Marta Omedes Pujol

The role of the counterion in the catalytic activity of Vanadium(V)(salen) complexes

Doctor of Philosophy Thesis

University of Newcastle upon Tyne

December 2011

Abstract

Over the last ten years, the North group has developed VO(salen)X complexes as an efficient catalytic system for the asymmetric addition of trimethylsilyl cyanide to aldehydes. It was found that the nature of the counterion X has a significant influence on the catalytic activity, but not on the enantioselectivity of the reaction. Complexes with the most coordinating counterions displayed the highest levels of catalytic activity. Kinetic studies revealed that the monometallic VO(salen)X complexes exist in equilibrium with bimetallic complexes, and both are catalytically active. This was supported by mass spectrometry which detected both $[VO(salen)]^+$ and $[VO(salen)]_2^+$ ions, with the latter involving both V(V) and V(IV) ions.

In this project, electron paramagnetic resonance spectroscopy (EPR) was used to monitor vanadium(IV) formation, revealing that the rate of formation is directly related to the catalytic activity of the complex. Also using EPR, cyanide was found to be the reducing agent and to be oxidized to cyanogen via a non-radical mechanism. Oxovanadium complexes bearing highly coordinating counterions were most rapidly reduced to vanadium(IV), thus favouring the formation of highly reactive bimetallic species. In contrast, less coordinating counterions resulted in the formation of much lower amounts of dinuclear species.

The potential of the counterion to display Lewis-base catalysis became increasingly clear during this project. A Hammett plot based on a series of *para*- and *meta*-substituted benzaldehydes, was used to determine the relative importance of Lewis-acid and Lewis-base catalysis within VO(salen)X complexes. As expected, the vanadium catalysts studied gave a positive reaction constant indicating that there is an increase in electron density at the benzylic carbon during the transition state. However, a less positive reaction constant (ρ = 1.2) was found for VO(salen)NCS which possessed a strongly coordinating counterion, compared to that of VO(salen) $EtOSO_3$ (ρ = 1.9) which possessed an ionic counterion, which indicates a possible Lewis base influence from the thiocyanate counterion. These complexes were also compared to metal(salen) complexes of titanium and aluminium. The latter required the presence of triphenylphosphine oxide as an achiral Lewis-base cocatalyst, and exhibited predominantly Lewis base catalysis with a reaction constant of 0.7, whereas the titanium catalyst was found to function almost entirely as a Lewis-acid catalyst with a reaction constant ρ = 2.4. Thiocyanate was also found to be an excellent Lewis base

catalyst for racemic cyanohydrin synthesis, for which a mechanism involving activation of the trimethylsilyl cyanide through a hypervalent silicon bond was suggested.

The use of propylene carbonate as an alternative solvent to dichloromethane was shown to affect the rate of cyanohydrin synthesis when VO(salen)NCS was used as the catalyst. Thus, a mechanistic study was undertaken. The reaction was found to obey second order kinetics in both propylene carbonate and dichloromethane. However, when the order with respect to the catalyst was determined, it became evident that propylene carbonate altered the monomer-dimer equilibrium towards the monomer. The monomer was the most abundant species in solution and hence was responsible for most of the catalytic activity. ^{51}V-NMR experiments provided evidence for propylene carbonate coordination to VO(salen)NCS, blocking the sixth coordination site, and hence inhibiting both dimer formation and aldehyde coordination. Further evidence for this effect was provided by a Hammett analysis, which showed that Lewis base catalysis was more pronounced when propylene carbonate was the solvent.

Dedication

Dedico aquesta tesis al meu pare Albert Omedes Casals, qui ens va deixar el dia 29 de Juliol d'aquest mateix any, 2011, després de patir una malaltia mortal (càncer) que va consumir la seva vida en el seus 57 anys. Les seves ganes de viure m'han ensenyat a apreciar la vida; a ser feliç i a fer felices a totes les persones que ens fan sentir especials. També dedico aquesta tesis a la resta de la meva família per estimar-me, recolzar-me I creure en mi des del dia que vaig néixer. Per tots ells, orgullosos de veure'm partir tota sola cap a una terra desconeguda, deixant tots els amics enrere incloent el Català.

Aquests quatre anys m'han omplert de valor i força per afrontar tot el que vingui. Se m'ha ofert l'oportunitat de conèixer gent nova, no només d'Anglaterra, sino també d'altres paisos com Alemanya, França, Itàlia, Noruega, Suècia, Letònia, la India, Nova Zelanda, Austràlia, Japó i la China. He après una llengua nova, i el que és mes important, l'habilitat d' escriure i a parlar-la a nivell científic.

No sé cap on em conduirà aquest Doctorat, tant sols sé que és el principi de la meva carrera professional i el principi d'una vida sense pors ni fronteres. La vida són quatre dies i s'ha de disfrutar.

T'estimo papi.

I dedicate this thesis to my father Albert Omedes Casals, whom sadly passed away on the 29th July of this year 2011, after suffering a fatal disease (cancer) that took his life at the age of 57. His will to live has taught me to appreciate Life; to be happy and to make happy all those people that make us feel special. I also dedicate this thesis to the rest of my family for loving me, supporting me and believing in me since the day I was born. For all of them, proud to see me depart to a new country, leaving many friends behind as well as my mother tongue "Catalan".

During these four years I have been filled with courage and strength to face anything that comes. This experience has given me the opportunity to meet new people, not only from England but from other countries as well; such as Germany, France, Italy, Norway, Sweden, Latvia, India, New Zealand, Australia, Japan and China. I have

learned a new language, and more importantly, the ability to write and speak on a scientific level.

I do not know where this PhD will lead me as this is only the beginning of my professional career and the beginning of a life without fear or boundaries. Life is short and we have to enjoy it.

I love you Dad.

Acknowledgements

I would like to thank my supervisor Professor Michael North for giving me the opportunity to undertake my PhD studies, for the guidance and the confidence he gave me for the last four years. Thanks also to Dr. Victor Chechik and Dr. Marco Conte from the University of York for all the help they provided with the EPR experiments.

I would like to express my gratitude to all my collegues and friends in the Chemistry department, in particular to my fellow Spaniard Pedro, for his support and bright personality. However, my special thanks goes to Dr. Thierry Achard, an old member of MN group, who I met during my Masters Degree in Barcelona. Thierry encouraged me to come to England to continue my studies, and to take the chances when they come. His courage and self-confidence made me a stronger person. I have to say that this experience so far, has been very rewarding.

Table of contents

1 Introduction

1.1 Chirality

It is still uncertain how life started on our planet. Carbon rather than other elements, was chosen to build the backbone structure of all molecules that all living beings on Earth are composed of. Our minuscule building blocks, cells, made mainly of fatty acids, sugars, and amino acids, work in harmony to keep the balance between the inside and outside of living beings. One mistake in the process of synthesising and transcribing DNA and RNA into proteins can trigger a catastrophe for the entire community of cells causing an imbalance and death of the organism.

A major discovery, that revolutionised the worlds of chemistry, biology and medicine was made by Pasteur.[1] He observed that minerals and some organic molecules which possess exactly the same chemical properties can rotate the plane of polarised light clockwise or anticlockwise. These molecules are mirror images of one another and are known as stereoisomers. Life itself has adopted one of the two enantiomers to create all building blocks, proteins and genetic material, as all the amino acids exist in their L-form and all the sugars exist in their D-form. The reason for this homochirality is still being debated; but what is clear is that the abundance of L-amino acids and D-sugars was already present in our early origins.

Enzymes, our synthetic machinery, are responsible for most of the biochemical reactions that take place in our bodies. Most of the molecules that interact with our enzymes, activating or inhibiting their biological activity, are chiral. In fact, great care has to be taken to make the right interaction between enzyme and substrate, since different stereoisomers may not give the same response. A well known example is Thalidomide (*R*)-**1**.[2] This drug was administered as a racemic mixture to suppress early sickness in pregnant women. However, it was later found that whilst the (*R*)-enantiomer had the desired medicinal property, the (*S*)-enantiomer was the cause of severe foetal deformities. Hence, the requirement to produce an enantiomerically pure stereoisomer rather than a racemic mixture became extremely important for the pharmaceutical industry.

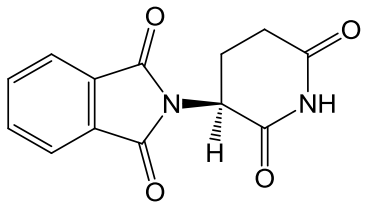

(*S*)-**1**

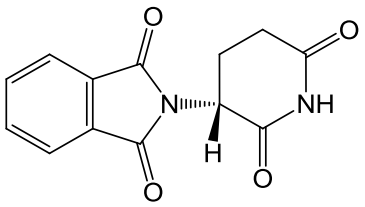

(*R*)-**1**

Amongst the methods to selectively produce enantiomerically pure compounds, there is a significant preference for asymmetric synthesis. This includes the use of chiral auxiliaries, chiral reagents and chiral catalysts. This thesis will focus on the latter approach which has become the most effective and hence preferred route. Chiral catalysts can be of a biological nature, i.e. enzymes, or synthetic, including many metal-based complexes which have been developed.

1.2 Asymmetric synthesis of cyanohydrins

Over the last century, the synthesis of non-racemic cyanohydrins has become one of the better studied reactions in organic chemistry. This is due to their potential as key intermediates for the preparation of other compounds of pharmaceutical interest. Cyanohydrins are most commonly prepared from the addition of cyanide to a carbonyl compound (**Scheme 1.1**). The product of this reaction bears two functional groups, a nitrile and an alcohol directly attached to a stereogenic centre; therefore, by using only simple chemical transformations, a wide variety of bifunctional molecules can be readily prepared. **Scheme 1.1** illustrates some examples of possible modifications to emphasise the importance of cyanohydrins as precursors to enantioenriched organic compounds including α-amino acids,[3] α-amino nitriles,[4] α-hydroxy acids[5] or hydroxy esters,[6] β-hydroxy amines[7] and α-sulfonyloxynitriles.[8]

The first cyanohydrin synthesis was reported by Winkler in 1832 by the nucleophilic addition of hydrogen cyanide to benzaldehyde in aqueous media.[9] Not much later, Wöhler identified an oxynitrilase enzyme in almonds, which catalyses the hydrolysis of mandelonitrile to hydrogen cyanide and benzaldehyde.[10] In view of this discovery, in 1908, Rosenthaler used emulsin (an extract from almonds) as a catalyst for the first asymmetric organic synthesis ever reported, the asymmetric synthesis of a cyanohydrin.[11] Emulsin contains glycosidase and oxynitrilase enzymes which degrade glycoside, the natural source of cyanohydrins in plants, first to mandelonitrile, then to benzaldehye and hydrogen cyanide (**Scheme 1.2**). Rosenthaler managed to optimise the

conditions to control the reverse reaction, and thus, enantioenriched (*R*)-mandelonitrile was first synthetically prepared with up to 97% enantiomeric excess.

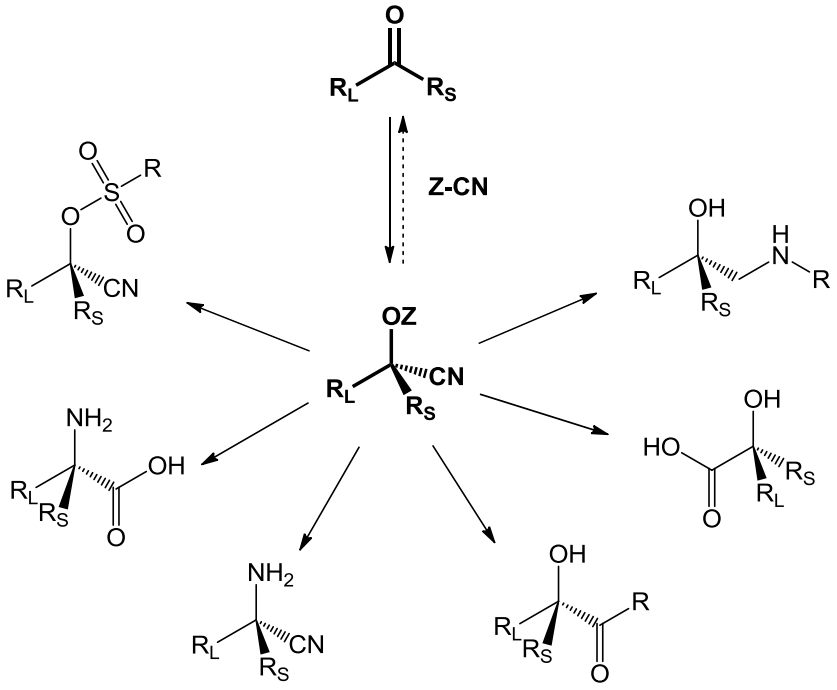

Scheme 1.1 Possible transformations from cyanohydrins, which are formed by the asymmetric addition of cyanide to an aldehyde (R_S = H) or ketone (R_S = alkyl or aryl)

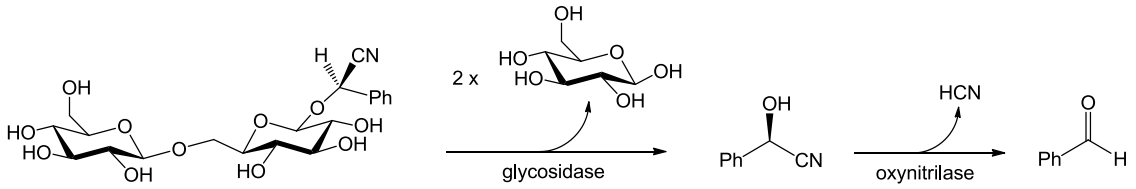

Scheme 1.2 Natural process of glycoside degradation and release of HCN occurring in almonds.

Although oxynitrilases display high regio- and stereoselectivity under mild reaction conditions; they still suffer from a few limitations including:

- Limited substrate tolerance
- pH and temperature dependence
- Poor availability, -whereas the (*R*)-oxynitrilase enzyme is abundant and easy to isolate from almonds, (*S*)-oxynitrilases are more time consuming to extract for use in asymmetric catalysis. However, this is no longer a major problem since the genes of natural (*R*)- and (*S*)-oxynitrilases have been cloned and over-expressed.

In 1902, Lapworth discovered that the addition of a base during cyanohydrin synthesis resulted in an increase in the rate of reaction.[12] Thus, the development of a whole new world of synthetic catalysts began. Chiral alkaloids, peptides and polyamines were amongst the first organocatalysts, derived from natural compounds that exerted some catalytic activity in the hydrocyanation of aldehydes; however, the enantioselectivity was rather mediocre (less than 20%). In 1979, Inoue and co-workers reported a novel synthetic catalytic system, diketopiperazines **2** and **3**.[13] These cyclic peptides showed exceptional levels of asymmetric induction in the addition of hydrogen cyanide to aldehydes (97% ee for mandelonitrile). Despite the fact that both amino acids from which catalysts **2** and **3** are formed have the (*S*)-configuration, catalyst **2** gives the (*R*)-cyanohydrin, whilst catalyst **3** gives the (*S*)-enantiomer. Attempts to investigate the mechanism of this reaction and improve the catalytic activity for a wider range of substrates were however, unsuccessful. This is due to the heterogeneous nature of the reaction conditions and the lack of modifications that can be made to structures **2** and **3**. For these reasons this system was abandoned and little progress was made in the development of new organocatalysts until the last few years (see section *1.4.2.1*).

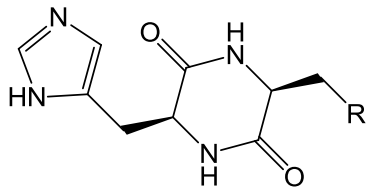

2 R = Ph
3 R= ^{i}Pr

1.3 Cyanide sources

All the early catalysts described above used hydrogen cyanide as the cyanide source. Although HCN is still widely used in industry, it is an extremely volatile compound (bp. 26 °C); which, when it comes into contact with water, releases cyanide anions, which halt cellular respiration and can rapidly cause human death. During the last few decades, several alternative cyanide sources have been successfully used in the cyanation of aldehydes and ketones using metal complexes as catalysts. Trimethylsilyl cyanide, sodium and potassium cyanide, alkyl cyanoformates, acetyl cyanide, acetone cyanohydrins and alkyl cyanophosphonates are examples of these cyanide sources. These alternative cyanide sources are stable at room temperature and lead to the formation of O-protected cyanohydrin derivatives which prevents racemisation (**Figure 1.1**). However, they often require reactions to be carried out at very low temperatures with long reaction times and high catalyst to substrate ratios. Despite its relatively high cost, trimethylsilyl cyanide (TMSCN) has been the most successful of these cyanide

sources and as a consequence, only catalytic systems using it will be described in this literature overview.

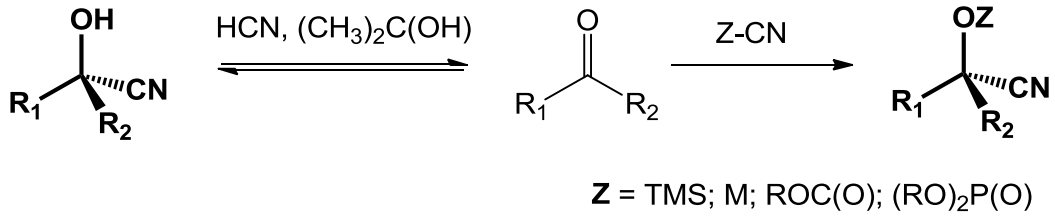

Figure 1.1 Cyanide sources used in the synthesis of cyanohydrins.

1.4 Metal-based catalysts for the asymmetric synthesis of cyanohydrins.

The real breakthrough in the field of asymmetric synthesis of cyanohydrins started with the use of transition metal complexes as catalysts. These compounds contain a Lewis acidic metal ion, embraced by a chiral ligand. The first complexes reported to catalyse the asymmetric synthesis of mandelonitrile from the reaction between TMSCN and benzaldehyde date from 1986 by Reetz.[14] Complexes **4** and **5** contain a boron ion and have C_2-symmetry which facilitated the transfer of asymmetry to the product. Although the asymmetric induction was low (12-16% ee), this demonstrated that Lewis acidic complexes have the potential to activate aldehydes and ketones for asymmetric cyanohydrin synthesis

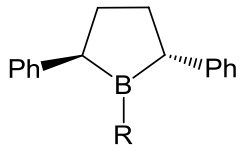

4 R = OMe
5 R = Cl

The role of the boron ion in the complexes is to activate the carbonyl compound by coordination. Therefore, in general, the metal ion has to be a good Lewis acid which can withdraw electron density from the prochiral centre thus increasing the rate of the nucleophilic addition. The ligand on the other hand, provides the chiral environment, and as a consequence regulates the stereochemistry of the reaction. However, the ability to make structural changes to the ligand makes it quite attractive to also incorporate other functionalities, such as Lewis basic groups which can activate the cyanide nucleophile, resulting in a lower energy transition state. Therefore, within this section, chiral ligands will be divided into two main groups, those that only influence the asymmetric induction, and those that can work cooperatively with the metal and activate

the cyanide. A further group of catalytic systems are those that include the use of additives and the three possibilities are illustrated in **Figure 1.2**. Therefore, a third subsection will be dedicated to those systems that require the addition of a chiral or non-chiral base which can separately activate the cyanide improving the catalytic activity and asymmetric induction. Only homogeneous reactions where the complex is soluble in the solvent system will be covered.

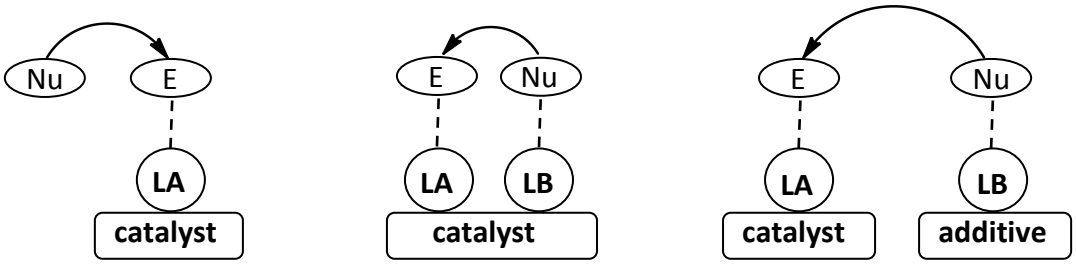

Figure 1.2 Lewis acid catalysis (left) *versus* dual Lewis acid – Lewis base catalysis using a bifunctional catalyst (centre) and use of two separate catalytic species (right).

1.4.1 Pure Lewis acid catalysis.

After the work of Reetz,[14] many other research groups have devoted their attention to the use of Lewis acidic complexes to activate carbonyl compounds for asymmetric cyanohydrin synthesis. The metal ion used most frequently has been titanium(IV). However, other electron deficient transition metals at the left hand side of the periodic table (with empty 4s and 3d orbitals) and some metals of the p-block (with empty s and p orbitals) have also been used as Lewis acidic ions. The associated ligand provides structural stability and a chiral environment for the cyanosilylation reaction to take place.

1.4.1.1 Chiral alcohol based ligands.

An early example of a chiral metal complex to be used in the asymmetric synthesis of silylated cyanohydrins was described by Narasaka in 1987.[15] The complex was formed *in situ* from the addition of chiral TADDOL **5a** to an equimolar amount of $TiCl_2(O^iPr)_2$. This system was shown to generate enantioenriched cyanohydrins from the reaction of several aromatic and aliphatic aldehydes with an excess of TMSCN. The best enantioselectivities (>73% ee) were obtained in toluene at -78 °C in the presence of 4 Å molecular sieves. Despite the encouraging enantioselectivities, this system was abandoned since a stoichiometric amount of the complex was essential to achieve any reactivity. Recently, Kim and co-workers prepared the titanium complex of TADDOL

5b, which also catalysed the silylcyanation of aldehydes, but only in the presence of triphenylphosphine oxide (see *section 1.4.3.4*).[16]

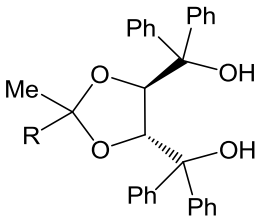

5a R = Ph
5b R = Me

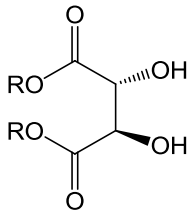

6a R = ^{i}Pr
6b R = Et

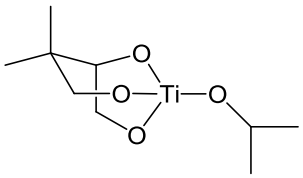

7

A similar approach was reported by Oguni using L-diisopropyl tartrate **6a** as the chiral ligand.[17] Addition of isopropanol was found to improve the reactivity and enantioselectivity, thus, this catalytic system can be included in the category of Lewis acid complexes used with additives (*section 1.4.3*). The use of 20 mol% of the catalyst generated *in situ* by treatment of **6a** with $Ti(O^{i}Pr)_4$ in equal ratio, and two equivalents of isopropanol in dichloromethane gave the optimal conditions for the asymmetric addition of TMSCN to several aldehydes, from which cyanohydrin O-trimethylsilyl ethers were obtained with high yields (>80%) and good enantioselectivities (60-91% ee). More recently, but resulting in inferior results to those of Oguni, Wada and Smith developed a similar system using bismuth(III) as the metal ion.[18] The complex was formed by the *in situ* addition of bismuth trichloride to L-diethyl tartrate **6b**. The best performance of this complex in the addition of TMSCN to aromatic and aliphatic aldehydes was observed when using 20 mol% of the catalyst in dichloromethane at -23 °C. The resulting O-trimethylsilylcyanohydrins were obtained with 100% yield after 3 hours, however, the enantioselectivities were rather poor (25-75% ee).

Another variant of a chiral alcohol metal based catalyst is the chiral complex **7** developed by de Vries in 1993.[19] The triol ligand was prepared by reduction of D-pantolactone with $LiAlH_4$ and subsequently coordinated to titanium by reaction with titanium(IV)tetraisopropoxide. Although initially designed to work with HCN, complex **7** did not show any reactivity towards benzaldehyde. However, when TMSCN was used instead of HCN, O-silylated mandelonitrile was obtained in 92% yield and with an enantiomeric excess of 76% after 2 hours. The optimal conditions were achieved in dichloromethane at -20 °C using stoichiometric amounts of complex **7**. When a substoichiometric protocol was attempted, both yield and enantioselectivity were dramatically reduced.

Despite the problems with low reactivity and poor selectivity associated with complex **7**, in 1997, Choi found an application for it. Complex **7** became the first example of a catalyst for the asymmetric cyanation of ketones. The best result was obtained at 18 °C and 0.8 GPa pressure for 18 hours when 1 mol% of complex **7** was used. Under these conditions, the cyanohydrin silyl ether obtained from acetophenone was prepared in 93% yield and with 60% enantioselectivity.[20]

1.4.1.2 Schiff Base ligands and derivatives

Inoue and Oguni were the pioneers of the most commonly used ligand structure in asymmetric cyanohydrin synthesis, Schiff bases. This ligand derives from the condensation of a salicylaldehyde unit and a chiral mono-amine or a 1,2-diamine in order to form a complex with C_1 or C_2 symmetry respectively (**Scheme 1.3**)

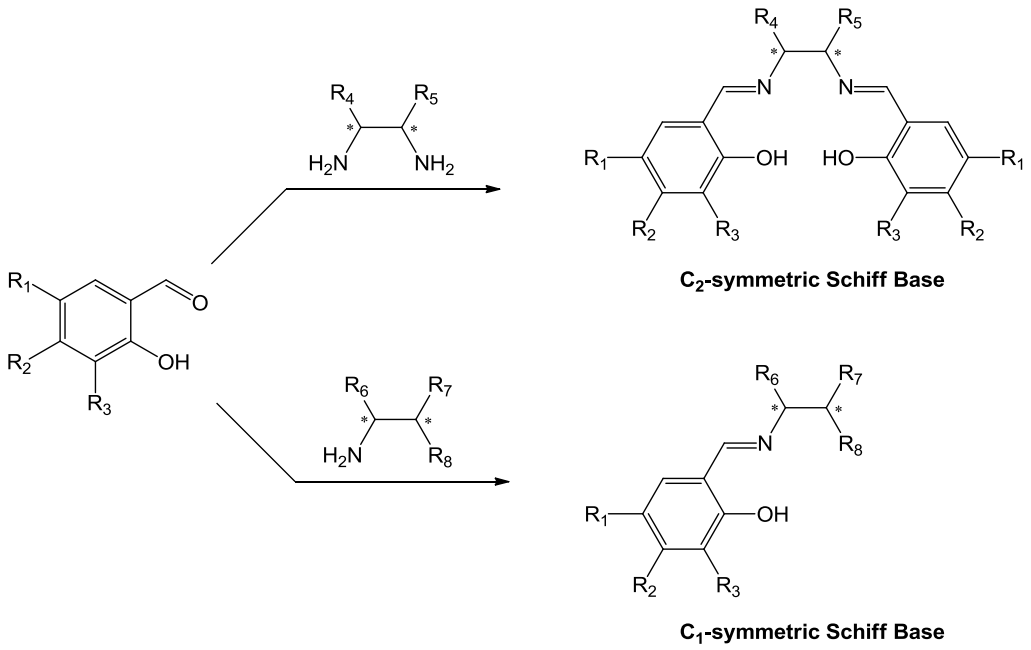

Scheme 1.3 Preparation of C_1 and C_2-symmetric Schiff's bases.

1.4.1.2.1 C_1-symmetric Schiff base ligands

Following on from his previous experience in using peptides as organocatalysts for the asymmetric synthesis of cyanohydrins (*Section 1.2*), Inoue prepared a range of Schiff bases **8-10** derived from amino acids and dipeptides.[21] All the Schiff bases were shown to catalyse the addition of HCN to aldehydes when combined with $Ti(O^iPr)_4$. After an extensive study of several catalyst structures, he noticed that ligands containing two amino acid residues (**8a-c**) gave better enantioselectivities than the ones with a single amino acid residue (**9-10**). This indicated that the selectivity was provided mostly by the C-terminal residue. When both amino acid residues within the ligand possessed

the same configuration (*S*,*S*), cyanohydrins were obtained with a better enantiomeric purity than those obtained when the residues had opposite configurations (*S*,*R*). However, all the complexes were found to be catalytically active and the best result was obtained using complex **8a** which gave a respectable asymmetric induction and chemical yield when benzaldehyde was used as a substrate (88% yield and 88% ee). However, attempts to conduct the reaction using TMSCN instead of HCN were ineffective even using stoichiometric amounts of the titanium complex. Therefore, Inoue investigated the effect of other metals such as aluminium.[22] Thus, novel complexes formed from ligands **8b** or **8c** with $AlMe_3$ (1:1 ratio) were prepared. This system catalysed the silylcyanation of several aromatic and aliphatic aldehydes with almost quantitative yields and moderate enantioselectivities (37-58% ee) in the presence of 20 mol% catalyst in toluene at -78 °C after 3 to 24 hours depending on the substrate.

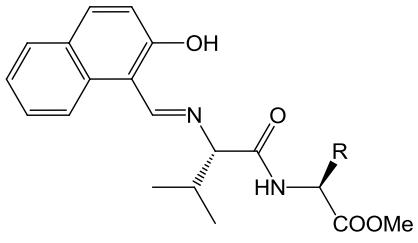

8a R = 3-indolyl
8b R = CH_2Ph
8c R = Cy

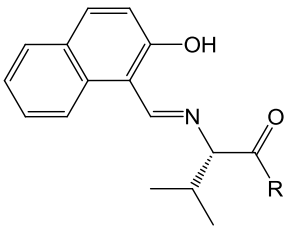

9a R = OMe
9b R = $NHCH_2Ph$

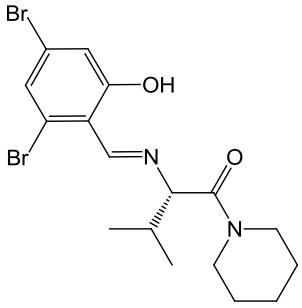

10

Oguni on the other hand, introduced β-amino alcohol derived Schiff bases as tridentate ligands. In this study, he treated a collection of tridentate ligands **11a-l** with $Ti(O^iPr)_4$ to prepare titanium complexes *in situ*, which were found to be effective catalysts for the addition of TMSCN to aldehydes (**Table 1.1**). Amongst these catalysts the titanium diisopropoxide complex derived from ligand **11f** (20 mol%) was found to be the most effective catalyst, affording cyanohydrin silyl ethers from various aromatic and aliphatic aldehydes in good yield and in some cases with excellent enantiomeric purities. A low reaction temperature was however essential to obtain cyanohydrins with high enantiomeric excesses, with the best results being obtained at -80 °C for one or two days. It is worth noting that the bulky substituent in the 3-position of the salicylaldehyde was the major factor influencing the enantioselectivity, since the lack of a substituent at this position gave a very low enantioselectivity.[23] Equally important was the discovery of the existence of two different complexes by NMR spectroscopy.[24] The complex obtained by the complexation of two equivalents of the β-amino alcohol derivative to

titanium(IV) led to the formation of a saturated hexacoordinated structure **A** which was shown to be catalytically inactive, whereas the coordinatively unsaturated bimetallic complex **B** formed from equimolar amounts of $Ti(O^iPr)_4$ and ligand **11f** is the catalytically active species.

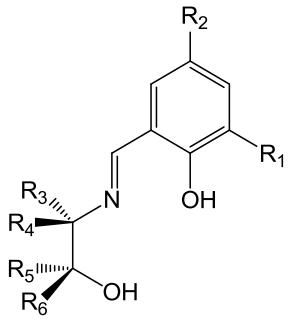

11

Schiff base	*R_1*	*R_2*	*R_3*	*R_4*	*R_5*	*R_6*	*Yield %*	*ee %*
(S)-**11a**	H	H	*i*-Pr	H	H	H	69	22 *(S)*
(S)-**11b**	H	H	*i*-Pr	H	Ph	Ph	28	60 *(R)*
(S)-**11c**	H	H	*t*-Bu	H	H	H	40	40 *(S)*
(S)-**11d**	*t*-Bu	H	Me	H	H	H	60	60 *(R)*
(R)-**11e**	*t*-Bu	H	H	Et	H	H	72	80 *(S)*
(S)-**11f**	*t*-Bu	H	*i*-Pr	H	H	H	67	85 *(R)*
(S)-**11g**	*t*-Bu	H	*i*-Pr	H	Ph	Ph	54	64 *(R)*
(S)-**11h**	*t*-Bu	H	*t*-Bu	H	H	H	51	63 *(R)*
(R)-**11i**	*t*-Bu	H	H	Ph	H	H	41	40 *(S)*
(R)-**11j**	*t*-Bu	H	H	H	*t*-Bu	H	61	67 *(S)*
(S)-**11k**	*t*-Bu	Me	*i*-Pr	H	H	H	45	76 *(R)*
(S)-**11l**	*t*-Bu	*t*-Bu	*i*-Pr	H	H	H	38	67 *(R)*

Table 1.1

In view of the promising results obtained using Oguni's 1,2-amino alcohol Schiff base system, Jiang and co-workers developed ligand **12**, with 2-amino-1,2-diphenylethanol as the amino alcohol moiety. This ligand bears two stereogenic centres with opposite configurations. This proved to be beneficial to the enantioselectivity, giving silylated cyanohydrins in 85-97% yield and with 54-91% enantiomeric excess.[25]

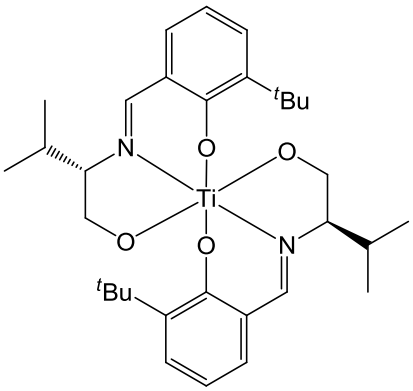

A
catalytically inactive

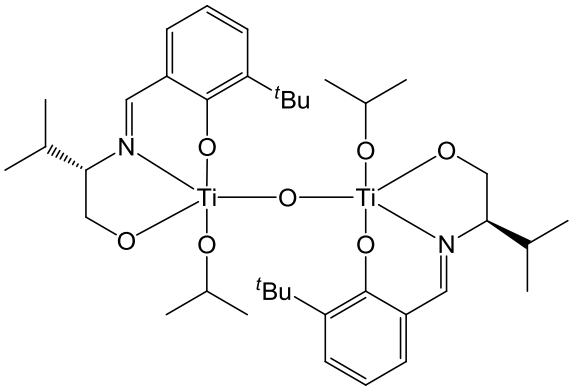

B
catalytically active

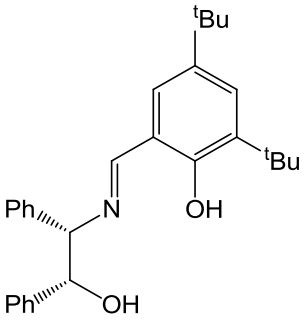

12

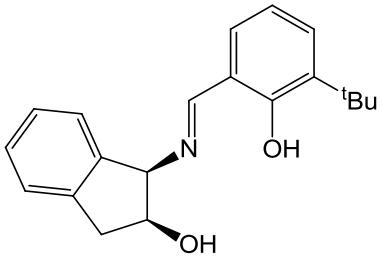

13

More recently, Walsh and Somanathan described another two-stereocentre amino alcohol Schiff base ligand, *cis*-1-amino-2-indanol **13.**[26] The introduction of an indanol group in the amino alcohol moiety was designed to restrict the mobility around the C_1-C_2 bond. Consistent with Oguni's findings, they also observed that the coordinatively saturated form of the complex *L_2Ti had very little activity in the silylcyanation of aldehydes since compared to the unsaturated complex *LTi(O^iPr)$_2$, very low yields and enantiomeric excesses were afforded. More interestingly, they discovered that the substituent *ortho* to the phenolic OH, not only had a determining influence on the enantioselectivity, but also had a major effect on the structure of the catalyst.[27] Thus, they showed that a larger group will provide more steric hindrance and hence favours the formation of the catalytically active mono-Schiff base complex *LTi(O^iPr)$_2$. The best results were obtained for the reaction of TMSCN with benzaldehyde, using an equal amount of Schiff base ligand **13,** bearing a *tert*-butyl group adjacent to the phenolic OH, and Ti(O^iPr)$_4$ (20 mol%) at -78°C in dichloromethane for 36 hours (64% yield, 85% ee).

Moyano *et al*. synthesised a library of amino alcohols derived from ferrocene.[28] They found that the C_1-symmetrical disubstituted amino alcohol **14**, when treated with

equimolar amounts of $Ti(O^iPr)_4$ in dichloromethane at -60 °C, gave (*S*)-mandelonitrile in 91% yield and with 94% ee after 64 hours. In contrast, when the methyl substituent was at the C_1-position, both the rate and enantioselectivity of the reaction were diminished, affording (*S*)-mandelonitrile with only 54% enantiomeric purity.

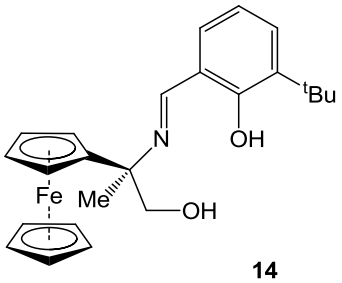

14

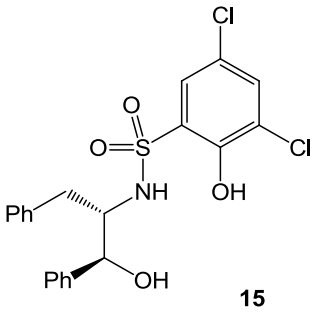

15

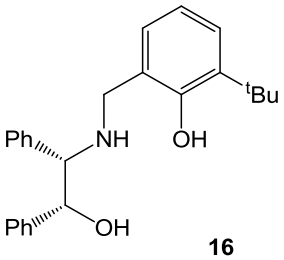

16

The β-amino alcohol Schiff base derivatives described so far, have been structurally modified in order to improve the enantioselectivity of the cyanosilylation reaction, mainly by changing the substituents on the phenol ring and at the 1,2-positions of the amino alcohol. However, Choi's group developed ligand **15**; an amino alcohol attached to a phenol, not through an imine but by a sulfonamide group.[29] This structural change was shown to be beneficial in the asymmetric catalysis of cyanohydrin synthesis. The amino alcohol moiety bearing two stereogenic centres of opposite configuration was shown to be a key factor in the transfer of asymmetry. When the complex, formed by treatment of ligand **15** with one equivalent of $Ti(O^iPr)_4$ (5-10 mol%), was used to catalyse the silylcyanation of benzaldehyde (in CH_2Cl_2 at -65 °C in the presence of 4A molecular sieves), (*R*)-mandelonitrile was obtained with total conversion and with an optical purity of 96% after 48 hours.

Following on from Oguni's β-amino alcohol Schiff base **11**-$Ti(O^iPr)_4$ complexes, Feng's group studied the reduced Schiff base analogue **16.** Ligand **16**, with two stereogenic centres of opposite absolute configuration and a methyl group *ortho*- to the phenolic OH, was the optimised structure from a series of ligands. When this was combined with one equivalent of $Ti(O^iPr)_4$, it was found to exhibit the best asymmetric induction in the cyanosilylation of benzaldehyde (98% yield and 94% ee). The process was carried out using 5 mol% of the catalyst and two equivalents of TMSCN relative to benzaldehyde at 0.5 M in dichloromethane at -20 °C for 20 hours. Under the same conditions, this complex was employed as a catalyst for the cyanosilylation of a range of substituted aromatic aldehydes. With the exception of 2-chlorobenzaldehyde, the

reaction led to the formation of the products with very similar *ee* values to that of benzaldehyde (87-93% ee). Contrary to Oguni's catalytic system, the *Re* face of the prochiral aldehyde is the preferred side for nucleophilic attack, since it is less sterically hindered, thus resulting in the formation of the (*S*)-enantiomer of the cyanohydrins (**Figure 1.2**). This is partly due to the formation of a covalent N-Ti bond, so, only one isopropoxy group is required to complete the titanium valence shell.

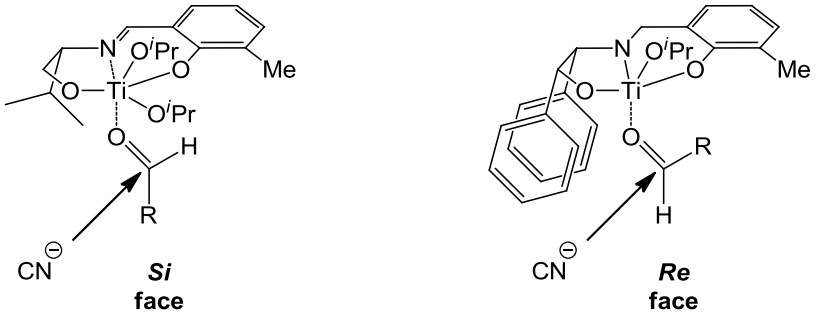

Figure 1.2 Proposed model for the asymmetric addition of cyanide to aldehydes catalysed by Oguni's catalyst **11f** (left) and Feng's catalyst **16** (right).

Very recently, the most efficient catalytic system of this type for the enantioselective silylcyanation of aldehydes and ketones was described by Yoshinaga and co-workers.[30] The complex was prepared from partially hydrolysed Ti(O^{i}Pr)$_4$ and ligand (*S*)-**11l** previously introduced by Oguni[23b] (**Scheme 1.4**). Only 0.2-1 mol% of the catalyst was needed to afford the O-trimethylsilyl cyanohydrin of a range of aromatic and aliphatic aldehydes with almost quantitative yields and excellent enantiomeric excesses (86-97% ee) after only two hours at room temperature. The same level of asymmetric induction was obtained for cyanohydrins derived from two ketones, acetophenone and cyclohexylmethylketone, which gave products with 88 and 90% enantiomeric excess respectively after 24 hours.

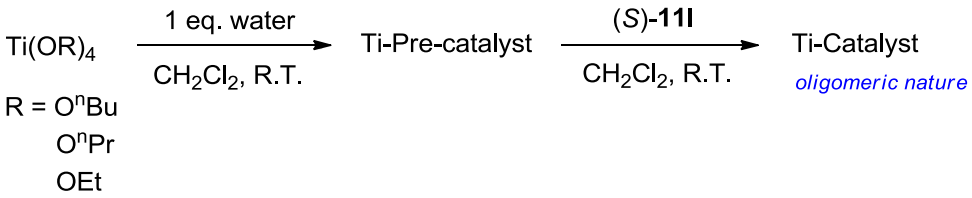

Scheme 1.4 Preparation of Yoshinaga's active catalyst from the pre-hydrolysed Ti(OR)$_4$ and Schiff base ligand (*S*)-**11l**.

1.4.1.2.2 C_2-symmetric Schiff base ligands

By applying the same strategy used to make C_1-symmetric Schiff base ligands, salicylaldehyde can be reacted with diamines to form a tetradentate C_2-symmetric ligand known as salen. Optically active metalosalen complexes derived from transition metals had been successfully used as catalysts for a wide variety of transformations including epoxidations,[31] cyclopropanations,[32] sulfoxidations[31a, 33] and Diels-Alder reactions.[34] Inspired by this precedent, Jiang's group prepared the titanium complexes of salen ligands **17a-d** and tested them as catalysts for the asymmetric cyanosilylation of aldehydes.[35] They observed that structural changes within the ligand significantly influenced the catalytic performance; and contrary to what had been observed for C_1-symmetric Schiff base complexes, the less sterically hindered the substituents on the phenolic rings, the higher the enantioselectivity achieved. As a result, the titanium complex obtained from the salen ligand with unsubstituted phenol rings (*S,S*)-**17d** was the most effective catalyst, converting a series of aldehydes into their respective (*R*)-cyanohydrins in 60-86% chemical yield and with 22-87% *ee* after 24 hours (10 mol% of catalyst, dichloromethane, -78°C).

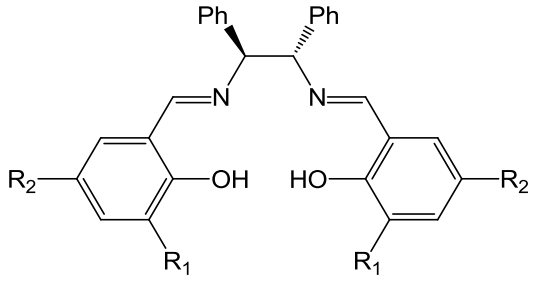

(*S,S*)-**17a** $R_1 = {}^t$Bu; $R_2 = {}^t$Bu
(*S,S*)-**17b** $R_1 = CHPh_2$; $R_2 = CH_3$
(*S,S*)-**17c** $R_1 = OCH_3$; $R_2 = H$
(*S,S*)-**17d** $R_1 = H$; $R_2 = H$

At the same time, Belokon and North reported another series of salen ligands derived from diaminocyclohexane and 3,5-disubstituted salicylaldehydes **18a-f**. In contrast to the system studied by Jiang, they found that steric hindrance in the *ortho*- and *para*-positions of the phenol rings was beneficial for the enantioselectivity of the cyanosilylation process. Thus, when 20 mol% of the titanium diisopropoxide complex derived from ligand (*R,R*)-**18e** was used to perform the asymmetric addition of TMSCN to a variety of aromatic and aliphatic aldehydes, (*S*)-cyanohydrin trimethylsilyl ethers were produced with the highest *ee* values (36-88%) and total conversion after 24-100 hours. The optimal conditions were found to be -80°C in dichloromethane. [36]

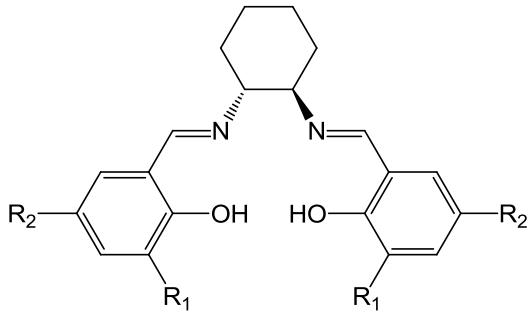

(*R,R*)-**18a** R_1 = H; R_2 = H
(*R,R*)-**18b** R_1 = ^{t}Bu; R_2 = H
(*R,R*)-**18c** R_1 = ^{t}Bu; R_2 = CH_3
(*R,R*)-**18d** R_1 = ^{t}Bu; R_2 = OCH_3
(*R,R*)-**18e** R_1 = ^{t}Bu; R_2 = ^{t}Bu
(*R,R*)-**18f** R_1 = Cl; R_2 = Cl

Despite the good stereoselectivities achieved with metalosalen systems, the optimal conditions were still unsatisfactory. The need for long reaction times, extremely low temperatures and the use of large catalyst to substrate ratios to obtain a respectable asymmetric induction for the cyanation of aldehydes all had room for improvement. In 1998, Belokon and North revealed the X-ray structure of complex **19** generated by the reaction of ligand **18e** with titanium tetrachloride.[37] This complex proved to be a superior catalyst to all the metal complexes published at that time. Thus, when benzaldehyde was used as a model substrate, only 0.1 mol% of the catalyst was required to give full conversion to O-trimethylsilyl mandelonitrile with 86% enantiomeric purity, from reactions carried out in dichloromethane, at ambient temperature for less than 24 hours.

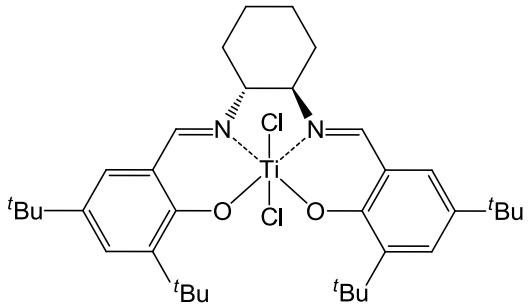

19

The authors found that the good results displayed by catalyst **19** were not reproducible, and that under extremely dry conditions the cyanosilylation reaction did not work at all using either the titanium complex generated by treatment of $Ti(O^iPr)_4$ with ligand **18e** or complex **19**. However, it was found that the addition of one equivalent of water formed an even more active catalyst for asymmetric cyanohydrin synthesis. Only 0.1 mol% of the catalyst was able to transform a set of aliphatic and aromatic aldehydes into their respective cyanohydrin silyl ethers with 80-90% ee in under one hour at room temperature. As the asymmetric induction was found to be the same or very similar to that obtained using catalyst **19**, the authors suggested that complex **19** is likely to be a precatalyst, which reacts with adventitious water to form

the active catalyst. This would explain why the lack of water had such a detrimental effect on the reaction. Therefore, in order to reveal the structure of the catalyst, complex **19** was treated with water, and a stable crystalline product was isolated, analysed by X-ray crystallography and shown to be the dimeric titanium complex **20**.[37b] Further kinetic studies revealed that a binuclear complex was the catalytically active species (See *section 1.5*). This allows both the aldehyde and cyanide to be simultaneously activated by the two metal centres. This cooperative mechanism lowers the energy barrier, and leads to an intramolecular reaction where the salen ligand attached to each metal in the dinuclear catalyst is forced to adopt a cis-β configuration, thus providing the excellent level of asymmetric induction (**Figure 1.3**).[38] The chiral nature of the salen ligand and the coordination of both reactants, predetermines the reaction trajectory towards one of the prochiral faces of the aldehyde resulting in cyanohydrin formation with excellent enantioselectivities (**Figure 1.3**).

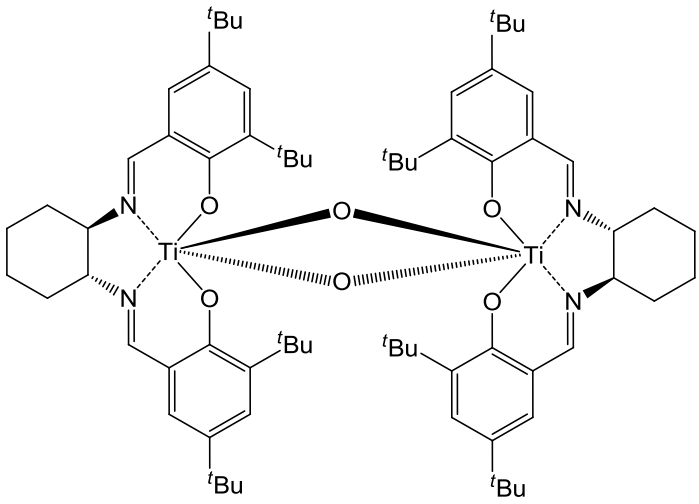

20

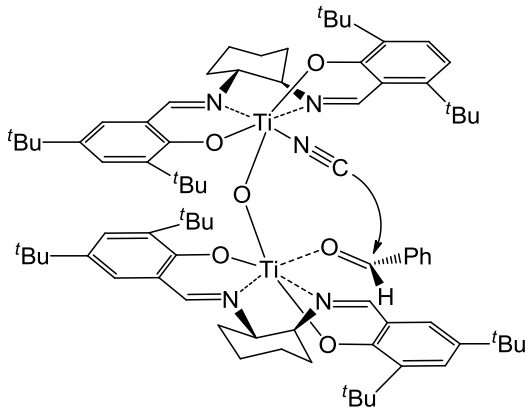

Figure 1.3 Proposed transition state for the catalytic asymmetric addition of cyanide to benzaldehyde using complex **20** as the catalyst.

The use of ketones as substrates for the silylcyanation reaction at room temperature using catalyst **20** also proved to be successful, albeit that much longer reaction times were required. Taking acetophenone as substrate, 38% conversion was obtained after one day in dichloromethane at ambient temperature, when 0.1 mol% of catalyst **20** was used, affording the (*S*)-cyanohydrin derivative with 70% ee. Increasing the amount of catalyst to 1 mol% or increasing the size of the alkyl group in the substrate negatively affected the enantioselectivity. Nevertheless, this was the first metal-based complex to perform the asymmetric addition of TMSCN to aromatic and aliphatic ketones at atmospheric pressure and gave respectable enantiomeric excesses (60-70%).[39] Complex **20** was also found to catalyse the addition of other cyanide sources to aldehydes, though this is beyond the scope of this review.[40]

Salen ligand **18e** was slightly modified by Bu and Liang by replacing the *tert*-butyl groups in the 3- and 5-positions of the aromatic ring with *tert*-pentyl groups. The catalyst obtained *in situ* from this salen ligand and $Ti(O^iPr)_4$ exhibited improved enantioselectivities compared to those obtained by using catalyst **20**. However, the reaction required temperatures of -78 °C and larger amounts of catalyst (5 mol%) to obtain reasonable reactivities.[41]

Belokon, North and co-workers discovered that the nature of the diamino moiety greatly affected the enantioselectivity of the reaction, since cyclic diamines, such as cyclohexanediamine, lock the ligand structure into a *gauche*-conformation; whereas acyclic diamine containing ligands, prefer to adopt the more stable *anti*-conformation (**Figure 1.4**). This was critical to the enantioselectivity of the process. A collection of ligands **17a** and **21a-d** were synthesised to study the effect of changing the diamine

structure on the cyanosilylation of aldehydes. The complexes obtained from these salen ligands and titanium tetrachloride all gave lower levels of asymmetric induction than that obtained using complex **19**.[42] With the exception of ligand **17a**, the cyanohydrin trimethylsilyl ethers obtained from the reaction between aldehydes and TMSCN catalysed by the titanium complexes of ligands **21a-d** had the opposite absolute configuration to that obtained using catalyst **20**. The flexibility of ligands **21a-d** results in a conformational change of the ligand structure, and hence it induces the opposite stereochemistry in the cyanohydrin to that obtained by catalysts **17a** and **20**.

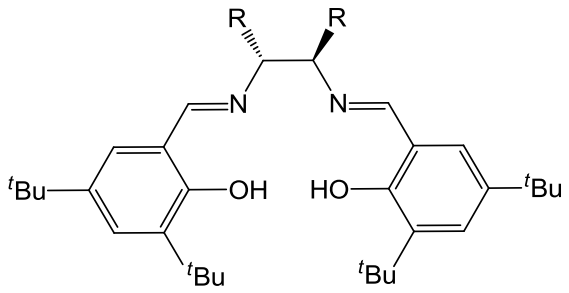

(*R,R*)-**17a** R = Ph
(*R,R*)-**21a** R = Me
(*R,R*)-**21b** R = ^{n}Pr
(*R,R*)-**21c** R = ^{i}Pr
(*R,R*)-**21d** R = ^{t}Bu

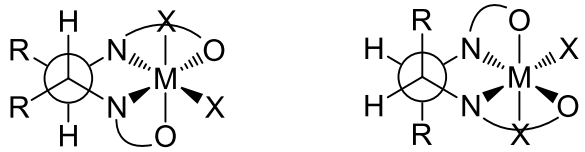

Figure 1.4 The *gauche*- and *anti*-conformations that a 1,2-diamine moiety can adopt in a salen ligand when it is coordinated to a metal.

With the aim of making a less reactive and hence more selective complex than bimetallic titanium complex **20**, Belokon and North attempted to prepare complex **22** based on vanadium(IV), a slightly less Lewis acidic centre. However, the reaction between Schiff base **18e** and $VOSO_4$ gave the oxidised catalyst **23a** with vanadium in the +5 oxidation state. The crystal structure of **23a** revealed an octahedral structure with the salen ligand occupying the four equatorial sites and the axial positions occupied by the oxo-group and a water molecule. Therefore, in the outer sphere, an ethylsulfate counterion (formed from $VOSO_4$ and ethanol used as the solvent in the synthesis) neutralizes the positive charge on the metal ion. When complex **23a** was used to catalyse the addition of TMSCN to benzaldehyde, under the same conditions used for complex **20** (0.1 mol% catalyst loading, in dichloromethane, at room temperature and air atmosphere), the reaction rate was significantly lower and there was an improvement

of the asymmetric induction. Subsequently, a range of aromatic and aliphatic aldehydes were converted into their O-protected cyanohydrins. After 24 hours all the aldehydes had fully reacted. Both aromatic and aliphatic cyanohydrins were obtained with higher enantiomeric excesses than those obtained using catalyst **20** (**Table 1.2**).[40b, 43]

Aldehyde	Catalyst (*R*,*R*)-**20** (*ee*)	Catalyst (*R*,*R*)-**23a** (*ee*)
PhCHO	88% (*S*)	94% (*S*)
4-$CH_3OC_6H_4CHO$	84% (*S*)	90% (*S*)
2-$CH_3C_6H_4CHO$	76% (*S*)	90% (*S*)
3-$CH_3C_6H_4CHO$	90% (*S*)	95% (*S*)
4-$CH_3C_6H_4CHO$	87% (*S*)	94% (*S*)
4-$NO_2C_6H_4CHO$	50% (*S*)	73% (*S*)
CH_3CH_2CHO	52% (*S*)	77% (*S*)
$(CH_3)_3CCHO$	66% (*S*)	68% (*S*)

Table 1.2

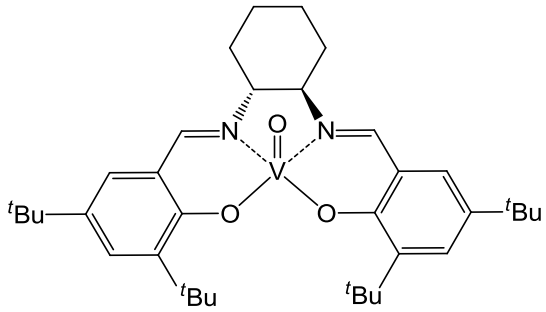

22

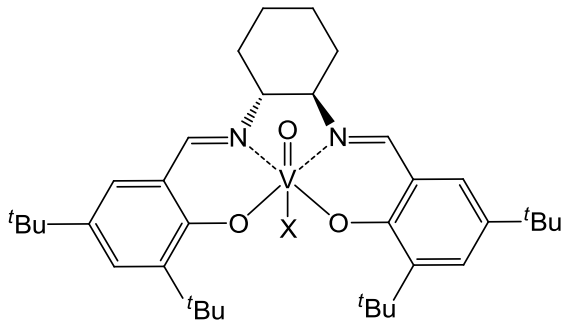

23a X = $EtOSO_3$
23b X = CF_3SO_3
23c X = BF_4
23d X = Br
23e X = NO_3
23f X = Cl
23g X = F
23h X = NCS

Further studies have shown that the counterion in complexes **23** plays an important role in the catalysis. Initially, the authors suggested that a less coordinating counterion such as triflate, would enhance the Lewis acidity of the central metal, and hence increase the rate of the reaction whilst maintaining the same level of asymmetric induction. However, the opposite effect was observed when vanadium(salen) complex

23b was found to be catalytically inactive. Therefore, complexes **23c-h** were prepared and tested as catalysts for the silylcyanation of benzaldehyde. Within this series, complex **23h** exhibited the highest catalytic activity, which appears to be determined by the basicity of the anion, increasing in the order: CF_3SO_3 <<< Br < $EtOSO_3$ < BF_4 < NO_3 < F < Cl < NCS, whilst the enantioselectivity is unaffected by changes in the counterion. X-ray analysis of complex **23h** confirmed that it was a mononuclear species. However, in this case, the NCS counterion was coordinated to the vanadium ion. Under the same conditions reported for complex **23a**, complex **23h** transfomed a series of aldehydes into their cyanohydrin silyl ethers in less than 2 hours giving the same high enantiomeric excesses as those obtained by complex **23a**.[44] The mechanism of asymmetric cyanohydrin synthesis catalysed by complexes **23** has been thoroughly investigated (See *section 1.5.2*). As will be explained, complex **23** is a precatalyst and in some instances, more than one $[VO(salen)]^+$ unit can be involved in the rate determining step of the catalytic cycle. Hence, this is another example of cooperative catalysis.

Complex **20** which had been found to exist as a dinuclear species in the solid state, was found to coexist in equilibrium with its monomer **24** when dissolved in chlorinated solvents (**Scheme 1.5**).[38] Taking advantage of this dynamic equilibrium, and also the monometallic nature of complex **23a** allowed the development of heterobimetallic catalyst **25**, which combined the high catalytic activity of titanium complex **20** and the high level of enantioselectivity of vanadium complex **23a**.[45] Thus, a series of mixtures of different ratios of complexes **20** and **23a** with opposite absolute configuration were prepared and tested as catalysts for the asymmetric addition of TMSCN to benzaldehyde in dichloromethane at room temperature (**Scheme 1.6**).

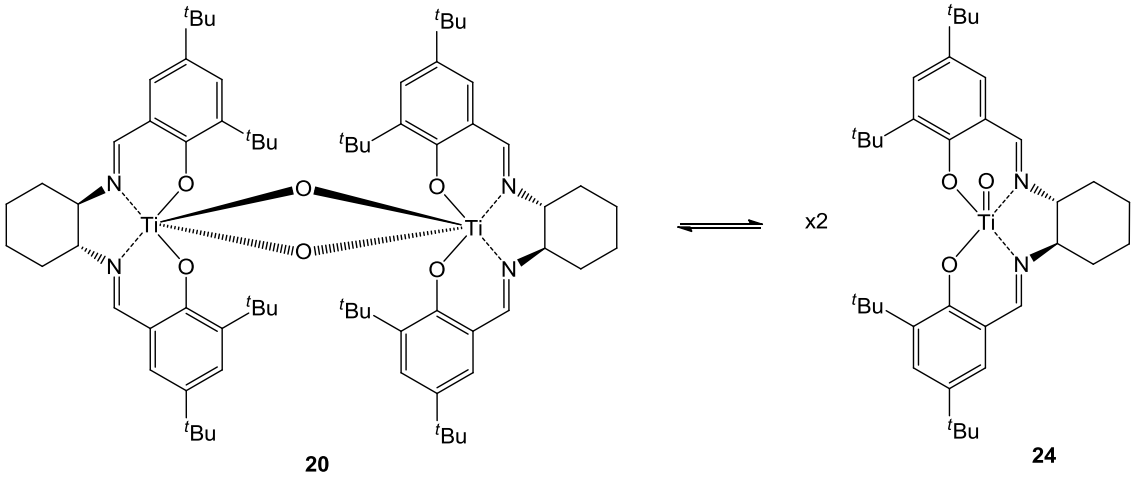

20 **24**

Scheme 1.5 Dynamic dimer-monomer equilibrium in chlorinated solvents.

The best result was obtained when a mixture of complexes (*R,R*)-**20** and (*S,S*)-**23a** in a 1:2 molar ratio was used for the catalysis. This gave (*R*)-mandelonitrile O-trimethylsilyl ether in 95% yield and with 89% ee after 30 minutes. Surprisingly, the absolute configuration of the product, was the opposite to that of the vanadium(salen) moiety. In addition, when the enantioselectivity was monitored versus time, (using 1:1 to 1:4 mixtures of Ti/V complexes), during the early stages of the reaction, the cyanohydrins obtained had the opposite configuration to that of titanium-based catalyst **20**, while towards the end of the reaction, the stereochemistry of the product was determined by the vanadium-based catalyst. This can be explained if during the early stages of the reaction, the enantioselectivity results from simultaneous catalysis by complexes **20** and **23a** when these are still present as individual catalysts. However, as the mixed complex is formed the vanadium fragment predominantly activates the aldehyde whilst the titanium moiety activates the cyanide. As a result, the enantiomeric excess of the product is determined by the stereochemistry of the salen ligand attached to vanadium.

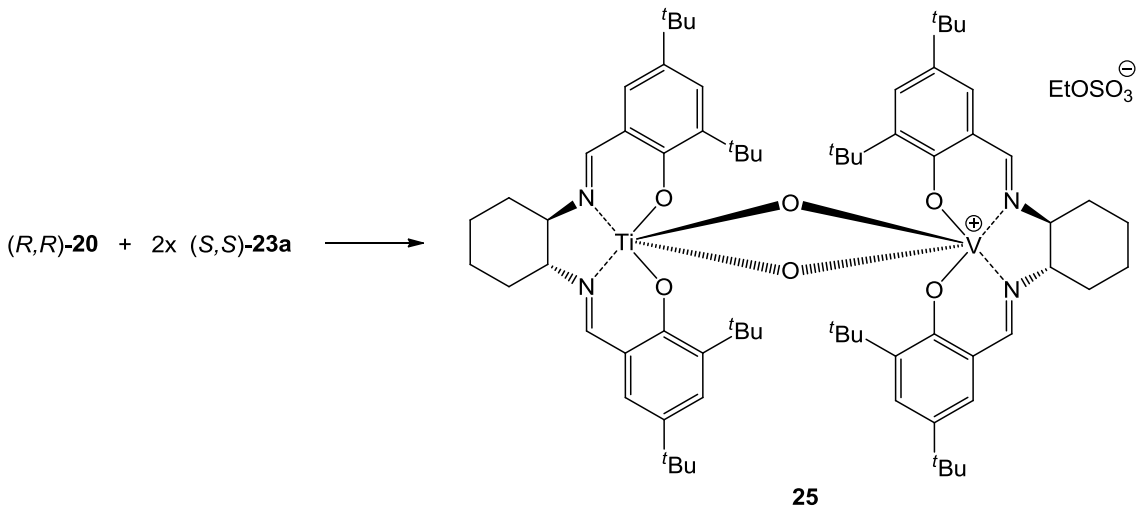

25

Scheme 1.6 Formation of Ti-V heterometallic complex **25**.

In the example discussed above, the authors took advantage of the dimer-monomer equilibrium (**Scheme 1.5**), as it enabled the formation of heterobimetallic complexes. However, the existence of this equilibrium is a drawback for the catalytic activity of bimetallic titanium(salen) complex **20**, as the dissociated form is catalytically inactive. Therefore, Ding *et al*. designed a series of bis(salen) ligands **26a-f** covalently linked by a spacer. Once the titanium complex was formed by treatment with $Ti(O^iPr)_4$ and subsequently with water, this was expected to fix the complex into its dimeric form. Ligand **26a** with a linear rigid spacer did not allow the two fragments to fold over one another resulting in very poor catalytic activity (27% yield after 72 hours) and

enantioselectivity (51%) during the cyanosilylation of benzaldehyde. This result provides support for the existence of a bimetallic transition state. Linkers **26b,c** were found to be too flexible and amongst **26d-f**, the titanium complex formed from ligand **26e** displayed superior catalytic activity and enantioselectivity to that of complex **20.** A catalyst loading of 0.05 mol% sufficed to convert benzaldehyde quantitatively into its O-protected cyanohydrin with 96% ee after 5 minutes at room temperature. The catalyst loading could be reduced still further to 0.02-0.005 mol% and the reaction scope was extended to the use of other aromatic and aliphatic aldehydes, which after optimizing the reaction conditions all gave products with enantiomeric purities higher than 90%.[46]

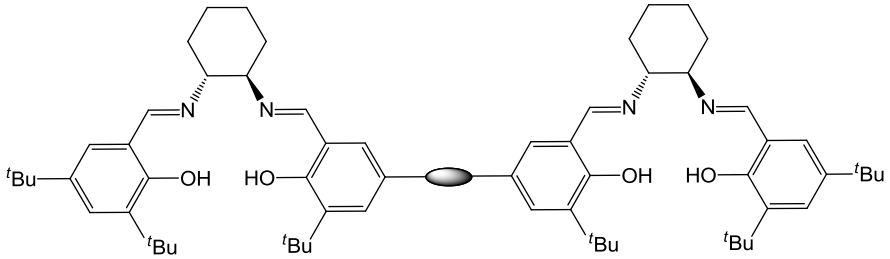

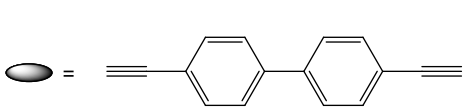

26a

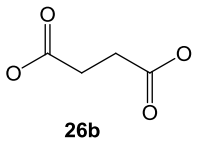

26b

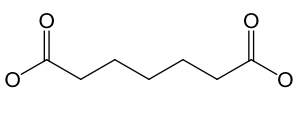

26c

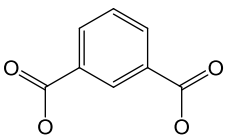

26d

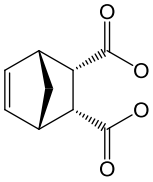

26e

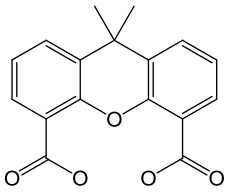

26f

Salen complexes of manganese(II) and aluminium(III) have also been used as catalysts for asymmetric cyanohydrin synthesis;[44b, 47] however, none managed to achieve comparable catalytic activity and selectivity to those obtained with titanium and vanadium complexes. However, with the addition of a Lewis base to activate the cyanide, these complexes can become good catalytic systems for the asymmetric addition of TMSCN to ketones as will be discussed in *section 1.4.3.2.*

1.4.1.3 BINOL and BINAM Ligands

BINOL-based metal complexes have proven to be very successful catalysts for the asymmetric cyanosilylation of aldehydes. The first complex of this type dates from 1986, and was reported by Reetz *et al*.[48] They demonstrated that 20 mol% of complex **27a** formed *in situ* from BINOL and $TiCl_4$ could induce some chirality to the reaction

between TMSCN and isobutanal in toluene at -78 °C, affording the corresponding cyanohydrin silyl ether in 85% yield and with 82% ee after 10 hours.

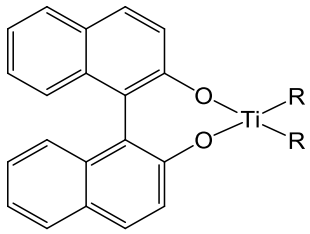

27a R = Cl
27b R = O^{i}Pr
27c R = CN

A similar system was developed a decade later by the Nakai's group. They used a different titanium source (Ti(O^{i}Pr)$_4$) which was mixed with (*R*)-BINOL to form the precatalyst **27b**. The best results were obtained for aliphatic aldehydes when the cyanosilylation was carried out in the presence of 20 mol% catalyst in dichloromethane at 0 °C. Under these conditions (*S*)-cyanohydrins were obtained in yields over 90% and with enantioselectivities up to 75%. The authors suggested that the active catalyst was dicyano complex **27c** which was only formed at temperatures above -30°C, since the reaction did not occur catalytically at lower temperatures.[49]

Using lanthanum as the metal ion source, Qian and co-workers developed a set of (*S*)-BINOL-based catalytically active complexes prepared by treatment of ligands **28a-d** with La(O^{t}Bu)$_4$. They found that the nature of the substituents at the 3,3'-position of the BINOL ligand was critical to the catalytic activity and enantioselectivity of the complex. Thus, the best result was obtained using the catalyst obtained from ligand **28d** (10 mol%) for the trimethylsilylcyanation of *p*-methylbenzaldehyde in dichloromethane at -78 °C for 10 hours (80% yield, 73% ee).[50]

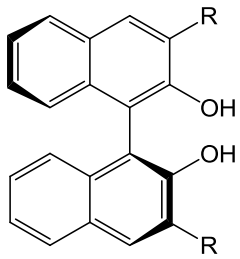

28a R = H
28b R = $SiMe_3$
28c R = Ph
28d R = $CH_2CH_2OCH_3$

Pu and co-workers synthesised BINOL-derivative **29** from the condensation of binaphthyl aldehyde and cyclohexanediamine. Ligand **29** (10 mol%) combined with an equimolar amount of Ti(O^{i}Pr)$_4$ was found to catalyse the asymmetric synthesis of cyanohydrin silyl ethers with good enantioselectivities at room temperature in dichloromethane (78% yield, 85% ee for benzaldehyde after 4 hours). The absolute

configuration of the cyanohydrin product was determined to be the same as that of the diamine moiety.[51]

Using the same synthetic strategy, *Belokon*'s group designed the C_2-symmetric chiral Schiff base **30** aiming to develop a binuclear titanium catalyst for the asymmetric addition of TMSCN to aldehydes which could achieve the same levels of catalyst activity and asymmetric induction as those achieved by other bimetallic systems such as complex **20**. The use of a 1:2 molar ratio of ligand **30**/ $Ti(O^iPr)_4$ was found to be ideal, indicating that the precatalyst had a binuclear nature. The best asymmetric induction was obtained for benzaldehyde (100% yield, 86% ee) when 20 mol% of the catalyst obtained from (*S*)-BINOL and (*R*)-valinol was used in dichloromethane at 6 °C for 4 hours.[52]

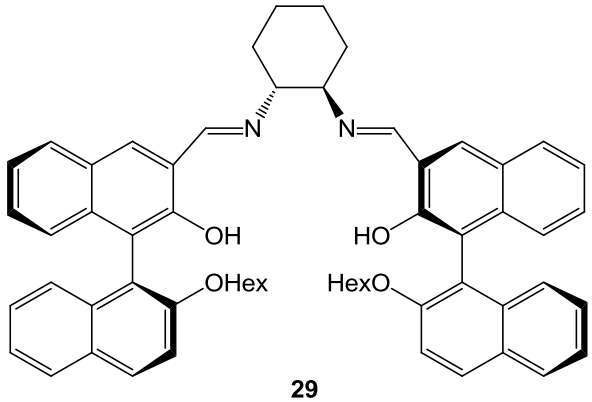

29

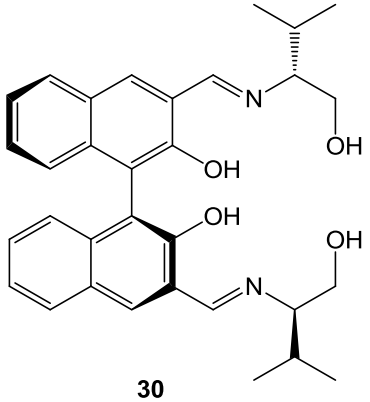

30

Building on the good results achieved with metalosalen complexes for the asymmetric synthesis of cyanohydrins, Che and co-workers developed a group of bi- tri- and tetradentate ligands **31a,b** and **32**, based on a binaphthyl unit conjugated to 3,5-disubstituted salicylaldehydes.[53] Titanium and ruthenium complexes were generated by mixing ligand **32** with $Ti(O^iPr)_4$ and $[Ru^{II}(NO)Cl_3(PPh_3)_2]$ respectively. While the titanium complex of ligand **32** proved to be very difficult to characterise, the ruthenium complex could be isolated and its structure determined by X-ray crystallography. The complex possessed a cis-β configuration of the ligand, the same structure as adopted by the salen ligand of catalyst **20** during the transition state for asymmetric cyanohydrin synthesis. When the cyanosilylation of a number of aliphatic and aromatic aldehydes was conducted under the optimized conditions (20 mol% catalyst, in dichloromethane, at -78°C, for 36-120 hours) the best performance was obtained by the titanium complex of ligand **31b**. The highest asymmetric induction was achieved with benzaldehyde as the substrate (94% chemical yield, 93% ee after 36 h). As expected, the groups in the 3,

3’ positions had a strong effect on the enantioselectiviy and the absolute configuration of the product was the opposite to that of the Schiff base.

The use of aluminium complexes of modified binol ligands which incorporates a Lewis or Brönsted base also showed some chiral induction.[54] However, this family of complexes has a greater impact as bifunctional catalysts (See section *1.4.2.3*).

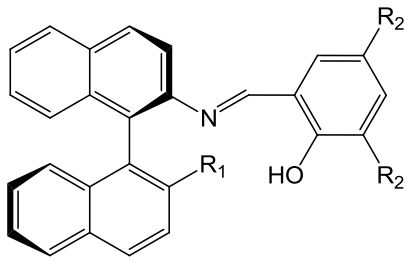

31a R_1 = OH; R_2 = Cl
31b R_1 = NH_2; R_2 = ^{t}Bu

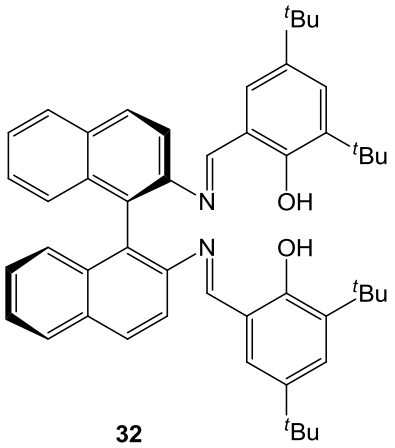

32

1.4.1.4 Amide-based ligands

A new catalytic system for the enantioselective addition of TMSCN to aldehydes based on C_2-symmetric diamide ligand **33a** was first designed by Uang’s group. A 15 mol% loading of the catalyst prepared *in situ* by treatment of ligand **33a** with Ti(O^iPr)$_4$ in dichloromethane at -78°C, converted a range of aromatic and aliphatic aldehydes into their O-silylated cyanohydrins with excellent enantioselectivities and chemical yields (>87% ee for aliphatic substrates and >94% ee for aromatic substrates).[55]

Encouraged by the results obtained with the Ti(O^iPr)$_4$-**33** catalytic system, the same authors replaced the cyclohexanediamine moiety by a diphenylethylenediamine (**33b**), which after complexation with Ti(O^iPr)$_4$ and under the same conditions reported above, was able to transform the same series of aromatic and aliphatic cyanohydrins to their O-cyanosilylated derivatives with higher enantiomeric purity. Ligands **33a** and **33b** were both recovered in 92 % yield and they could both be reused without any loss of activity.[56]

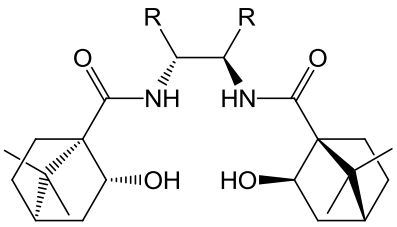

33a R = -$(CH_2)_4$-
33b R = Ph

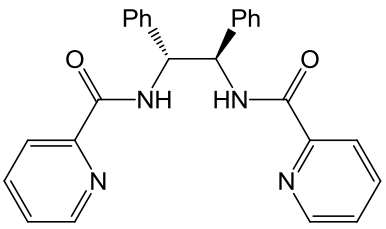

34

A variant of ligands **33a**,**b** was described by Belda and Moberg by replacing the camphor residues with pyridine groups (**34**). The best asymmetric induction was achieved when 1 mol% of the derived titanium catalyst was used in the cyanosilylation of benzaldehyde in dichloromethane at room temperature (70% ee). The use of a larger catalyst loading and lower temperature did not lead to any improvement in the enantioselectivity.[57]

Another system based on C_2-symmetric diamide ligands was elaborated by Feng and co-workers. They investigated the catalytic properties of a number of tetraaza ligands derived from L-proline and other cyclic amine carboxylic acid derivatives. Among them, the complex formed by the *in situ* addition of Ti(^{i}PrO)$_4$ to ligand **35** catalysed the formation of O-trimethylsilyl cyanohydrins giving the highest degree of selectivity when benzaldehyde was the substrate (93% yield, 84% ee). The process was conducted with 15 mol% of Ti(O^{i}Pr)$_4$/**35** as catalyst in a 1:2 molar ratio, at 0 °C in dichloromethane for 17 hours. Using these optimal conditions, a range of aromatic and aliphatic aldehydes were converted into their respective O-trimethylsilyl cyanohydrins in good chemical yields and with moderate to good enantioselectivities. The absolute configuration of the cyanohydrin is determined by the configuration of the chiral diamine moiety, thus, ligand **35**, derived from (*R*,*R*)-1,2-diphenylethylenediamine produces cyanohydrins with (*S*)-configuration.[58]

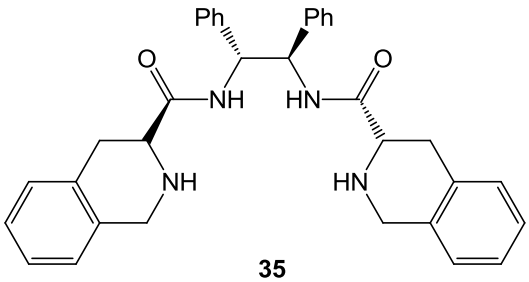

35

1.4.1.5 PyBOX ligand

The catalytic system formed by the tridentate Pybox ligand **36** and $AlCl_3$ was first investigated by Iovel's group for the catalytic asymmetric addition of TMSCN to aldehydes. In the presence of 20 mol% of catalyst, mandelonitrile was produced in 92% isolated yield and with 90% enantiomeric excess after 4 hours in dichloromethane at 0 °C. Identical conditions were used for the cyanosilylation of heterocyclic aldehydes which gave the corresponding cyanohydrins with good enantiomeric purity (85-96%).

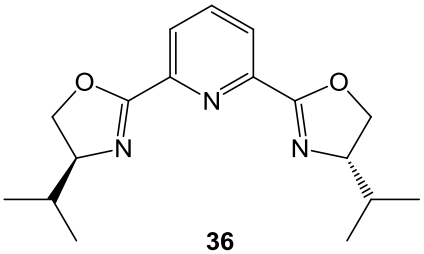

36

Aspinall, Greeves and collaborators explored the use of other metals. Thus, Pybox ligand **36** could also be coordinated to lanthanides, of which ytterbium gave the best result. Conducting the reaction with 1 mol% of the catalyst using a 2:1 molar ratio of **36** to $YbCl_3$, a series of aliphatic and aromatic aldehydes were converted to their respective cyanohydrin silyl ethers in 60-98% isolated yield and with 45-89% ee after 1-16 hours. The optimal conditions were found to be in acetonitrile at room temperature.

1.4.1.6 Peptide ligands

A unique example of this type is the aluminium catalyst of oligopeptide **37** disclosed by Snapper and his team in 2002.[59] This was, and still is, one of the best catalytic systems for the asymmetric cyanosilylation of ketones. The authors established the best conditions to be toluene as solvent, in the presence of 20 mol% of **37**-Al(^{i}PrO)$_3$, 20 mol% of MeOH and 3 Å MS, at -78 °C for 48 hours. The asymmetric induction was not particularly affected by the electronic nature of the aryl substituted ketones, giving the cyanohydrins with 85-94% ee and in 67-98% yields. Interestingly, when sterically hindered ethyl and cyclic ketones were tested, there was no substantial decrease in the catalytic efficiency or enantioselectivity of the reaction. Acyclic aliphatic ketones were also found to be excellent substrates for this system, affording enantioselectivities of 80-95% with isolated yields >65%. In addition, this was the first system to catalyse the asymmetric synthesis of alkynyl cyanohydrin derivatives. Although a large amount of catalyst is required, this could be recovered and reused without any loss of activity.

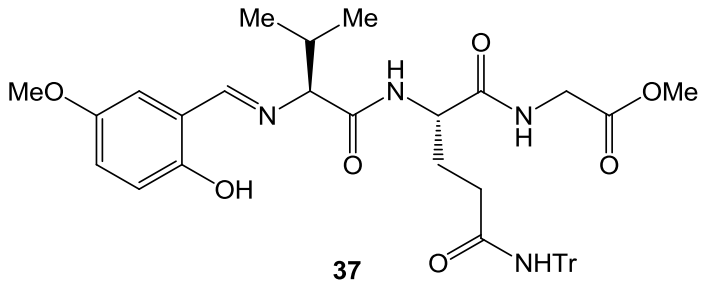

37

In summary, this section has explored several catalytic systems that are believed to behave as pure Lewis acids, thus activating primarily the carbonyl reagent. Interestingly, binuclear systems can assist the addition of cyanide to aldehydes in a more efficient manner, through a co-operative intramolecular pathway, where a second metal can also activate the cyanide reagent. Amongst these, titanium^{IV}salen dimer **20** and oxovanadium^{V}salen **23** have given the best results. In order to understand why these catalysts are so effective for the asymmetric addition of TMSCN to aldehydes, kinetic and spectroscopic studies were conducted and will be described in detail in *section 1.5*. Despite the large number of highly effective catalysts for the enantioselective cyanosilylation of aldehydes, there are fewer examples capable of promoting the asymmetric addition of TMSCN to ketones (only those of Belokon and North, and Snapper). As we will see in the next section, simple activation of the carbonyl is not effective enough to achieve this and hence, a different strategy is required.

1.4.2 Dual Lewis acid and Lewis base catalysis. Bifunctional catalysts.

This section will deal with bifunctional metal-based complexes bearing a Lewis base moiety in their structure. This type of complex makes it possible to have co-operative transition states where both the aldehyde and cyanide are simultaneously activated and allowed to react intramolecularly, thus achieving a lower energy transition state. Moreover, this also facilitated the development of a number of catalysts capable of performing the enantioselective silylcyanation of ketones. Ketones are much less reactive than aldehydes; therefore, only by fixing the carbonyl reagent in a chiral enviroment (*via* Lewis acid coordination) and activating the cyanide by a Lewis base can the facile synthesis of chiral tertiary cyanohydrins be achieved.

1.4.2.1 O-Hydroxyaryl diazaphospholidine oxides.

In 1999, Buono and co-workers reported ligand **38**, which was the first example of this type, with a phosphoryl group acting as a Lewis base. The *in situ* complexation of 40 mol% of ligand **38** to 10 mol% of Ti(O^iPr)$_4$ in dichloromethane at 20 °C produced a catalyst which had the ability to catalyse the asymmetric cyanosilylation of

benzaldehyde in high yield, but which exhibited only 31% enantioselectivitiy. Interestingly though, the addition of two equivalents of isopropanol per titanium significantly improved the asymmetric induction, giving mandelonitrile with 94% enantiomeric excess. Unfortunately, the degree of selectivity was rather poor when other aromatic aldehydes were used as substrates.[60]

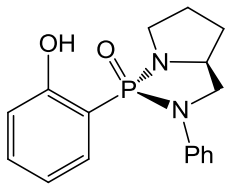

38

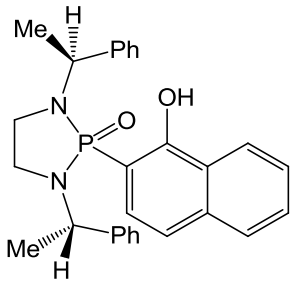

39

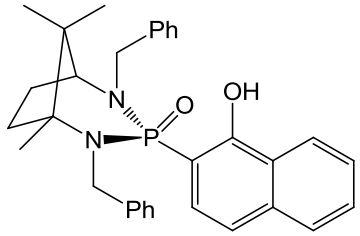

40

Zhou, Tang and co-workers designed a modified version of ligand **38**, which turned out to be a more efficient catalyst than that of Buono, without the need to use additives. Thus, when a 1:4 molar ratio of $Ti(O^iPr)_4$ and ligand **39** was used at the optimal temperature of 0 °C in dichloromethane, a range of *ortho*, *meta* and *para* substituted aromatic aldehydes was converted into their corresponding cyanohydrins in excellent yields but with highly variable enantioselectivities (8-90% ee). The chiral ligand could be recovered in quantitative yield, and reused to afford the same catalytic activity and selectivity.[61]

The same authors further optimised the catalyst structure to ligand **40** in which the ethylenediamine fragment of ligand **39** was replaced by a camphor derivative. This structural change considerably improved the enantioselectivity of asymmetric cyanohydrin synthesis. Under the same optimised conditions reported for the **39**/$Ti(O^iPr)_4$ system, the best results were obtained for substituted aromatic aldehydes bearing electron donating groups (54-98% ee); although, the position of the substituent also affected the enantioselectivity of the reaction, whereas aromatic aldehydes bearing electron withdrawing substituents only gave moderate enantioselectivities (33-53% ee).[62]

1.4.2.2 N-oxides

Feng and co-workers have focused on the synthesis of titanium complexes of chiral N-oxides and their use as bifunctional catalysts for the asymmetric addition of TMSCN to aldehydes and ketones. In view of the known ability of N-oxide groups to activate TMSCN,[63] the first efforts were devoted to the synthesis of an optimal chiral

ligand containing an N-oxide. The authors developed bidentate ligand **41** which contains two chiral stereocentres. The best catalytic activity was obtained when 20 mol% of (1*R*,2*S*)-**41** combined with one equivalent of Ti(O^iPr)$_4$ was used for the cyanosilylation of acetophenone, producing the (*R*)-cyanohydrin in 48% chemical yield and with 51% ee. The reaction was conducted in dichloromethane at 0 °C for 30 hours. Other ketones were used as substrates, however, they gave products with only low ee's. Interestingly, ligand **42** which lacks the N-oxide group, formed a catalytically inactive complex **42**-Ti(O^iPr)$_4$. This suggests that simple coordination of the ketone to the metal centre was not sufficient to promote product formation. The authors also investigated the catalytic activity of the ligand itself as a potential Lewis base catalyst, however, no reactivity was observed after 70 hours, when 20 mol% of ligand **41** was used in the absence of Ti(O^iPr)$_4$.[64]

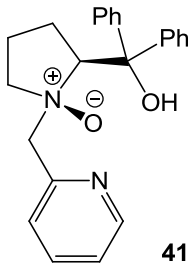

41

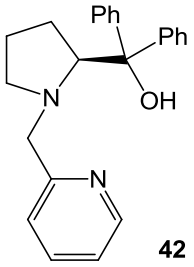

42

Some achiral N-oxides have been reported to catalyse the addition of TMSCN to aldehydes without the action of a metal ion.[63c, 65] Therefore, in 2005, Feng's group designed a chiral proline-based C_2-symmetric N,N-dioxide (**43**) capable of generating O-trimethylsilyl cyanohydrin ethers derived from aromatic, heteroaromatic and aliphatic aldehydes in almost quantitative yields with 53-73% enantiomeric purities. The optimised conditions were found to be 5 mol% of catalyst in dichloromethane at -78 °C for 80 hours.[66]

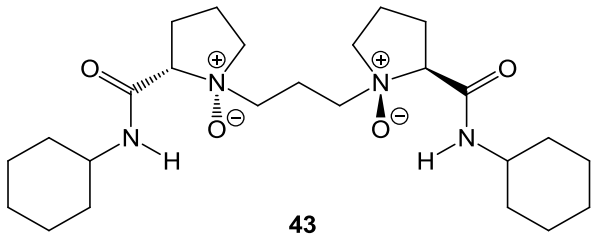

43

Inspired by catalyst **43**, the authors prepared the analogue **44** which also bears two N-oxides. The complex prepared by treatment of ligand **44** with Ti(O^iPr)$_4$ (in a 2:1 molar ratio) was used to induce the asymmetric addition of TMSCN to benzaldehyde. Under the optimised conditions (5 mol% catalyst loading in dichloromethane, -78°C, for

52 hours) (*R*)-mandelonitrile was produced in 83% yield and with 65% ee. This could be improved by the addition of 4-methylbenzoic acid (20 mol%) to the reaction, which gave rise to trimethylsilyl cyanohydrin ether formation with enantiomeric excesses up to 80%. Consistent with the previous results obtained with ligand **41**, no product was obtained when ligand **44** was used alone, or when the two N-oxides were replaced by amino groups. The authors suggest that in the transition state two units of ligand **44** are coordinated to the titanium through the pyrrolidine N-oxide and the nitrogen atom of the amide. Aldehyde and TMSCN are activated simultaneously by the metal ion, and the N-oxide of the pyridine respectively. Cyanide attack then occurs intramolecularly to the *si*-face of the aldehyde, since the *re*-face is largely hindered by the two phenyl groups, thus resulting in the formation of the product with *R*-configuration (**Figure 1.5**).[67]

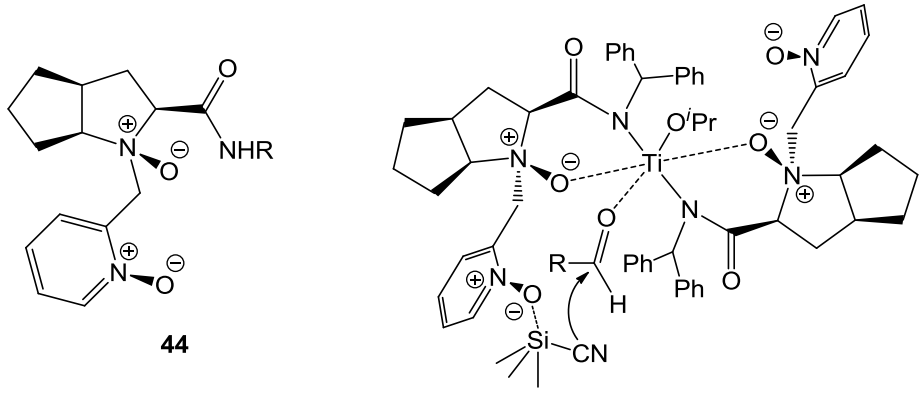

Figure 1.5 Transition state for the asymmetric addition of TMSCN to aldehydes catalysed by complex **44**-Ti(O^{i}Pr)$_4$.

1.4.2.3 Schiff bases, and salen ligands

Not many examples of Schiff base metallocomplexes incorporating both a Lewis acidic and Lewis basic site have been reported in the literature, generally due to their problematic synthesis.

Pericàs's previous experience on the asymmetric synthesis of β-amino alcohols,[68] allowed the preparation of a family of chiral amino alcohols *via* a regioselective and stereospecific ring opening of optically active epoxyalcohols with an azide, followed by reduction with $LiAlH_4$. These amino alcohols were then reacted with salicylaldehyde to obtain Schiff bases (**Scheme 1.7**). Among them, the complex formed by ligand **45** and Ti(O^{i}Pr)$_4$ was found to display the best reactivity and asymmetric induction for the reaction of TMSCN with a series of aromatic and aliphatic aldehydes

(87-100% conversions, up to 77% ee). The results were obtained using 20 mol% catalyst loading, in dichloromethane at -40 °C for 4 days.[69]

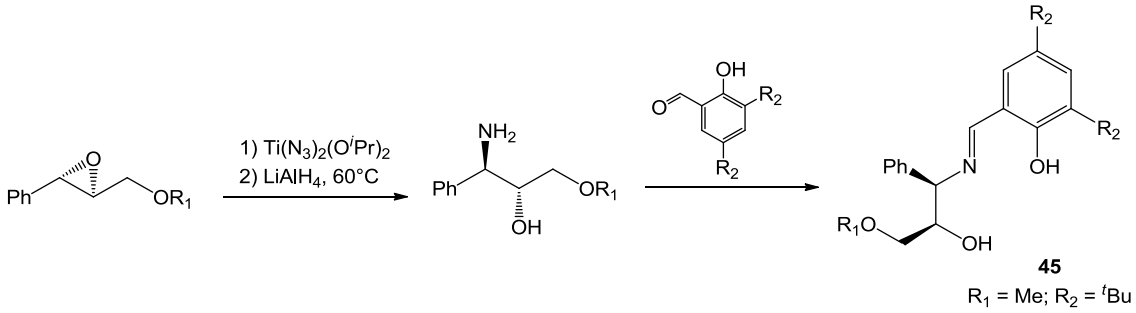

Scheme 1.7 Synthesis of chiral β-amino alcohols and their corresponding Schiff bases.

The good performance of this catalytic system was associated with the activation of both reagents. Thus, in the transition state proposed by the authors, the methoxy group assists cyanide delivery to the *si*-face of the aldehyde, which is activated by the titanium ion (**Figure** 1.**6**).

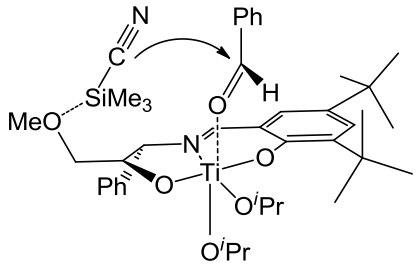

Figure 1.6 Dual activation of TMSCN and benzaldehyde in the transition state using the titanium complex of ligand **45.**

Very recently, Lu and co-workers explored the effect of incorporating a Lewis basic group as part of the salen ligand structure on the catalytic activity for the cyanosilylation of aldehydes.[70] A range of unsymmetrical racemic salen ligands bearing a Lewis basic group at the 3-position of one of the aromatic rings were prepared and tested as catalysts for the preparation of racemic cyanohydrins. Ligand **46** with a diethylamino group, together with $Ti(O^iPr)_4$, exhibited the highest reactivity. Only 0.05 mol% of catalyst was sufficient to transform benzaldehyde quantitatively into mandelonitrile in less than 10 minutes at ambient temperature using dichloromethane as the solvent. Notably, when the complex formed from Jacobsen's salen ligand **18e** and $Ti(O^iPr)_4$ was used to catalyse the reaction in the presence of Et_3N, only 20% conversion was observed under the same conditions after 1.5 hours. This result indicates that a cooperative mechanism is taking place, which enables the simultaneous activation

of the two substrates. Encouraged by this result, the asymmetric addition of TMSCN was attempted using a non-racemic version of complex **46**-Ti(O^iPr)$_4$. Although excellent yields were obtained, only a small group of aromatic aldehydes gave reasonable enantiomeric excesses (81-88 %ee).

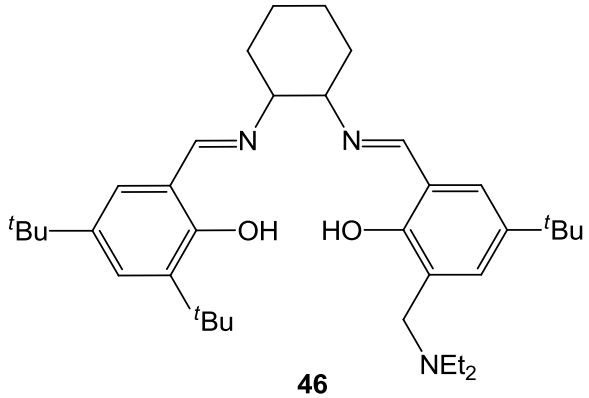

46

1.4.2.4 BINOL and BINOLAM ligands.

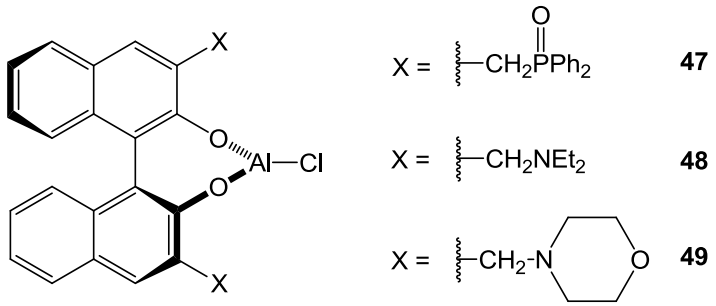

In 1999, with the aim of integrating a Lewis acid and a Lewis base into the same structural motif, Shibasaki described a novel catalytic system based on BINOL with pendant groups in the 3- and 3'-positions.[54a] He found that complex **47** (9 mol%), formed by treatment of the binaphthol ligand with Et_2AlCl, was able to catalyse the asymmetric cyanosilylation of benzaldehyde in 91% yield and with 87% asymmetric induction with absolute configuration opposite to that of the complex. This result was obtained at -40 °C with dichloromethane as solvent after 37 hours reaction. Interestingly, under the same conditions, in the presence of a phosphine oxide (36 mol%) an increase in the rate of reaction as well as in the enantioselectivity (98% yield, 96% ee for benzaldehyde) was observed. Kinetic studies revealed that this additive is not involved in the activation of cyanide. Instead, it coordinates to the aluminium ion changing the catalyst geometry from tetrahedral to trigonal bipyramidal (**Figure 1.7**).[54a, 54b, 71] This structural change brings the two activated reagents closer to one another, facilitating an intramolecular reaction. Thus, in the transition state, when (*R*)-**47** is used as catalyst, the delivery of cyanide (activated by the internal phosphine

oxide) occurs predominantly on the *re*-face of the aldehyde when this is coordinated to the aluminium *trans* to the phosphine oxide unit, resulting in the observed asymmetric induction. Complex **47** was shown to catalyse asymmetric cyanohydrin synthesis from a wide variety of aldehydes, producing the O-trimethylsilyl protected products with exceptional levels of enantioselectivity (almost quantitative yields, 83-99% ee).

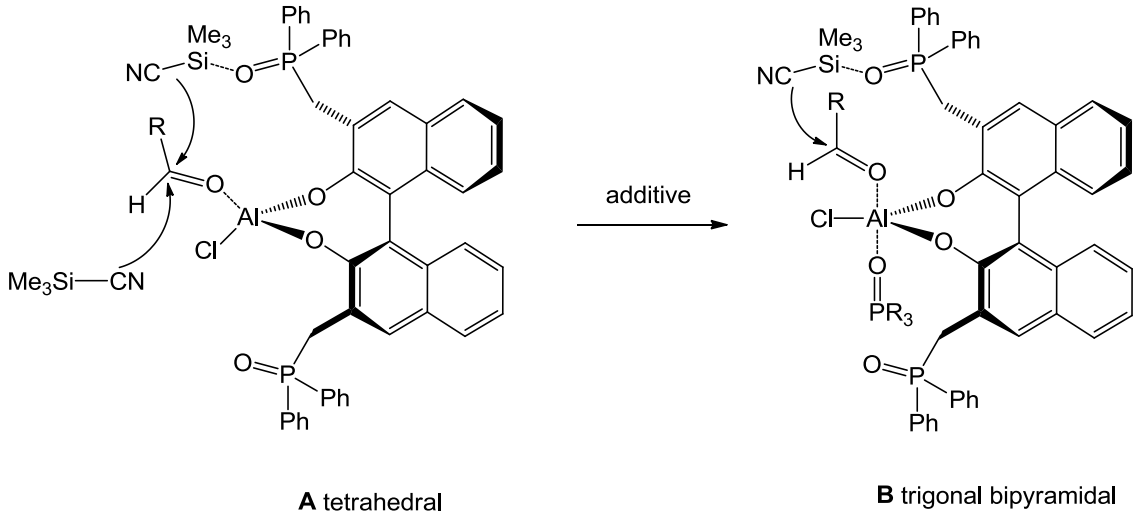

Figure 1.7 The action of the additive in the catalytic transition state of TMSCN addition to aldehydes catalysed by complex **47.**

Following this work, Nájera, Sáa *et al*. developed a similar symmetrical complex (**48**), which had the ability to catalyse the enantioselective addition of TMSCN to aldehydes. A catalyst loading of 10 mol% with respect to the aldehyde, at -20 °C, in the presence of 40 mol% of triphenylphosphine oxide and 4 Å MS in toluene were found to be the best conditions. In this way, enantiomerically enriched cyanohydrins (66-98% ee) were obtained from a broad range of aromatic, heteroaromatic, aliphatic and α,β-unsaturated aldehydes after 6-12 hours, the best results being obtained with aromatic aldehydes. The BINOL ligand could be recovered in >95% yield and reused without any loss of activity.[54c]

The phosphine oxide additive was again involved in a structural change of the catalyst, forcing the complex to adopt a trigonal bipyramidal geometry. This allowed the diethylaminomethyl arms to act as a Brönsted base, activating the HCN, which was found to be the real cyanating agent, generated by the reaction of TMSCN with traces of water stored in the 4 Å MS. At the same time, the aldehyde, interacting with the Lewis acidic Al-Cl moiety, sits on a plane parallel to the equatorial plane of the complex formed by the BINOL oxygens and chloride aluminium bonds, thus allowing the

nucleophilic attack to occur to the *si*-face of the aldehyde when the (*S*)-BINOL complex **48** was used as the catalyst, giving rise to the (*R*)-enantiomer of the cyanohydrin as shown in **Figure 1.8**.[54d]

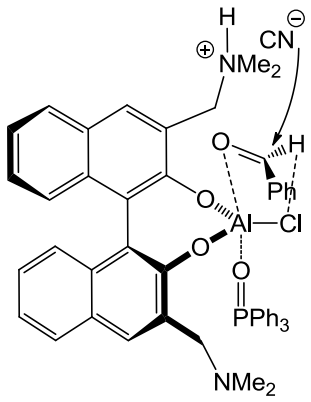

Figure 1.8 Transition state of the dual activation and intramolecular reaction using complex **48**.

Based on the good results for asymmetric cyanohydrin synthesis using 3,3'-disubstituted BINOL-AlCl type complexes, Pu and co-workers slightly modified Najera's ligand structure changing the diethylamine groups to morpholine. Using the best conditions obtained by Najera (10% catalyst, 40% additive, in the presence of 4Å MS at -20°C in toluene), complex **49** proved to be a more effective catalyst, particularly for aliphatic aldehydes. The reaction conditions could be further optimized by changing the Ph_3PO additive to HMPA which accelerated the reaction whilst leaving the enantioselectivity unaffected. In addition, when diethyl ether was use as solvent, an increase in the enantioselectivity was observed. Thus, after 24 hours octanal was totally converted into its O-TMS cyanohydrin which was produced with a 97% enantiomeric purity. Using these optimised conditions, other aliphatic aldehydes were also found to give excellent chemical yields (70-92%) and enantioselectivities (92-99% ee).

Recently, Lu *et al.* described the monosubstituted BINOL-Ti complex **50**, which was designed to act as a bifuntional catalyst.[54f] The authors noticed that the imidazole group was the most common basic site used by enzymes to activate a nucleophile, and for that reason, they decided to incorporate it into the BINOL-structure. When ligand **50** was combined with $Ti(O^iPr)_4$, in a 1:1 ratio, the asymmetric addition of TMSCN to benzaldehyde went smoothly to form mandelonitrile silyl ether in 97% yield and with 98% enantiomeric excess without the need for additives. Dichloromethane and -40 °C were found to be the optimal conditions. Interestingly, the authors observed that the use of a linker between the imidazole and the binol group induced an internal coordination

and hence a loss in the catalytic activity and selectivity. Moreover, the use of extremely dry TMSCN also diminished the yield and enantioselectivity. According to this observation, the authors suggested that the small amount of HCN in commercial TMSCN was sufficient to initiate the first catalytic cycle and hence that the imidazole was acting as a Brönsted base. The same protocol could be applied to a larger group of aromatic and aliphatic aldehydes, all of which gave excellent yields (91-99%) of cyanohydrins with enantiomeric excesses of 95-98%.

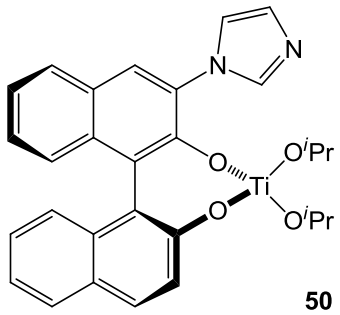

50

1.4.2.5 Proline derived ligands.

Building on the successful application of the **35**/Ti(O^{i}Pr)$_4$ catalytic system for the asymmetric silylcyanation of aldehydes (*section 1.4.1.4*), Feng decided to expand the scope of his C_2-symmetrical amide ligands to the asymmetric cyanosilylation of ketones. Taking acetophenone as the model substrate, the best results were afforded by the catalyst formed by combining equimolar amounts of ligand **51** and Ti(O^{i}Pr)$_4$. The optimal enantioselectivity (92% ee) and catalytic activity (70% isolated yield, after 100 h) were obtained when the reaction was carried out at -45 °C in dichloromethane, in the presence of 30 mol% of the catalyst and 2.5 equivalents of TMSCN. Comparable results were obtained for monosubstituted-aromatic ketones, promoting the formation of their corresponding optically active quaternary cyanohydrins in 48-90% yield and with 61-94% ee. However, aliphatic ketones gave inferior results in terms of enantioselectivity (84-89% yield and 51% ee).[72]

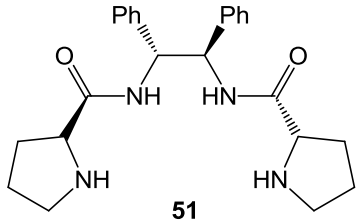

51

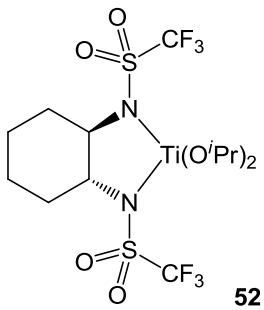

52

Initially, it was unclear whether compound **51** was binding to the metal centre as a bidentate, or tetradentate ligand, the latter having been suggested for compound **35**. Due to the structural similarity to the titanium-*N*,*N*-[(1*R*,2*R*)-cyclohexane-1,2-diyl]bis(trifluoromethyanesulfonamide) complex **52**,[73] the authors suggested that in the case of ligand **51**, only the two amide nitrogen atoms were coordinated to the titanium ion, together with two isopropoxyl groups (**Figure 1.9**). Therefore, the catalysis is accomplished by dual activation of the TMSCN by the free pyrrolidinyl groups, and the ketone by the metal centre. The nucleophilic addition of cyanide is then directed to the less sterically hindered face of the ketone giving rise to the product enantiomer with absolute configuration opposite to that of the ligand.

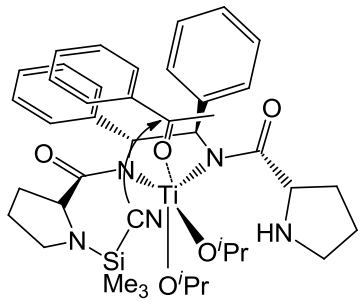

Figure 1.9 Possible dual-activation model of the transition state for the addition of TMSCN to acetophenone using **51**/Ti(O^iPr)$_4$ as catalyst.

Trost *et al.* independently developed another bifunctional proline derived catalyst formed from the reaction of ligand **53** with $AlMe_3$. This complex proved to be a good catalyst for the asymmetric cyanosilylation of aldehydes, producing a collection of chiral trimethylsilylcyanohydrin ethers in high yield and with 57-86% enantiomeric excess using 11 mol% of catalyst, in chlorobenzene, at 4 °C. There is spectroscopic evidence that suggests that the active catalyst has a non-symmetrical structure. Thus, the authors proposed that one of the proline amino alcohols might coordinate to the aluminium ion (as shown in structure **54**), whereas the other functions as a Brönsted base, donating a proton and hence generating hydrogen cyanide.[74]

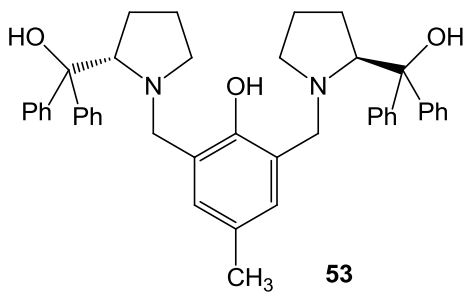

53

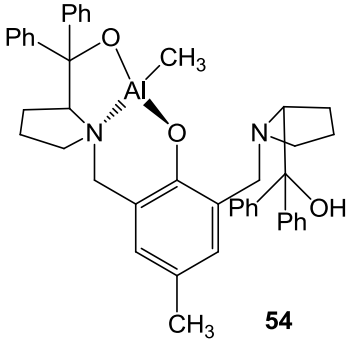

54

Kim's group reported a similar chiral ligand to that of Trost. Using the same strategy as Shibasaki and his bifunctional Al-BINOL catalyst, they incorporated phosphine oxide groups on both pyrrolidine rings. The complex formed by the treatment of $Ti(O^iPr)_4$ with ligand **55** afforded the best chemical yield and enantioselectivity amongst other titanium, aluminium and magnesium complexes. In agreement with Shibasaki's system, the addition of two equivalents of triphenylphosphine oxide with respect to the catalyst, had a positive effect on the reactivity and enantioselectivity of the process, presumably by inducing a conformational change on the structure of the catalyst during the transition state; but it was the internal phosphine oxide groups which play the role of cyanide activators. This system was used with a wide range of aldehydes, from which the corresponding O-trimethylsilyl cyanohydrin ethers were obtained in moderate to good yields and with enantioselectivities of up to 95% ee of the (*R*)-enantiomer. The reactions were catalysed by 10 mol% of **55**-$Ti(O^iPr)_4$ in combination with 20 mol% of Ph_3PO in dichloromethane for 24 hours at -20 °C.[75]

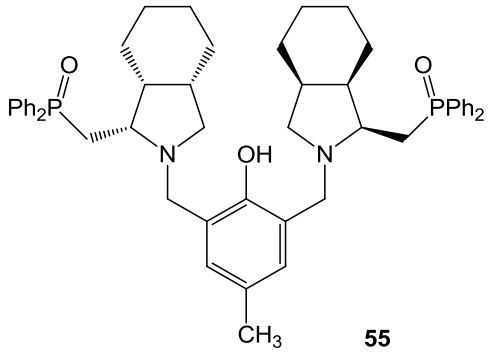

55

1.4.2.6 Sugar-derived ligands

In 2000, *Shibasaki* and his team developed, a chiral carbohydrate-derived aluminium complex (**58**) as a potential bifuntional catalyst for the enantioselective addition of TMSCN to aldehydes. Complex **58** was initially prepared by the *in situ* reaction of Me_2AlCl with the corresponding glycal **56**. Under optimised conditions (5-9 mol% of catalyst, dichloromethane, -60 °C) O-trimethylsilyl mandelonitrile was produced with 46% enantiomeric excess. However, this could be further improved by incorporating a phenyl group at the carbon alpha to the phosphine oxide (ligand **57**), which raised the enantioselectivity to 80%. This result could be explained by a structural change, which brought the Lewis base and Lewis acid sites closer together in space, thus allowing the intramolecular nucleophilic attack to occur more smoothly (**Figure 1.10**). In addition, catalyst **59** was successfully used for the catalytic

asymmetric production of the quaternary cyanohydrin derived from acetophenone (20% ee) when the reaction was carried out at -10 °C.[76]

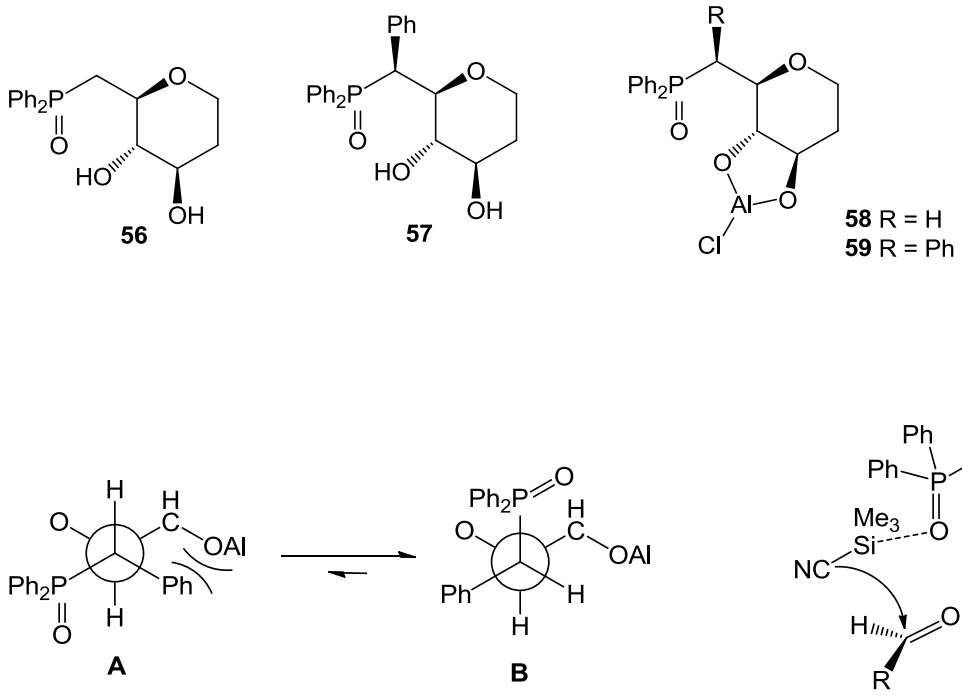

Figure 1.10 Conformational equilibrium favoured towards conformer B for complex **59**, and its transition state during the formation of cyanohydrins.

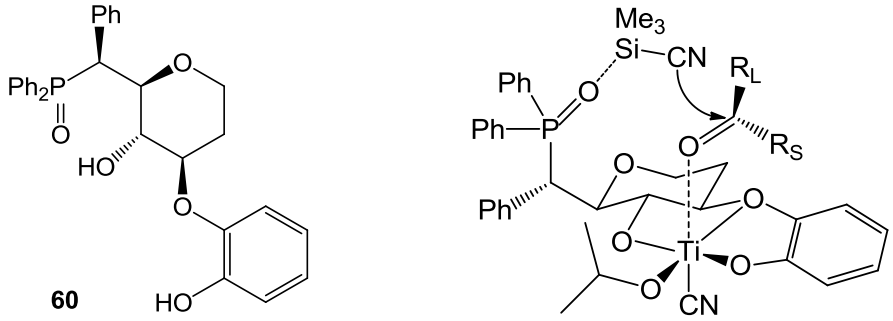

Figure 1.11 Proposed transition state for the enantioselective addition of TMSCN to prochiral ketones using the titanium complex of ligand **60.**

Further structural modifications to ligand **57,** and a change of the metal led to the formation of complex **60**-Ti(O^iPr)$_4$, a remarkably effective catalyst for the asymmetric nucleophilic addition of TMSCN to ketones. Thus, using 10 mol% of the catalyst in THF at the optimal temperature of -30 °C, a wide array of ketones of different electronic and steric properties could be transformed into their O-protected cyanohydrins with high yields (up to 92 %) and enantiomeric excesses (69-92 % in favour of the (*R*)-enantiomer). The catalyst structure was confirmed by NMR studies by

mixing equimolar amounts of catalyst and TMSCN, which resulted in the formation of titanium monocyanide species (**Figure 1.11**). Furthermore, labelling experiments using TMS^{13}CN showed that the cyanide coordinated to the metal was not incorporated into the cyanohydrins. Based on all these results, a transition state was proposed as depicted in **Figure 1.11**.[77]

In summary, amongst all the bifunctional catalysts described in this section, BINOL-derived catalysts described by Shibasaki, Nàjera, Pu and Lu are the best choice for the asymmetric cyanosilylation of aldehydes, whereas the chiral titanium complex derived from carbohydrate ligand **60** reported by Shibasaki is undoubtedly the best option for the catalytic asymmetric addition of TMSCN to ketones. Despite the high yields and enantiomeric excesses obtained, all these catalysts still suffer from a few drawbacks. All require large amounts of complex (5-40 mol%), as well as lengthy reaction times, especially for those that involve low reaction temperatures. Thus, complexes **20** and **23h** are still the best choice overall.

1.4.3 Dual Lewis acid-Lewis base catalysis. Two separate entities.

This last group of metal-based catalysts also involves a dual activation mechanism, in which aldehyde and TMSCN are activated simultaneously by a Lewis acid and a Lewis base respectively. However, unlike the previous section these two sites are found in two separate species. Thus, we will see that the metallocomplex itself can catalyse the asymmetric cyanosilylation reaction of aldehydes or ketones to an extent, but that a significant rate and enantioselectivity enhancement can be achieved by adding a chiral or achiral Lewis base to the reaction. This strategy has revolutionised the asymmetric cyanosilylation of ketones.

1.4.3.1 Magnesium and boron Corey's complexes

The first example of this type of catalyst is the bisoxazoline-magnesium complex **61** developed by Corey and his team. This system was initially tested for the addition of two equivalents of TMSCN to cyclohexane carboxaldehyde in a solvent mixture of 3:1 dichloromethane-propionitrile at -78°C. Using 20 mol% of the bisoxazoline catalyst **61** alone, the chiral cyanohydrin was produced in 85% yield and with 65% enantiomeric excess after 25 hours. Interestingly, the authors observed that, under the same optimised conditions with the addition of 12 mol% of bisoxazoline **62**, the catalytic activity and enantioselectivity increased, giving product with 95% yield and 94% ee after only 4 hours (**Scheme 1.8**). When the opposite enantiomer to **62** was

used as the co-catalyst, the enantioselectivity dropped to 38%. This represents a case of dual activation, where bisoxazoline **62** is acting as a chiral cyanide donor, which together with complex **61** to activate the aldehyde, can catalyse enantioselective cyanohydrin formation.[78]

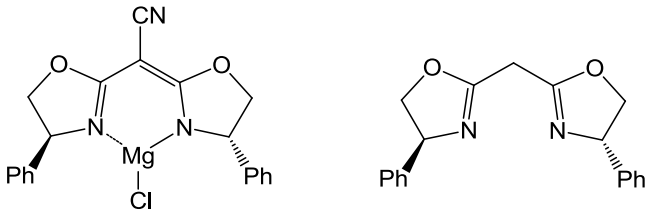

61 **62**

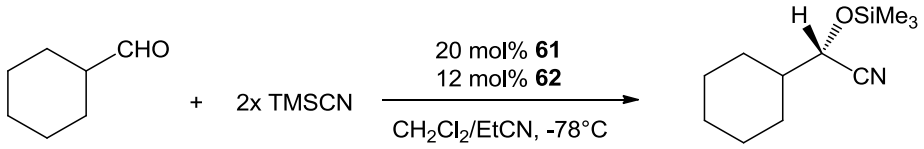

Scheme 1.8 Asymmetric addition of TMSCN to cyclohexane carboxaldehyde using catalyst **61** and co-catalyst **62**.

Another well known example of this type of dual-activation catalysis, is the oxazoborolidinium salt **63** reported by Corey in 2004. The B-O moiety acts as a Lewis acid by coordination of the carbonyl oxygen to the boron and a C-H···O hydrogen bond positions the aldehyde into the chiral environment provided by the surrounding ligands (**Figure 1.12**). The reaction takes place without the need of an additive. However, a significant improvement in the rate and enantioselectivity was observed when triphenylphosphine oxide was added to the reaction. After extensive spectroscopic studies, the authors suggested that the active species formed by mixing Ph_3PO and TMSCN had the structure $Ph_3P(OTMS)(N{=}C{:})$. Therefore, in the transition state, this newly formed cyanide donor would deliver the cyanide to the *si* face of the activated aldehyde, forming the (*R*)-cyanohydrin.[79]

This system turned out to be very efficient for both aldehydes and methyl ketones, which could be transformed into their respective cyanohydrin derivatives with excellent chemical yield and enantioselectivities (**Table 1.3**). The best reaction conditions established for the reaction of TMSCN with aldehydes involved the use of toluene at -20 °C in the presence of 10 mol% of complex **63** and 20 mol% of Ph_3PO. However, for the reaction of TMSCN with ketones, Ph_2MePO was the phosphine oxide of choice since it gave a higher catalytic activity and enantioselectiviy. The reaction

temperature was increased to 25-45 °C, and longer reaction times were required for ketones. The catalyst could be recovered in 96 % yield and reused, leading to the same level of reactivity and selectivity.[79-80]

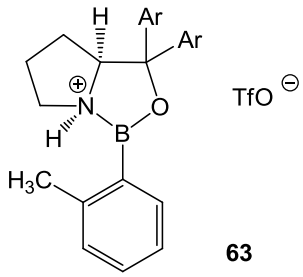

63

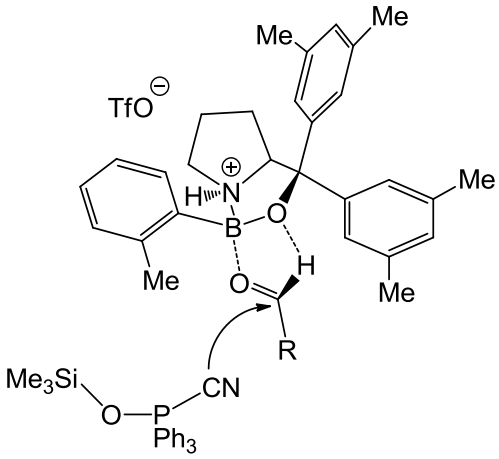

Figure 1.12 Transition state, involving dual activation of cyanide and aldehyde by the catalytic system **63**/Ph_3PO.

Substrate	Temperature	Reaction time	% yield	% *ee*
Aldehydes	-20 °C	40-144 hours	91-98	90-97
Methyl ketones	25-45 °C	2-14 days	45-97	32-96

Table 1.3 Reaction conditions for the asymmetric addition of TMSCN to aldehydes and ketones using 10 mol% of catalyst **63** and 20 mol% of co-catalyst Ph_3PO (for aldehydes) or Ph_2MePO (for ketones).

1.4.3.2 Salen-derived ligands

In view of the ability of N-oxides to activate TMSCN, and based on the encouraging results obtained with titanium(salen) complexes in the catalytic asymmetric cyanosilylation of aldehydes, Feng's group evaluated the effect of combining Lewis acid **17a**-Ti(O^iPr)$_4$ with a set of achiral N-oxides for the enantioselective addition of TMSCN to ketones. Yields of 37-85% and enantioselectivities of 64-84% were obtained for a set of aromatic and aliphatic ketones.

When N-oxide **64** was used as the Lewis base, the optimal procedure for the catalysis involved the separate formation of the titanium complex by treatment of Ti(^{i}PrO)$_4$ with ligand **17a**, evaporation of the released isopropanol, then addition of the ketone. A solution of N-oxide **64** and TMSCN was then added. Under these conditions,

the best result was obtained using two equivalents of TMSCN in the presence of 2 mol% of complex **17a**- Ti(O^iPr)$_4$ and 1 mol% of N-oxide **64** at -20 °C (75% yield and 85% ee after 4 days when acetophenone was the substrate). The authors believe that if all the reaction components were mixed at the start, coordination of N-oxide to the metal centre may occur, negatively affecting the catalyst performance. As expected, the addition of a Lewis base, proved to be beneficial to the reactivity and enantioselectivity, since the titanium complex of **17a** alone only afforded a 3% yield and 66% asymmetric induction under the same reaction conditions. On the basis of the experimental data, the authors proposed a double-activation mechanism in which Lewis acid and Lewis base units separately, but simultaneously, activate the ketone and TMSCN respectively.[81]

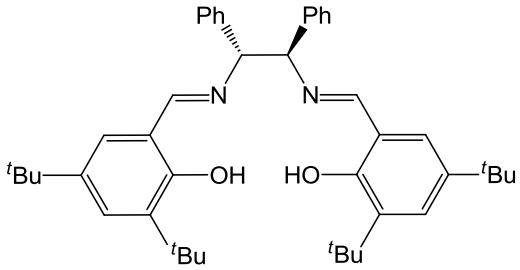

17a

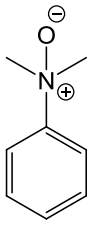

64

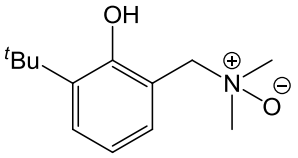

65

Searching further for a more suitable N-oxide, the same authors found an alternative Lewis acid-Lewis base combination, by using N-oxide **65** instead of **64**. This catalyst system transformed a range of aromatic and aliphatic ketones to their respective cyanohydrin silyl ethers in 58-95% yield and with 56-82% ee, similar values to those afforded by the previous system. The reaction was conducted in dichloromethane using 10 mol% of **17a**-Ti(O^iPr)$_4$ and 1 mol% of N-oxide **65** at -20°C for 96 hours. Unlike the previous system, catalyst **17a**-Ti(O^iPr)$_4$ and co-catalyst **65** were premixed at the start of the reaction and the reagents were subsequently added. This suggested that, during the transition state, the phenolic N-oxide is coordinated to the titanium centre through the phenolate group. Therefore, this is the active catalyst which can then activate both substrates and facilitate intramolecular cyanide transfer to the activated aldehyde as illustrated in **Figure 1.13**.[82] In agreement with the results obtained by Belokon and North the cyanohydrins had the opposite absolute configuration to that of the catalyst; thus, when (*R,R*)-**17a**-Ti(O^iPr)$_4$ was the catalyst, the (*S*)-cyanohydrin was obtained as the major enantiomer.

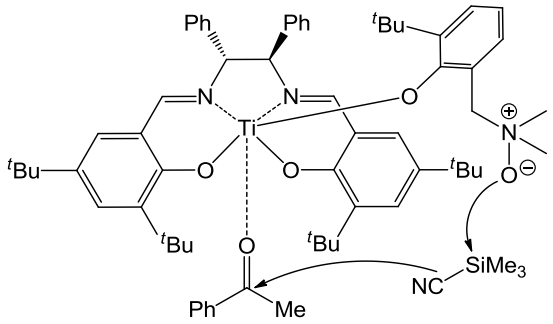

Figure 1.13 Proposed double-activation catalysis carried out by catalyst **17a**-Ti(O^iPr)$_4$, and co-catalyst **65**.

After a laborious screening of salen ligands (with substituents of different electronic nature), metal ions and various N-oxides, Feng's group found that the best complementary Lewis acid-Lewis base catalyst-co-catalyst was **66**-$AlEt_3$/**64**. This turned out to be a highly efficient dual-activation catalyst system with a high substrate tolerance, which afforded levels of enantioselectivity of up to 94% in almost quantitative yields after reaction times of a few hours to days depending on the substrate. The major advantage of this system was the use of very low catalyst loadings without affecting the enantioselectivity of the process. Thus, the best conditions were found to be in THF at -20 °C, in the presence of 0.1 mol% of **66**-$AlEt_3$ complex and 0.05 mol% of N-oxide **64**.

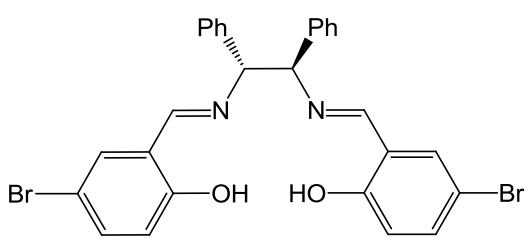

66

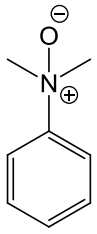

64

Kim and co-workers successfully employed mononuclear aluminium(III) and manganese(III) salen complexes **67** and **68** together with triphenylphosphine oxide for the enantioselective addition of TMSCN to aldehydes and ketones. The addition of Ph_3PO had a positive effect on both the reactivity and asymmetric induction especially when **67** was used as the catalyst, whereas only a slight enhancement to the enantioselectivity was observed for the catalytic system involving complex **68**.[47a, 47c, 83] The best molar ratio of catalyst to co-catalyst was found to be 1:10, and the optimal conditions for the catalysis are summarised in **Table 1.4**. Generally, the **67**/Ph_3PO system appears to be a more effective catalyst than **68**/Ph_3PO, however, neither of them

was able to achieve comparable catalytic activities or enantioselectivities to those obtained with complexes **20** and **23h** described by Belokon and North for the asymmetric cyanosilylation of aldehydes (*Section 1.4.1.2.2*), or systems **37**-$AlCl_3$ and **58** reported by Snapper or Shibasaki when ketones were the substrate (*Sections 1.4.1.6 and 1.4.2.6*).

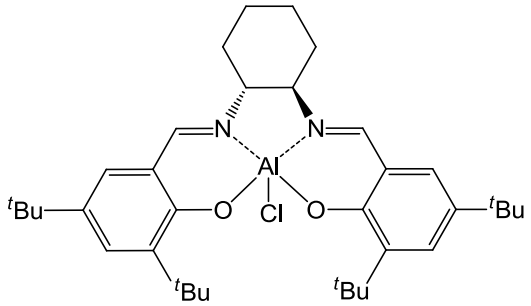

67

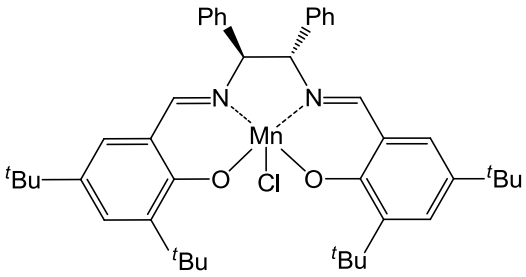

68

Substrate	M(salen) (mol%)	Ph_3PO (mol%)	T (°C)	Time (h)	% yield	% ee
C_6H_5CHO	1 (**67**)	10	-50	18	94	86(*S*)
4-$ClC_6H_4COCH_3$	1 (**67**)	10	r.t.	11	98	77(*S*)
C_6H_5CHO	5 (**68**)	10	0	24	94	58(*R*)
4-$ClC_6H_4COCH_3$	5 (**68**)	50	r.t.	26	90	57(*R*)

Table 1.4 Cyanosilylation of benzaldehyde and 4-chloroacetophenone under the best conditions using catalysts **67** and **68** with Ph_3PO as co-catalyst in CH_2Cl_2.

Building on the successful application of complexes **20** and **23** for the cyanosilylation of aldehydes, North *et al*. investigated the use of bimetallic aluminium complex **69**. This metal complex had previously been used as a catalyst in other organic transformations such as the pioneering work of cyclic carbonate synthesis from epoxides and carbon dioxide, developed by the same authors.[84] Initially, the reaction between benzaldehyde and TMSCN was conducted at room temperature in dichloromethane and in the presence of 10 mol% catalyst. Under these conditions O-trimethylsilyl mandelonitrile was only produced in 55% yield and with 50% enantioselectivity after 16 hours. However, the addition of Ph_3PO was found to enhance both catalytic activity and the asymmetric induction. The highest enantioselectivity (89% ee) was obtained when 2 mol% of the catalyst **69** and 10 mol% of Ph_3PO were used at -40 °C for 16 hours affording the product in 88% yield. Under the optimised,

conditions a range of electron-rich and electron-deficient aromatic aldehydes were found to be as good substrates as benzaldehyde.[85]

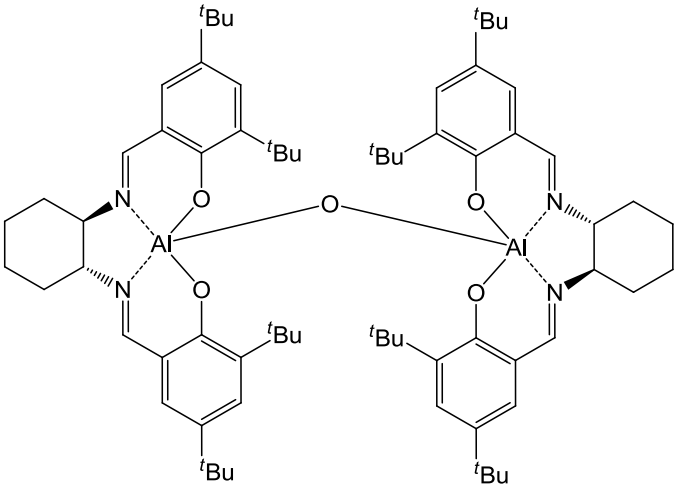

69

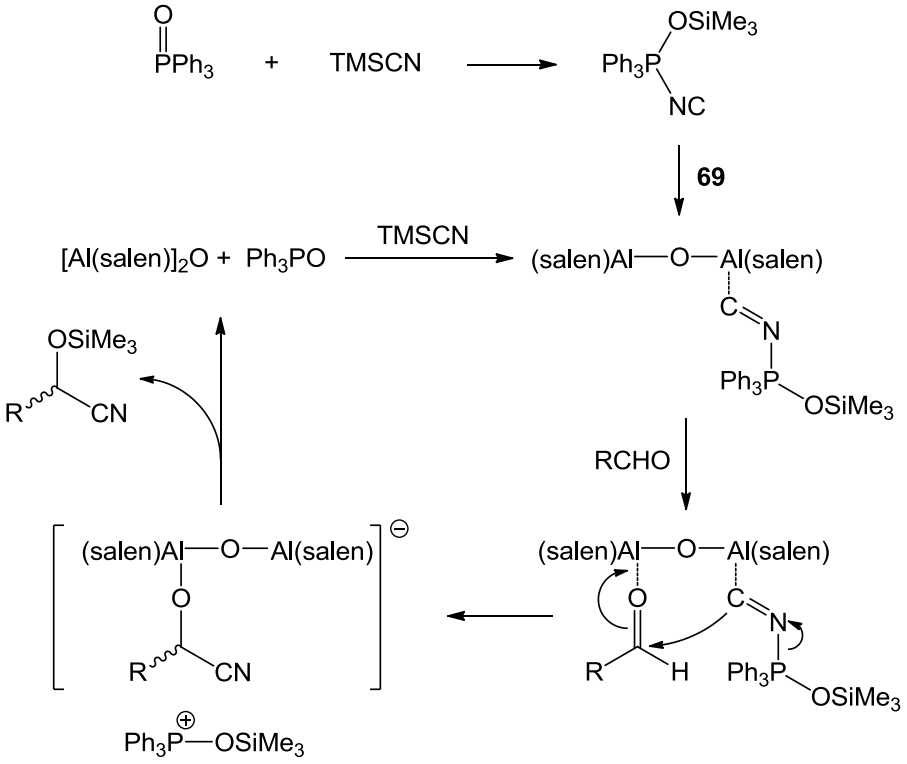

Scheme 1.9 Catalytic mechanism for complex **69**.

The reaction kinetics for the addition of TMSCN to benzaldehyde catalysed by **69** and Ph_3PO were investigated and overall first order kinetics were observed with the rate depending on the concentration of TMSCN, but not benzaldehyde. By carrying out reactions at various concentrations of catalyst and co-catalyst, the order with respect to

these two components could be determined and the reaction was first order in each component. Thus, the authors proposed a mechanism (**Scheme 1.9**) which involves first the activation of TMSCN by the Ph_3PO forming the activated species $Ph_3P(OTMS)(N{=}C{:})$ as previously described by Corey.[79] This subsequently coordinates to one of the aluminium ions, whilst the other activates the aldehyde. This facilitates an intramolecular nucleophilic attack to afford the chiral cyanohydrin O-trimethylsilyl ether with opposite absolute configuration to that of the salen ligand.[71, 85]

Sun and co-workers designed salen ligands **70** and **71**, derived from pyrrolidine and pyrrolidine N-oxide groups respectively. When the catalytic activity of the pre-formed titanium complexes was investigated in the cyanosilylation of benzaldehyde under the same standard conditions (0 °C, in CH_2Cl_2, for 15 hours), both gave similar reactivity but very different enantioselectivity (81% ee (*S*) and 24% ee (*R*) when **70**-Ti(O^iPr)$_4$ and **71**-Ti(O^iPr)$_4$ were the catalysts respectively). The authors explained the reduced asymmetric induction when complex **71**-Ti(O^iPr)$_4$ was used as the catalyst, as being due to an interaction between the N-oxide and the titanium centre. This also induced a structural change within the catalyst during the transition state of the reaction, since the cyanohydrin product was obtained with the opposite absolute configuration to that obtained by complex **70**-Ti(O^iPr)$_4$. Therefore, to improve the catalytic performance, **70**-Ti(O^iPr)$_4$ was used in combination with an achiral N-oxide (**64**), and this system formed cyanohydrin silyl ethers with almost quantitative yields and with enantiomeric excesses up to 90%. The best conditions were found to be at -10 °C, in dichloromethane in the presence of 1 mol% of a 1:1 molar ratio of **70**-Ti(O^iPr)$_4$ to **64** for 24 hours.[86]

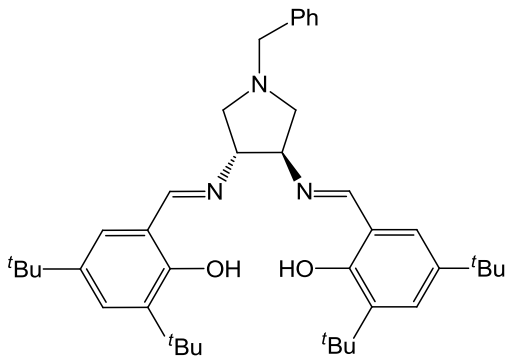

70

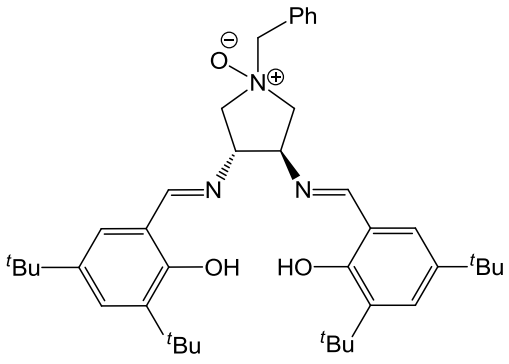

71

1.4.3.3 Proline-derived ligands

Feng's group developed ligand **72** prepared from L-proline and an aminodiphenylmethane.[87] This is structurally very similar to ligands **53** and **55**, for which the respective metal complexes were shown to effectively catalyse the

asymmetric cyanosilylation of aldehydes (*section 1.4.2.5*). Initially, the titanium complex **72**-Ti(O^iPr)$_4$ was found to catalyse the asymmetric addition of TMSCN to acetophenone, exhibiting good reactivity but rather poor enantioselectivity. Therefore, the authors decided to explore the use of additives, of which N-oxide **73** gave the most promising results. The optimal conditions were 2.5 mol% of **72**/ Ti(O^iPr)$_4$/ **73** in a molar ratio of 1:1:1, with 1.5 equivalents of TMSCN in THF at -45 °C. With a concentration of acetophenone of 1.0 M, this was transformed into its corresponding cyanohydrin trimethylsilyl ether in 96% yield and 90% ee. The nature of the catalytic species was believed to be in equilibrium with a dimer or a more complex species since nonlinear effects were observed during the course of the reaction.[88] Thus, similarly to the model of the proposed transition state for catalytic system **17a**-Ti(O^iPr)$_4$/ **65**, the N-oxide binds to the titanium centre through the phenolic oxygen. This would act as a Lewis base activating the TMSCN, and hence the cyanide delivery would take place to the less sterically hindered face of the ketone, which is at the same time activated by the Lewis acidic metal centre.

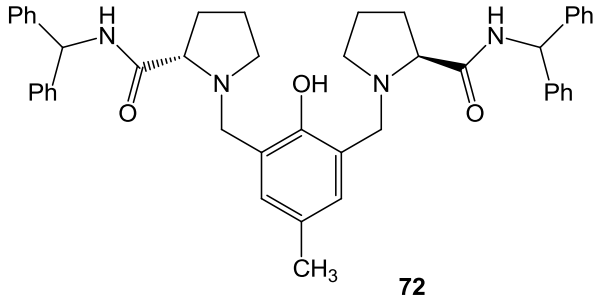

72

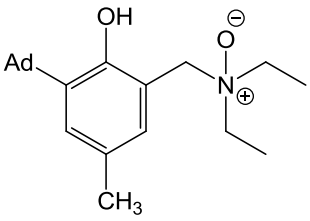

73

1.4.3.4 Diol-derived ligands

Kim and co-workers examined the use of TADDOL **5b** as a chiral ligand for the asymmetric synthesis of cyanohydrins. The titanium complex of this, in conjunction with triphenylphosphine oxide, displayed the highest enantioselectivity, which was rather moderate even in the best conditions of -10 °C in chloroform in the presence of 10 mol% of both catalyst **5b**-Ti(O^iPr)$_4$ and Ph_3PO co-catalyst (95% yield and 50% ee after 20 hours). The proposed transition state involved the simultaneous activation of aldehyde and TMSCN by the metallic centre and the phosphine oxide respectively.[89]

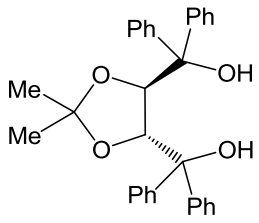

5b

So far, many systems have been shown to catalyse the formation of cyanohydrins from ketones in good yield and enantioselectivity. Most of them require an additive or the presence of a Lewis or Brönsted base in the ligand structure, which in conjunction with the Lewis acidic metal ion can simultaneously activate both the nucleophile and electrophile. This dual-activation also regulates the orientation of the two substrates resulting in better stereocontrol of the reaction.

1.5 Mechanistic studies of M(salen) complexes

At the beginning of this project we believed that the vanadium(salen)X system was somewhat exceptional as the counterion (X) played an important role in the catalytic activity. In this section, this will be explained in more detail and the mechanistic studies previously carried out on vanadium(V)(salen)X complexes **23** will be compared with the well established mechanism for asymmetric cyanohydrin synthesis catalysed by bimetallic titanium complex **20** developed in our group. The Lewis acidity and Lewis basicity of these catalysts provide to the activation of both reagents will be discussed.

Although catalysts **20** and **23** are not the most enantioselective catalytic systems for the cyanosilyation of aldehydes and ketones, they meet most of the industrial requirements. They are prepared from inexpensive and readily available chemicals through a two step synthesis, and they can promote cyanohydrin formation under the very mild conditions of atmospheric pressure, room temperature and in air. Moreover, only a catalyst loading of 0.1 mol% is required to transform a wide diversity of aldehydes (aromatic, heteroaromatic, aliphatic and α,β-unsaturated) into their O-trimethylsilyl cyanohydrins with high conversions and with enantioselectivities up to 95%. Due to these advantageous properties, Belokon and North's groups studied the kinetics of reactions catalysed by complexes **20** and **23** and searched for intermediates which together allowed a mechanism to be proposed for each catalyst.

1.5.1 Mechanistic studies of $[Ti(salen)]_2O_2$ catalyst

Titanium complex **20**, a bimetallic compound in the solid state, was observed to exist in a concentration dependent equilibrium with its monomer (**24**) when chloroform or dichloromethane were used as solvents (**Scheme 1.5**, *section 1.4.1.2.2*).[38] This implies a dissociation of the coordinatively saturated complex **20**, thus allowing small electron-rich molecules such as aldehydes and ketones to interact with the metal centre. Evidence for this interaction was seen in the formation of metalo-acetal **74**, detected by ^{1}H NMR spectroscopy, which is formed by a formal [2+2] cycloaddition between the Ti=O bond of monomer **24** and the C=O bond from hexafluoroacetone, when this was added to a solution of complex **20** in CD_2Cl_2 (**Scheme 1.10**).

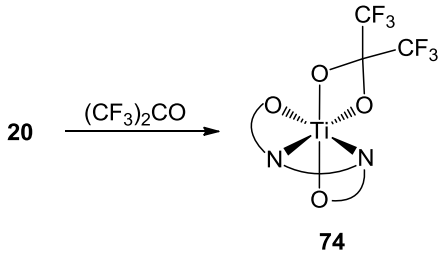

74

Scheme 1.10 Metalo-acetal formation from a mixture of precatalyst **20** and $(CF_3)_2CO$.

On the other hand, the ^{1}H NMR spectrum of complex **20** in $CDCl_3$ mixed with 10 to 30 equivalents of TMSCN showed the formation of C_2-symmetric species **75** in which the two oxygen bridges were coordinated to $Si(CH_3)_3$ and two CN anions were in the outer coordination sphere. This adduct seemed to decompose to monomeric species **76-78**, of which the bis-cyanide complex **78** was suggested to combine with metalo-acetal **79** to form the key intermediate, complex **80**.

Kinetic studies revealed an overall first order reaction with rate equation Rate = k_{app} [TMSCN], where $k_{app} = k[\mathbf{20}]^n$, showing a zero-order dependence on the aldehyde concentration and a first order dependence on TMSCN concentration. This indicates that the aldehyde is only involved in the catalytic cycle after the rate limiting step. When kinetic experiments were conducted at different catalyst concentrations, the order with respect to catalyst **20** was determined and a value n = 1.34 was obtained. This value gives information about the oligomeric nature of the catalytically active species in solution and the number of Ti(salen) units involved in the catalytic cycle. Thus, a value $1< n \leq 2$ implies that the catalytic species has a binuclear nature and exists in equilibrium with a catalytically inactive mononuclear species. Taking this into account, the authors proposed the catalytic cycle illustrated in **Scheme 1.11**.

The mechanism involves first the formation of catalytically active species **80** by the recombination of complexes **78** and **79**; with one metal ion acting as a Lewis acid to activate the aldehyde, while the other binds to the cyanide. Both salen ligands adopt cis-β configurations in order to bring the two reagents closer in space and to eventually promote an intramolecular reaction giving rise to the chiral cyanohydrin. The rate determining step is the silylation of the cyanohydrin, in which a molecule of TMSCN is involved. This step releases the O-trimethylsilyl cyanohydrin ether and forms complex **82**, which rapidly reacts with a molecule of aldehyde to form complex **80**, allowing the catalytic cycle to start again. This scheme is consistent with the kinetic and spectroscopic experiments and is nowadays well accepted.

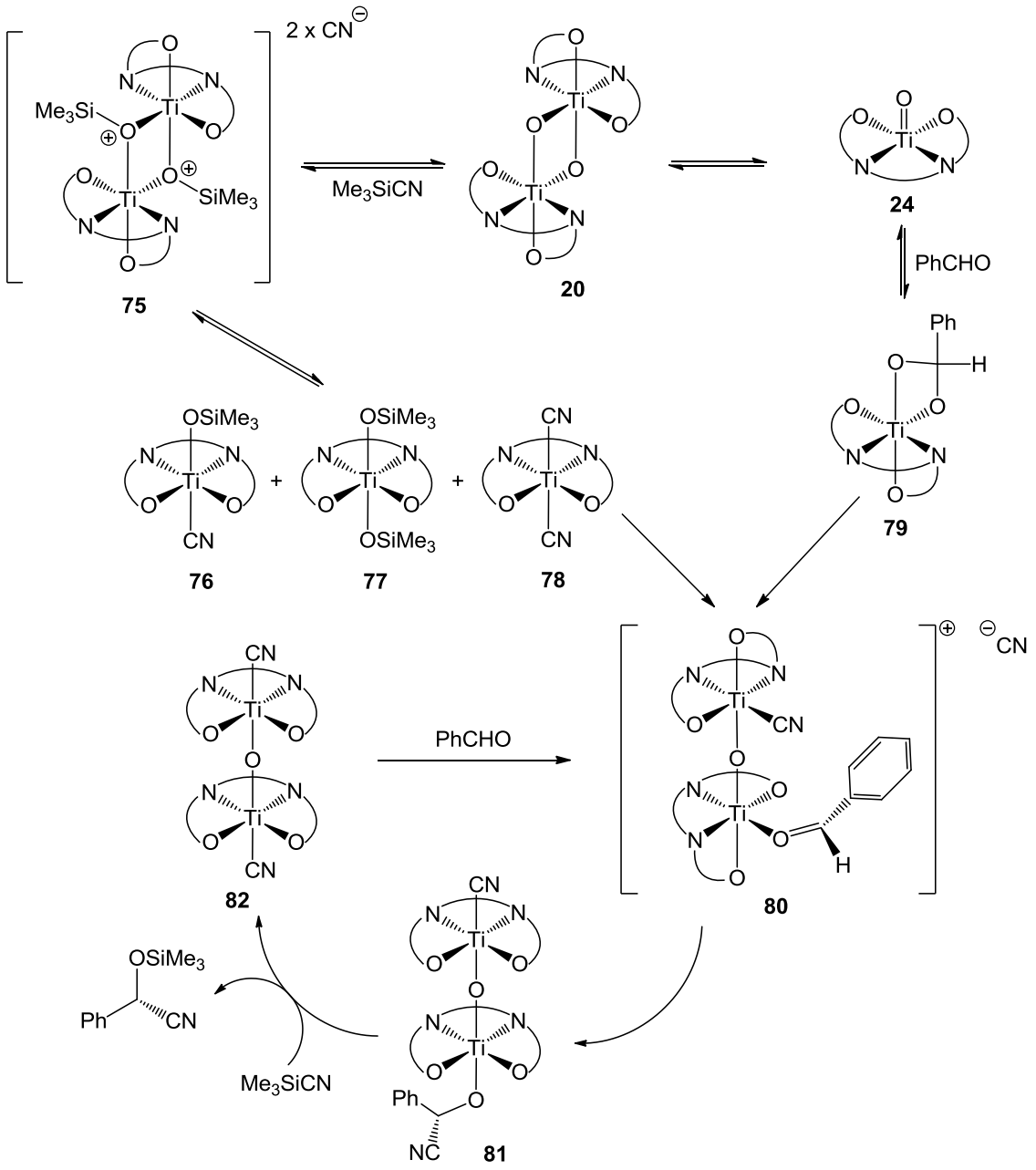

Scheme 1.11 Proposed catalytic cycle exhibited by complex **20**.

1.5.2 Mechanistic studies of VO(salen)X catalysts

Complex **20** was shown to be an extremely active catalyst for the silylcyanation of aldehydes, however the asymmetric induction still had room to be improved. Belokon and North thought that this could be achieved by making a less reactive catalyst, in order to increase the enantioselectivity.[43] This catalyst had to be structurally similar to complex **20**, with the monomer-dimer equilibrium slightly more favoured towards that of the monomer, which is catalytically inactive. Oxovanadium(IV)(salen) complexes were found to the best choice, as they either exist as a monomer containing a V=O bond,[90] or as oligomers possessing −V−O−V−O− bonds;[91] the monomeric form

being more stable. Thus, VO(salen) complex (**22**) was prepared by refluxing a mixture of salen ligand (**18e**) and $VOSO_4$ in ethanol under an air atmosphere. Initially, complex **22** was thought to be the product of the reaction and hence, the catalytically active species. However, X-ray analysis revealed that the real complex had a monomeric structure with the vanadium ion in its +5 oxidation state, the salen ligand occupying the four equatorial positions, an oxygen double bond occupying an axial position, and a water molecule *trans* to the V=O bond taking the sixth coordination site. An ethyl sulphate anion was found outside the coordination sphere, neutralizing the positive charge of the complex (see **Figure 1.14**). As mentioned in *section 1.4.1.2.2*, VO(salen)$EtOSO_3$ (**23a**) has been found to catalyse the asymmetric addition of TMSCN to benzaldehyde in high yield (>99%) and with excellent enantioselectivity (up to 91%ee) after 24 hours. However, complex **22**, which was prepared using the same protocol as for complex **23a** but without the presence of oxygen, was found to be catalytically inactive.[44a]

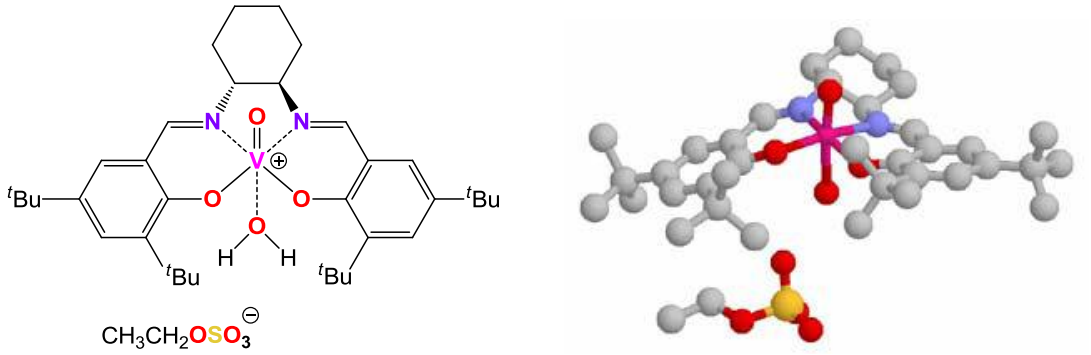

Figure 1.14 X-ray structure of complex **23a**

Unlike catalyst **20**, which exhibited overall first-order kinetics, catalyst **23a** was found to obey second order kinetics in which both the aldehyde and the TMSCN are involved in the rate equation (rate = k_{app}[PhCHO][TMSCN], where k_{app} = k[**23a**]^n). Thus, this indicates that the mechanism of action of the oxovanadium(salen) catalyst is different to that of the titanium catalyst.[44]

In order to study the effect of the counterion on the catalytic activity, a series of complexes **23b-h** were prepared. With the exception of complexes **23f** and **23g,** which were prepared by treatment of salen ligand with VOF_3 and $VOCl_3$ respectively (**Scheme 1.12**), all the other complexes were prepared either by ion exchange chromatography using Dowex® resin from complex **23a** (**Scheme 1.13**), or by direct ion exchange between **23a** and the counterion salt in solution. These complexes were tested as

catalysts for the asymmetric addition of TMSCN to benzaldehyde. As shown in **Table 1.5**, the counterion had a major impact on the kinetics of the reaction. Complex **23a** was the least effective catalyst in terms of reaction rate ($t_{50\%}$), whereas complex **23h** exhibited higher catalytic activity than titanium complex **20**. Interestingly, those complexes in which the counterion covalently binds to the vanadium ion (**23f-h**) displayed the highest catalytic activity and ionic complexes (**23a,c-e**) showed lower reactivity. Surprisingly, complex **23b**, which possesses the most highly Lewis acidic metal ion was found to be catalytically inactive. The nature of the counterion however, did not significantly influence the enantioselectivity of the product. This indicates that the counterion is not involved in the stereodetermining step of the reaction, but is involved in the rate determining step of the mechanism.

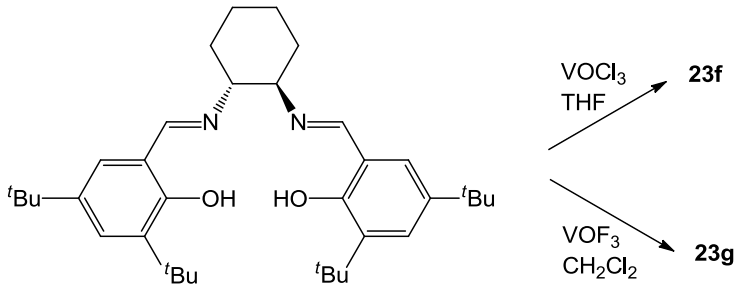

Scheme 1.12 Synthesis of vanadium-based complexes **23f** and **23g**.

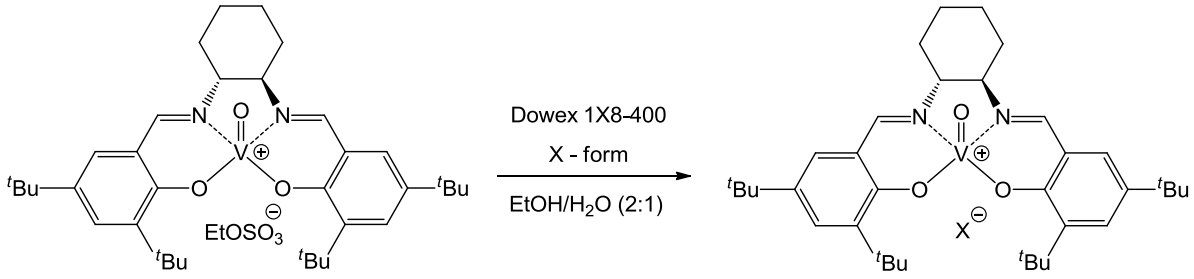

Scheme 1.13 Ion exchange chromatography procedure to form complexes **23b-e**

Complex	Counterion	$t_{50\%}$ (min)	*ee* (%)
23a	$EtOSO_3$	370.0	91(*S*)
23b	CF_3SO_3	-	-
23c	BF_4	80.1	90(*S*)
23d	Br	68.1	94(*S*)
23e	NO_3	48.5	95(*S*)
23f	Cl	12.5	93(*S*)
23g	F	9.2	91(*S*)
23h	NCS	3.8	95(*S*)
20	-	4.1	84(*S*)

Table 1.5

In order to obtain structural information on these complexes in solution, the order with respect to the catalyst was determined. The results shown in **Table 1.6** were highly unexpected as orders from 0.6 to 2.5 were observed, which suggests that the vanadium complexes can form dimers in solution (or polymers in the case of fluoride complex **23g**), and that these are in equilibrium with their monomers. For catalysts **23a** and **23c-f**, $n < 1$ suggesting that the catalytically active species is the monomer, whilst for catalysts **20**, **23g**, **23h**, $n > 1$ which is indicative of a dimer or a larger aggregate being the active species.

Complex	Counterion	Order with respect to the catalyst
23a	$EtOSO_3$	0.64
23c	BF_4	0.84
23d	Br	0.74
23e	NO_3	0.77
23f	Cl	0.88
23g	F	2.45
23h	NCS	1.23
20	-	1.34

Table 1.6

All the kinetic experiments were conducted at 0 °C. Surprisingly though, at this temperature, catalysts **23c** and **23d** showed zero rather than second order kinetics; and when the temperature was reduced to -10 °C catalyst **23e** also exhibited zero order kinetics. However, when the temperature was increased to 20 °C, all the complexes

exhibited second order kinetics. This observation implies a change in the rate determining step of the mechanism on changing the temperature.

Another parameter which was found to be critical to the catalyst performance was the atmosphere and this gave the first glimpse that a redox process could be taking place. When the catalytic reaction was conducted under argon, the reaction kinetics were clearly retarded and the reaction eventually stopped. In addition, the colour changed from dark green to light green through the course of the reaction. The fact that an inert atmosphere had such a detrimental effect on the catalytic activity was found to be caused by the reduction of vanadium(V)(salen) complexes to the catalytically inactive vanadium(IV)(salen) complex **22**. Therefore, when air was bubbled through the solution, the catalytic activity could be recovered, indicating that the catalyst can be converted back into the active vanadium(V)(salen) species simply by the presence of air. Thus, an oxygen atmosphere was essential to maintain the catalyst activity. This hypothesis was valid for all catalysts, with the exception of **23f** and **23h** as these catalysts did not deactivate; even under extremely inert conditions.

$[VO(salen)]^+$ and $[VO(salen)]_2^+$ species could be identified by electrospray mass spectrometry analysis of complexes **23a** and **23c-h**. The latter corresponds to a dimer containing vanadium ions in two oxidation states, +4 and +5.[44b] In accordance with data from the Cambridge Crystal structure database, a mixed-oxidation state vanadium dimer is much more common than both vanadium ions having the same oxidation state.[92] This was supported by previous reports from our group in which the formation of heterobimetallic complexes containing Ti(IV) and V(V) ions have been described.[45] These are also mixed oxidation states complexes containing a V(V) coordinated to Ti(IV) bound through two bridging oxygen atoms (see complex **25**, *section 1.4.1.2.2*).

In view of the above results, a mechanism for asymmetric cyanohydrin synthesis catalysed by VO(salen)X complexes was postulated. Building on the monomer-dimer equilibrium, and knowing that both can be catalytically active, two different catalytic cycles were suggested (**Scheme 1.14**).

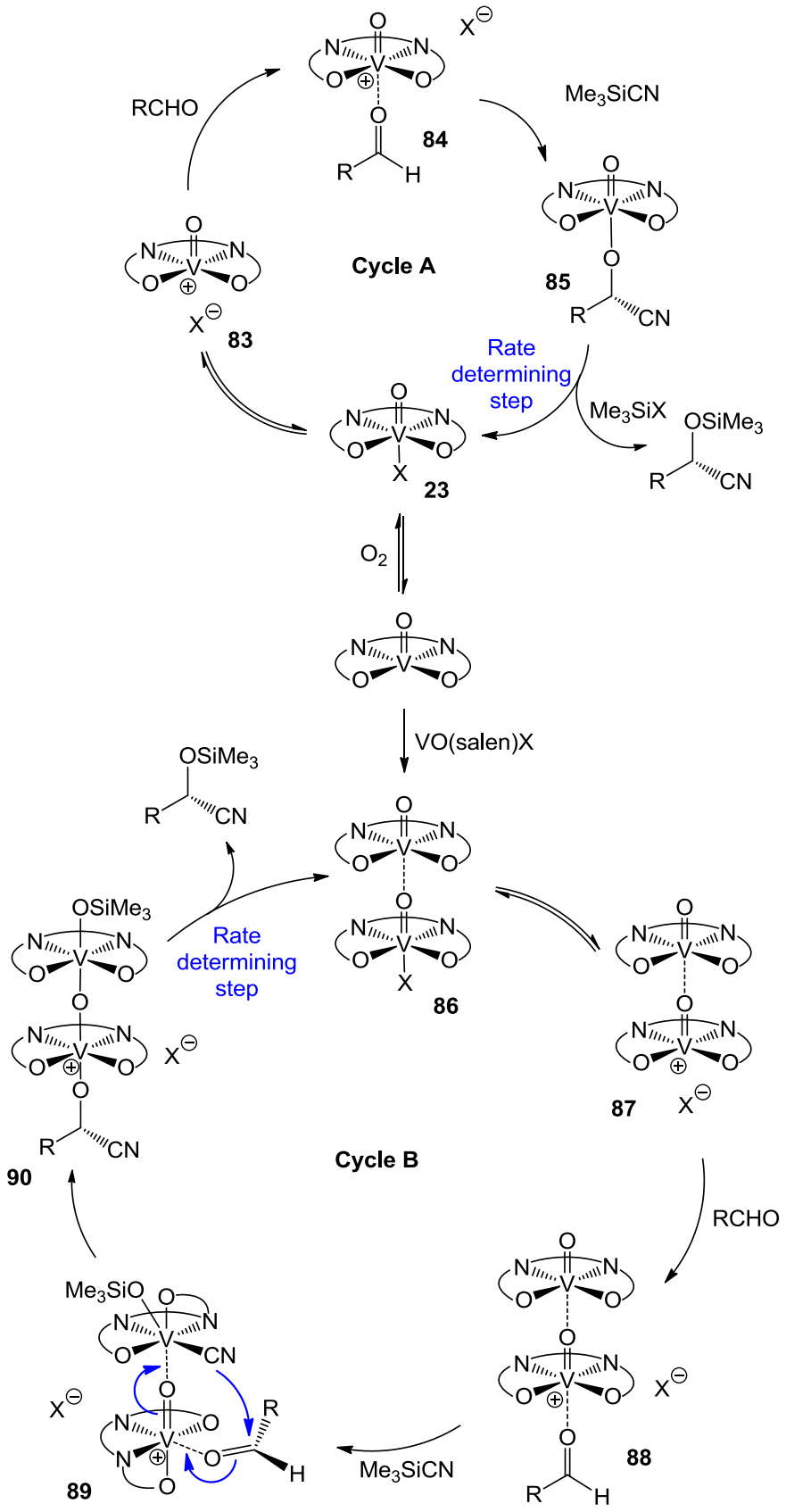

Scheme 1.14 Monometallic and bimetallic catalytic cycles for asymmetric cyanohydrin synthesis

For those complexes that were found to have a reaction order with respect to the catalyst lower than one, the mechanism involves a mononuclear species as the predominant catalytically active species (**Cycle A, Scheme 1.14**). The coordinatively saturated catalyst **23** first dissociates the counterion (to give complex **83**), permitting the aldehyde to coordinate to the Lewis acidic metal centre to form species **84**. Then, enantioselective nucleophilic attack of cyanide onto the activated carbonyl generates a stereogenic centre. With the cyanohydrin still coordinated to the vanadium ion (**85**), the re-coordination of the counterion results in the extrusion of the cyanohydrin $RCH(CN)O^-$, which is subsequently silylated, and catalyst **23** regenerated. The sluggish reactivity of complex **23a** could be related to the bond strength of V−OCH(CN)R. Thus, on changing the counterion to a more strongly coordinating one, the release of the cyanohydrin product (the rate determining step) would be more favoured. This could explain the lower catalytic activity shown by complex **23b**, as being due to the low nucleophilicity of the triflate anion.

For those complexes that were determined to have a reaction order of one or higher with respect to the catalyst (**Cycle B, Scheme 1.14**), the catalytic cycle proposed involved dinuclear species **86**, which had a vanadium ion in each oxidation state (+4 and +5). In the same way as for the monometallic cycle, dissociation of the counterion occurs first (to form **87**), followed by the activation of the aldehyde by the Lewis acidic vanadium ion, with the higher oxidation state. A molecule of TMSCN reacts with the vanadium ion of complex **88** to form complex **89**. This highly active catalyst can then deliver the cyanide intramolecularly, forming the cyanohydrin through a lower energy transition state to that of the monometallic catalytic cycle. In the rate determining step, the cyanohydrin is expelled by the counterion, which regenerates catalyst **86** and produces the trimethylsilyl cyanohydrin ether in a silylation reaction.

It is likely that both the mononuclear **23** and binuclear **86** species are catalytically active, and the nature of the counterion is responsible for altering the position of the equilibrium between the monomer and dimer. Thus, both catalytic cycles could be taking place at the same time. As the simultaneous activation of the aldehyde and the cyanide is followed by an intramolecular reaction in the bimetallic catalyst, it can be expected to be more effective than the monometallic catalyst, which only activates the aldehyde, and a non-coordinated cyanide anion performs the nucleophilic attack. While the role of the oxygen is not well understood, it seems to be essential to generate the binuclear species. This however, can also be detrimental if the rate of

formation of vanadium(IV) is faster than that of the oxidation reaction. In fact, when the temperature drops below 273 K, for some catalysts, the reoxidation of vanadium(IV) to vanadium(V) becomes the rate determining step, and thus they show overall zero order kinetics.

1.6 Aims of the project

All of the work in this project was concerned with the asymmetric cyanation of aldehydes or ketones using metal(salen) complexes as catalysts. The thesis is divided into three main sections, presented as follows:

a) A detailed study of the redox reaction which occurs during the catalytic asymmetric cyanation of aldehydes when oxovanadium(V)salen complexes are used as catalysts. Electron paramagnetic resonance spectroscopy was mainly used to detect and quantify the formation of V(IV) species and an array of analytical and chemical techniques were used to detect the reducing agent as well as its oxidized form. This provided a better understanding of the structure of the catalytically active species, and of the monomer-dimer catalyst equilibrium postulated previously.

b) A study of the relative importance of the Lewis acid and Lewis base character of the metal(salen) catalytic systems $[Ti(salen)O]_2$, VO(salen)X (X = $EtOSO_3^-$ and NCS^-) and $[Al(salen)]_2O/Ph_3PO$ in the asymmetric synthesis of cyanohydrins. Kinetics were conducted on a series of *para*- and *meta*- substituted aromatic aldehydes and a Hammett plot was constructed. The study was extended to the use of additives in the asymmetric cyanation of ketones.

c) The use of cyclic carbonates as a solvent system for the asymmetric addition of TMSCN to aldehydes using titanium and vanadium(salen) based complexes as catalysts. This was aimed to address the growing industrial demand for the development of a more environmentally friendly and economic process. In addition, a kinetic study in this solvent system was conducted in order to provide information on the solvent effect in the catalytic activity of the VO(salen)NCS catalyst in the asymmetric cyanation of aldehydes.

2 Study of the redox process in asymmetric cyanohydrin synthesis using VO(salen)X complexes as catalysts.

2.1 Introduction

VO(salen)X complexes are amongst the most effective catalysts for the asymmetric addition of TMSCN to aldehydes (**Scheme 2.1**), displaying excellent asymmetric inductions for a wide range of substrates.[43] The mechanistic studies described in *section 1.5* have shown that the catalytic activity, but not the enantioselectivity of vanadium(V)(salen) complexes (VO(salen)X) is highly dependent on the counterion X, and this correlates with the coordinating nature of the counterion (**Table 2.1**).[44b]

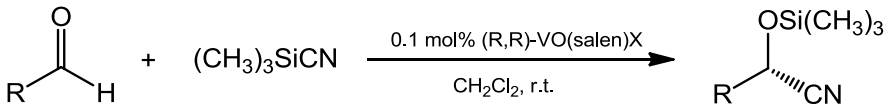

Scheme 2.1 Standard conditions for the asymmetric addition of TMSCN to aldehydes catalysed by VO(salen)X complexes.

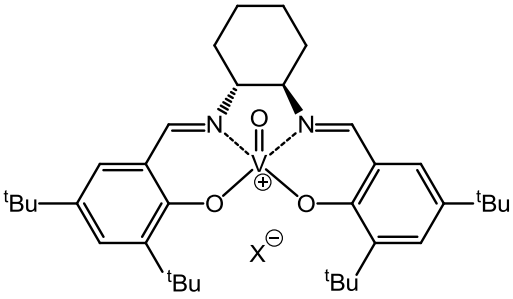

23

Complex	Counterion X	$t_{50\%}$ (min)	*ee* (%)
23a	$EtOSO_3$	370.0	91
23b	CF_3SO_3	-	-
23c	BF_4	80.1	90
23d	Br	68.1	94
23e	NO_3	48.5	95
23f	Cl	12.5	93
23g	F	9.2	91
23h	NCS	3.8	95

Table 2.1 Catalyst activity in the asymmetric addition of TMSCN to benzaldehyde in dichloromethane at room temperature using 0.1 mol% of catalyst.

The ability of the counterion to bind to the vanadium ion was not the only factor involved in the catalytic activity. Kinetic studies also showed that the monomeric complex could exist in solution in equilibrium with dinuclear species, or even larger aggregates such as trimers. Moreover, according to mass spectrometry (ESI-TOF), the dimer or dinuclear species is a mixed-valence species, wherein one of the vanadium ions is in the +5 oxidation state and the other is present as the reduced +4 form.[44b] Both monomer and dimer were found to be catalytically active; thus, two parallel catalytic cycles were proposed to perform the catalysis, a monometallic and a bimetallic cycle. The latter is expected to be the more efficient, since it can activate both the aldehyde and the cyanide and allows an intramolecular reaction to take place (see *section 1.5*). It is the nature of the counterion that determines the position of the equilibrium between monomer and dimer. Thus, the more coordinating counterions exhibited a reaction order in catalyst concentration greater than one which indicates that two VO(salen) units are involved in the catalysis. In contrast, the poorly coordinating counterions show an order in catalyst concentration lower than one, which clearly indicates that despite being in equilibrium to their bimetallic counterpart, the catalysis is predominantly performed through a monometallic cycle.

At the start of this project there was considerable evidence for the existence of a redox process during asymmetric cyanohydrin synthesis catalysed by VO(salen)X complexes; and the formation of V(IV) species seemed to be necessary to promote the generation of bimetallic species, and hence a more catalytically active catalyst. However, when vanadium(IV)(salen) species are in excess, the catalytic activity diminishes showing catalyst deactivation. This explains the observed decay of the catalytic activity when the reaction is carried out under an inert atmosphere. Therefore, an oxidative atmosphere, either air or pure oxygen was essential to maintain the balance between V(V) and V(IV) species in solution.[44b] The reaction temperature was also found to affect the redox process, by slowing the reoxidation process as the temperature was lowered. The role of oxygen was critical in the catalysis; however, the origin of the reduction phenomenon which promotes the formation of vanadium(IV)(salen) species remained unknown. Therefore, with the aim of fully understanding the chemistry involved in the redox process and the role that the counterion plays, a detailed study of the *in situ* formation of vanadium(IV) species during VO(salen)X catalysed asymmetric cyanohydrin synthesis was undertaken.

2.2 Electron paramagnetic resonance spectroscopy

The catalyst loadings used in asymmetric cyanohydrin synthesis (typically 0.2 mol%) are too low to be detected by ^{1}H NMR spectroscopy. Moreover, the signals are broad due to the presence of paramagnetic V(IV) containing species. Analysis by ^{51}V-NMR spectroscopy was considered, however, the close proximity of the V(V) and V(IV) chemical shifts and the line broadening made the two species indistinguishable. In contrast, and taking advantage of the paramagnetism of V(IV), electron paramagnetic resonance (EPR) was found to be an ideal technique to follow the course of the reaction as it can detect paramagnetic species. This technique is widely used in inorganic laboratories to characterise organometallic compounds possessing nuclei with unpaired electrons. In our case, vanadium(V)(salen) species have an even number of electrons and are invisible to EPR. However, vanadium(IV)(salen) species, have an unpaired electron of spin ½, so by applying microwave irradiation within a magnetic field, this electron can be promoted to the first excited state ($\Delta m_s = 1$). As the ^{51}V nucleus has a non-zero nuclear spin ($I = 7/2$), each electronic spin level (m_s) will split into $2I + 1$ energy levels. This explains the origin of the characteristic eight line signal of vanadium(IV) species.

2.3 Preliminary EPR results

In order to test the ability of EPR spectroscopy to detect the very small amounts of V(IV) present in asymmetric cyanation reactions, the spectrum of a 10 mM solution of VO(salen) **22** in dichloromethane was recorded. As expected, a characteristic eight line spectrum was observed (**Figure 2.1**, top). Subsequently, spectra of 10 mM solutions of VO(salen)$EtOSO_3$ **23a**, VO(salen)Cl **23f** and VO(salen)NCS **23h** complexes in dichloromethane were recorded and found to contain 3-6 % of V(IV) impurity (**Figure 2.1**). The unequal intensities of the eight lines within these spectra is due to the size of the VO(salen) molecule. This is so big that it tumbles slowly on the EPR timescale and the spectrometer can therefore start to distinguish the g_x, g_y and g_z components (spatial Cartesian axes) of the spectra. If the paramagnetic species was very small, such as an inorganic salt, it would tumble rapidly on the EPR timescale and appear as a solid sphere. In this case, all the lines within the multiplet would be of equal intensity.

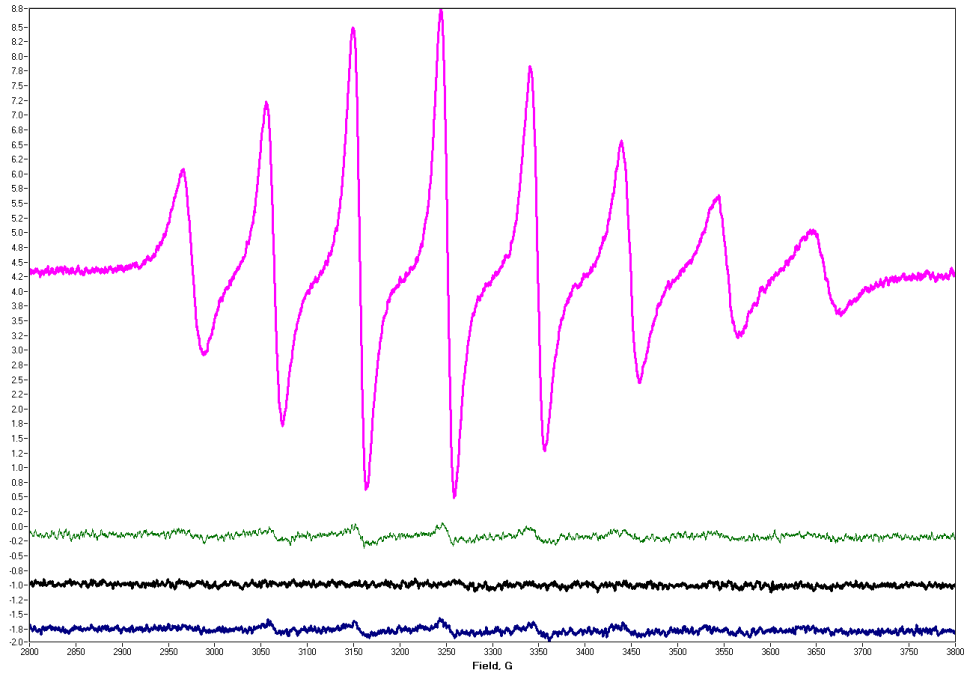

Figure 2.1 From top to bottom, the spectra of 10 mM solutions of complex **22**, **23h**, **23f** and **23a**.

2.4 EPR monitoring of cyanation reactions

Having shown that VO(salen) species could be easily detected by EPR spectroscopy, the next step was to determine if any vanadium(IV) species were formed during asymmetric cyanohydrin synthesis. Complexes VO(salen)$EtOSO_3$ **23a** and VO(salen)NCS **23h** were chosen as examples of catalysts, predominantly active as monometallic and bimetallic species respectively, and VO(salen)Cl **23f** was included as an intermediate catalyst. Thus, to a standard solution of catalyst in dichloromethane, benzaldehyde and TMSCN were sequentially added and a series of EPR spectra were recorded every 5 minutes. All three catalysts **23a, 23f** and **23h** showed the same general trend; a rapid increase of V(IV) signal intensity to a maximum value which is then maintained and ultimately slowly decreased (see *Appendix 1, 1.2*). In order to quantify the amount of V(V) transformed into V(IV) during the course of the reaction, the EPR signal of the reaction mixtures at the highest intensity were compared to the signal intensity of a VO(salen) sample prepared under the same conditions, at the same concentration. Then, the percentage of V(V) converted to V(IV) could be estimated and is shown in **Figure 2.2**.

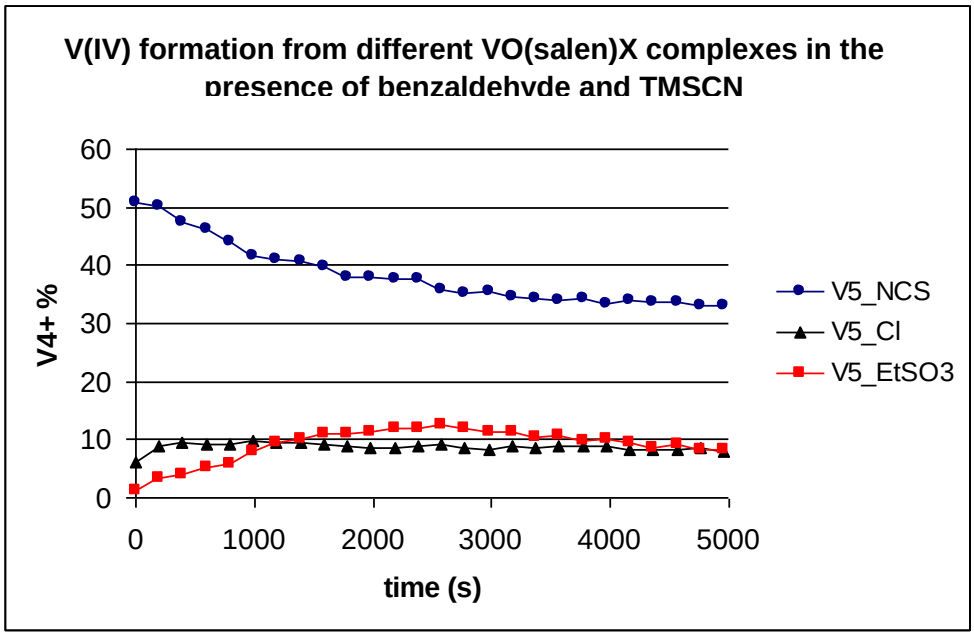

Figure 2.2 Percentage of V(IV) species present vs. time during the asymmetric addition of TMSCN to benzaldehyde starting from minute 5 which is the time it takes to record the spectrum. Thus, the extremely high percentage of V(IV) reached in the case of VO(salen)NCS, is achieved during the first 5 minutes of reaction.

The results show a well defined trend, wherein the VO(salen)$EtOSO_3$ catalyst **23a** bearing the least coordinating counterion generates a maximum of a 12% of V(IV) species in the reaction mixture, suggesting that this catalyst performs the catalysis mainly through a monometallic cycle. In contrast, for VO(salen)NCS **23h**, with a covalently bound counterion, approximately 50% of the V(V) is transformed to V(IV), and assuming that every unit of V(IV) combines with a unit of V(V), forming a mixed-valence bimetallic catalyst, the catalysis would occur entirely through a bimetallic cycle. VO(salen)Cl **23f** gave an unexpectedly low conversion; only 10% of V(V) was reduced to V(IV). This is comparable to the less reactive catalyst VO(salen)$EtOSO_3$, which indicates that the catalysis using this complex as catalyst also takes place mainly though a monometallic cycle.

2.5 The nature of the reducing agent

Having established that vanadium(IV) species were formed during asymmetric cyanohydrin synthesis catalysed by VO(salen)X (X=$EtOSO_3$, Cl, NCS) complexes, the question which remained was which species was acting as the reducing agent?

2.5.1 Aldehyde as reducing agent

The most likely reducing agent was thought to be benzaldehyde, which could be oxidized to benzoic acid. This would also explain why ketones are not good substrates for cyanohydrin synthesis using vanadium-based complexes as catalysts, since they cannot be oxidised. Thus, the addition of benzaldehyde to solutions of VO(salen)$EtOSO_3$, VO(salen)Cl and VO(salen)NCS complexes in dichloromethane was monitored by EPR. However, this did not lead to any significant change in the spectra apart from a decrease in the signal intensity due to the effect of sample dilution (see *Appendix 1, 1.3*). In addition, HPLC, GCMS and LCMS were used to analyse these samples in an attempt to detect traces of benzoic acid, which presumably should be the product of the oxidation process. However, all these techniques failed to find any evidence for benzaldehyde oxidation.

2.5.2 Cyanide as reducing agent

The remaining species that could act as a reducing agent were the cyanohydrin product or cyanide reagent, which could be oxidised, for example, to benzoyl cyanide and cyanogen respectively. Therefore, samples of mandelonitrile and TMSCN were separately added to a solution of VO(salen)NCS complex **23h** in dichloromethane. Immediately after the addition of TMSCN, formation of a large amount of V(IV) species was detected by EPR spectroscopy. In contrast, addition of mandelonitrile to complex **23h** did not lead to any vanadium reduction. The experiment was repeated for all three catalysts **23a**, **23f** and **23h**. The solutions were degassed prior to TMSCN addition, and the evolution of the EPR signal was monitored over a period of two hours at room temperature (**Figure 2.3**) (see *Appendix 1, 1.4*).

A clear trend in the amount of V(V) converted to V(IV) was observed following the order according to the counterion used: NCS > Cl > $EtOSO_3$, which also correlates with the catalytic activity. VO(salen)NCS **23h**, the most active catalyst of the series, showed the largest amount of V(V) reduction (40%), resulting in catalysis dominated by a bimetallic catalyst. VO(salen)$EtOSO_3$ **23a**, for which only 5% of V(V) is reduced to V(IV), must exist predominantly as a monomer, and this will be responsible for most of the catalysis. In the case of VO(salen)Cl **23f**, 20% of V(V) was reduced to V(IV), indicating that both monometallic and bimetallic species are likely to be involved in the catalysis.

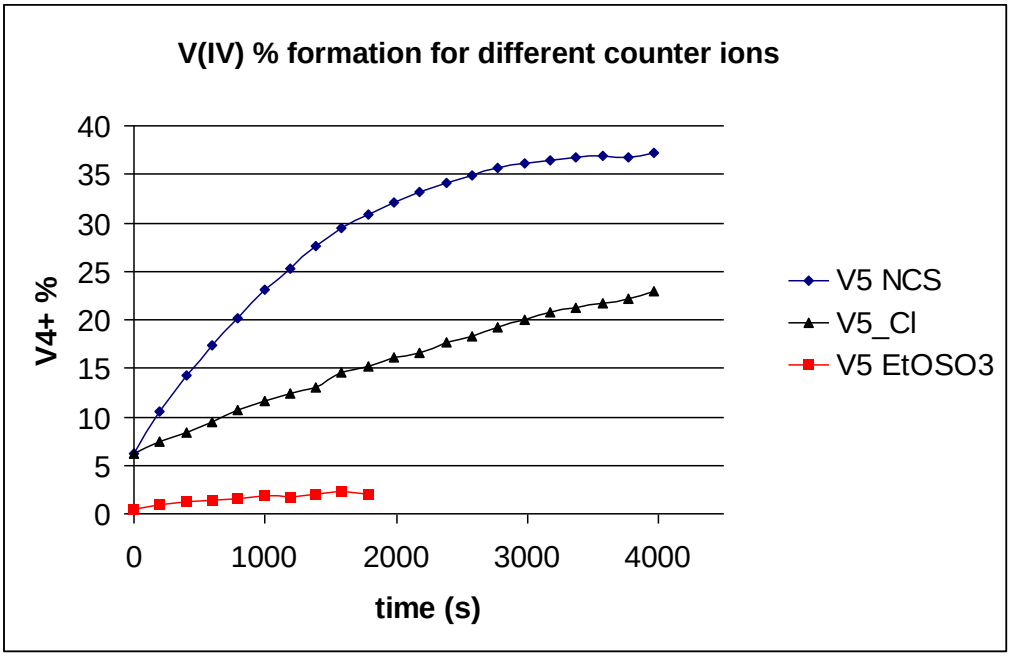

Figure 2.3 The addition of TMSCN to a solution of complex **23a**, **23f** and **23h**. The formation of vanadium(IV) species is monitored.

If cyanide is responsible for the reduction of vanadium(V), then other cyanide sources should give similar results to those obtained using TMSCN. Thus, based on previous reports in which potassium cyanide was found to be a good cyanating agent in asymmetric cyanation reactions catalysed by oxovanadium(V)salen complexes,[40a, 93] a mixture of VO(salen)NCS **23h** and potassium cyanide in dichloromethane was prepared. *Tert*-butanol and water were then added to increase the solubility of the cyanide salt, and the mixture was then subjected to EPR analysis. 16% of V(IV) species formation could be quantified after a period of one hour. Thus, in this case, free cyanide anions are the reducing agent. (see *Appendix 1, 1.5*)

In summary,

- The reduction of V(V) to V(IV) during the asymmetric addition of TMSCN to benzaldehyde has been confirmed and quantified.
- A correlation of V(IV) formation with catalyst activity has been established. A bimetallic catalytic cycle dominates over the monometallic catalytic cycle when complexes with strongly coordinated counterions are used in the catalysis. In contrast, for less coordinating counterions a monometallic cycle dominates.
- Benzaldehyde was not involved in the reduction of vanadium(V) species, whilst cyanide was found to be the reducing agent.
- The catalyst counterion is clearly involved in the redox process.

2.6 Investigation of cyanide oxidation

2.6.1 Possible products of cyanide oxidation

There are many possible compounds that cyanide might be oxidized too. Amongst these are cyanogen, cyanate and carbon dioxide. Most of these species are gases at room temperature and this makes their detection quite a difficult task.

2.6.1.1 FT-IR studies

In view of a literature report[94] on a study of the detection of cyanogen and its derivatives which used gas-phase FT-IR, wherein the reaction was carried out in a gas cell, attempts were made to detect cyanogen using FT-IR spectroscopy. As we did not possess a gas cell, the experiment was carried out in solution. The solution was placed in a FT-IR solution cell made of NaCl, which contains a cavity where the solution is introduced and conveniently sealed. Spectra were then recorded *in situ*. The stretching frequencies of all compounds of interest are localised in the region of 1800 to 2400 cm^{-1}. A background experiment showed that solutions of VO(salen), VO(salen)Cl, and VO(salen)$EtOSO_3$ gave no signal in this region; only VO(salen)NCS with a υ_{max} = 2064 cm^{-1} due to the N=CS stretching absorbed in this region. Therefore, when a large excess of TMSCN was added to these solutions, two new IR bands were detected at υ = 2190 cm^{-1} and υ = 2090 cm^{-1}, which could be assigned to TMSCN and HCN respectively.[94] There was no evidence for the formation of any cyanogen derivatives. However, it is worth noting that the band corresponding to NCS stretching present in the spectrum of VO(salen)NCS prior to TMSCN addition, vanished when TMSCN was added. The isothiocyanate anion has a great affinity for silicon, and it possibly reacted with TMSCN, to form TMS-NCS.

2.6.1.2 GC-MS studies

In order to set up a method and optimise the conditions for cyanogen detection, it was necessary to synthesise some cyanogen. Thus, the gas generated in the reaction of aqueous solutions of copper(II)sulphate and potassium cyanide (**Scheme 2.2**), was carried by a stream of inert gas (N_2) into a cooled solution of dichloromethane as described in the literature.[95] This solution, which was expected to contain cyanogen, was directly injected into a GC-MS system. The chromatogram exhibited a clear peak with retention time 13.54 minutes, which could be assigned to cyanogen by the mass sensitive detector (m/z 52) (see *Appendix 1, 1.6*)

Scheme 2.2 Generation of cyanogen from aqueous copper sulphate and potassium cyanide.

In order to identify the products of the redox reaction between VO(salen)NCS and TMSCN, samples of the reaction mixture were directly injected into the GCMS, which did show a signal for cyanogen. A control reaction in the absence of vanadium complex showed no detectable cyanogen. Moreover, formation of cyanogen could be monitored over time (**Figure 2.4**). The maximum cyanogen concentration was reached after *ca*. 1 hour, consistent with the EPR data for vanadium(IV) formation (*section 2.5.2*). To exclude the possibility of cyanogen formation occurring only in the injection chamber of the GC apparatus, N_2 gas was bubbled through the reaction mixture and the gaseous products carried by the gas were collected in a cold dichloromethane trap. Cyanogen was still clearly detected in the dichloromethane solution (**Figure 2.4**, red dot).

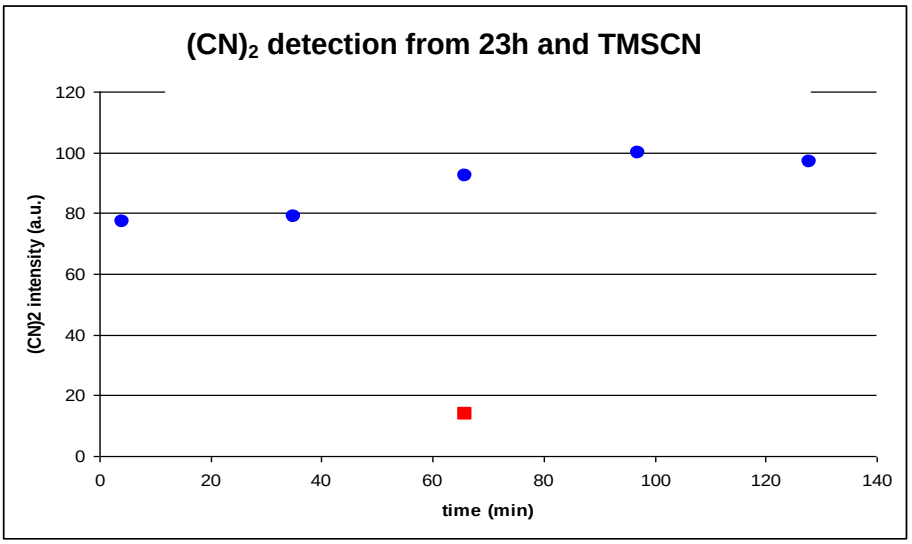

Figure 2.4 (blue dots) cyanogen signal accumulation for the reaction between VO(salen)NCS **23h** and TMSCN in dichloromethane monitored by GC-MS. (red dot) cyanogen signal for the reaction between VO(salen)NCS and TMSCN in dichloromethane, carried by N_2 and collected in a cold trap containing dichloromethane.

2.6.2 How is cyanide oxidised?

2.6.2.1 Attempts to detect cyanide radicals

Cyanide (a soft Lewis base) is not a good ligand for V(V), or for Ti(IV) (both hard Lewis acids), though the latter has been shown to incorporate cyanide in its coordination sphere.[96] In both cases, oxygen is always a preferred ligand. The Cambridge Crystal Structure ConQuest Database provides a few examples of isocyanides bound to V(II), V(III) or V(IV),[97] but none with a direct bond to V(V). Manganese, chromium, iron and ruthenium(salen) complexes have been found to coordinate cyanide, but not vanadium(salen) complexes.[98] This explains the failure of attempts to synthesise the VO(salen)CN complex. In view of this, it was expected that, if VO(salen)CN does form *in situ*, it would rapidly decompose to VO(salen) and a cyanide radical. This radical, an extremely reactive species, can dimerise to form cyanogen (**Scheme 2.3**).

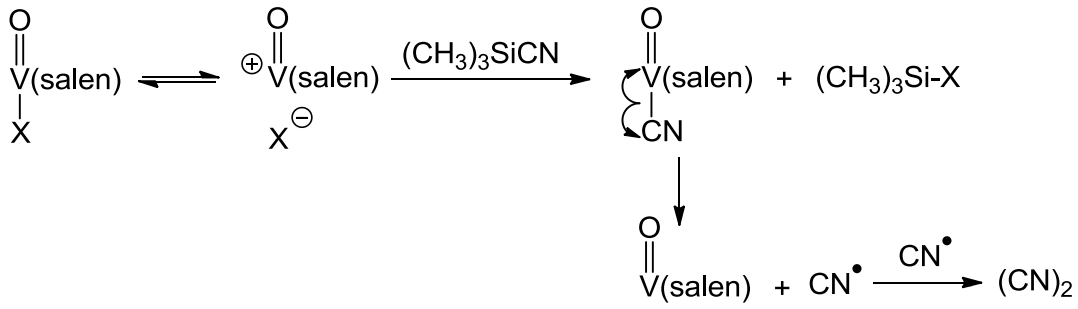

Scheme 2.3 Possible mechanism for the redox reaction, through a radical pathway.

Radicals are usually short-lived species and their detection is not trivial. Nonetheless, their unpaired electron makes EPR a very attractive technique to use. The direct detection of short-lived radicals by EPR is a method that requires special equipment and works with frozen solutions using an argon matrix at temperatures close to absolute zero. Nowadays indirect methods to detect radicals are more often employed. Amongst them, radical traps and scavengers to capture the radical are most commonly used. These species are intended to react rapidly with the cyanide radical, forming a longer-lived species.

2.6.2.1.1 Spin trapping

This technique consists of the rapid addition of short-lived radicals to a diamagnetic spin trap. The product of such an addition is a persistent free radical, with a longer lifetime, which can then be detected by EPR measurements (**Scheme 2.4**).

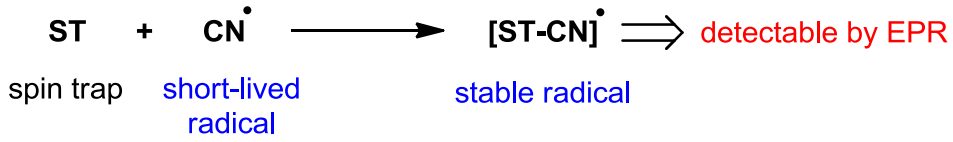

Scheme 2.4 Mechanism by which a spin trap captures a cyanide radical and transforms it into a more stable species.

It must be borne in mind that the observation of an EPR signal does not necessarily indicate that the expected short-lived radical is present. The stable radical adduct may have been formed by a different pathway. In addition, failure to detect radicals does not always mean that their generation is not occurring. If the short-lived radicals form too rapidly, they will react equally rapidly with the spin trap and with the already generated spin adduct (a radical), thus, affecting the stability and lifetime of the spin adduct, which may never be detected, since it will be consumed as it is formed.

5,5-Dimethyl-1-pyrrolidine N-oxide (DMPO), N-*tert*-butyl-α-phenylnitrone (PBN) and 2-methyl-2-nitrosopropane (MNP) are the three spin traps used in this study. As shown in **Table 2.2**, all three belong to the same family of compounds, possessing an N-oxide group in their structure. Hence, their EPR signals will appear in the same spectral region. MNP exists in equilibrium with its dimer and gives a three-line EPR signal on its own. Hence, this was conveniently used as the reference to find the spectral region where the radical adducts will appear.

The experiments were carried out by mixing a solution of spin trap (DMPO, PBN or MNP) in toluene and a solution of complex (**23a**, **23f** or **23h**) in dichloromethane. The mixture was degassed (treatment with N_2), and TMSCN was then added to it. Immediately thereafter, EPR spectra were recorded every 5 minutes over a period of 15 to 30 minutes to observe the evolution of the EPR signal with time.

Spin trap	Spin trap structure	Spin adduct
5,5-dimethyl-1-pyrrolidine N-oxide (DMPO)	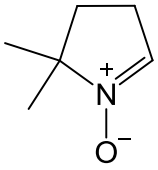	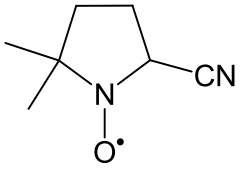
N-*tert*-butyl-α-phenylnitrone (PBN)	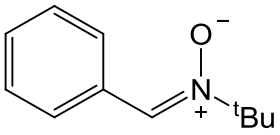	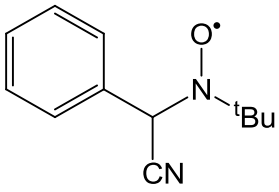
2-methyl-2-nitrosopropane (MNP)	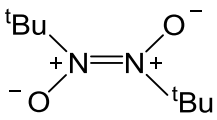 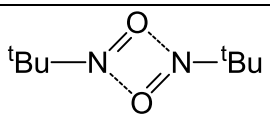	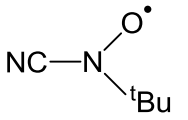

Table 2.2 Structures of spin trap and their spin adducts with cyanide radicals

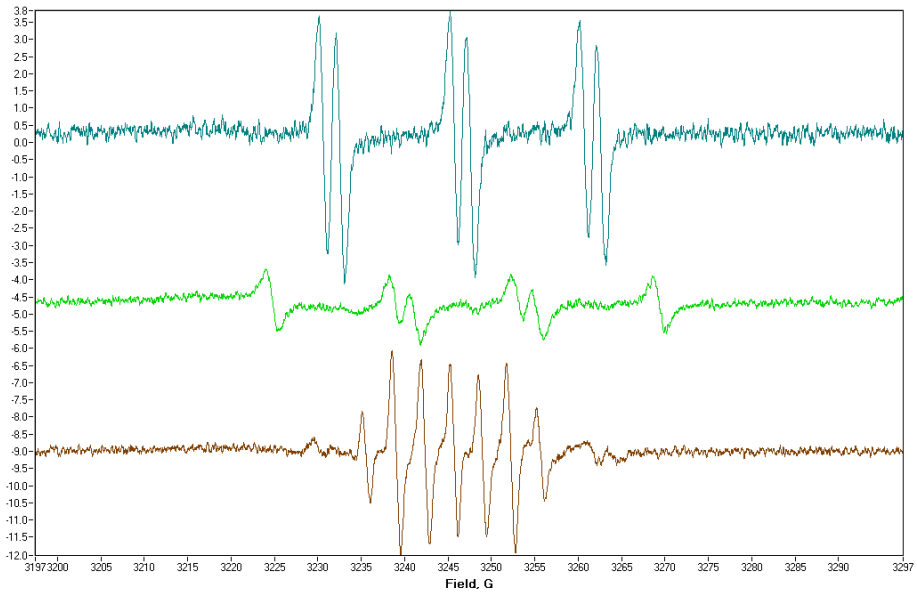

Figure 2.4 Top and middle: PBN-CN and DMPO-CN adducts generated by the reaction between VO(salen)EtOSO$_3$, TMSCN and the corresponding spin trap in dichloromethane. The bottom spectrum is the oxidised form of DMPO (DMPOx), observed when mixing the vanadium complex with the spin trap in the absence of TMSCN.

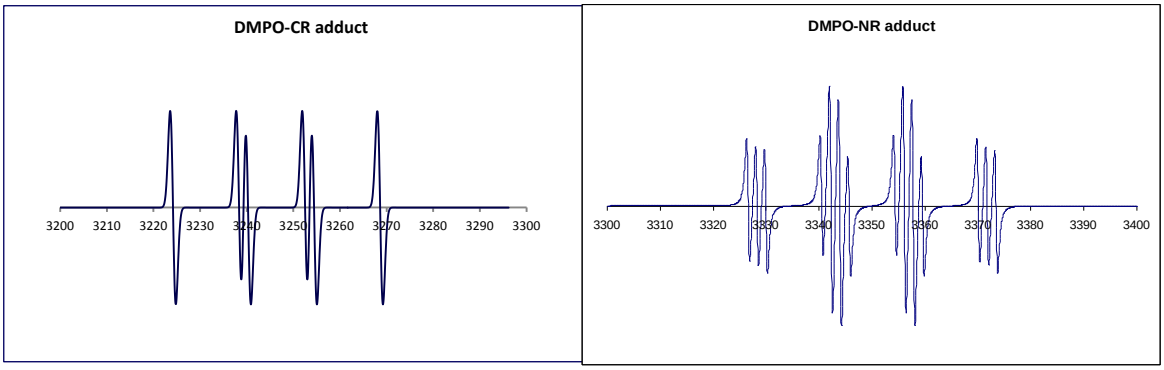

Figure 2.5 Simulations of DMPO-CN and DMPO-NC respectively.

No spin adduct was detected when MNP was used, but a spin adduct was clearly detected for PBN and DMPO (**Figure 2.4**). Both gave characteristic six-line signals corresponding to a carbon-centred radical, rather than a nitrogen-centred radical (see simulations **Figure 2.5**). The spacing of the six lines of the two adducts (CN-PBN, CN-DMPO) are different and this reflects the structural differences between them even though the spin trap contains the same reactive centre ($C=N^{+}\text{-}O^{-}$). All three oxovanadium(V)salen complexes (**23a**, **23f** and **23h**) led to the formation of the same CN-adducts with coupling constants of a_N = 14.15 and a_H = 16.24 Gauss for the DMPO adduct, and a_N = 15.02 and a_H = 1.87 Gauss for the PBN adduct. The coupling constants of PBN are comparable to and consistent with values present in the literature for a PBN-CN adduct,[99] but this is not the case for the DMPO adduct.[100] However, the solvent used in our experiments and that reported in the database was not the same. Thus, in order to eliminate discrepancies due to different reaction media, a UV irradiation test was carried out. A solution of TMSCN in dichloromethane was mixed with a solution of DMPO spin trap in toluene and irradiated with a UV lamp. This provided an alternative synthesis of the DMPO-CN spin adduct and gave exactly the same coupling constants as those observed using VO(salen)X complexes (**Figure 2.6**). This unambiguously proved the formation of the DMPO-CN adduct in the presence of VO(salen)X complexes.

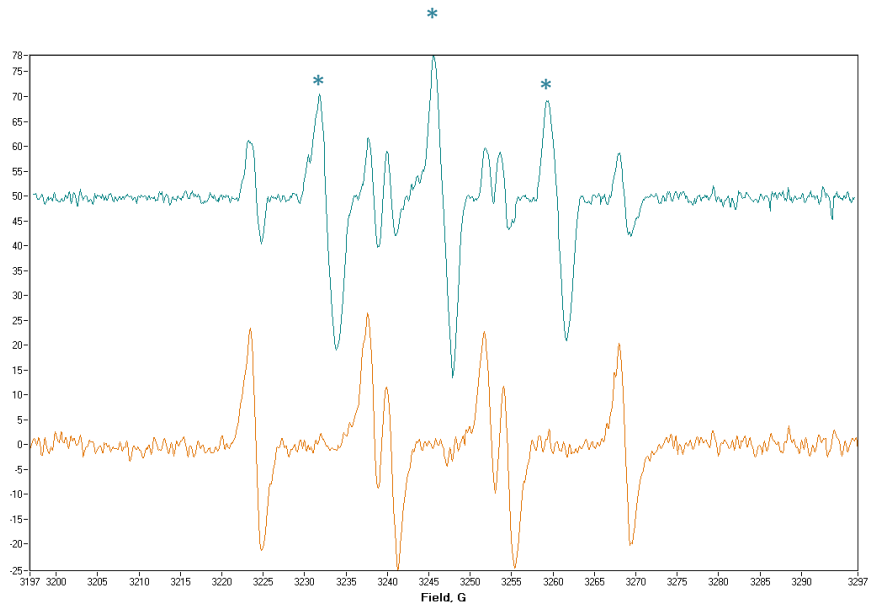

Figure 2.6 EPR spectra of the spin adduct formed in a solution (toluene/dichloromethane) of DMPO and TMSCN irradiated by UV light (top), and the spin adduct generated during the reaction between DMPO and TMSCN in the presence of VO(salen)$EtOSO_3$ in the same solvent media (bottom). * The three more intense lines are a nitroso compound formed from DMPO.

The stability of the spin adducts was found to be strongly dependent on the counterion. In fact, when VO(salen)NCS was used, the radical could not be efficiently captured by the spin trap resulting in the rapid disappearance of the spin adduct signal. A similar effect was observed when VO(salen)Cl was used, however, the rate at which the signal decreased was not as pronounced. In contrast, VO(salen)$EtOSO_3$ slowly generated cyanide radicals which permitted their efficient capture and the spin trap could sustain a constant rate of CN-adduct formation. The EPR signal intensity thus increases to a maximum after 30 minutes (see *Appendix 1, 1.7*). These results show that the nature of the counterion is directly related to the rate of cyanide radical formation.

It is clear from the above results that a CN-adduct is being formed. However, all the pathways by which this can be created have to be considered. The presence of DMPOx (see **Figure 2.4**, bottom spectrum), formed when solutions of catalyst and DMPO were mixed together in the absence of TMSCN suggests that the vanadium(V) complex, being a good oxidizing agent, can oxidise DMPO. The DMPOx can then undergo nucleophilic addition with a cyanide anion to give the same DMPO-CN adduct (**Scheme 2.5**). Previous studies reported in the literature[101] support the formation of spin adducts through multiple pathways, in which reaction with anions or radicals leads to the formation of the same spin adduct.

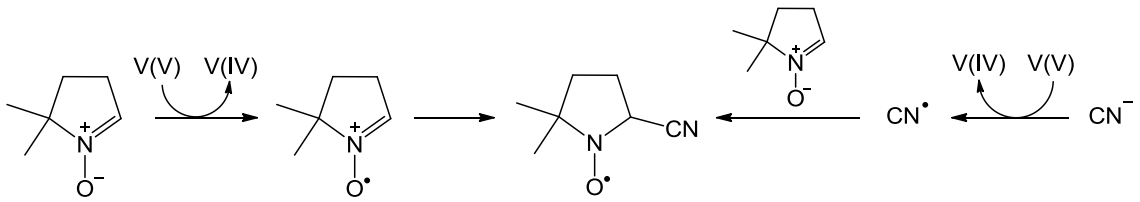

Scheme 2.5 Formation of DMPO-CN spin adduct by pathways involving cyanide anions and cyanide radicals.

2.6.2.1.2 TEMPO experiments

In order to ascertain if the observed CN-spin trap is formed through an anionic or radical pathway or by both routes, TEMPO (2,2,6,6-tetramethyl-piperidin-1-oxyl) was used as a radical scavenger. This compound is a stable radical itself, which makes it suitable for this purpose. The nitroxyl group will react with any cyanide radical (**Scheme 2.6**), resulting in the decay of the TEMPO EPR signal. This would support the hypothesis that cyanide radicals are generated *in situ*.

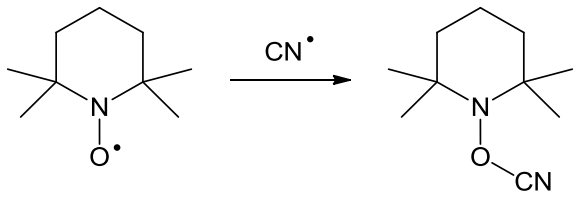

Scheme 2.6 Cyanide radical capture using TEMPO as a scavenger.

Initially, TEMPO was mixed separately with each of the reaction components to see if they could lead to decay of the TEMPO EPR signal by themselves. The spectrum of a solution of VO(salen)X and TEMPO was virtually the same as that of TEMPO itself. When TEMPO was mixed with VO(salen), line broadening and a decrease in the signal intensity was observed, though this effect can be accounted for by the simultaneous presence of two paramagnetic species and their interaction. In contrast a mixture of TEMPO and TMSCN led to a significant decrease in EPR signal intensity. This can be explained by the presence of traces of hydrolysed TMSCN due to atmospheric moisture. Nevertheless, after the initial decrease in signal intensity, the signal remained unaltered versus time (see *Appendix 1, 1.8*).

Subsequently, the EPR signal of a reaction mixture containing VO(salen)NCS, TEMPO, benzaldehyde and TMSCN was monitored. A decrease in the TEMPO EPR signal intensity with time was observed, and there was no detectable line broadening (**Figures 2.7** and **2.8**). This suggests that the observed signal intensity decay was real

and was not due to interactions with V(IV) species. In principle, these results suggest that TEMPO-CN is formed *in situ*. However, no direct evidence for the formation of TEMPO-CN species could be obtained by electron impact GC mass spectrometry (see *Appendix 1, 1.8*).

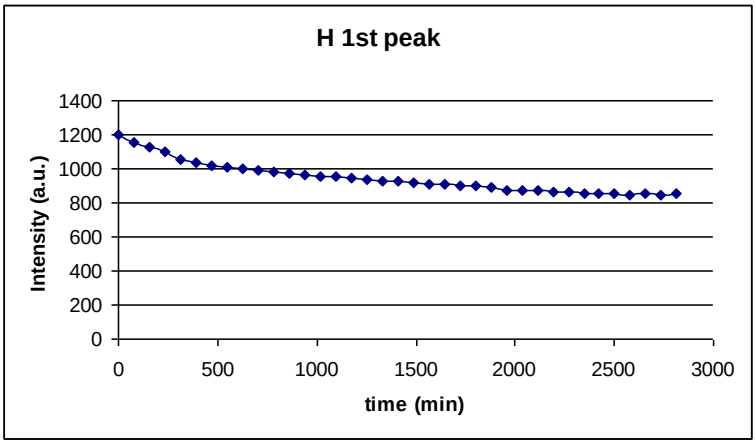

Figure 2.7 TEMPO EPR signal intensity during the cyanosilylation of benzaldehyde catalysed by VO(salen)NCS.

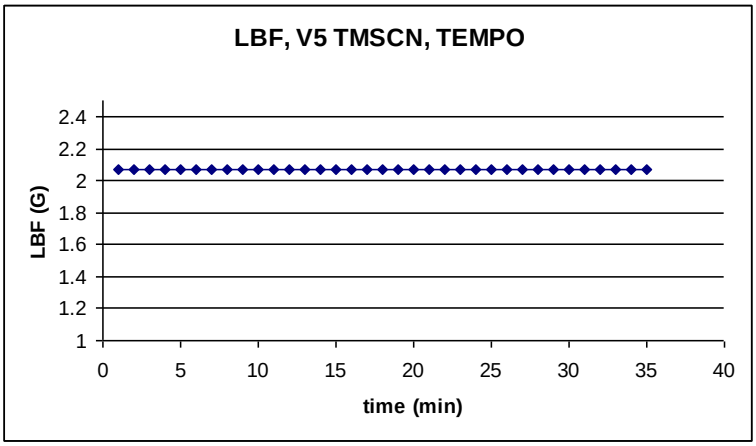

Figure 2.8 TEMPO EPR line width during the cyanosilylation of benzaldehyde catalysed by VO(salen)NCS.

2.6.2.1.3 Styrene oligomerisation

At this stage there was not enough evidence to unambiguously say that cyanide radical formation was occurring. Therefore, a less common but equally effective method to indicate carbon-centred radical formation was used: styrene polymerisation (**Scheme 2.7**).[102] This reaction requires a carbon-centred radical to initiate the polymerisation process. Thus, the presence of a radical source, would lead to polymer generation.

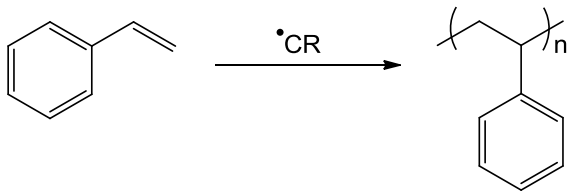

Scheme 2.7 Styrene polymerisation initiated by a carbon-centred radical.

In a sealed EPR tube, the reaction of VO(salen)NCS with TMSCN was carried out in the presence of styrene. If any polymerisation occurred, the solution viscosity would increase which would slow down the tumbling of the vanadium(IV)(salen) complex, resulting in EPR signal distortion. A comparison of spectra of a solution of VO(salen) complex and the reaction mixture, both in the presence of styrene, are shown in **Figure 2.9** after 40 minutes, 2.5 hours and 18 hours.

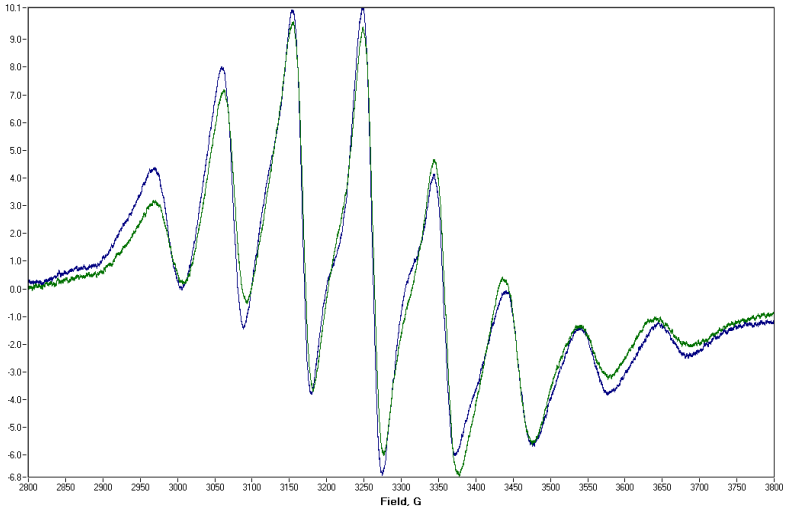

A

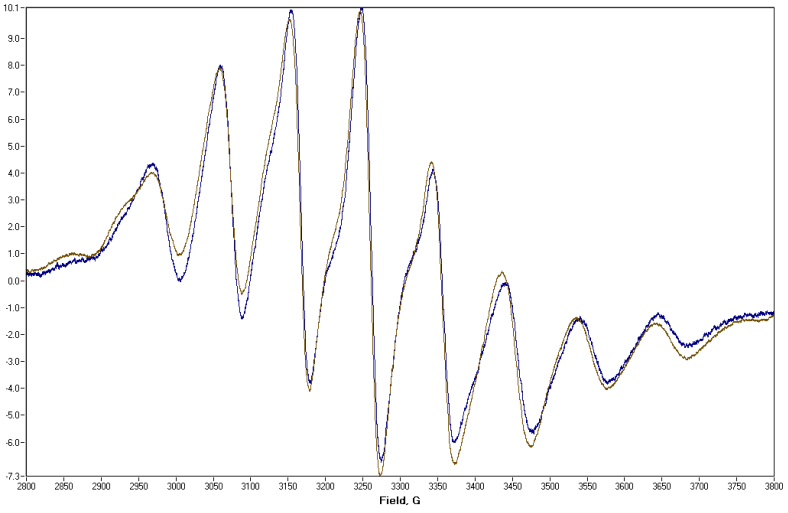

B

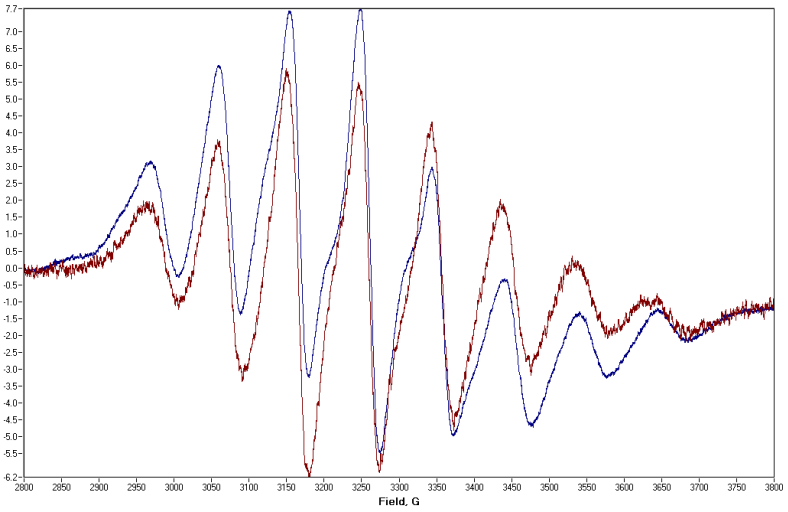

C

Figure 2.9 EPR spectra of a mixture of VO(salen) in styrene (blue) and a mixture of VO(salen)NCS and TMSCN in styrene after 40 min.(A), 2.5 hours (B) and 18 hours (C).

The spectra are all very similar, and the minor variations are considered to be due to a loss of solvent over the long reaction times. It was observed that the solution gradually turned brown, but the viscosity appeared to remain constant, even after a period of 18 hours. A sample of this reaction mixture was analysed by mass spectrometry, and styrene polymerisation was not observed. The brown colour could be associated with catalyst decomposition. To prove that cyanide radicals initiate styrene polymerisation, a control experiment was carried out. In a small flask, a solution of TMSCN in styrene was irradiated with UV light (λ = 254 nm) for 18 hours. A significant increase in viscosity and the presence of broad bands in the aliphatic and aromatic regions in the ^{1}H NMR spectrum of the crude material indicates that cyanide radicals could initiate styrene polymerisation. Overall therefore, the polymerisation results provide no evidence for the homolytic cleavage of the V-CN bond of VO(salen)CN species.

2.6.2.1.4 Reaction of cyanide radicals with an electron-rich alkene

A final attempt to trap cyanide radicals was made using electron-rich vinyl ethers. The electron-rich nature of the alkene group makes it a potential candidate to undergo reaction with electron-deficient radicals. The substrate chosen was vinyl ether **91** which, after undergoing radical addition could generate a bromine radical and at the same time form vinyl nitrile **92**. The bromine radical could perhaps reoxidise the V(IV) complex to V(V) which would start the catalytic cycle again (**Scheme 2.8**).

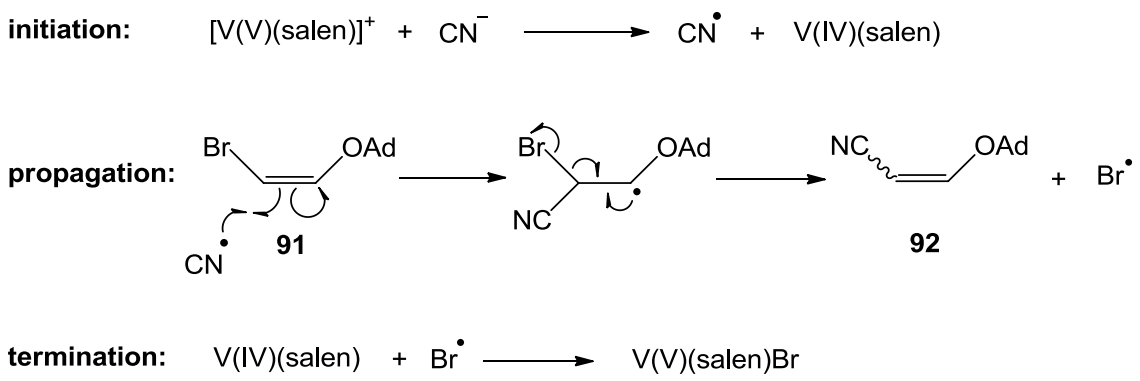

Scheme 2.8 Cyanide radical capture by reaction with an electron-rich alkene, and possible catalyst reoxidation.

A two step synthesis reported by Pericàs *et al.*,[103] was used for the preparation of Z-1-(1-adamantyloxy)-2-bromoethene. Thus, bromination of a solution of ethyl vinyl ether (**93**) in chloroform followed by the addition of 1-adamantanol, formed the mixed acetal compound 1-(1-adamantyloxy)-2-bromo-1-ethoxyethane **94**. Treatment of **94** with phosphorus pentachloride in dichloromethane led to the chemoselective cleavage of the ethoxy group. Finally, triethylamine was added, resulting in the formation of Z-1-(1-adamantyloxy)-2-bromoethene **91** (**Scheme 2.9**).

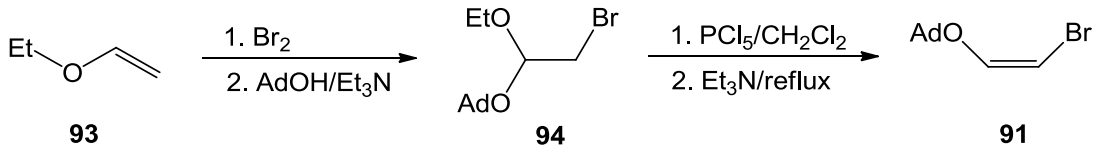

Scheme 2.9 Two-step synthesis of (Z)-1-(1-adamanyloxy)-2-bromoethene.

Vinyl ether **91** was then used in attempts to trap cyanide radicals. Thus, one equivalent of TMSCN was added to a solution of **91** and VO(salen)X (10 mol%) in dichloromethane. After a number of attempts, using three different oxovanadium(V)salen complexes (**23a**, **23d** and **23g**) at different temperatures (0 to 25 ^{o}C), the only products that could be isolated were the unreacted vinyl ether and 1-adamantol.

In conclusion, all attempts to detect cyanide radical formation during VO(salen)X catalysed cyanohydrin synthesis were unsuccessful, which suggested that free radicals may not be involved in the mechanism.

2.7 Possible mechanism: a non-radical pathway

The lack of evidence for a radical pathway, but the detection of cyanogen when VO(salen)X is reacted with TMSCN led to the consideration of a non-radical mechanism for the redox reaction (**Scheme 2.10**). Initially, a simple ion exchange between complex **23** and TMSCN forms TMS-X species and complex VO(salen)CN (**95**). Two molecules of **95** associate to form the dimer **96** (there is literature precedent for the formation of oligomeric VO(salen) complexes)[104] which rapidly eliminates cyanogen intramolecularly, forming two VO(salen) units. Atmospheric oxygen can then reoxidize V(IV) to regenerate V(V) complexes which can reenter the redox cycle. This process also allows the formation of mixed-valence bimetallic species **86**. Thus, under the reaction conditions, VO(salen)X complexes can combine with VO(salen) to form a highly active bimetallic catalyst for the asymmetric synthesis of cyanohydrins. Complex **86** is the dominant catalyst when the counterion is strongly coordinating, whereas less coordinating anions favour a mechanism for cyanohydrin synthesis catalysed by monometallic species. In other words, the counterion controls the formation of VO(salen) species and hence the balance between monomeric and dimeric species, thus directing the catalysis through the monometallic or bimetallic catalytic cycle.

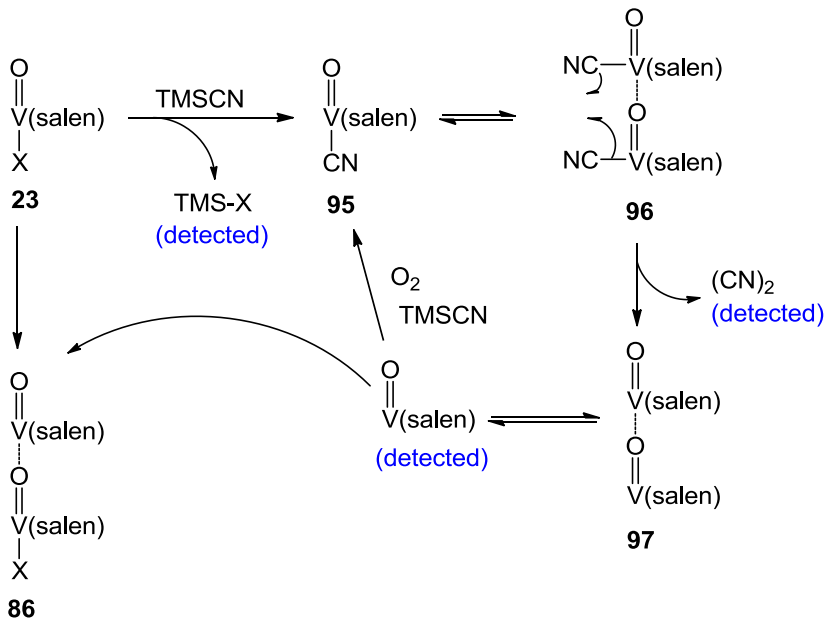

Scheme 2.10 Possible mechanism for the redox process in conjunction with the mixed-valence more active bimetallic catalyst formation.

2.8 The role of the counterion in the reduction of vanadium(V)(salen) complexes.

According to the mechanism proposed in **Scheme 2.10** for the redox process, during the first step, TMSCN reacts with the counterion X^- to generate species such as TMS-X. The ability of the counterion to bind to the silicon atom could be the key factor for the activation of TMSCN; and thus would promote the reduction of vanadium(V)(salen) complexes to vanadium(IV)(salen).

To support this hypothesis, a study of the ability of the counterion X^- to form TMS-X species was carried out. GCMS analysis of solutions of VO(salen)NCS and VO(salen)$EtOSO_3$ with TMSCN in dichloromethane showed the presence of TMS-NCS, but not TMS-O_3SOEt (see *Appendix 1, 1.9*). These results are consistent with the EPR data and suggest that the activation of TMSCN by the counterion is essential for the generation of vanadium(IV) species and as a consequence this favours a bimetallic catalytic cycle over a less efficient monometallic one, due to the conjugation of two VO(salen) units (one in each oxidation state +4 and +5). The low affinity of $EtOSO_3^-$ for silicon was evident since TMS-OSO_3Et could not be detected by GCMS analysis. As a result, the generation of V(IV) was almost negligible compared to the use of VO(salen)NCS (See **Figure 2.3**, *section 2.5.2*)

2.9 Conclusions

The existence of a redox cycle during VO(salen)X catalysed asymmetric cyanohydrin synthesis could be demonstrated by detection of vanadium(IV) species during the catalytic process using electron paramagnetic resonance spectroscopy. Vanadium(IV) species are generated by reaction with cyanide anions rather than benzaldehyde. As a result, cyanide is oxidised to cyanogen *via* a non-radical mechanism at the same time that the oxovanadium(V)(salen) complex is reduced to oxovanadium(IV)(salen). The latter can then combine with a non-reduced oxovanadium(V)(salen) unit to form a highly active bimetallic catalyst. The presence of oxygen is essential for the reoxidation of vanadium(IV) to vanadium(V) in order to avoid catalyst deactivation during the course of the reaction. The counterion has a significant effect on the catalysis, not only in the rate determining step, but also in the activation of TMSCN to form VO(salen)CN. When the counterion X has low affinity towards silicon, the activation of cyanide does not occur and the VO(salen)X complex as a monomer is mainly responsible for the catalysis.

The idea of cyanide activation by the counterion X^- led us to think about the importance of electronic properties, not only during the redox process, but also during the actual formation of cyanohydrins. This suggested that, the counterion might be acting as a Lewis base activating the TMSCN, whilst the metal(salen) complex acts as a Lewis acid, activating the aldehyde. Thus, further investigations of the influence of the Lewis basicity of the counterion on the rate of asymmetric cyanohydrin synthesis were carried out and will be discussed in the next chapter.

3 Lewis acid – Lewis base catalysis in the asymmetric addition of trimethylsilyl cyanide to aldehydes

3.1 Introduction

Vanadium(V)(salen) complexes, in common with many other transition metal complexes, have excellent Lewis acidic properties. For this reason, all the previous mechanistic studies on asymmetric cyanohydrin synthesis and hence all the proposed intermediates involved in the catalytic cycle focused on the activation of the aldehyde.

At the start of this project, the counterion X was thought to be involved only in the rate-determining step of the catalytic mechanism. However, the results reported in Chapter 2 have shown that it has a wider influence in the catalytic process. The detection of TMS-X species by GCMS, while investigating the redox process (*Section 2.8*), provided the first evidence of the counterion being involved in cyanide activation. Hence, the importance of a Lewis base contribution to the catalysis by the counterion was considered. Catalysts with both Lewis acidic and Lewis basic sites have been shown to be the most effective catalysts for asymmetric cyanohydrin synthesis, as they can activate both the aldehyde and cyanide simultaneously.[105] A good example of this dual activation is the *bis*-*N*-oxide organocatalyst **43** developed by Feng *et. al.* (**Scheme 3.1**).[66] This compound was designed to act as a chiral Lewis base catalyst producing chiral cyanide by the interaction of TMSCN with the *N*-oxides, which have been shown to be excellent trimethylsilyl cyanide activators; however, one of the secondary amides can also activate the aldehyde, thus acting as a Brönsted acid.

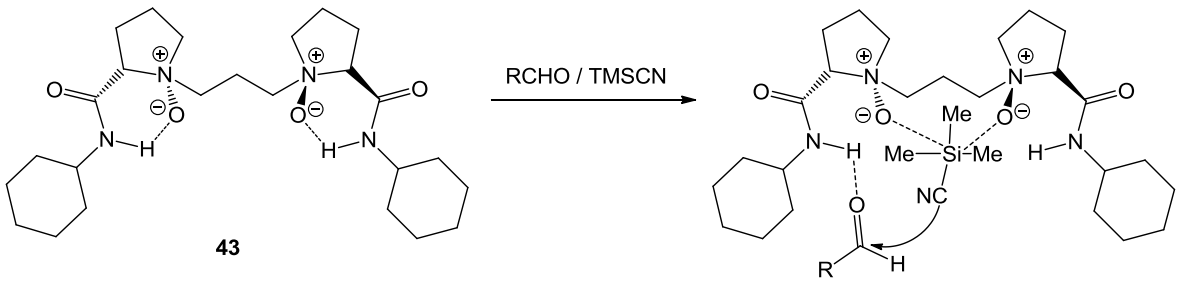

Scheme 3.1 Catalytic cyanosilylation of aldehydes in which the aldehyde and TMSCN are simultaneously activated by a bifuntional catalyst.

This bifunctional *bis*-*N*-oxide catalyst has both acidic and basic active sites incorporated into the same structure. However, this is not the usual approach to dual activation. Lewis acid and Lewis base sites are more commonly found as two separate entities, one or both of which have to be optically active in order to transfer chiral information to the substrate. An excellent example is the magnesium(bisoxazolidine) complex **61** along with bisoxazolidine **62** developed by Corey.[106]

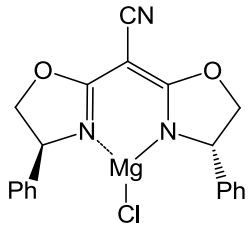

61

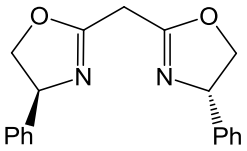

62

The activation of TMSCN can occur through various mechanisms. In the two examples just mentioned, the moiety responsible for the activation of TMSCN is a nucleophile (a heteroatom) which by coordination to the silicon atom promotes the formation of hypervalent silicon species (**Scheme 3.2, A**). However, there are other methods to activate the TMSCN, which do not necessarily involve a hypervalent silicon complex. Phosphine oxides, well known Lewis base catalysts, have been used as additives in many catalytic systems in order to enhance the catalytic activity.[54b, 71, 83a, 89, 107] In a communication in 2004, by the team led by Corey, a new approach to the activation of TMSCN was introduced. Corey was studying the effect of adding phosphine oxide to the reaction of TMSCN addition to aldehydes catalysed by oxazaborolidinium catalyst **98**. Phosphine oxide addition resulted in a significant improvement in both the catalytic activity and the asymmetric induction. In view of these results, Corey *et al.* carried out spectroscopic experiments which suggested the formation of a $Ph_3P(OTMS)(N{=}C{:})$ adduct (**Scheme 3.2, B**).[79] A final and less common way to activate TMSCN is by coordination to a metal. Cyanide anions are found in many organometallic compounds as a passive ligand; however, these can in some cases be involved in a carbon-carbon bond formation such as cyanohydrin synthesis (**Scheme 3.2, C**). A first example of this phenomenon is the alkoxytitanium complex **99** developed by Narasaka .[108] However, the best example of this type is bimetallic titanium(salen) complex **20** developed in our group. In the transition state,

one of the titanium ions bears the aldehyde and the other the cyanide. Hence, these two units cooperate to form the cyanohydrin by an intramolecular nucleophilic addition.[38]

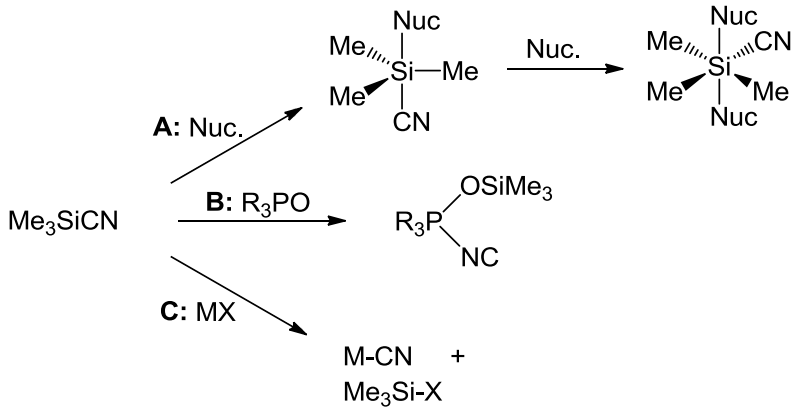

Scheme 3.2 Activation of trimethylsilyl cyanide by Lewis base catalysis.

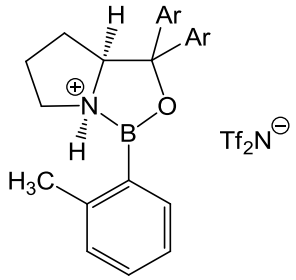

98

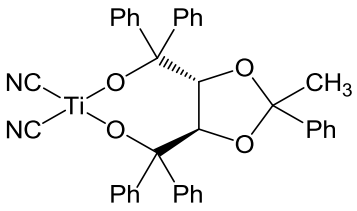

99

In view of the potential importance of Lewis base catalysis in the asymmetric addition of TMSCN to aldehydes, this chapter will focus on the particular case of VO(salen)X complexes. Thus, a study of the basicity of the counterion and its influence in the catalytic activation of TMSCN as well as an investigation of the relative importance of Lewis basicity and Lewis acidity was undertaken.

3.2 The basic character of the counterion

The ability of the counterion X^- to coordinate to the metal is a clear sign of its Lewis basic character. This supports the hypothesis of the recoordination of the counterion with cyanohydrin liberation being the rate limiting step in the catalytic cycle (**Scheme 3.3**). This also explains why the complex with $CF_3SO_3^-$ as the counterion which is unable to coordinate to the vanadium ion, is catalytically inactive even though it has the most Lewis acidic vanadium centre. The ability of the counterion to

coordinate to the silicon atom of TMSCN is expected to follow the same trend; and thus will further contribute to lowering the energy barrier during the transition state in which the cyanohydrin is formed.

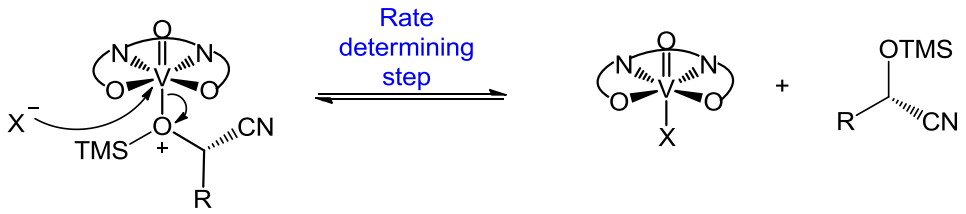

Scheme 3.3 Rate determining step of the catalytic cycle.

An investigation of the nucleophilic effect of the counterion was carried out in our group.[44b] The experiment examined the effect of the addition of an excess of the counterion to the catalytic reaction. VO(salen)Cl **23f** was used as the catalyst and tetrabutylammonium chloride as the source of additional chloride. When chloride was present in excess, the results showed an increase in the rate of the reaction without affecting the enantioselectivity, however a higher concentration of the chloride anion led to a decrease of the reaction rate (**Figure 3.1**). This was consistent with the chloride anion attaching to the complex and subsequent release of the cyanohydrin being the rate determining step. However, the addition of a larger amount of chloride, accelerated this step, so that it was no longer rate-limiting. As a result, competition between chloride and the aldehyde for the vanadium's sixth coordination site in the early steps of the catalytic cycle becomes rate limiting. This inhibits substrate coordination, and results in a decrease in the rate of reaction. A control experiment in which tetrabutylammonium chloride was used as a catalyst in the absence of VO(salen)Cl, showed that the reaction was 150 times slower. This agrees with the unaffected enantioselectivity, since the non-asymmetric reaction cannot compete with the asymmetric reaction catalysed by VO(salen)Cl. This indicates that chloride is not able to effectively coordinate to the silicon and activate the cyanide.

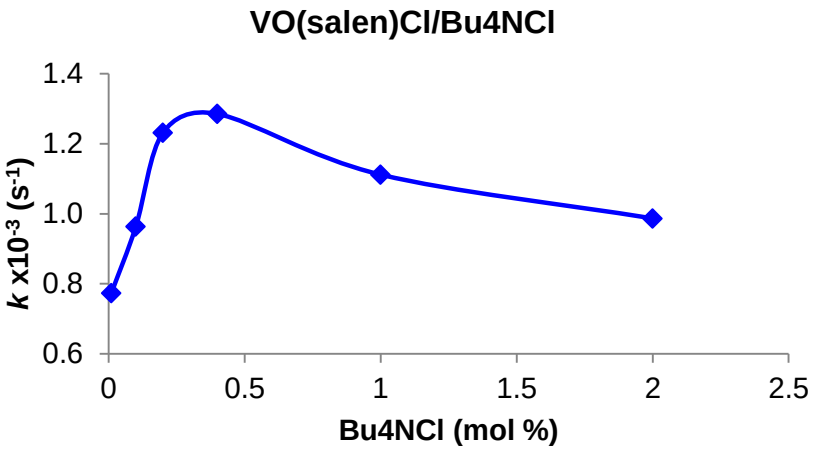

Figure 3.1 The contribution of an excess of Cl^- counterions to the rate of the asymmetric addition of TMSCN to benzaldehyde catalysed by VO(salen)Cl, with Bu_4NCl as the source of the added chloride (0.01-2 mol%). The enantioselectivity remains unaffected at 93±3 % ee.

In view of these results, it was decided that this experiment should be repeated using isothiocyanate as the counterion since VO(salen)NCS **23h** is the most active of the VO(salen)X series of catalysts. In contrast to the previous case, the control experiment when tetrabutylammonium thiocyanate was used alone, showed pronounced catalytic activity. The higher affinity of isothiocyanate for silicon and hence the formation of species such as $[SCN\text{-}TMS\text{-}CN]^-$ can explain this result. Furthermore, a loss of enantioselectivity was observed when the isothiocyanate concentration was increased in the presence of a fixed amount of VO(salen)NCS (**Figure 3.2**). This supports the hypothesis that the counterion is directly involved in the activation of TMSCN, and hence the racemic reaction begins to show.

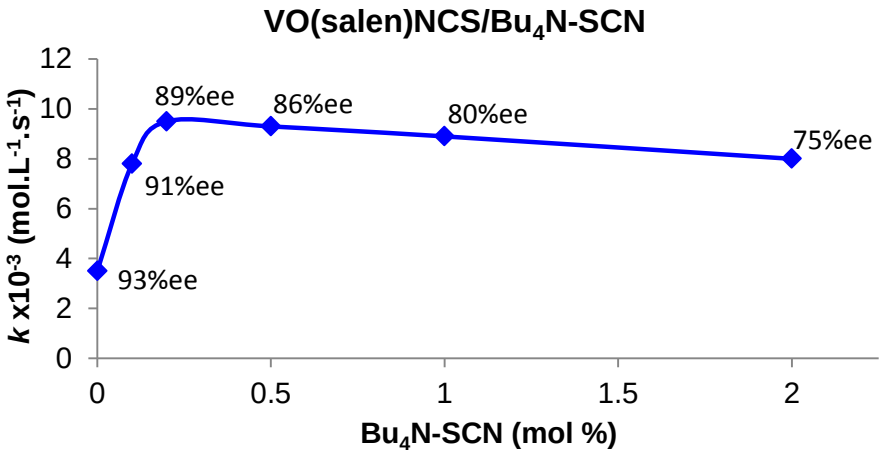

Figure 3.2 Contribution of an excess of the counterion NCS to the rate of the asymmetric addition of TMSCN to benzaldehyde catalysed by VO(salen)NCS.

In conclusion, the VO(salen)X catalyst is believed to dissociate the X^- ligand during the catalytic cycle which leads to the formation of highly active $[VO(salen)]^+$ species. This cationic complex contains a highly Lewis acidic metallic centre, due to its positive charge, which is responsible for aldehyde activation. At the same time, formation of a Lewis base (X^-) occurs, and depending on its basic character, this could enable cyanide activation by coordinating to the silicon of TMSCN. Taking this into account, it would be expected that the catalysts bearing the least coordinating counterions which are unable to coordinate to the silicon, will perform the catalysis entirely by Lewis acid catalysis, which would be consistent with a monometallic catalytic cycle wherein only the aldehyde is activated. On the other hand, the catalysts bearing the most coordinating counterions, are expected to have a degree of Lewis base character, which added to the already established Lewis acid character of the metal centre explains the dual activation of aldehyde and cyanide proposed to occur in the bimetallic catalytic cycle.

3.3 Relative importance of Lewis acidity and Lewis basicity in the VO(salen)X catalytic system

3.3.1 Introduction to the Hammett equation

A method which can be used to quantify the importance of Lewis acid and Lewis base catalysis during the cyanosilylation of aldehydes using VO(salen)X complexes as catalysts is to study the electronic effects of an array of substituents (X) relative to hydrogen. This will give information on the changes of the free energy relationship of the transition state relative to the reactant state of a particular bond formation; in this case, the formation of the C-C bond which will lead to the formation of the cyanohydrin. These X groups must be appropriately placed into the reagent, close enough to the reaction centre in order to provide an electronic effect to it, but without having a steric influence on the reaction.

There are two classes of free energy relationships. Class I or Bronsted free energy relationships are those in which the rate of a specific reaction is directly compared to the equilibrium constant of the same process ($\log k = a \cdot \log K_{eq} + b$). This is applicable only to proton transfer reactions, since the measurement of equilibrium constants becomes more difficult when these diverge from a simple K_a (HA). Therefore, a Class II free energy relationship is used instead. This relates the rate or equilibrium

constant of a studied reaction to the rate or equilibrium constant of another unconnected but similar reaction (($\Delta G = a \cdot \Delta G_s + b$), where $\Delta G = \log k$ or $\log K_{eq}$)

The Hammett equation is the first formulated Class II free energy relationship.[109] Hammett observed that a linear correlation exists between the reactivity of a *para*- or *meta*- substituted phenyl derivative and the proton dissociation constant (pK_a) of the correspondingly *para*- or *meta*- substituted benzoic acid (**Scheme 3.4**) (Equation (1)-(4)). The σ_x values ($\sigma_x = pK_a^H - pK_a^X$) were then determined and tabulated for a wide range of substituents with different polarities.

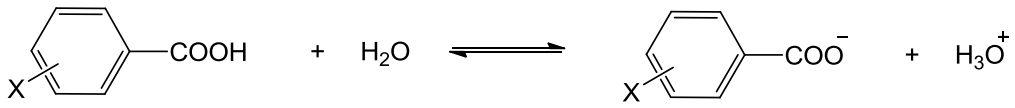

Scheme 3.4

$$\text{Log}(k_X) = -\rho\, pK_a^X + C \qquad (1)$$

$$\text{Log}(k_H) = -\rho\, pK_a^H + C \qquad (2)$$

$$\text{Log}(k_X) = \rho\, (pK_a^H - pK_a^X) + \log(k_H) \qquad (3)$$

$$\text{Log}(k_X) = \rho\, \sigma_x + \log(k_H) \qquad (4)$$

The different nature of these substituents will bring about changes in the transition state stability, and this will result in a change in the rate of the reaction, which can be experimentally measured.

3.3.2 Hammett plot analysis

In order to undertake a Hammett correlation study on our catalytic system, $VO(salen)EtOSO_3$ (**23a**) and VO(salen)NCS (**23h**) complexes were chosen as the least and most active complexes respectively, as well as being representative examples of catalysts performing the catalysis through monometallic and bimetallic pathways respectively.

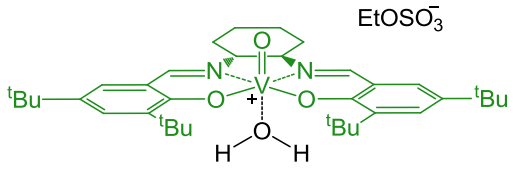

23a

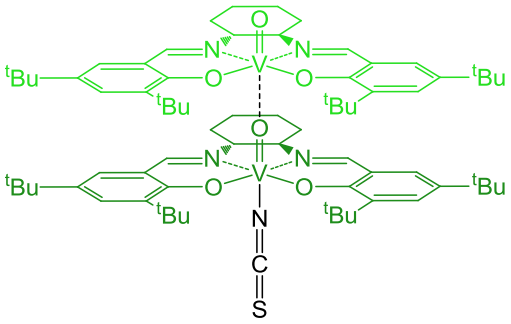

22-23h

Due to the ability of the metal complex to activate the aldehyde, a Hammett plot was constructed by using a series of *para*- and *meta*-substituted benzaldehyde derivatives. Thereby, if the Lewis acidity of the catalyst is dominant in the catalytic process, a non-zero reaction constant will be observed in the Hammett plot. In contrast, if the catalyst functions predominantly as a Lewis base, activating the TMSCN, then the electronic nature of the *para*- and *meta*-substituted benzaldehyde will not affect the reaction rate and a reaction constant of approximately zero would be expected (**Scheme 3.5**).

Two steps are involved in Lewis acid-catalysed cyanohydrin formation (**Scheme 3.5 A**). The first is the coordination of the aldehyde to the complex. The metal ion will withdraw electron density from the carbonyl, generating a partial positive charge on the carbon atom. This process will be favoured by electron donating substituents *para* and *meta* to the carbonyl group, thus giving a negative reaction constant on the Hammett plot. The second step is the nucleophilic attack, in which the cyanide donates electron density to the carbonyl giving rise to the product formation. In contrast to the previous step, a lack of electron density on the carbonyl group will favour the nucleophilic attack, thus giving a positive reaction constant on the Hammett plot. Hence, an electron deficient aldehyde will pull electron density from the cyanide to the carbonyl, therefore, the transition state will be more evolved towards the product, whereas, an electron rich aldehyde will build-up a negative charge on the carbonyl, discouraging the nucleophilic attack, which results in an earlier transition state. Both steps are in competition. Thus, the Hammett plot will inform which process, the coordination of the aldehyde to the metal, or the nucleophilic attack, shows a greater effect on the catalysis.

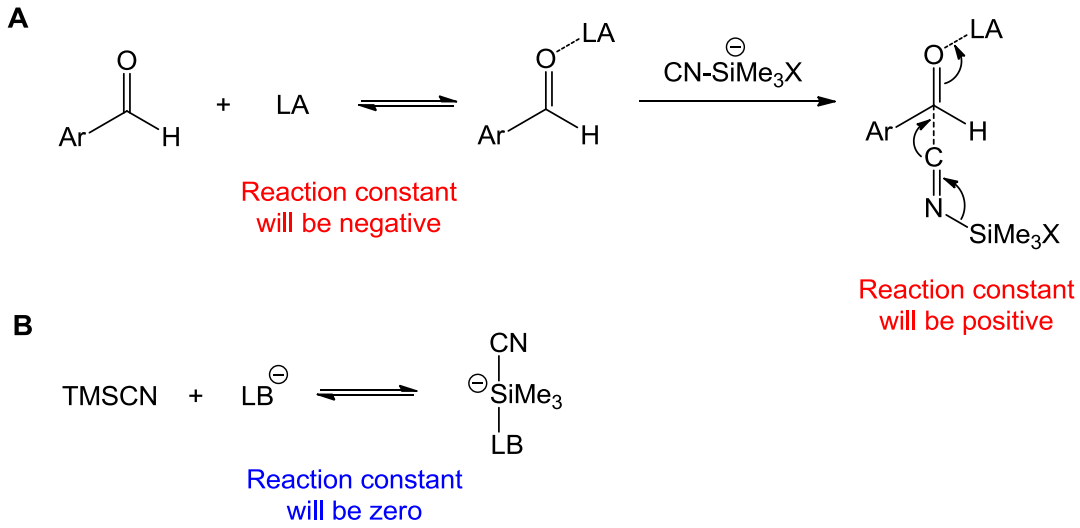

Scheme 3.5

3.3.3 Kinetic studies for the Hammett plot

All the aldehydes used in this study absorbed very strongly between 240-315 nm, whilst their cyanohydrin derivatives absorbed only very slightly in this region. Thus, the progress of the reaction could be monitored by the aldehyde UV absorbance decay. Initially, a solution of catalyst dissolved in dichloromethane was used to provide a background reading for the UV spectrophotometer. Kinetic experiments were conducted in an ice/water bath at 0 °C. Aliquots (0.5 μL) were removed from the reaction mixture at appropriate recorded times and diluted into 3.5 mL of dichloromethane before being analysed in a UV-visible spectrophotometer. The absorbance measurements were used to calculate the aldehyde concentration and these were used to produce kinetics profiles for zero, first (in aldehyde or TMSCN) and second (in aldehyde, TMSCN or both) orders, these correspond to the rate equations (5), (6), (7) and (8).

$[A] = [A]_o - k\,t$ (5) *zero order*

$\ln[A] = \ln[A]_o - k\,t$ (6) *first order*

$1/[A] = 1/[A]_o + k\,t$ (7) *second order in* A

$\ln([A]/[B]) = \ln([A]_o/[B]_o) + k\,t\,([A]_o - [B]_o)$ (8) *second order overall, first order in both* A *and* B

The order for every substituted aldehyde was determined by the graph which gave the best fit to a straight line. Reactions catalysed by VO(salen)NCS **23h** and

VO(salen)$EtOSO_3$ **23a** gave a good fit to second order kinetic equation (8) for all *para* and *meta* substituted aldehydes screened in this study. **Figures 3.3** and **3.4** show the second order plots when VO(salen)NCS and VO(salen)$EtOSO_3$ were used as catalysts in the asymmetric addition of TMSCN to benzaldehyde, with rate constants of 3.4×10^{-3} and 7.0×10^{-5} $mol.L^{-1}.s^{-1}$ respectively. This agrees with previous work, where the rate equations of product formation for VO(salen)NCS and VO(salen)$EtOSO_3$, were found to be first order in aldehyde and first order in TMSCN as shown below.[44b]

Rate = k[**23h**]$^{1.2}$ [PhCHO][TMSCN] = k_{obs}[PhCHO][TMSCN]

Rate = k[**23a**]$^{0.6}$ [PhCHO][TMSCN] = k_{obs}[PhCHO][TMSCN]

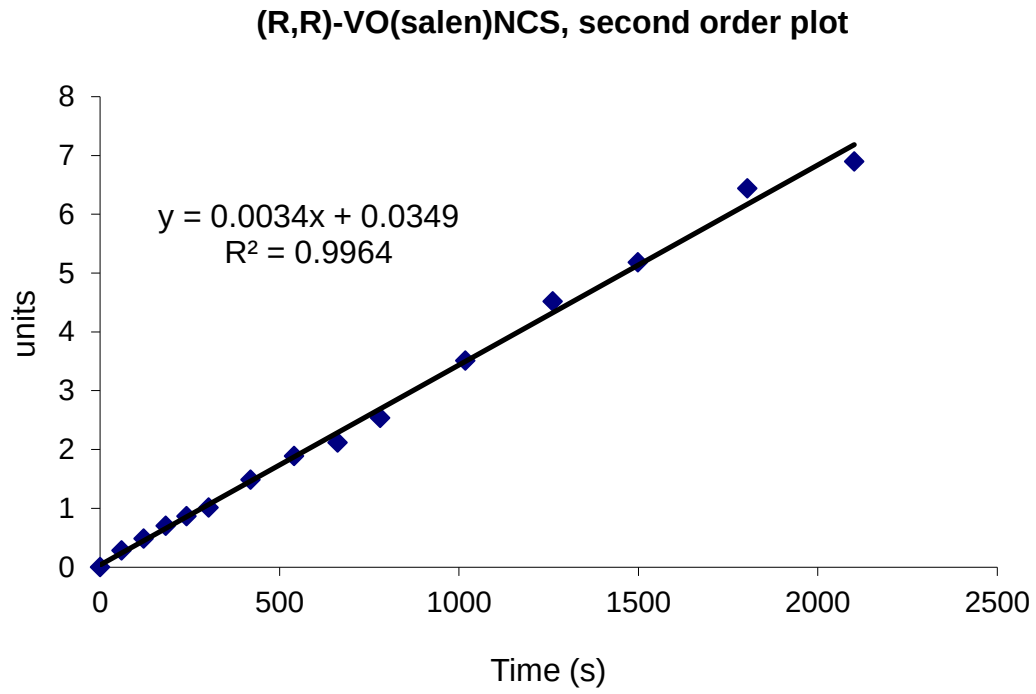

Figure 3.3 Second order kinetics plot for the use of VO(salen)NCS (**23h**) to catalyse the cyanosilylation of benzaldehyde. The units for the y-axis are: $([PhCHO]_o-[Me_3SiCN]_o)^{-1}\ln([Me_3SiCN]_o[PhCHO]_t[Me_3SiCN]_t^{-1}[PhCHO]_o^{-1})$ where the subscripts ø and t refer to initial concentrations and concentrations at time t respectively.

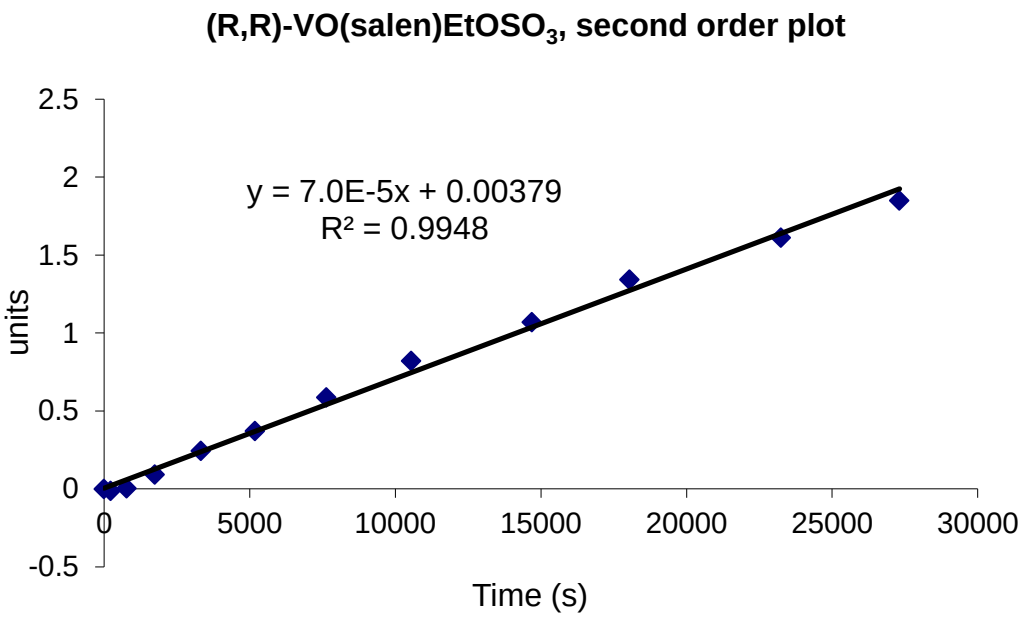

Figure 3.4 Second order kinetics plot for the use of VO(salen)$EtOSO_3$ (**23a**) to catalyse the cyanosilylation of benzaldehyde. The units for the y-axis are: $([PhCHO]_o–[Me_3SiCN]_o)^{-1}ln([Me_3SiCN]_o[PhCHO]_t[Me_3SiCN]_t^{-1}[PhCHO]_o^{-1})$ where the subscripts ø and t refer to initial concentrations and concentrations at time t respectively.

The enantiomeric excess of the cyanohydrins were determined by chiral GC after converting the trimethylsilyl ether to the acetate derivative using Kagan's method with acetic anhydride and 10 mol% scandium(III) triflate in acetonitrile.[110] However, the cyanohydrin derivatives from 4-methoxybenzaldehyde, 3,4-dimethylbenzaldehyde and 3,4-dichlorobenzaldehyde could not be separated by chiral GC, so their enaniomeric excesses were determined by ^{1}H-NMR spectroscopy of the free cyanohydrin using *(R)*-mandelic acid and DMAP as a chiral shift reagent as described in the literature.[111] The preparation of the free cyanohydin was achieved by a two-day transesterification of the acetate derivative using $TsOHxH_2O$ in ethanol at room temperature.[112] This method could not be applied to the cyanohydrin derived from 4-methoxybenzaldehyde as it gave the cyanohydrin with virtually 0% *ee*. This is due to the rapid racemisation of the free cyanohydrin when there is an electron-donating group in the *para* position of the aromatic ring (**Scheme 3.6**). In this case, the enantiomeric excess was determined by comparing the optical rotation of the cyanohydrin trimethylsilyl ether with the literature value.[113]

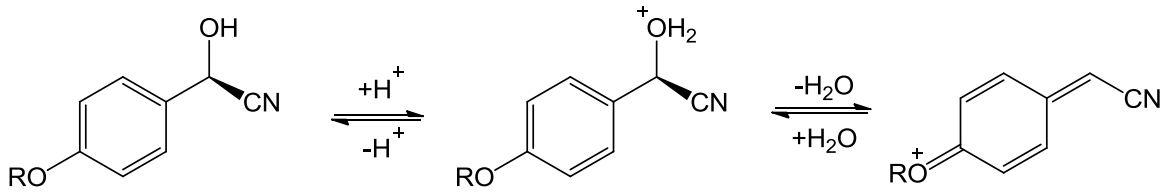

Scheme 3.6 Rapid racemisation reaction of the free cyanohydrin of 4-methoxybenzaldehyde.

3.3.4 Hammett correlation using VO(salen)NCS as catalyst

When VO(salen)NCS (0.2 mol%) was used as the catalyst, a total of fourteen aldehydes were examined in the Hammett study (**Scheme 3.7**). In all cases, the reactions obeyed second order kinetics, giving a good fit to equation (8) being first order in aldehyde and first order in TMSCN. The kinetics experiments were repeated a minimum of two times per substrate and the average of the two closest values were used to construct the Hammett plot (**Table 3.1**). The second order kinetic plots for each of these aldehydes are presented in the appendix. In order to transform the rate constants into a Hammett plot, benzaldehyde was taken as the reference point and all the substituted benzylaldehyde rate constants were divided by its rate constant. Finally, the logarithm of the resulting rate ratio was plotted against the corresponding substituent constant σ (**Figure 3.5**).

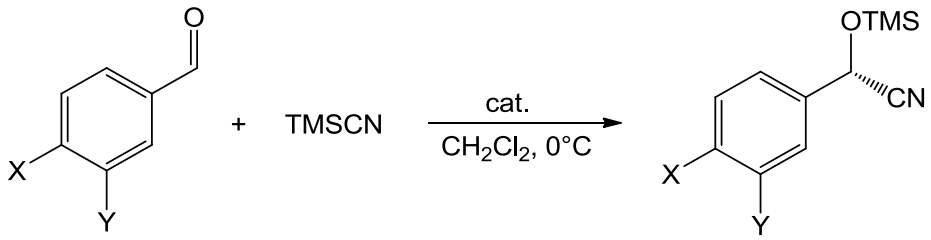

Scheme 3.7 Catalysed reaction between substituted aromatic aldehydes and TMSCN.

Entry	Aldehyde	σ	k_1 ($M^{-1}.s^{-1}$)	k_2 ($M^{-1}.s^{-1}$)	$k_{average} \times 10^{-3}$ ($M^{-1}.s^{-1}$)	*ee* (%)
1	PhCHO	0	0.0034	0.0041	3.75±0.5	87*(S)*
2	3,5-FC_6H_3CHO	0.68	0.0318	0.0338	32.80±1.4	75*(S)*
3	3,4-ClC_6H_3CHO	0.60	0.0091	0.0113	10.20±1.6	86*(S)*
4	4-$CF_3C_6H_4CHO$	0.53	0.0105	0.0095	10.00±0.7	75*(S)*
5	3-ClC_6H_4CHO	0.37	0.0083	0.0081	8.20±0.1	77*(S)*
6	3-FC_6H_4CHO	0.34	0.0111	0.0108	10.95±0.2	86*(S)*
7	4-ClC_6H_4CHO	0.23	0.0062	0.0067	6.45±0.4	84*(S)*
8	4-BrC_6H_4CHO	0.21	0.0070	0.0071	7.05±0.1	81*(S)*
9	4-FC_6H_4CHO	0.06	0.0048	0.0048	4.80±0.0	85*(S)*
10	4-$CH_3SC_6H_4CHO$	0	0.0023	0.0032	2.75±0.6	57*(S)*
11	3-CH_3C_6H4CHO	-0.06	0.0037	0.0035	3.60±0.1	78*(S)*
12	4-$CH_3C_6H_4CHO$	-0.14	0.0018	0.0021	1.95±0.2	85*(S)*
13	3,4-$CH_3C_6H_3CHO$	-0.20	0.0013	0.0012	1.25±0.1	76*(S)*
14	4-$CH_3OC_6H_4CHO$	-0.27	0.0003	0.0003	0.30±0.0	96*(S)*
15	4-^{t}BuOC_6H_4CHO	-0.27	0.0012	0.0013	1.25±0.1	78*(S)*

Table 3.1 All reactions were carried out in dichloromethane at 0 °C, using 0.5 M aldehyde, 0.55 M TMSCN and 0.2 mol% of VO(salen)NCS **23h**. k_1 and k_2 are the observed rate constants in two different reactions and $k_{average}$ is the average of these.

The rate data showed good reproducibility and when incorporated into a Hammett plot, a linear correlation was obtained for all of the aldehydes but one, 4-methoxybenzaldehyde. 4-Thiomethylbenzaldehyde showed a similar deviation from the best fit line, though this was not as pronounced as for 4-methoxybenzaldehyde. In view of this observation, it appeared that the heteroatoms (S and O) of these two substrates could be coordinating to the vanadium ion, thus inhibiting its catalytic activity. Therefore, it was decided to study their effect by replacing the small methoxy group by a bulky *tert*-butoxy group in order to shield the oxygen and thus prevent its coordination to the vanadium ion (entry 15, **Table 3.1**). This was successful and 4-*tert*-butoxybenzaldehyde could be fitted into the same straight line as the other 13 substrates (R^2 = 0.9014), giving a Hammett plot with a positive slope of 1.24. The enantiomeric excesses of the cyanohydrin derivatives were between 57-96% in favour of the *S* enantiomer, confirming that the catalysed and not the uncatalysed reaction was being monitored.

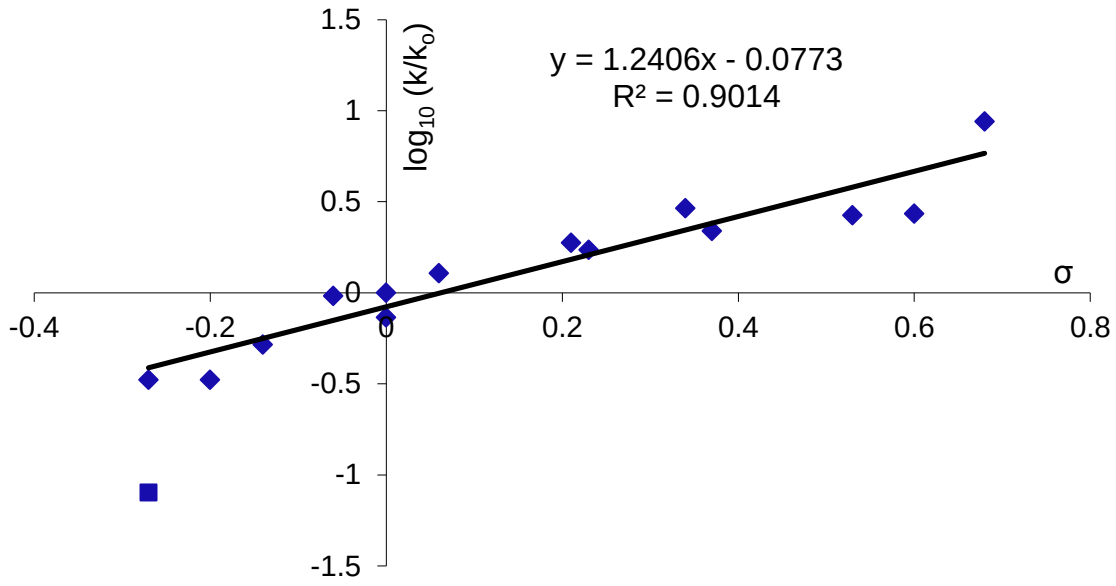

Figure 3.5 Hammett plot for the asymmetric addition of TMSCN to 3- and 4-substituted aromatic aldehydes catalysed by VO(salen)NCS **23h**. The square point (4-methoxybenzaldehyde) is not included in the best fit line.

3.3.5 Hammett correlation using VO(salen)EtOSO$_3$ as catalyst

The VO(salen)EtOSO$_3$ complex is not as active catalyst as VO(salen)NCS, therefore it catalysed reactions with lower rates. In order to allow direct comparison with the data recorded using the VO(salen)NCS catalyst, the 0.2 mol% catalyst loading was maintained in the kinetics experiments, so significantly smaller rate constants than those obtained when using the VO(salen)NCS catalyst were observed (**Table 3.2**). The decrease in rate was such, that reactions using benzaldehydes bearing electron-donating substituents did not reach 30 % conversion even after reaction times of eight hours. All the kinetics showed a good fit to second order kinetics as in the case of VO(salen)NCS catalysed reactions. The rate constants of duplicated kinetic experiments showed good reproducibility, and the average rate data gave a good fit to a straight line ($R^2 = 0.9249$) when converted to a Hammett plot, producing a positive slope of 1.87 (**Figure 3.6**). Again, the reaction with 4-methoxybenzaldehyde showed a significant deviation from the linear fit, and this reaction did not exceed 3% conversion after 8 hours reaction time. The use of 4-*tert*-butoxybenzaldehyde again gave a rate constant which gave a better fit to the linear correlation. The generated cyanohydrin derivatives produced in these

reactions had good enantioselectivities, 58 % being the lowest, which confirms that the process being monitored is the catalysed rather than the uncatalysed reaction.

Entry	**Aldehyde**	**σ**	$k_1 \times 10^{-3}$ ($M^{-1}.s^{-1}$)	$k_2 \times 10^{-3}$ ($M^{-1}.s^{-1}$)	$k_{average} \times 10^{-5}$ ($M^{-1}.s^{-1}$)	***ee*** **(%)**
1	PhCHO	0	0.070	0.061	6.55±0.5	86*(S)*
2	3,5-FC_6H_3CHO	0.68	0.573	0.500	53.65±3.7	82*(S)*
3	3,4-ClC_6H_3CHO	0.60	1.425	1.506	146.55±4.1	78*(S)*
4	4-$CF_3C_6H_4CHO$	0.53	0.286	0.242	26.40±2.2	77*(S)*
5	3-ClC_6H_4CHO	0.37	0.295	0.355	32.50±3.0	72*(S)*
6	3-FC_6H_4CHO	0.34	0.276	0.250	26.30±1.3	88*(S)*
7	4-ClC_6H_4CHO	0.23	0.129	0.152	14.05±1.2	86*(S)*
8	4-BrC_6H_4CHO	0.21	0.122	0.114	11.80±0.4	84*(S)*
9	4-FC_6H_4CHO	0.06	0.088	0.082	8.50±0.3	89*(S)*
10	4-$CH_3SC_6H_4CHO$	0	0.025	0.017	2.10±0.4	68*(S)*
11	3-$CH_3C_6H_4CHO$	-0.06	0.033	0.031	3.20±0.1	86*(S)*
12	4-$CH_3C_6H_4CHO$	-0.14	0.023	0.021	2.20±0.1	68*(S)*
13	3,4-$CH_3C_6H_3CHO$	-0.20	0.016	0.017	1.65±0.1	65*(S)*
14	4-^{t}BuOC_6H_4CHO	-0.27	0.024	0.012	1.80±0.6	58*(S)*

Table 3.2 All reactions were carried out in dichloromethane at 0 °C, using 0.5 M aldehyde, 0.55 M TMSCN and 0.2 mol% of VO(salen)$EtOSO_3$ **23a**. k_1 and k_2 are the observed rate constants in two different reactions and $k_{average}$ is the average of these.

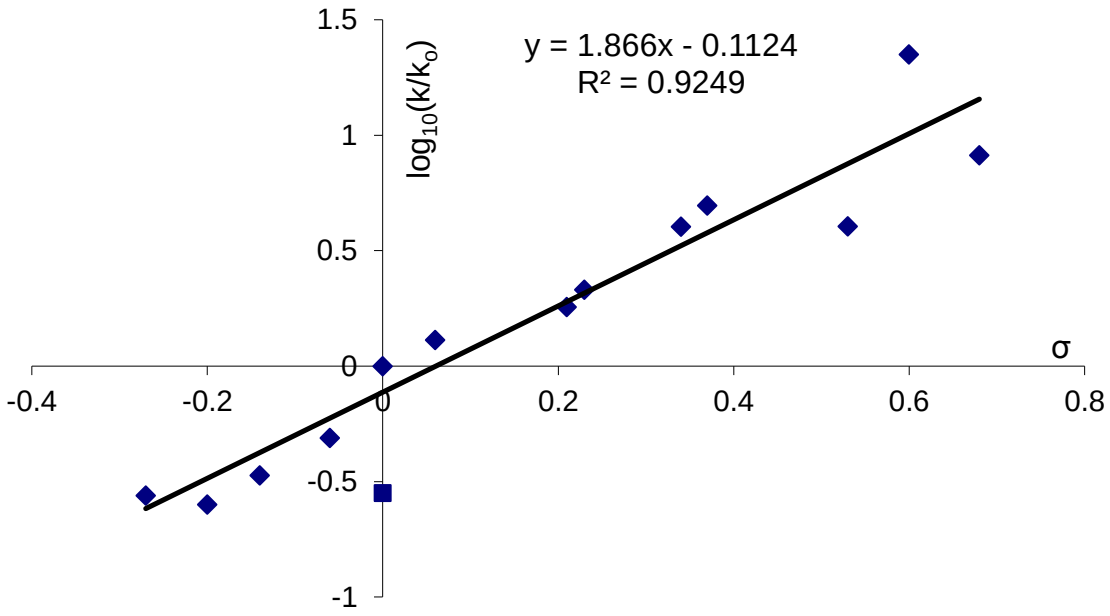

Figure 3.6 Hammett plot for the asymmetric addition of TMSCN to 3- and 4-substituted aromatic aldehydes catalysed by VO(salen)$EtOSO_3$ **23a**. The square point (4-$CH_3SC_6H_4CHO$) has not been considered in the linear trend.

3.3.6 A model to explain the influence of the Lewis basicity of the counterion in the VO(salen)X catalytic system

Figure 3.7 presents the two sets of Hammett data on the same axes to facilitate comparison of the vanadium based catalysts. The slope in both cases is positive; which indicates that the reaction rate increases as the σ value increases. Thus, benzaldehydes with electron-withdrawing substituents lower the activation energy by facilitating electronic density transfer from cyanide towards the activated carbonyl during the transition state. In contrast, benzaldehydes bearing electron-donating groups increase the energy barrier associated with the transition state, since these groups stabilize the aldehyde.

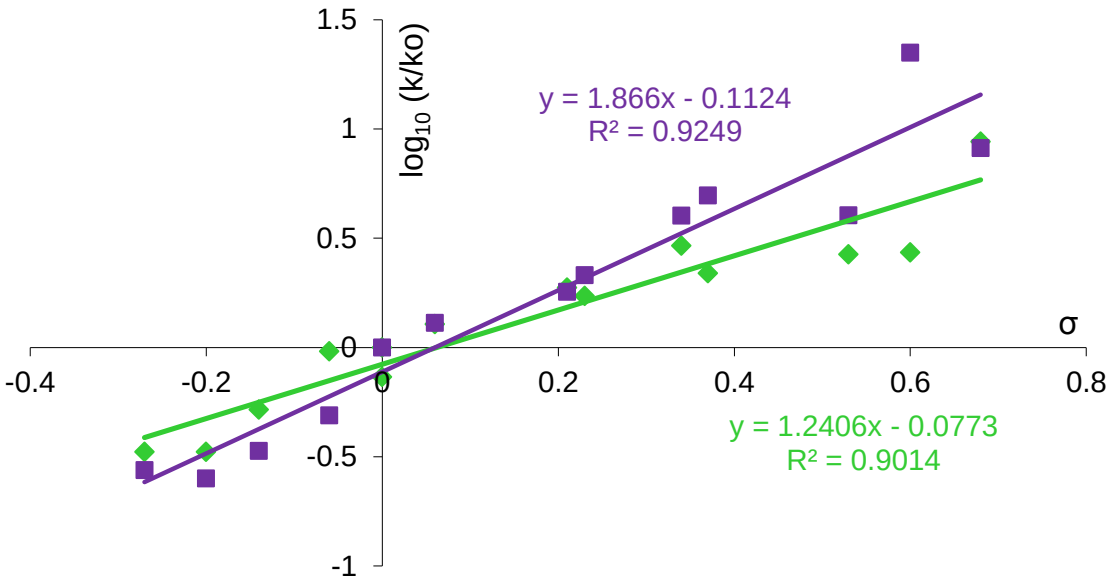

Figure 3.7 Superimposition of the Hammett plots obtained using VO(salen)$EtOSO_3$ (purple) and VO(salen)NCS (green).

Both vanadium(V)(salen) catalysts gave a good correlation to a straight line in a Hammett plot with positive reaction constants of 1.86 and 1.24 respectively, which indicates that all the aldehydes used in this study are coordinated to the metal center during the catalytic process; thus, indicating that Lewis acid catalysis is dominant in the catalytic process for both vanadium catalysts, regardless of their counterion. However, the lower reaction constant observed when VO(salen)NCS is used as the catalyst, indicates that some degree of Lewis base catalysis is also operating in this system.

The unexpectedly close reaction constant values cannot explain the significant difference in reaction rate, in which the VO(salen)NCS complex catalyses cyanohydrin synthesis 100 times faster than the VO(salen)$EtOSO_3$ complex. This suggests that it is not the counterion that induces the majority of the Lewis base catalysis, instead, this could be associated mainly with the oxo group due to its ability to form oligomers as well as its affinity for silicon. On this basis, a transition state model which involves catalyst dimer formation is proposed (**Scheme 3.8**). Thus, the vanadium centre with higher oxidation state (+5), being the stronger Lewis acid, will coordinate to the aldehyde, whereas the vanadium centre with +4 oxidation state, will bind to the silicon through the *oxo*-group, forming a pentacoordinate hypervalent silicon species. Therefore, the influence of the counterion can be explained according to the two models

shown in **Scheme 3.8**. Model **B** represents the highly coordinating counterions, in which the counterion binds to the silicon expanding its coordination sphere to a hexacoordinated species; this results in the weakening of the silicon-cyanide bond, and hence, further facilitates cyanohydrin synthesis. On the other hand, when the counterion is poorly coordinating (model **A**), it stays in the outer sphere. Finally, the transition state can be represented as a transfer of the electron density of the cyanide towards the activated carbonyl, generating a carbon-carbon bond and hence ultimately forming the cyanohydrin.

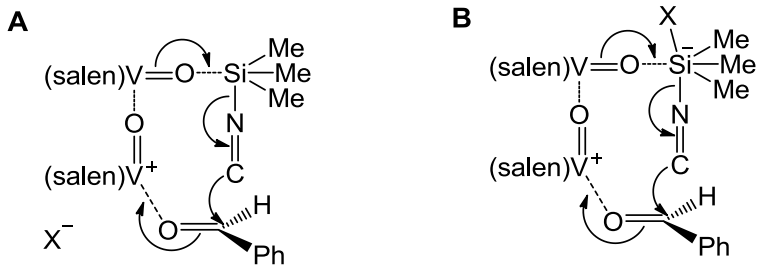

Scheme 3.8 Possible transition state model involving both Lewis acid and Lewis base catalysis. Model **A** corresponds to a non-coordinating counterion such as $EtOSO_3^-$, and model **B** corresponds to a highly coordinating counterion such as thiocyanate.

3.4 Other metals bearing a salen ligand.

In view of the promising result obtained with oxovanadium(V)(salen) catalysts, it was decided to extend the Hammett study to other metal(salen) complexes such as bimetallic titanium complex **20** and the aluminium dimer **69** (**Figure 3.8**). Both of these complexes were developed by our group and shown to be excellent catalysts for the asymmetric addition of TMSCN to aldehydes.[37b, 85] In addition, like the vanadium complexes, these incorporate a tetradentate salen ligand in their structure. Thus, in view of the structural differences (both **20** and **69** are bimetallic in the solid state, whilst vanadium complexes **23a** and **23h** are monometallic) it was interesting to compare the relative importance of Lewis acidity and Lewis basicity in asymmetric cyanohydrin synthesis catalysed by these complexes with the vanadium catalysts. Titanium(IV)(salen) complex **20** is known to be an excellent Lewis acid, whereas aluminium(III)(salen) complex **69**, due to its relatively poor Lewis acidic character performs better as a catalyst in the presence of a Lewis basic additive.

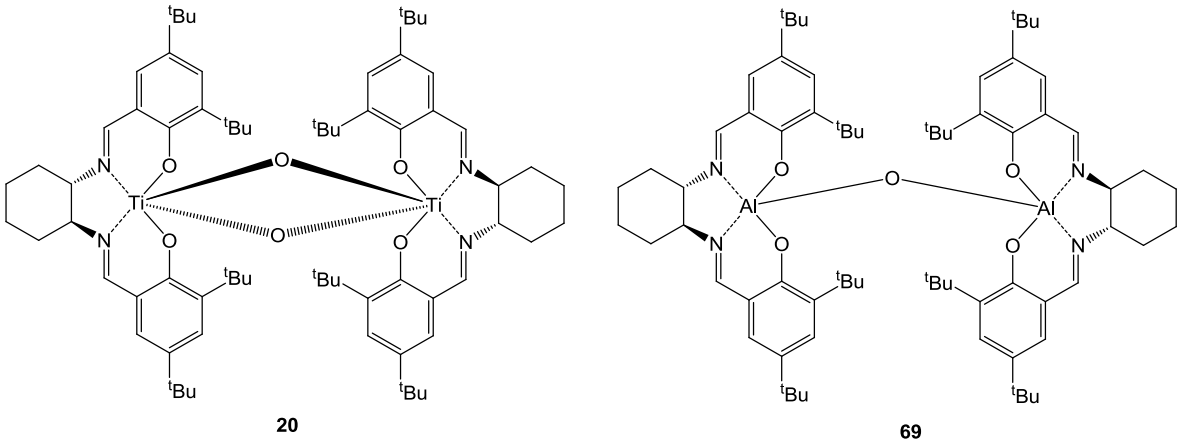

Figure 3.8 Bimetallic catalysts for the asymmetric addition of TMSCN to aldehydes.

3.4.1 Hammett correlation using [Ti(salen)O]$_2$ as catalyst

When bimetallic titanium complex **20** was used as catalyst, only ten aldehydes could be included in the Hammett study since the most electron-deficient aldehydes; 3,4-dichloro-, 3,5-difluoro- and 4-trifluoromethylbenzaldehyde reacted too rapidly to monitor; in less than 10 seconds all the aldehyde was converted to cyanohydrin. 4-Bromobenzaldehyde could not be included in the study since it was unreactive. This substrate appeared to be unable to coordinate to the metal, since after its addition to the catalyst solution, no colour change was observed unlike the other substrates. This was the first sign that no Lewis base activation was present in this system; otherwise, cyanide activation by the Lewis base would have enabled cyanohydrin formation even if the substrate could not be activated by the Lewis acidic metal. Only 0.1 mol% of complex was used for the kinetic study, and all ten aldehydes were found to obey first order kinetics (**Figure 3.9**); which is assumed to be first order with respect to TMSCN and thus, independent of the aldehyde concentration as has previously been determined for benzaldehyde,[38] for which the rate equation corresponds to:

Rate = k[**20**]$^{1.3}$ [TMSCN] = k_{obs}[TMSCN]

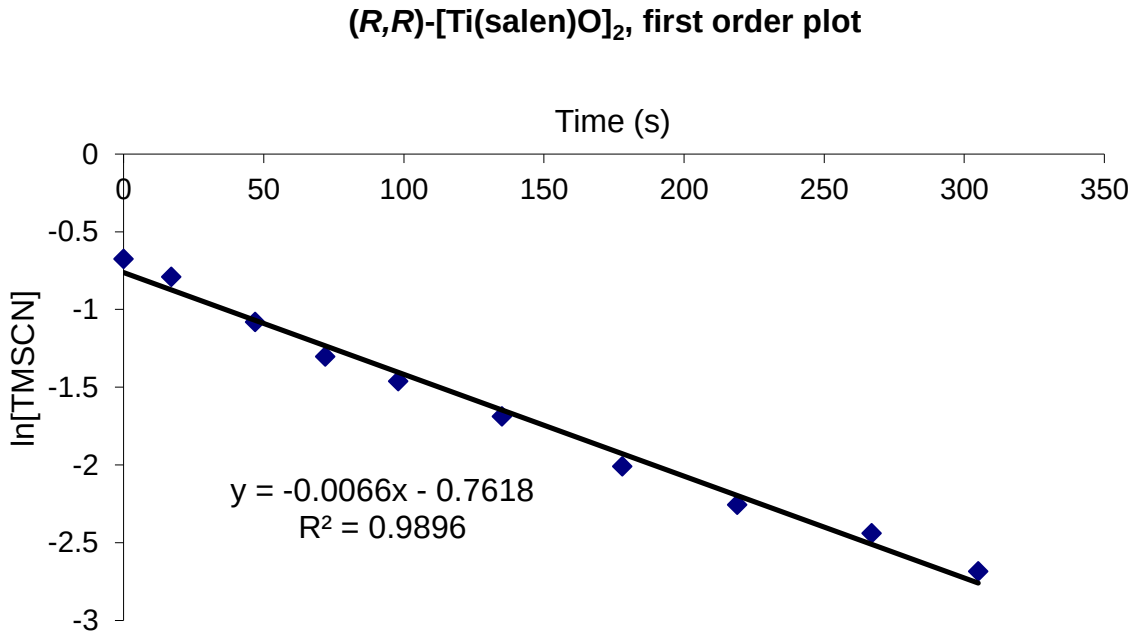

Figure 3.9 First order kinetics plot for the asymmetric addition of TMSCN to benzaldehyde with $[Ti(salen)O]_2$ (**20**) complex as the catalyst.

Entry	**Aldehyde**	**σ**	**k_1 (s^{-1})**	**k_2 (s^{-1})**	**$k_{average}$ $\times 10^{-3}$ (s^{-1})**	***ee*** **(%)**
1	PhCHO	0	0.00655	0.00751	7.01±0.7	84*(S)*
2	3-ClC_6H_4CHO	0.37	0.04220	0.04321	42.71±0.7	84*(S)*
3	3-FC_6H_4CHO	0.34	0.03749	0.03872	38.11±0.9	87*(S)*
4	4-ClC_6H_4CHO	0.23	0.03115	0.03189	31.52±0.5	87*(S)*
5	4-FC_6H_4CHO	0.06	0.00857	0.01061	9.59±1.4	88*(S)*
6	4-$CH_3SC_6H_4CHO$	0	0.00397	0.00468	4.33±0.5	55*(S)*
7	3-$CH_3C_6H_4CHO$	-0.06	0.00724	0.00620	6.72±0.7	95*(S)*
8	4-$CH_3C_6H_4CHO$	-0.14	0.00245	0.00200	2.23±0.3	79*(S)*
9	3,4-$CH_3C_6H_3CHO$	-0.20	0.00329	0.00334	3.32±0.1	57*(S)*
10	4-$CH_3OC_6H_4CHO$	-0.27	0.00117	0.00110	1.14±0.1	46*(S)*

Table 3.3 All reactions were carried out in dichloromethane at 0 °C, using 0.5 M aldehyde, 0.55 M TMSCN and 0.1 mol% of $[Ti(salen)O]_2$ **20**. k_1 and k_2 are the observed rate constants in two different reactions and $k_{average}$ is the average of these.

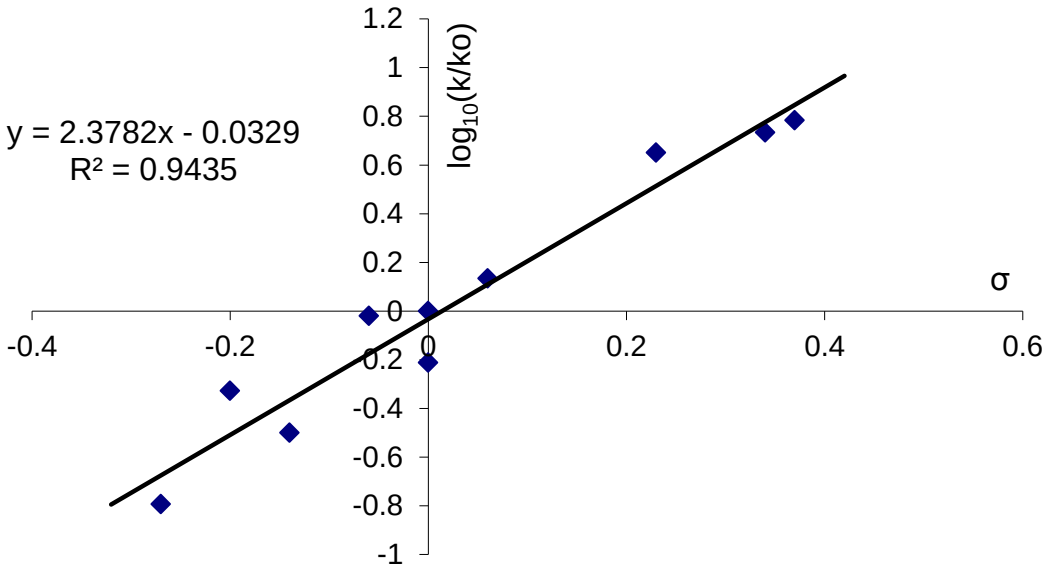

Figure 3.10 Hammett plot for the asymmetric addition of TMSCN to 3- and 4-substituted aromatic aldehydes catalysed by $[Ti(salen)O]_2$ **20**.

The rate data, when converted to a Hammett plot, fitted reasonably well (R^2 = 0.9435) to a straight line, with a pronounced positive reaction constant of 2.38 (**Figure 3.10**). The enantiomeric excesses for all the aldehydes were found to be higher than 46% in favour of the *S* enantiomer, which is consistent with the reaction being catalysed by (*R*,*R*)-$[Ti(salen)O]_2$.

3.4.2 Hammett correlation using $[Al(salen)]_2O$ / Ph_3PO as catalyst

The study of the aluminium(III)(salen) and phosphine oxide system was undertaken by another member of our group;[85] however, it is useful to include it in this analysis as it further illustrates the effect of Lewis acids and Lewis bases in the catalysis of asymmetric cyanohydrin synthesis. This system uses a catalyst loading of 2 mol% (10-fold higher than the vanadium(V)(salen) catalysts) and requires the addition of triphenylphosphine oxide in 5:1 ratio with respect to the catalyst. If compared with the vanadium and titanium based catalytic systems, a decrease in the catalytic activity is clearly evident, indicating that the aluminium complex is not as good a Lewis acid. This can be observed in the rate constants which are three times lower than for $VO(salen)EtOSO_3$ (**Table 3.4**). All the aldehydes obeyed first order kinetics with respect to TMSCN and the rate equation was determined to be: Rate = *k*[**69**][Ph_3PO][TMSCN], which could be simplified to Rate = k_{obs} [TMSCN], where k_{obs} equals *k*[**69**][Ph_3PO]; however, the rate data did not follow a linear trend when they

were incorporated into a Hammett plot (**Figure 3.11**). The enantiomeric excesses were also not as good as in the case of titanium and vanadium catalysts, but were still found to be higher than 35%. Only benzaldehydes bearing electron-donating groups can reasonably be correlated to a straight line (R^2 = 0.7412), with a reaction constant of 0.67. However, those substrates with σ-values higher than +0.35 show only a very weak interaction with the aluminium ion which affects the enantioselectivity, as the enantiomeric excesses have the lowest values.

Entry	**Aldehyde**	**σ**	$k_1 \times 10^{-3}$ (s^{-1})	$k_2 \times 10^{-3}$ (s^{-1})	$k_{average} \times 10^{-5}$ (s^{-1})	***ee*** **(%)**
1	PhCHO	0	0.0258	0.0275	2.67±0.1	64*(S)*
2	3,5-FC_6H_3CHO	0.68	0.0417	0.0580	4.99±1.2	38*(S)*
3	3,4-ClC_6H_3CHO	0.60	0.0281	0.0324	3.03±0.3	50*(S)*
4	4-$CF_3C_6H_4CHO$	0.53	0.0334	0.0348	3.41±0.1	49*(S)*
5	3-ClC_6H_4CHO	0.37	0.0407	0.0314	3.61±0.7	54*(S)*
6	3-FC_6H_4CHO	0.34	0.0542	0.0466	5.04±0.5	61*(S)*
7	4-ClC_6H_4CHO	0.23	0.0348	0.0328	3.38±0.1	61*(S)*
8	4-BrC_6H_4CHO	0.21	0.0303	0.0263	2.83±0.3	60*(S)*
9	4-FC_6H_4CHO	0.06	0.0325	0.0396	3.61±0.5	69*(S)*
10	4-$CH_3SC_6H_4CHO$	0	0.0178	0.0217	1.98±0.3	40*(S)*
11	3-$CH_3C_6H_4CHO$	-0.06	0.0254	0.0270	2.62±0.1	73*(S)*
12	4-$CH_3C_6H_4CHO$	-0.14	0.0268	0.0249	2.59±0.1	65*(S)*
13	3,4-$CH_3C_6H_3CHO$	-0.20	0.0174	0.0194	1.84±0.1	68*(S)*
14	4-$CH_3OC_6H_4CHO$	-0.27	0.0121	0.0105	1.13±0.1	71*(S)*
15	4-^{t}BuOC_6H_4CHO	-0.27	0.0139	0.0162	1.51±0.2	58*(S)*

Table 3.4 All the reactions were carried out in dichloromethane at 0 °C, using 0.5 M aldehyde, 0.55 M TMSCN, 2 mol% of [Al(salen)]O_2 **69** and 10 mol% of Ph_3PO. k_1 and k_2 are the observed rate constants in two different reactions and $k_{average}$ is the average of these.

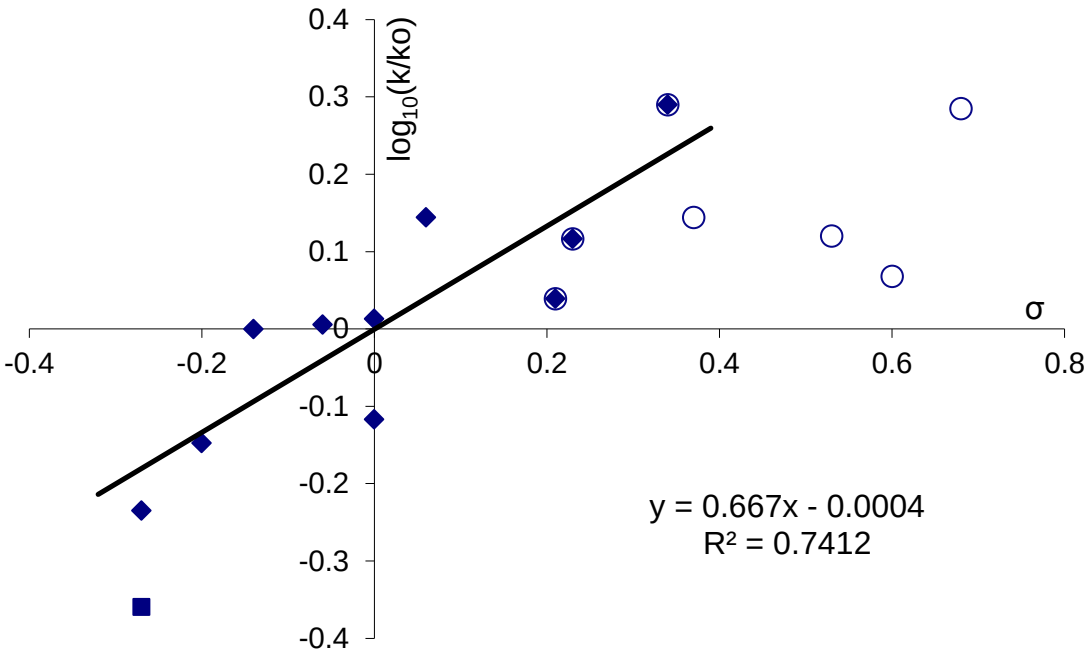

Figure 3.11 Hammett correlation of 15 aldehydes using $[Al(salen)]_2O$ as the catalyst. The square point corresponds to 4-methoxybenzaldehyde. Filled blue diamonds represent the aldehydes bearing the more electron-donating groups, which can be correlated to a straight line. Empty blue circles are those that do not fit to a straight line.

3.4.3 Comparison of the four systems

By replotting the Hammett data for the four metal(salen) complexes on the same axes (**Figure 3.12**) some conclusions can be drawn. The large positive reaction constant when titanium(salen) is used as the catalyst, indicates that the catalysis is dominated by Lewis acid catalysis, therefore a model wherein negative charge is transferred to the carbonyl during the transition state can be proposed (**Scheme 3.9, A**). On the other hand, the aluminium(salen) dimer used along with triphenylphosphine oxide gives a Hammett plot with a slope close to zero, reflecting catalysis predominantly by the triphenylphosphine oxide acting as a Lewis base to activate the TMSCN. However, the level of enantioselectivity indicates that the aldehyde must be interacting to some extent with one of the aluminium centres, since it is the salen ligand that provides the chiral environment. In this case, during the transition state, the negative charge is located mostly on the TMSCN, with little or no charge being transferred to the carbonyl (**Scheme 3.9, B**). The reaction constants determined for the vanadium catalysts are intermediate between the titanium and aluminium catalysts, indicating that both Lewis acid and Lewis base catalysis are operating in the catalytic process. Vanadium

complexes, being better catalysts than the aluminium(salen) complex in terms of catalytic activity and better than titanium(salen) complex in terms of enantioselectivity, this demonstrates that dual activation of the aldehyde and TMSCN leads to the most effective catalysts.

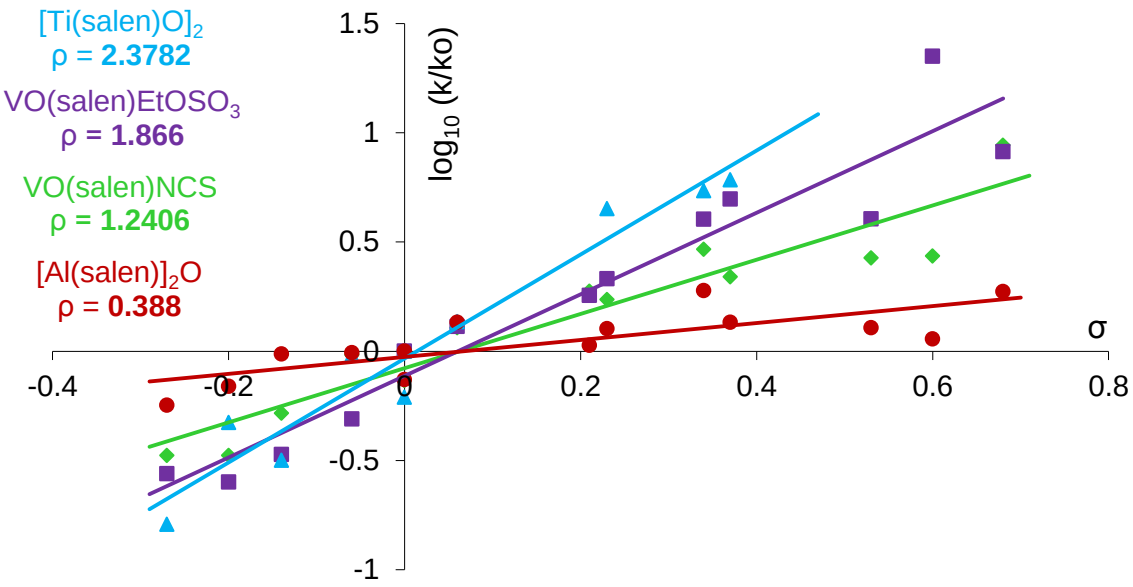

Figure 3.12 Comparison of the Hammett plots. Circles $[Al(salen)]_2O/Ph_3PO$, diamonds VO(salen)NCS, squares $VO(salen)EtOSO_3$ and triangles $[Ti(salen)O]_2$.

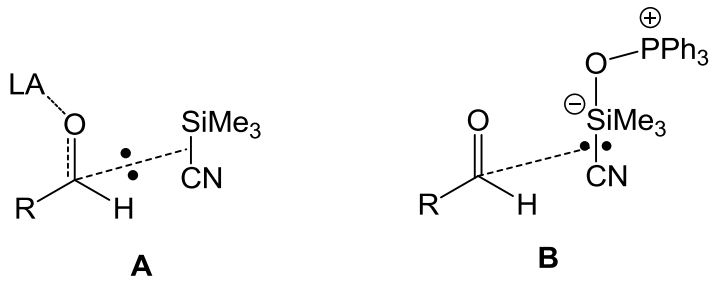

Scheme 3.9 Rate determining transition states for asymmetric cyanohydrin synthesis. Model **A** when Lewis acid catalysis is dominant, model **B** when Lewis base catalysis is dominant.

In addition to the Hammett correlation, another method to determine the relative importance of Lewis acid and Lewis base catalysis in the asymmetric addition of TMSCN to aldehydes, albeit not as precise, is by observing the enantioselectivities of the formed cyanohydrins (**Figure 3.13**). The asymmetric induction for all four catalytic systems is provided by the optically active salen ligand, which is coordinated to the metallic centre, this being the Lewis acidic moiety. In order to provide chirality to the

substrate, the aldehyde must be coordinated to the metal during the enantioselectivity determining step. Titanium(IV) and vanadium(V) based catalytic systems show the highest asymmetric induction. Moreover, the observed enantiomeric excesses are consistently high regardless of the nature of the *para*- and *meta*-substituents on the aromatic ring. In contrast, the aluminium(III) complex, shows a progressive decrease on the asymmetric induction as the nature of the *para*- and *meta*-substituted benzaldehydes become more electron-withdrawing, thus indicating that the aldehydes are only weakly coordinated to the metal, and it is the activation of the TMSCN which catalyses cyanohydrin formation.

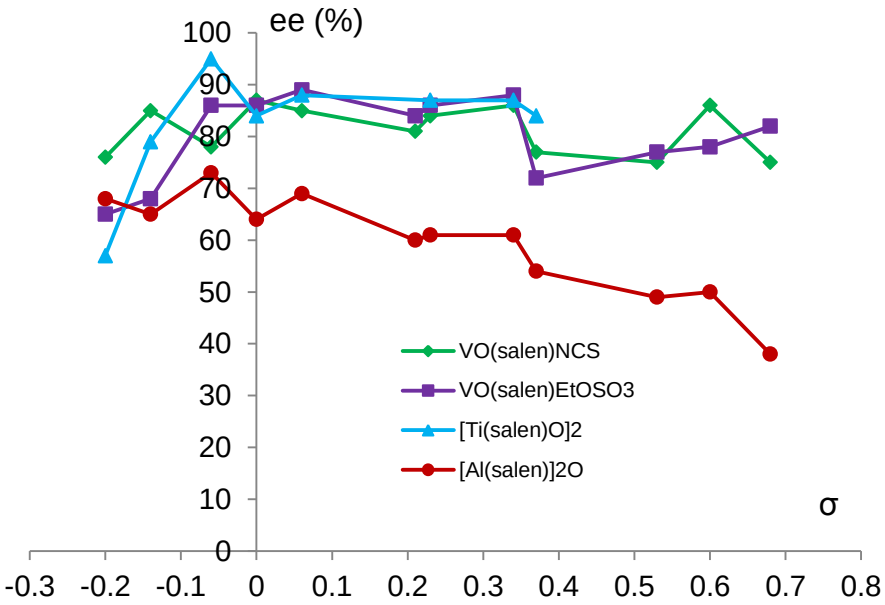

Figure 3.13

3.5 Racemic cyanohydrin synthesis by Lewis acid or Lewis base catalysis

In order to optimise the methods to separate the cyanohydrin enantiomers by chiral gas chromatography, racemic samples had to be prepared. As mentioned at the beginning of this chapter, the silylcyanation of aldehydes can be catalysed by a Lewis acid, by a Lewis base, or by a combination of both. Initially, a Lewis acid catalysed strategy was explored, since this has been the most utilised non-chiral catalyst class reported in the literature.[114] A first report, dating from 1973 by Evans,[114a] described a list of metal compounds capable of catalysing racemic cyanohydrin synthesis with variable reactivity. Amongst them zinc iodide exhibited the highest catalytic activity. Therefore, zinc iodide and a range of other metal salts were at our disposal, including

aluminium, iron, titanium and zinc derivatives. These were tested in the catalytic achiral addition of TMSCN to benzaldehyde, this being the model substrate (**Scheme 3.10**). The reaction conditions were chosen to be in dichloromethane at room temperature using 10 mol% catalyst loading for 1 hour. **Table 3.5** shows the results. Titanium isopropoxide gave the worst result with only a 20 % conversion of aldehyde to trimethylsilyl cyanohydrin. This was probably due to decomposition of the catalyst in the reaction vessel producing titanium dioxide, as a cloudy solution was observed five minutes after TMSCN was added. Zinc iodide gave better results than zinc bromide, however, aluminium triflate gave the best result of all (98% conversion).

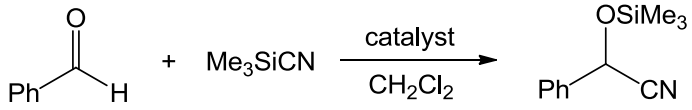

Scheme 3.10 Racemic synthesis of cyanohydrins from aldehydes.

Catalyst (10 mol%)	**Conversion**
$AlCl_3$	73%
$Al(OTf)_3$	98%
$FeCl_3$	88%
$Ti(O^iPr)_4$	20%
$ZnBr_2$	28%
ZnI_2	83%

Table 3.5

Therefore, initially aluminium triflate was used to produce the racemic trimethylsilyl cyanohydrin ethers from a range of aromatic and aliphatic aldehydes. The catalysis experiments were conducted in the presence of 5 mol% of catalyst at room temperature in dichloromethane, with the reaction time extended to two hours. The results illustrated in **Table 3.6** show excellent conversions for electron deficient substrates, but moderate to low conversions for electron rich substrates. Aliphatic aldehydes were also found to be good substrates, particularly pivaldehyde. However, attempts to perform kinetic studies were unsuccessful. This could be explained by the poor solubility of the catalyst in chlorinated solvents.

Another catalyst tested was tetrabutylammonium thiocyanate. The thiocyanate anion was previously found to catalyse the silylcyanation of benzaldehyde as part of a

study on the effect of the counterion in the enhancement of catalytic activity, when VO(salen)NCS was the catalyst (*Section 3.2*). Surprisingly, although there is precedent for Lewis acid catalysed addition of TMSCN to aldehydes and ketones not much work has been done on achiral Lewis base catalysis.[115] Thus, the catalytic activity of tetrabutylammonium thiocyanate was compared to that of aluminium triflate under the same conditions. After two hours, all the electron deficient and aliphatic aldehydes were quantitatively transformed into their corresponding O-protected cyanohydrins. Tetrabutylammonium thiocyanate proved to be a better catalyst than the Lewis acid aluminium triflate for all the substrates tested (**Table 3.6**).

Aldehyde	**Conv.** $Al(OTf)_3$ (5 mol%)	**Conv.** Bu_4N-NCS (5 mol%)
PhCHO	81%	94%
3,5-FC_6H_3CHO	93%	100%
3,4-ClC_6H_3CHO	96%	100%
4-$CF_3C_6H_4CHO$	77%	100%
3-ClC_6H_4CHO	84%	100%
3-FC_6H_4CHO	62%	100%
4-ClC_6H_4CHO	64%	100%
4-BrC_6H_4CHO	63%	100%
4-FC_6H_4CHO	68%	91%
4-$CH_3SC_6H_4CHO$	72%	88%
3-CH_3C_6H4CHO	58%	80%
4-$CH_3C_6H_4CHO$	55%	87%
3,4-$CH_3C_6H_3CHO$	50%	76%
4-$CH_3OC_6H_4CHO$	41%	66%
4-^{t}BuOC_6H_4CHO	-	72%
CyCHO	82%	100%
$(CH_3)_3CCHO$	100%	100%
$CH_3(CH_2)_7CHO$	72%	100%

Table 3.6

A kinetic study was carried out using equimolar amounts of benzaldehyde and TMSCN, in the presence of 1 mol% of tetrabutylammonium thiocyanate in CH_2Cl_2 at 0 °C. The reaction showed overall second order kinetics (**Figure 3.14**); presumably first order with respect to both the aldehyde and TMSCN. By varying the concentration of catalyst (5×10^{-3}, 1×10^{-2} and 2×10^{-2} M) the reaction was shown to be first order in

tetrabutylammonium thiocyanate (**Figures 3.15** and **3.16**). In view of these results a catalytic cycle could be proposed (**Scheme 3.11)**. Tetrabutylammonium thiocyanate acts as a source of free thiocyanate anions in solution, which can activate the TMSCN as a hypervalent silicon species (**Scheme 3.2**, route A). This could then react with the aldehyde to form the cyanohydrin anion and trimethylsilyl thiocyanate, which we previously detected by mass spectrometry (see *Section 2.8*). Then, the final step would be the cyanohydrin silylation, as oxygen has a higher affinity for silicon than sulphur. According to the overall second order reaction kinetics, this should be the rate determining step.

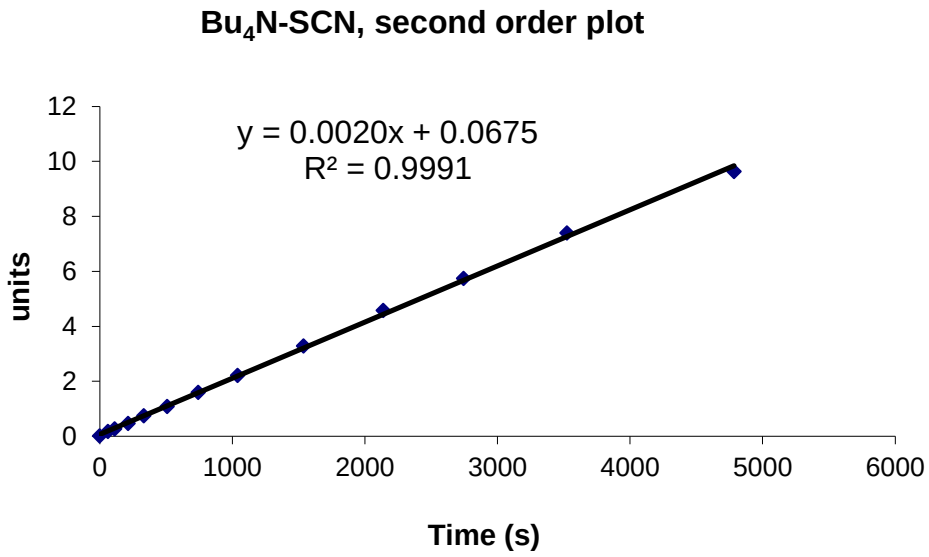

Figure 3.14 Kinetics of the addition of TMSCN to benzaldehyde using 1 mol% Bu_4N-NCS catalyst at 0 °C, in dichloromethane. The units for the y-axis are: $([PhCHO]_o–[Me_3SiCN]_o)^{-1}\ln([Me_3SiCN]_o[PhCHO]_t[Me_3SiCN]_t^{-1}[PhCHO]_o^{-1})$ where the subscripts ø and t refer to initial concentrations and concentrations at time t respectively.

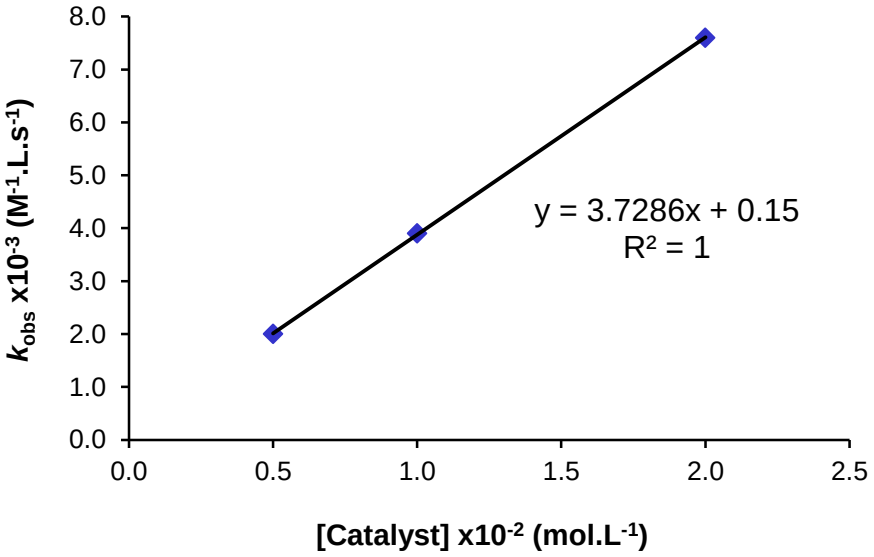

Figure 3.15 Plot of k_{obs} against [catalyst] at three different concentrations of Bu_4N-NCS.

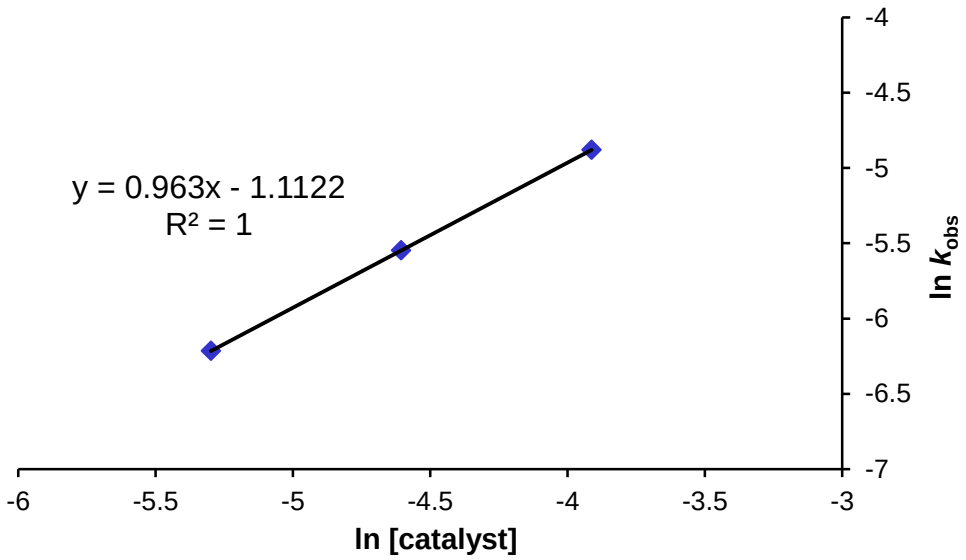

Figure 3.16 Plot of ln k_{obs} against ln[catalyst], the gradient gives information on the order with respect to Bu_4N-NCS.

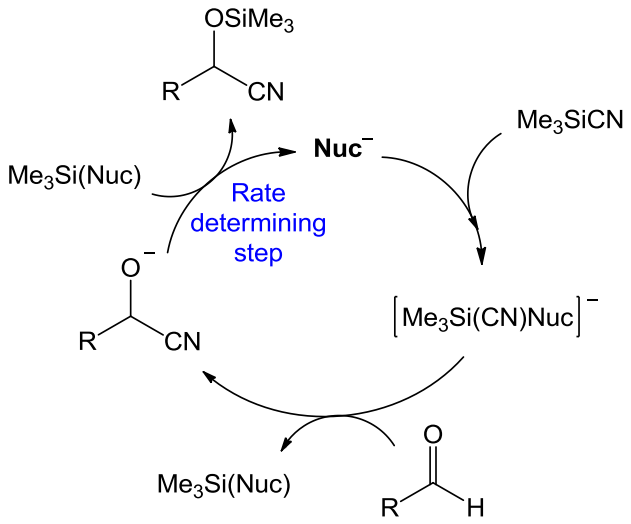

Scheme 3.11 Possible mechanism for racemic cyanohydrin synthesis catalysed by tetrabutylammonium thiocyanate.

3.6 Lewis base catalysis to promote cyanohydrin synthesis from ketones.

Ketones are known to be less reactive than aldehydes, and their use as substrates in asymmetric cyanohydrin synthesis has always been a challenge. Titanium catalyst **20** has been shown to be an effective system for the asymmetric addition of TMSCN to ketones; able to transform a variety of aromatic and aliphatic acetophenones into their respective trimethylsilyl cyanohydrin ethers.[39, 40b] This reactivity was associated with the highly Lewis acidic character of the metallic center. Recently, within the same family of metal(salen) complexes, aluminium dimer **69** in conjunction with phosphine oxide, was also shown to be a potential catalyst to carry out this transformation, since ketone derived cyanohydrins with fairly good enantioselectivities and yields were obtained (**Table 3.7**).[116] In this case, the reactivity is associated mainly to the Lewis basic character of the phosphine oxide, leading to cyanide activation, which suffices for the reaction to occur (See *section 1.4.3.2*).

Entry	Ketone	Conversion (%)	ee (%)
1	PhCOMe	85	51 (*S*)
2	4-Cl-$C_6H_4COCH_3$	99	51 (*S*)
3	3-Cl-$C_6H_4COCH_3$	99	47 (*S*)
4	4-Br-$C_6H_4COCH_3$	99	49 (*S*)
5	4-F-$C_6H_4COCH_3$	91	55 (*S*)
6	4-CH_3-$C_6H_4COCH_3$	62	50 (*S*)
7	4-CH_3O-$C_6H_4COCH_3$	54	55 (*S*)
8	$CH_3CH_2CH_2COCH_3$	100	44 (*S*)

Table 3.7 Asymmetric addition of TMSCN to ketones catalysed by $[Al(salen)]_2O$ and triphenylphospine oxide.[116]

The use of vanadium(salen) complexes **23a** and **23h** to catalyse the addition of TMSCN to acetophenone was investigated, but no cyanohydrin product was obtained. According to the Hammett analysis, this could be due to the insufficient Lewis acidic or Lewis basic character of these complexes. Therefore, the addition of triphenylphosphine oxide was expected to enhance the formation of chiral cyanohydrins as occurs in the case of the aluminium system. However, vanadium(salen) complexes **23a** and **23h** were again found to be unable to perform the reaction. In order to explain this phenomenon, the possibility of catalyst inhibition was suggested. Thus, triphenylphosphine oxide could instead of activating the cyanide, displace the counterion in the VO(salen)X complex, occupying its position and remaining strongly coordinated. This would inhibit dimer formation and prevent carbonyl coordination to the metallic centre.

^{51}V NMR spectroscopy was used to provide some support for this hypothesis. A 24 mM solution of VO(salen)NCS in dichloromethane was compared to a solution of equal concentration with a large excess of triphenylphosphine oxide (500 eq.) added to it. Analysis of the spectra (**Figure 3.17**) showed a change in the chemical shift of VO(salen)NCS from δ = -580.5 ppm to δ = -577.0 ppm after the addition of Ph_3PO. This chemical shift change is consistent with coordination of the vanadium ion to a more electronegative heteroatom (replacement of nitrogen for oxygen), thus giving a higher value for the chemical shift. This supports the assumption that the triphenylphosphine oxide strongly coordinates to the vanadium ion inhibiting the coordination of ketones and hence not allowing carbonyl activation. Therefore, as

ketones are generally less reactive, the activation of the cyanide is not enough for the reaction to occur.

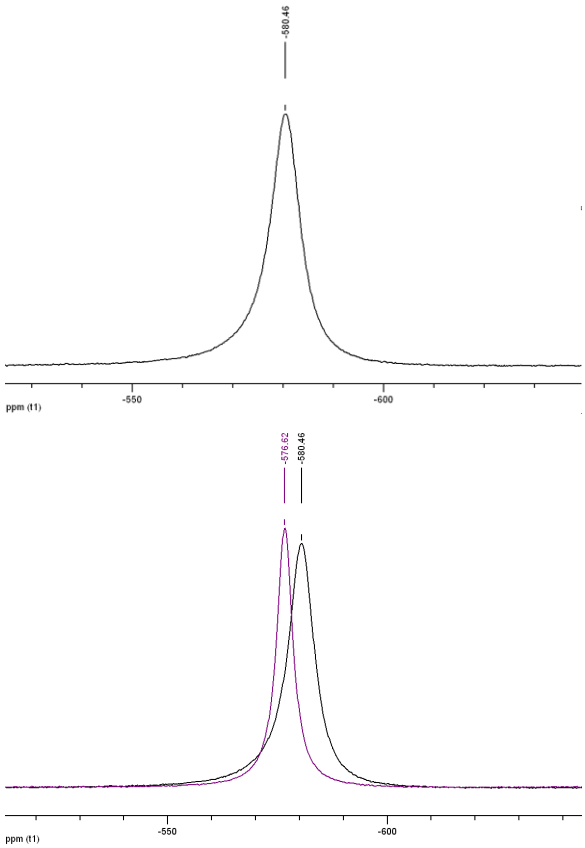

Figure 3.17 ^{51}V-NMR spectra of complex VO(salen)NCS recorded at 50 °C. Top: spectrum in dichloromethane (δ = -580.5 ppm). On the bottom: spectrum in dichloromethane with 500 equivalents of Ph_3PO added (δ = -577.0 ppm) overlaid on the spectrum in dichloromethane for comparison.

3.7 Conclusions

It has been demonstrated that Hammett analyses can provide detailed information on the relative importance of Lewis acid and Lewis base catalysis in asymmetric cyanohydrin synthesis. Amongst the metal(salen) complexes, the VO(salen)X complexes are the most effective catalysts for the addition of TMSCN to aldehydes, and this is due to dual activation of both substrates. The counterion has been shown to be partially involved in the Lewis basic character, however, the major Lewis base catalytic contribution is due to the oxo group, thus supporting the formation of bimetallic $O=V^{IV}$-$O=V^{V}$ species.

Three metal(salen) catalytic systems have been compared. All three ions studied in this section, titanium(IV), vanadium(V) and aluminium(III) are hard acids according

to the Pearson HSAB concept, and hence they are predetermined to be excellent Lewis acids since they have the 3*s*, 3*d* and 3*p* valence shell empty. However, it is the environment (ligands) which in this case determines the Lewis acidity of the metallic centre. The dinuclear titanium precatalyst can break one of the oxygen bridges and strongly coordinate the aldehyde. The vanadium precatalyst can also decoordinate the X ligand to create a highly Lewis acidic cationic species ($[VO(salen)]^{+}$) which will also strongly coordinate the aldehyde. In contrast, in the case of the bimetallic aluminium catalyst, the only oxygen bridge is unfavourable to be broken, as it is very stable. Therefore the aldehyde coordination is very weak. Hence, this system needs a Lewis base to achieve the same catalytic activity as the other two.

In contrast, whereas titanium and aluminium salen complexes were found to be good catalysts for the asymmetric addition of TMSCN to ketones, vanadium complexes turned out to be the worst catalysts for the asymmetric addition of TMSCN to ketones. This reaction requires a good Lewis acid or a good Lewis base catalyst such as $[Ti(salen)O]_2$ and $[Al(salen)]_2O/Ph_3PO$ respectively.

In addition to catalysts **20**, **23** and **69** which led to the formation of chiral trimethylsilyl cyanohydrin ethers, an achiral Lewis base has been described as an excellent catalyst for the racemic synthesis of cyanohydrins. A mechanistic study revealed that the reaction exhibits overall second order kinetics, and first order with respect to the catalyst. This suggests that the thiocyanate anion activates the TMSCN followed by the addition of cyanide to the aldehyde forming a cyanohydrin anion and TMS-SCN. Finally, the transfer of the silyl group to the cyanohydrin is the rate limiting step, this being consistent with a second order reaction.

4 Use of propylene carbonate as solvent for asymmetric cyanohydrin synthesis catalysed by metal(salen) complexes

4.1 Introduction

From an environmental point of view, the 100% atom economical asymmetric synthesis of cyanohydrins from aldehydes and ketones catalysed by titanium and vanadium(salen) complexes, has accomplished many of the required industrial demands. Amongst the benefits that can be highlighted are the low catalyst to substrate ratio (1:1000), and the ability to prepare highly enantiomerically enriched and conveniently protected cyanohydrins at room temperature.[37b] The use of alternative more stable and inexpensive cyanide sources such as potassium cyanide / acetic anhydride,[40a, 93a, 117] cyanoformates[40c, 40d, 118] and acyl cyanides[118b, 118c, 119] has also been achieved when using a bimetallic titanium(salen) complex as the catalyst. Unlike the titanium(salen) catalyst, vanadium(salen) complexes had been found to only accept potassium cyanide / acetic anhydride as an alternative to TMSCN. Recently, some work published by Khan *et. al*. showed that oxovanadium(V)(salen) chloride and ethylsulfonate complexes can induce the asymmetric addition of ethyl cyanoformate to aldehydes by using an additive such as imidazole.[120] Nevertheless, the best catalytic activity for the majority of the metal-based catalysts used in asymmetric cyanohydrin synthesis is achieved in chlorinated solvents. Ionic liquids have been successfully used in the vanadium-based catalysed reaction; however, at the expense of a higher catalyst loading.[121] Moreover, due to their unknown toxicity, the green credentials of ionic liquids are still being questioned. Recently, Zhou *et. al*. [122] reported a catalytic system formed from manganese(III) acetate and the water soluble Schiff-base ligands **100a,b** and **18e**, which can perform the asymmetric addition of sodium cyanide to aldehydes in methanol at room temperature, affording good yields and excellent enantiomeric excesses.

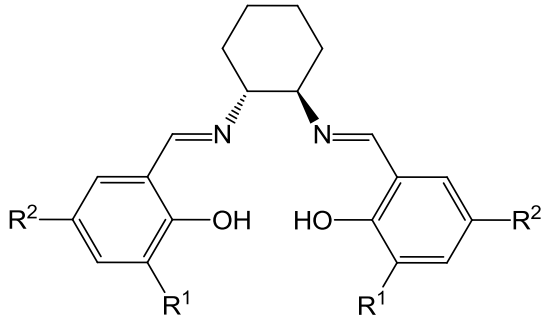

100a - R^1 = H, R^2 = SO_3Na
100b - R^1 = ^{t}Bu, R^2 = SO_3Na
18e - R^1 = R^2 = ^{t}Bu

4.1.1 Propylene carbonate as solvent

Organic carbonates such as **101-107,** especially propylene carbonate **105**, have started attracting interest as green solvents which can be used as alternatives to the more commonly used organic solvents (**Figure 4.1**). Propylene carbonate has been tested and shown to possess very low toxicity resulting in its use as a co-solvent for cleaning products and cosmetics.[123] In addition, due to its high dielectric constant (ε = 65), propylene carbonate is used as an electrolyte in lithium batteries,[124] and its large molecular dipole moment (4.9 D) and wide liquid range (mp -49 °C, bp 242 °C) makes it suitable for use as a polar aprotic solvent.[125]

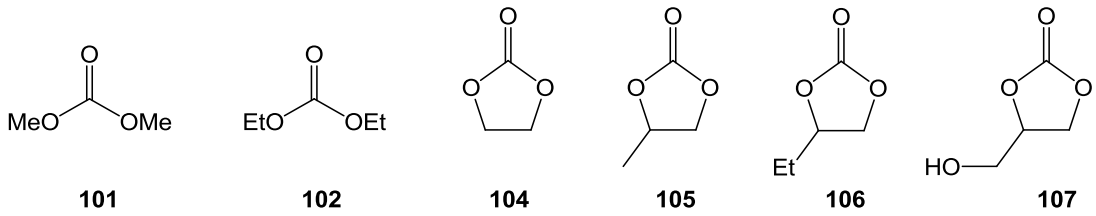

101 **102** **104** **105** **106** **107**

Figure 4.1 Most common organic carbonates used as solvents.

4.1.2 Homogeneous catalysis in propylene carbonate

Propylene carbonate has already seen several applications as a solvent for metal catalysed reactions. Amongst these, the work of Reetz *et al*. who introduced the use of propylene carbonate as a solvent in palladium-catalysed Heck reactions is notable.[126] More interesting from our point of view, are the examples of asymmetric reactions in propylene carbonate; in particular, the work done by Börner *et al*. on rhodium-catalysed asymmetric hydrogenation of prochiral olefins,[127] and the asymmetric allylic alkylation catalysed by palladium complexes reported by Schäffner *et al*.,[128] both of which gave good enantioselectivities and high catalytic activities for reactions carried out in propylene carbonate. In 2009, our group started investigating the use of ethylene and propylene carbonate in *(S)*-proline-catalysed cross-aldol reactions, for which best results had been obtained in DMSO as solvent.[129] Propylene carbonate was demonstrated to be a better solvent system than DMSO, giving excellent diastereo- and enantioselectivities, however, the addition of water to help dissolve the proline was a drawback.[130] This research is now being extended to the use of amino acids other than proline which are more soluble in propylene carbonate (**Scheme 4.1**).[131]

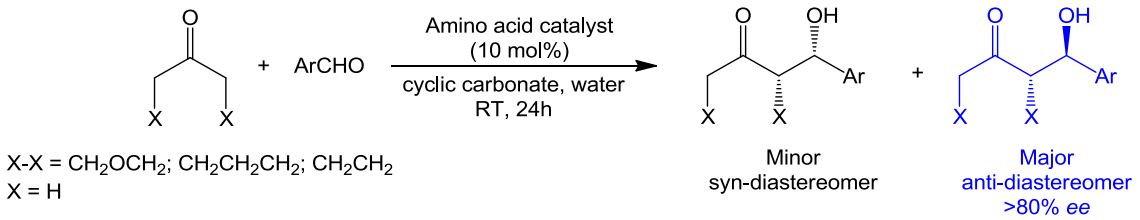

Scheme 4.1 Model cross-aldol reaction catalysed by chiral aminoacids in propylene carbonate as solvent.

4.1.3 Propylene carbonate preparation

The most commonly employed industrial route to obtain cyclic carbonates is the reaction between epoxides and carbon dioxide (**Scheme 4.2**).[132] Several recent improvements have allowed the propylene oxide required for this process, which was rather difficult to produce, to be obtained in a one-pot reaction involving *in situ* preparation of hydrogen peroxide from molecular hydrogen and oxygen.[133] The industrial preparation of ethylene **104** and propylene **105** carbonates uses pressurised procedures, which require a lot of energy. In 2007, a new catalyst based on an aluminium(salen) complex developed in our group enabled the preparation of cyclic carbonates at atmospheric pressure and room temperature when the catalysis was carried out in batch mode, or at 100 °C in a gas-phase flow reactor.[84] The flow reactor results were achieved by immobilisation of the catalyst onto a solid support. This process can also reduce the carbon dioxide emissions of power stations, since the catalyst was shown to be highly active even in the presence of the fuel-gases of a real power station. Another advantage of this catalyst is that it can be reactivated and reused over 60 cycles.

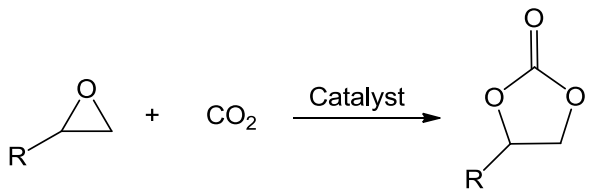

Scheme 4.2 Synthesis of cyclic carbonates from epoxides and CO_2.

4.2 Preliminary results

To determine whether propylene carbonate could be an effective alternative solvent to dichloromethane for the catalysed asymmetric addition of TMSCN to aldehydes, when this was catalysed by $[Ti(salen)O]_2$ and VO(salen)NCS complexes, a standard set of conditions, known to be ideal when using dichloromethane as the

solvent, was applied to a range of aromatic and aliphatic aldehydes. These conditions involved the use of concentrations of 0.49 M aldehyde and 0.55 M TMSCN with 0.1 mol% of the metal(salen) complex relative to the aldehyde and a reaction time of two hours at room temperature. In order to provide comparison data on the effectiveness of the catalytic process in both solvent systems, the experiments were carried out in parallel using both dichloromethane and propylene carbonate as solvents. The conversion was determined by ^{1}H-NMR spectroscopy integrating the peaks of the aldehyde and the cyanohydrin, and the enantiomeric excesses were measured by gas chromatography after transforming the protected cyanohydrin trimethylsilylether into the corresponding acetate using acetic anhydride catalysed by 10 mol% of scandium(III) triflate in propylene carbonate.[110]

4.2.1 [Ti(salen)]$_2$O$_2$ as the catalyst

When the bimetallic titanium complex **20** was used as the catalyst, the use of propylene carbonate led to a significant decrease in the asymmetric induction for all of the aldehydes screened in this study as illustrated in **Table 4.1**. The use of propylene carbonate also had a detrimental effect on the catalytic activity for all of the aromatic aldehydes; however, the aliphatic aldehydes generally gave better conversions in propylene carbonate than those obtained from reactions in dichloromethane.

Aldehydes	**Dichloromethane**		**Propylene carbonate**	
	Conversion (%)	*ee(%)*	*Conversion (%)*	*ee(%)*
PhCHO	95	78	33	40
4-FC$_6$H$_4$CHO	40	76	24	35
3-ClC$_6$H$_4$CHO	83	84	53	46
4-ClC$_6$H$_4$CHO	98	83	20	25
2-MeC$_6$H$_4$CHO	76	89	47	36
3-MeC$_6$H$_4$CHO	95	97	30	57
4-MeC$_6$H$_4$CHO	82	68	16	49
CH$_3$(CH$_2$)$_7$CHO	71	73	98	45
(CH$_3$)$_3$CCHO	93	47	100	10
CyCHO	100	66	97	19

Table 4.1 Asymmetric synthesis of trimethylsilyl cyanohydrins using 0.1 mol% of[Ti(salen)O]$_2$ **20** as catalyst for 2 hours at room temperature.

The reason for this general decrease in catalytic activity and enantioselectivity is probably due to the greater polarity of propylene carbonate compared to dichloromethane, which favours the dissociation of the catalytically active bimetallic complex **20** into its monometallic catalytically inactive counterpart **24** (**Scheme 4.3**). It has previously been demonstrated by ^{1}H-NMR spectroscopy that the bimetallic titanium complex exists in equilibrium with its monomer, and this equilibrium is affected by the nature of the solvent as well as by the catalyst concentration and temperature.[117b] For this reason, and because of the high affinity of titanium(IV) for oxygen, it is believed that solvation of the Ti=O bond displaces the position of the equilibrium towards the monomer, and thus the concentration of the catalytically active bimetallic species diminishes, resulting in loss of catalyst effectiveness.

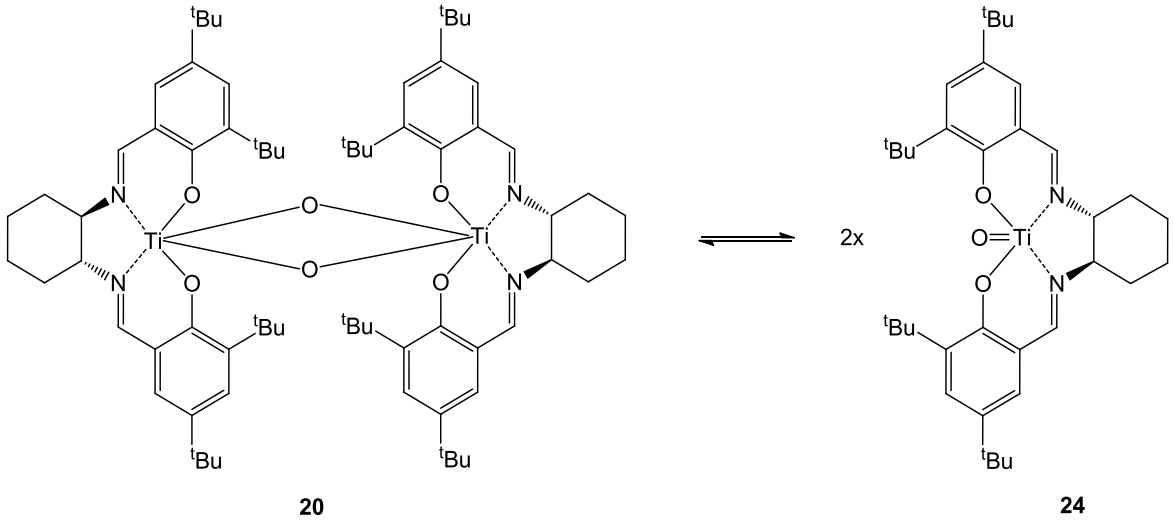

20 **24**

Scheme 4.3 Monomer-dimer equilibrium for $[Ti(salen)O]_2$ in solution.

4.2.2 VO(salen)NCS as the catalyst

The results summarised in **Table 4.2** are the corresponding conversions and enantiomeric excesses obtained for the asymmetric addition of TMSCN to aldehydes when VO(salen)NCS was used as catalyst. In this case, the solvent change also affected the catalyst performance, nonetheless, this effect is far less pronounced than reactions catalysed by $[Ti(salen)O]_2$. Again, the catalytic activity when aliphatic aldehydes are used as substrates is essentially unaffected or slightly better in propylene carbonate that it is in dichloromethane.

Aldehyde	Dichloromethane		Propylene carbonate	
	Conversion (%)	*ee(%)*	*Conversion (%)*	*ee(%)*
PhCHO	100	86	73	80
4-FC_6H_4CHO	81	91	67	76
3-ClC_6H_4CHO	83	89	56	62
4-ClC_6H_4CHO	90	93	73	76
2-MeC_6H_4CHO	81	96	78	73
3-MeC_6H_4CHO	100	99	67	93
4-MeC_6H_4CHO	86	87	56	86
$CH_3(CH_2)_7CHO$	88	83	96	67
$(CH_3)_3CCHO$	100	86	99	76
CyCHO	100	88	97	67

Table 4.2 Asymmetric synthesis of trimethylsilyl cyanohydrins using 0.1 mol% VO(salen)NCS as catalyst for 2 hours at room temperature.

The reason for this general decrease in both catalytic activity and enantioselectivity probably has the same cause as discussed above for titanium(salen) complex **20** catalysed reactions, i.e. catalyst dissociation. Even though the VO(salen)NCS complex is a monomer in its solid state,[44b] kinetic studies showed that in solution, this complex coexists with a mixed-valence bimetallic complex (**Scheme 4.4**), and both monometallic and bimetallic species are catalytically active.[44b] Mechanistic studies carried out with VO(salen)NCS precatalyst showed that the catalysis occurs predominantly through a bimetallic species. Therefore, when a highly polar solvent such as propylene carbonate is employed, it facilitates the dissociation of the bimetallic complex **22-23h** (**Scheme 4.4**) which results in a decrease in the catalytic activity. However, in this case, unlike titanium complex **20**, the monomer of **23h** is also catalytically active, which makes the reaction generally slower but almost equally as effective.

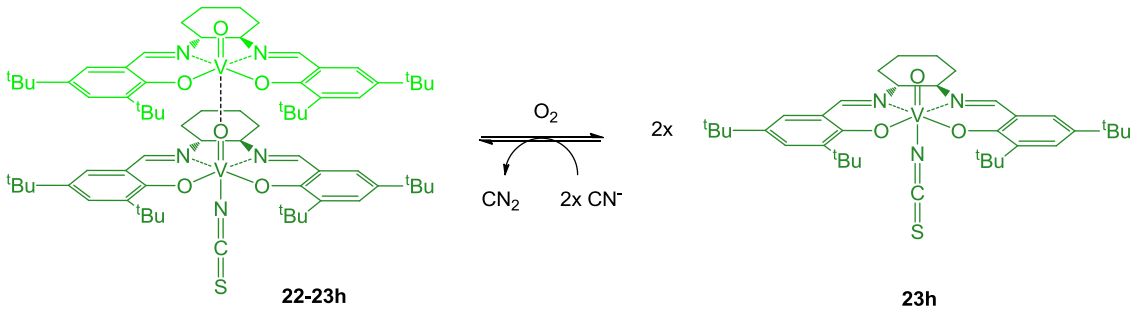

Scheme 4.4 Monomer-dimer equilibrium wherein the binuclear species is a mixed-valence species.

In order to optimise the reaction conditions for the asymmetric synthesis of cyanohydrins using VO(salen)NCS as catalyst in propylene carbonate, the reaction times were extended and the reaction temperature reduced. The results of this study are illustrated in **Table 4.3**. Thus, starting with benzaldehyde, when the reaction time was extended to 4 and 24 hours at room temperature (entries 1 and 2), this had a beneficial effect on the conversion, whilst the enantioselectivity remained constant. A similar conversion was also obtained when the amount of catalyst was doubled and the reaction time kept at two hours (entry 3). However, the enantioselectivity of the reaction still required improvement. Therefore, the reaction temperature was reduced to 0 °C and the reaction time extended to 18 hours to obtain an identical enantioselectivity to that obtained after 2 hours reaction at room temperature with dichloromethane as the solvent (entry 4). In the case of electron-rich aromatic aldehydes, for which the enantioselectivities were far less affected by the change in solvent, a 24 hour reaction time sufficed to raise the conversions to the level obtained after 2 hours reaction in dichloromethane (entries 9, 10 and 11). In contrast, the enantioselectivities for electron-deficient aromatic aldehydes, which were significantly reduced by the change of solvent, required a temperature of 0°C to achieve reasonably high asymmetric induction (entries 5, 6 and 7, **Table 4.3**). Therefore, in order to obtain the same conversions as those observed in dichloromethane at room temperature, the reaction times were extended to 24 hours. For the aliphatic aldehydes, a decrease in the reaction temperature to 0 °C with a reaction time of 18 hours slightly increased the asymmetric induction, achieving enantiomeric excesses of 60-80% (entries 12, 13 and 14, **Table 4.3**); however, these are not comparable to those obtained in dichloromethane. Therefore, in order to further enhance the enantioselectivity of the reactions, the reaction temperature was lowered to -20 °C (entries 15, 16 and 17, **Table 4.3**), which resulted in a further improvement in enantioselectivity to 75-80%.

Entry	Aldehyde	T (°C)	Time (h)	Cat. (mol%)	Conversion (%)	ee (%)
1	PhCHO	rt	4	0.1	83	83
2	PhCHO	rt	24	0.1	92	80
3	PhCHO	rt	2	0.2	86	85
4	PhCHO	0	18	0.1	73	86
5	4-FC_6H_4CHO	0	24	0.1	88	88
6	3-ClC_6H_4CHO	0	24	0.1	89	82
7	4-ClC_6H_4CHO	0	24	0.1	86	80
8	4-MeC_6H_4CHO	0	18	0.1	63	90
9	2-MeC_6H_4CHO	rt	24	0.1	100	81
10	3-MeC_6H_4CHO	rt	24	0.1	93	89
11	4-MeC_6H_4CHO	rt	24	0.1	90	83
12	$CH_3(CH_2)_7CHO$	0	18	0.1	100	61
13	$(CH_3)_3CCHO$	0	18	0.1	92	76
14	CyCHO	0	18	0.1	100	80
15	$CH_3(CH_2)_7CHO$	-20	24	0.1	98	75
16	$(CH_3)_3CCHO$	-20	24	0.1	88	77
17	CyCHO	-20	24	0.1	100	80

Table 4.3 Optimisation of the asymmetric synthesis of cyanohydrins catalysed by VO(salen)NCS in propylene carbonate.

The cyanohydrin trimethylsilyl ether could not be separated from the propylene carbonate. Due to its high boiling point, propylene carbonate cannot be removed by evaporation. In addition, the conventional extractive methods did not allow the product to be separated from the solvent, since propylene carbonate is miscible with the majority of organic solvents and water. Distillation was not successful since the product co-distils with the solvent, and attempted purification by chromatography led to product decomposition. Nevertheless, one of the most common synthetic applications for cyanohydrins is the production of chiral α-hydroxy acids.[134] Thus, it was possible to obtain (S)-mandelic acid in 60% isolated yield, by reaction of the mixture of propylene carbonate and mandelonitrile trimethylsilylether (81% *ee*) with 12 N hydrochloric acid under reflux for 6 hours (**Scheme 4.5**). The product of this reaction could be crystallised

from an ether/hexane mixture, giving the expected product as a white crystalline solid. In order to prove that no racemisation took place during this transformation, the mandelic acid was converted to methyl mandelate, allowing its enantiomeric excess to be determined as 81% by chiral HPLC.

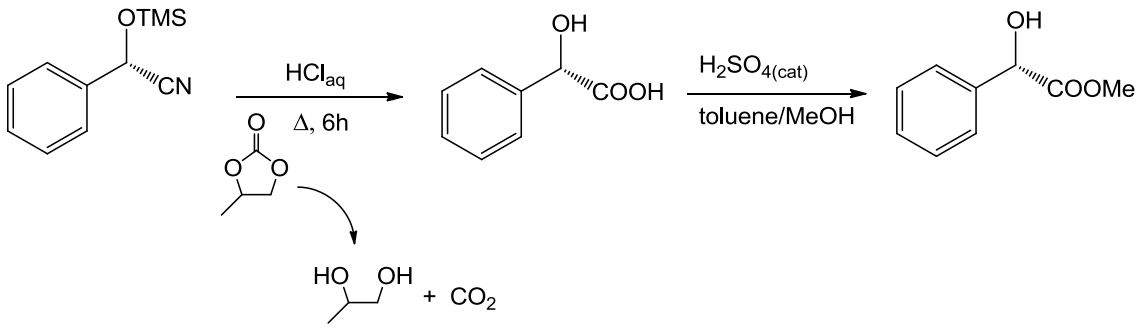

Scheme 4.5 Synthesis of mandelic acid, followed by an esterification to form methyl mandelate.

4.3 Initial kinetic studies in propylene carbonate using benzaldehyde as substrate.

The use of conversions after a specific reaction time does not always allow the relative activity of a catalyst in different media to be determined. The catalysis may proceed more slowly due to catalyst decomposition rather than just a simple interaction with the solvent. Thus, a highly active catalyst that undergoes decomposition may appear to be a much less active catalyst. Therefore, a kinetic study of asymmetric cyanohydrin synthesis in propylene carbonate was undertaken, in which the reaction course was monitored against time.

It is known from previous studies that the asymmetric addition of TMSCN to benzaldehyde in dichloromethane catalysed by vanadium(salen)X complexes obeys overall second order kinetics; and by carrying out reactions at different concentrations of benzaldehyde and TMSCN, the order with respect to each of them was determined and the reaction was found to be first order in both benzaldehyde and TMSCN concentrations. This allowed the following rate equation to be formulated:[44b]

$$\text{Rate} = k_{obs}[\text{PhCHO}][\text{TMSCN}]$$

(Rate of trimethylsilyl cyanohydrin formation)

In order to provide direct comparison with the kinetic profile obtained in dichloromethane, identical kinetic conditions were used for the reaction carried out in

propylene carbonate. Thus, the kinetic experiments were conducted at 0 °C using a 0.2 mol% catalyst loading, with initial concentrations of 0.49 M and 0.56 M for benzaldehyde and TMSCN respectively. The progression of the reaction was monitored by UV-vis spectrophotometry at a wavelength of 240-260 nm where benzaldehyde has its maximum absorbance. Thus, aliquots were extracted from the reaction mixture at appropriate time intervals and analysed by measuring the aldehyde decay over a period of 2.5 hours (**Figure 4.2**).

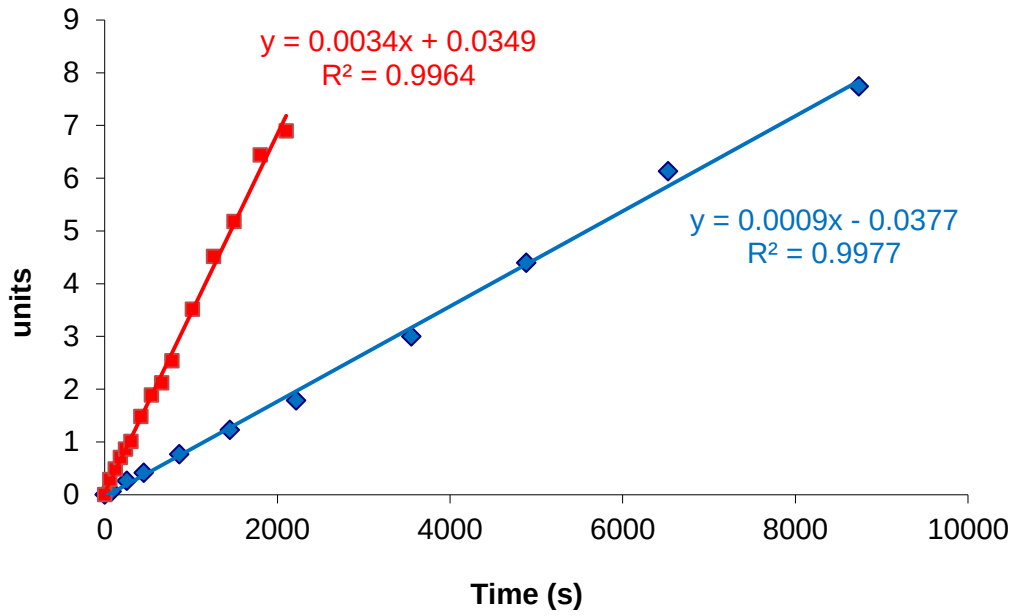

Figure 4.2 Second-order kinetic plots for the addition of TMSCN to benzaldehyde at 0 °C using 0.2 mol% of catalyst in dichloromethane (squares) and propylene carbonate (diamonds). The units for the y-axis are: $([PhCHO]_o–[Me_3SiCN]_o)^{-1}\ln([Me_3SiCN]_o[PhCHO]_t[Me_3SiCN]_t^{-1}[PhCHO]_o^{-1})$ where the subscripts ø and t refer to initial concentrations and concentrations at time t respectively.

The good fit to second order kinetics observed in both dichloromethane and propylene carbonate, indicates that the decrease in the rate of the reaction is due to the effect of the propylene carbonate being a more polar solvent rather than catalyst decomposition. There is also the possibility of facing a catalytic inhibition from solvent, as propylene carbonate bears a carbonyl group in its structure (this will be considered later on in the chapter). Nevertheless, the excellent fit to second order kinetics suggests that the catalytic mechanism remains the same in both solvents used. Thus, as previously suggested, the solvent affects the aggregation state of the catalyst in solution and hence the rate of reaction.

4.4 Kinetic studies at different catalyst concentrations

A method to get information on the monomer-dimer equilibrium of the catalyst under the reaction conditions is to determine the order with respect to the catalyst. It is known, that the asymmetric addition of TMSCN to benzaldehyde catalysed by VO(salen)X complexes in dichloromethane, all obey a second order rate equation (1), first order in both benzaldehyde and TMSCN concentrations.

$$\text{rate} = k_{obs}[\text{PhCHO}][\text{TMSCN}] \qquad (1)$$

$$k_{obs} = k[\text{catalyst}]^n \qquad (2)$$

$$\ln(k_{obs}) = \ln(k) + n\ln([\text{catalyst}]) \qquad (3)$$

As the catalyst is not consumed during the reaction, its concentration can be considered a constant and this is included in the observed rate constant (k_{obs}), obtained in the kinetic experiments. k_{obs} can then be expressed as in the equation (2), where k is the rate constant and the exponential n is the order with respect to the catalyst. This number provides information on the level of organization of the precatalyst in solution and the number of VO(salen) units involved in the catalytic cycle. Thus, when the precatalyst VO(salen)X is added to the reaction mixture, this rapidly establishes an equilibrium between monometallic and bimetallic species **A** and **B** (**Scheme 4.6**), where **B** is a mixed-valence species.

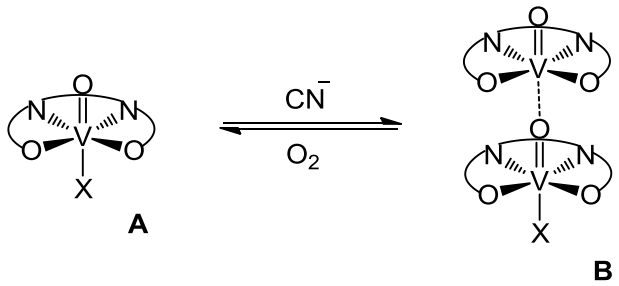

Scheme 4.6 VO(salen)X reduction and aggregation process.

Thus, if [cat] is the concentration of catalyst added to a reaction, then:

$$[\text{cat}] = [\text{A}] + 2[\text{B}]$$

And if K_{eq} is the equilibrium constant between A and B then:

$$[B] = K_{eq}[A]^2$$

This allows four limiting cases to be considered:

- If the catalytically active species is the monomer (rate = k[A]), and this is the predominant form in solution, then [cat] ≈ [A], **rate = k[cat]^1**
- If the catalytically active species is the monomer (rate = k[A]), but in solution the catalyst exists predominantly as a dimer, then [cat] ≈ 2[B], **rate = k[cat]$^{0.5}$**
- If the catalytically active species is the dimer (rate = k[B]), but in solution the catalyst exists predominantly a monomer, then [cat] ≈ [A], **rate = k[cat]^2**
- If the catalytically active species is the dimer (rate = k[B]), and the equilibrium in solution is inclined towards the dimeric form, then [cat] ≈ 2[B], **rate = k[cat]^1**

For VO(salen)NCS, the order with respect to the catalyst in dichloromethane was found to be 1.2, which suggests that the precatalyst (or monomeric form) exists in solution in equilibrium with a dimeric species, which is in turn predominantly responsible for the catalytic process. Therefore, in order to investigate the solvent effect on the catalytic addition of TMSCN to benzaldehyde when VO(salen)NCS was used as the catalyst, kinetic experiments at five different catalyst concentrations were carried out, whilst all the other parameters remained unchanged. The rate constant for each catalyst concentration was determined in triplicate using three different distilled batches of propylene carbonate which are listed in **Table 4.4** along with the average value. Then, rearrangement of equation (2), after taking the logarithm of both sides, gives equation (3). When ln(k_{obs}) was plotted against ln[catalyst] a slope of 0.980 was obtained, showing that, the asymmetric addition of TMSCN to benzaldehyde in propylene carbonate is first order with respect to the catalyst concentration, a result which is consistent with the catalyst existing only as monometallic species in propylene carbonate (**Figure 4.3**). In addition, when k_{obs} was plotted against the catalyst concentration, three straight lines were obtained (four with the average values) which all intercept the zero point (**Figure 4.4**).

Entry	VO(salen)NCS (mol%)	k_{obs} (1) ($M^{-1}s^{-1}$)	k_{obs} (2) ($M^{-1}s^{-1}$)	k_{obs} (3) ($M^{-1}s^{-1}$)	k_{obs} (average) $\times 10^{-3}$ ($M^{-1}s^{-1}$)
1	1.13 mM (0.2)	0.00057	0.00099	0.00090	0.82 ± 0.2
2	1.69 mM (0.3)	0.00087	0.00116	0.00127	1.10 ± 0.2
3	2.25 mM (0.4)	0.00100	0.00170	0.00155	1.42 ± 0.4
4	3.38 mM (0.6)	0.00220	0.00205	0.00229	2.18 ± 0.1
5	4.50 mM (0.8)	0.00296	0.00370	0.00296	3.21 ± 0.4

Table 4.4 Second order rate constants for the asymmetric addition of TMSCN to benzaldehyde ($mol.L^{-1}.s^{-1}$), at different catalyst concentrations.

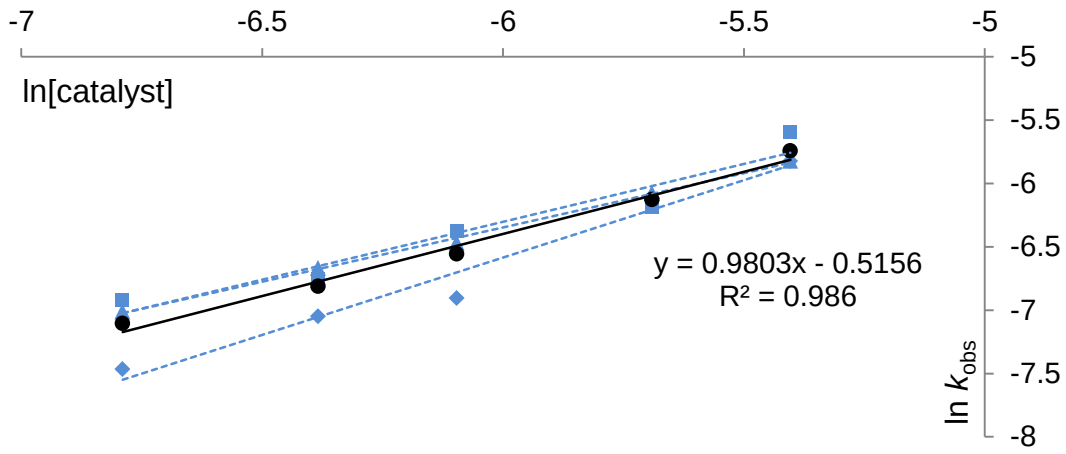

Figure 4.3 Plot of ln k_{obs} versus ln[catalyst], showing the order with respect to the catalyst VO(salen)NCS. The three sets of points with dotted lines (squares, triangles and diamonds) are the three individual measurements, whereas the solid line corresponds to the average of the three (circles).

VO(salen)NCS, being a highly polar molecule due to the dipolar nature of the V=O group, strongly interacts with propylene carbonate, which is a highly polar solvent (ε = 65), this will displace the monomer-dimer equilibrium towards the mononuclear species, which explains the observed decrease in catalytic activity and enantioselectivity.

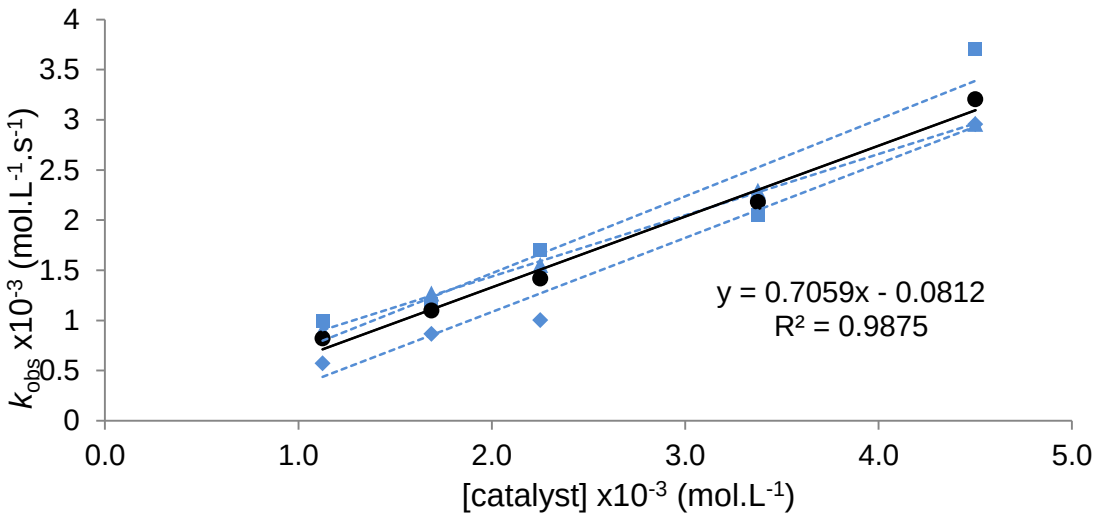

Figure 4.4 Plot of k_{obs} versus [catalyst], showing a good correlation to a straight line, which virtually intercepts at zero. The three sets of points with dotted lines(squares, triangles, and diamonds) represent the three individual measurements, whereas the solid line is the average correlation of the three (circles).

4.5 Introduction to thermodynamic parameters ΔH, ΔS and ΔG

The thermodynamic functions ΔH, ΔS and ΔG indicate whether or not a chemical reaction is energetically favourable. It is well understood that ΔG is the difference in free energy between the reagents and the products of a reaction. However, the fact that the products are energetically more stable than the reagents, does not ensure that the reaction will occur, since it does not take into account the energy profile through which the reagents are transformed to products. In the synthesis of cyanohydrins, a negative value for ΔG indicates that the reactants should evolve to products; however, the reaction does not occur in the absence of a catalyst (**Figure 4.5,** blue profile). This is due to the high energy barrier that the reagents have to overcome to evolve to products. The energy required to reach the peak or transition state is the Gibbs free energy of activation $\Delta G^{\ddagger}$. As is illustrated in **Figure 4.5**, $\Delta G^{\ddagger}$ can be affected by a catalyst (**Figure 4.5,** red profile). $\Delta G^{\ddagger}$ can also be affected by changes in the temperature, pressure, structure of the catalyst, solvent and other parameters.

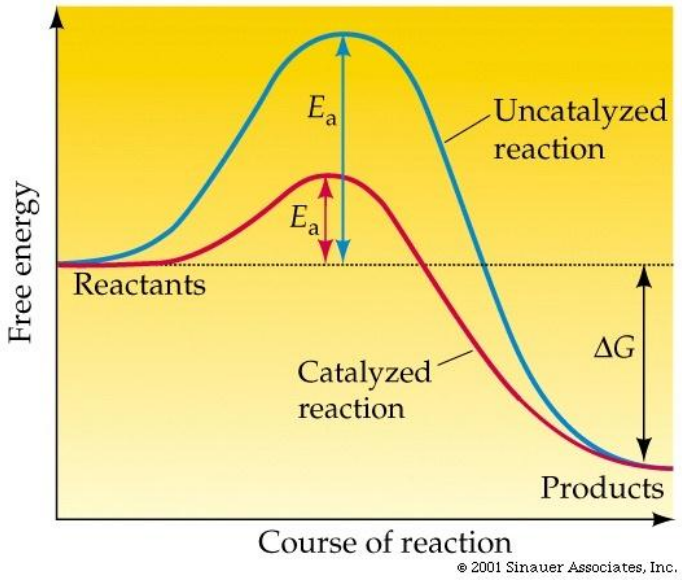

Figure 4.5 Free energy profile for a catalysed and uncatalysed reaction.

4.5.1 Variable temperature experiments

In order to fully understand the effect of the solvent during the transition state of cyanohydrin formation, the activation parameters $\Delta H^{\ddagger}$, $\Delta S^{\ddagger}$ and $\Delta G^{\ddagger}$ were determined. Therefore, comparison of the activation parameters in propylene carbonate with the ones found for reaction in dichloromethane should give a better understanding of the role of the solvent in the transition state of the reaction.

The Eyring equation (4), correlates the rate constants of a reaction to the enthalpy ($\Delta H^{\ddagger}$) and entropy ($\Delta S^{\ddagger}$) of activation. Thus, $\Delta H^{\ddagger}$ and $\Delta S^{\ddagger}$ can be experimentally determined by a variable temperature kinetic study. As it is more convenient to work with the k_{obs} ($k_{obs} = k[\text{catalyst}]^n$), directly available from the variable temperature experiments, equation (4) can be transformed to equation (5) by substituting k_{obs} into it and rearranging. Therefore, taking the logarithm of both sides, gives the final equation (6). Then, a plot of $\ln(k_{obs}/T)$ *vs.* 1/RT, should give a gradient equal to the negative value of $\Delta H^{\ddagger}$. The $\Delta S^{\ddagger}$ values can be obtained from the y-axis intercept by a simple mathematical rearrangement, since the order with respect to the catalyst has been determined (*Section 4.4*). Finally, the Gibbs free energy of activation ($\Delta G^{\ddagger}$) can be determined from the equation $\Delta G^{\ddagger} = \Delta H^{\ddagger} - T\,\Delta S^{\ddagger}$ at a given temperature.

$$k = (k_B \,.\, T \,.h^{-1}) \,.\, \exp(-\Delta H^{\ddagger}/\, RT) \,.\, \exp(\Delta S^{\ddagger}/\, R) \qquad (4)$$

$$k_{obs}/\, T = (k_B \,.h^{-1}) \,.\, [\text{catalyst}]^n \,.\, \exp(-\Delta H^{\ddagger}/\, RT) \,.\, \exp(\Delta S^{\ddagger}/\, R) \qquad (5)$$

$$\ln(k_{obs}/T) = (-\Delta H^{\ddagger}/RT) + (\Delta S^{\ddagger}/R) + \ln(k_B . h^{-1}) + n \ln[\text{catalyst}] \quad (6)$$

(k_B- Boltzmann's constant, h- Planck's constant, R- gas constant)

The kinetic experiments in propylene carbonate, using VO(salen)NCS as the catalyst, were conducted in duplicate at 5 different temperatures from 253 to 293K. Throughout the temperature range studied, all the reactions exhibited second order kinetics, with rate constants reported in **Table 4.5** which were then used to construct the Eyring plot shown in **Figure 4.6**.

Temperature (K)	k_{obs} **(1)** **($M^{-1}s^{-1}$)**	k_{obs} **(2)** **($M^{-1}s^{-1}$)**	k_{obs} **(average)** $\times 10^{-3}$ **($M^{-1}s^{-1}$)**
253	0.00011	0.00006	0.09±0.1
263	0.00029	0.00020	0.25±0.1
273	0.00057	0.00047	0.52±0.1
283	0.00150	0.00172	1.61±0.2
293	0.00255	0.00325	2.90±0.5

Table 4.5 Second order rate constants for the temperature range of 253 to 293 K for the asymmetric addition of TMSCN to benzaldehyde in propylene carbonate by VO(salen)NCS.

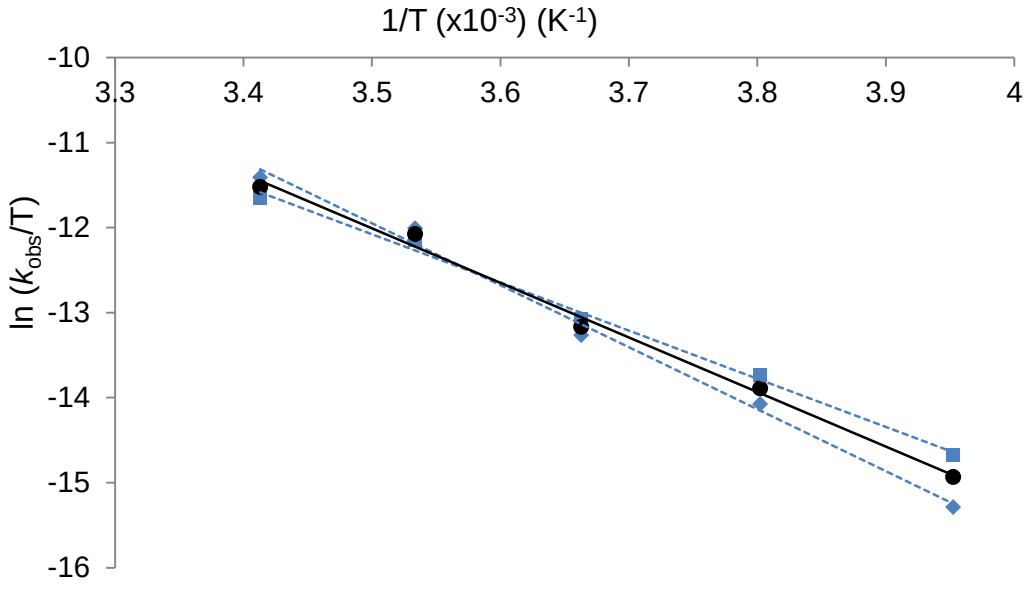

Figure 4.6 Eyring plot to determine the activation parameters for VO(salen)NCS catalyst in propylene carbonate. The two straight dotted lines (diamonds and squares) correspond to the two sets of data given in the **Table 4.5**, and the solid straight line (circles) to the average data.

The activation parameters in propylene carbonate were determined and are summarised in **Table 4.6** together with the activation parameters previously reported for reaction in dichloromethane.[44b] As can be seen, the enthalpy of activation was significantly greater in propylene carbonate than in dichloromethane. This is consistent with the earlier assumption that only one of the reagents is activated by the catalyst. In addition, the less negative entropy of activation when propylene carbonate is used as solvent supports the hypothesis that a monometallic species is responsible for the catalysis, which can only activate the aldehyde; then, an intermolecular nucleophilic attack from the separately activated TMSCN, will lead to the product formation. In contrast, when dichloromethane is the solvent, the transition state is more organized, since the predominant species in the catalysis is a bimetallic species, which activates both the aldehyde and the cyanide; therefore, the carbon-carbon bond formation is conducted intramolecularly. Despite the big difference in $\Delta H^{\ddagger}$ and $\Delta S^{\ddagger}$ between reactions carried out in dichloromethane and propylene carbonate, the values partially cancel each other out when $\Delta G^{\ddagger}$ is calculated at a given temperature (273K), giving more similar $\Delta G^{\ddagger}$ values. The slight increase in the Gibbs free energy of activation cannot fully explain the big difference in the rate constants, this being four-fold faster in dichloromethane than in propylene carbonate.

solvent	**$\Delta H^{\ddagger}$ (kJ mol^{-1})**	**$\Delta S^{\ddagger}$ (J mol^{-1} K^{-1})**	**$\Delta G^{\ddagger}$ (kJ mol^{-1})^{a}**
Dichloromethane	20.4	-136	57.5
Propylene carbonate	53.1	-54	67.8

Table 4.6 Activation parameters achieved by using Eyring equation (4) in two different solvent media**.** [a] T = 273 K.

An additional factor responsible for the lower reaction rate in propylene carbonate is an inhibition process. Propylene carbonate, having a carbonyl group in its structure, might compete with the carbonyl of the aldehyde and block the sixth coordination site of the $[VO(salen)]^{+}$ complex. Therefore, propylene carbonate being in a large excess compared to the aldehyde concentration, can reversibly occupy the sixth coordination site of the $[VO(salen)]^{+}$, resulting in lower abundance of catalytic sites, and hence a decrease in the reaction rate.

4.6 Vanadium nuclear magnetic resonance study

In order to support this hypothesis, a ^{51}V-NMR study was undertaken. Firstly, a spectrum of VO(salen)NCS in dichloromethane was recorded (**Figure 4.7a**), for which

the chemical shift appeared at -580 ppm. It is known by X-ray crystallography that the nitrogen from the isothiocyanate group is covalently bound to the vanadium ion. This, together with the effect of the other three oxygens and two nitrogens which form the octahedral geometry of the VO(salen)NCS complex results in a total of three oxygens and three nitrogen atoms coordinated to the vanadium ion. Then, when 500 equivalents of benzaldehyde were added to this solution a change in the chemical shift to a higher field was observed (-575 ppm) (**Figure 4.7b**). This is consistent with the substitution of a nitrogen atom (**N**CS) by oxygen (PhCH**O**) in the sixth coordination site, thus accounting in the formation of complex **A, (Figure 4.8)**. VO(salen)NCS was then dissolved in propylene carbonate. The ^{51}V-NMR signal was observed at -571 ppm (**Figure 4.7c)**. This is consistent with the formation of complex **B (Figure 4.8)**, in which, again, similarly to complex **A,** four oxygens and two nitrogen atoms are coordinated to the vanadium ion. This is an indication of the affinity of vanadium for the oxygen atom of the carbonyl group of the aldehyde and the cyclic carbonate. The addition of 500 equivalents of benzaldehyde to the solution of VO(salen)NCS in propylene carbonate did not lead to a significant change in the chemical shift (-569 ppm) (**Figure 4.7d**); however, when the half-widths of the ^{51}V-NMR signals in dichloromethane (930 Hz and 950 Hz for **Figure 4.7a** and **Figure 4.7b**, respectively) were compared to the corresponding signals in propylene carbonate (1730 Hz and 1510 Hz for **Figure 4.7c** and **Figure 4.7d**), the latter were much larger, indicating that an exchange process between species **A, B** and **C** could be taking place in propylene carbonate.

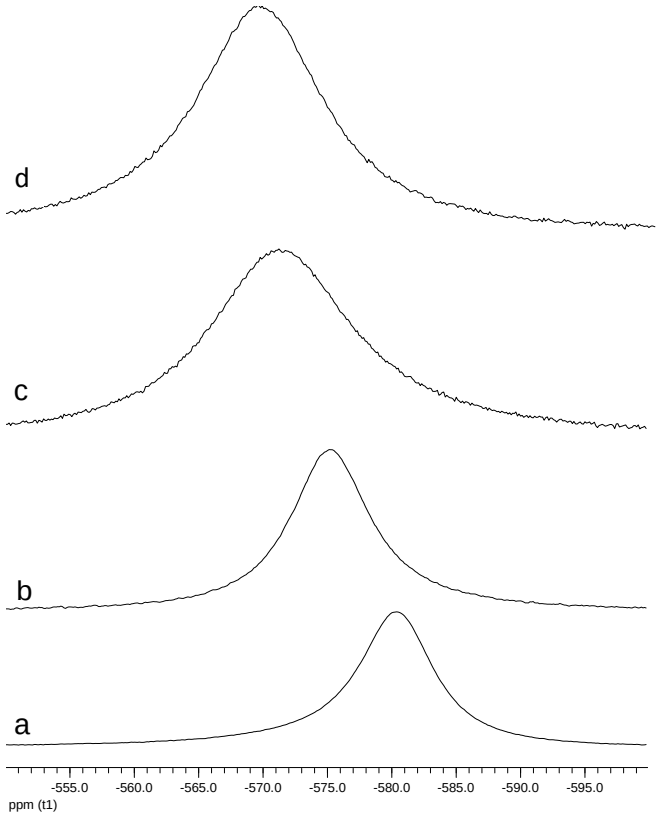

Figure 4.7 ^{51}V- NMR spectra of VO(salen)NCS in CH_2Cl_2 **a**, and in propylene carbonate **c**; and with 500 equivalents of benzaldehyde added **b** and **d.**

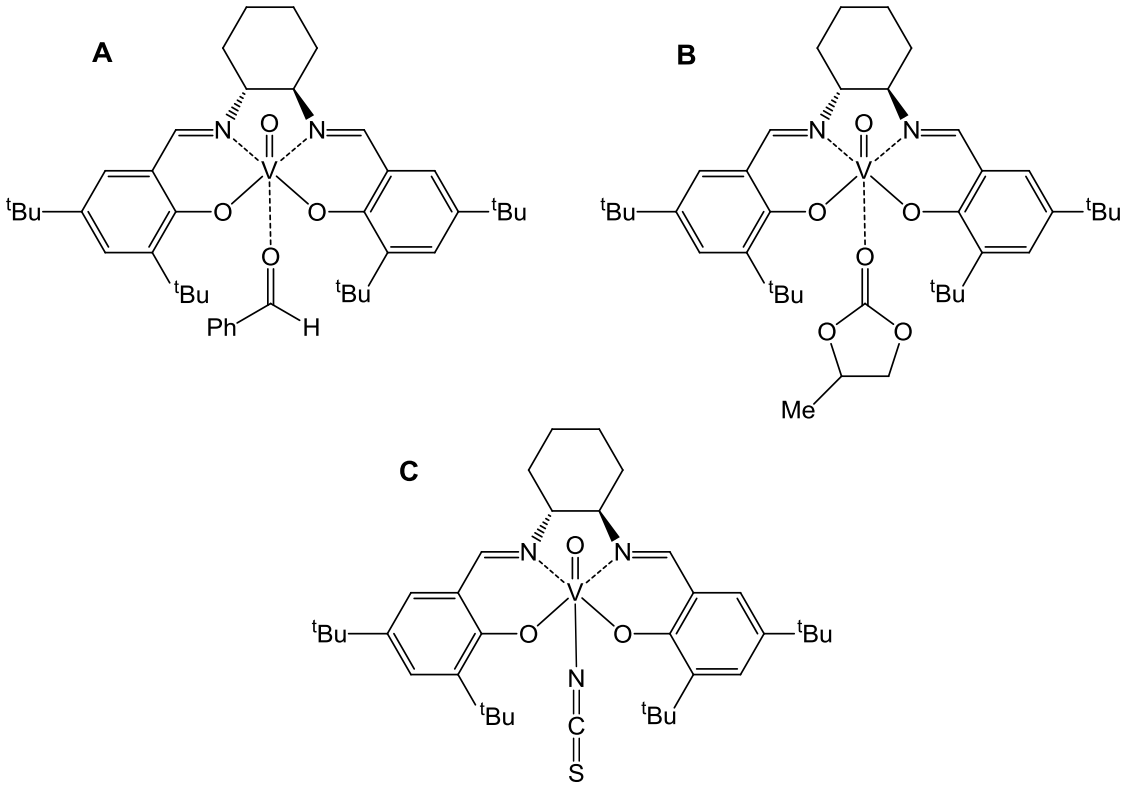

Figure 4.8 Structure of $[VO(salen)]^+$ according to the ^{51}V NMR spectra

4.7 Hammett analysis

As discussed in *Chapter 3*, Hammett studies on the asymmetric synthesis of cyanohydrins allowed the degree of Lewis acid and Lewis base catalysis to be determined for four different M(salen) complexes when the solvent was dichloromethane. Amongst these M(salen) complexes, two limiting cases were observed. The Hammett plot for the bimetallic aluminium(III)(salen) catalyst together with triphenylphosphine oxide, gave a gradient (ρ) very close to zero, which is indicative of a low level of Lewis acid catalysis. Thus, during the transition state, TMSCN will be largely activated, whereas the aldehyde is only slightly activated. The other limiting case, is observed with the bimetallic titanium(IV)(salen) catalyst. The large positive reaction constant (ρ) obtained in the Hammett correlation, indicates that the catalysis is entirely dominated by Lewis acid catalysis. Thus, it is the benzaldehyde which is activated during the transition state, as a result of a favourable coordination of the aldehyde to the metal. In the case of vanadium(V)(salen) complexes, regardless of the nature of the counterion, an intermediate value for the reaction constant was found. This indicates that both Lewis acid and Lewis base functionalities are operating during the catalysis.

Amongst the VO(salen)X complexes, and now taking into account the counterion, the monometallic or bimetallic nature of the catalytic species accounts for the activation of one or both reagents in the asymmetric silylation of aldehydes. The latter case is predominant when the catalysis is carried out in dichloromethane. However, it has been shown by both kinetic and spectroscopic studies that when propylene carbonate is the solvent, this directs the catalysis through a mononuclear transition state, due to the large solvation effect which inhibits bimetallic species formation. All the evidence suggests that, the catalysis by VO(salen)NCS in propylene carbonate would be similar to that observed when VO(salen)$EtOSO_3$ was the catalyst in dichloromethane, as this performs the catalysis in its monomeric form. Therefore, based on the previous Hammett correlation study, it was decided to investigate the solvent effect in catalytic cyanohydrin synthesis catalysed by VO(salen)NCS catalyst in propylene carbonate for the same set of aldehydes studied in the previous chapter.

Amongst the 14 aldehydes used for this study, only 12 were used to construct the Hammett plot, since 4-thiomethylbenzaldehyde and 4-methoxybenzaldehyde (entries 10 and 14, **Table 4.7**) did not fit onto a straight line. The reason for this could be explained

by the nature of the substituent. This, containing a heteroatom, might coordinate to the metallic centre thus, preventing the aldehyde from coordinating. In order to compare the data points obtained in propylene carbonate with the results obtained in dichloromethane, the experimental points for the 12 aldehydes were added to the same axes as shown in **Figure 4.9.**

Entry	**Aldehyde**	**σ**	k_1 **(M.s^{-1})**	k_2 **(M.s^{-1})**	$k_{average}$ **$\times 10^{-3}$ (M.s^{-1})**	***ee* (%)**
1	PhCHO	0	0.00090	0.00090	0.90±0.0	85
2	3,5-FC_6H_3CHO	0.68	0.00084	0.00110	0.97±0.2	45
3	3,4-ClC_6H_3CHO	0.6	0.00117	0.00124	1.20±0.1	40
4	4-$CF_3C_6H_4CHO$	0.53	0.00153	0.00173	1.63±0.1	44
5	3-ClC_6H_4CHO	0.37	0.00078	0.00090	0.84±0.1	57
6	3-FC_6H_4CHO	0.34	0.00104	0.00100	1.02±0.03	72
7	4-ClC_6H_4CHO	0.23	0.00093	0.00099	0.96±0.04	74
8	4-BrC_6H_4CHO	0.21	0.00089	0.00076	0.83±0.1	70
9	4-FC_6H_4CHO	0.06	0.00056	0.00048	0.52±0.1	84
10	*4-$CH_3SC_6H_4CHO$*	*0*	*0.00026*	*0.00025*	*0.26±0.01*	*60*
11	3-CH_3C_6H4CHO	-0.06	0.00068	0.00074	0.71±0.04	90
12	4-$CH_3C_6H_4CHO$	-0.14	0.00058	0.00058	0.58±0.0	77
13	3,4-$CH_3C_6H_3CHO$	-0.2	0.00055	0.00048	0.52±0.05	85
14	*4-$CH_3OC_6H_4CHO$*	*-0.27*	*0.00002*	*0.00004*	*0.03±0.01*	-

Table 4.7 Reactions kinetics carried out in propylene carbonate at 0ºC, using 0.5 M aldehyde, 0.55 M TMSCN and 0.2 mol% of VO(salen)NCS **23h**.

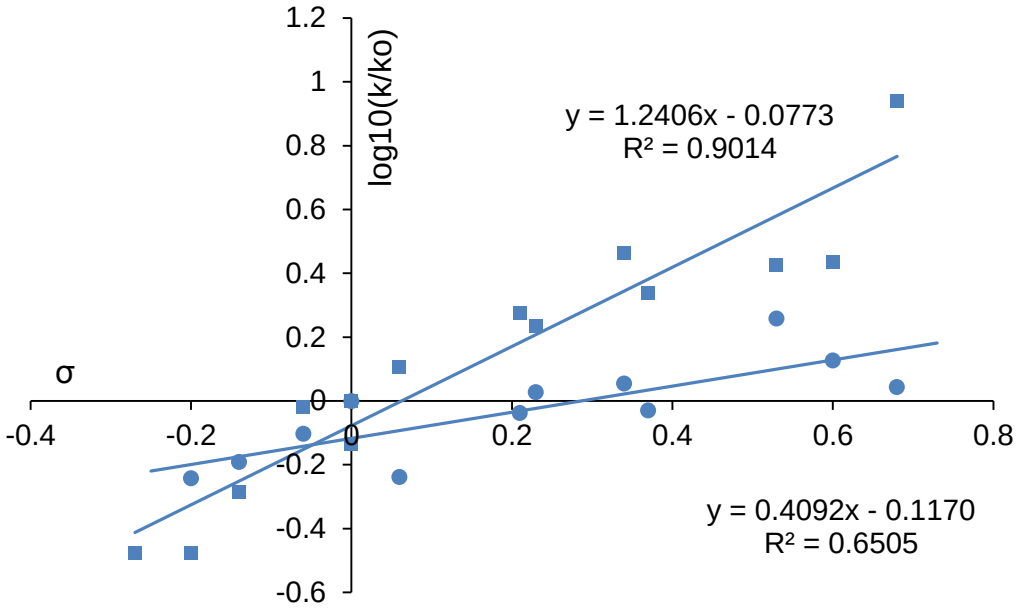

Figure 4.9 Hammett plot for the asymmetric addition of TMSCN to *para*- and *meta*-substituted aromatic aldehydes catalysed by VO(salen)NCS **23h** in dichloromethane (squares), and in propylene carbonate (circles).

Contrary to what was expected, VO(salen)NCS proved to be a better Lewis acid in dichloromethane than in propylene carbonate. The reaction constant ρ = + 0.4 indicates that the catalysis with VO(salen)NCS in propylene carbonate is almost entirely dominated by Lewis base catalysis as in the case of the $[Al(salen)]_2O$ / Ph_3PO catalytic system. Therefore, the high polarity of propylene carbonate may not only solvate the catalyst but also the aldehyde, making the approach of the aldehyde to the free sixth-coordination site difficult. Moreover, as shown by ^{51}V NMR, the affinity of vanadium(V) for oxygen, results in a competition process between the aldehyde and the solvent for the sixth coordination site. It is apparent by the decrease in the rate of the reaction, that fewer molecules of aldehyde can coordinate to the catalyst due to the competition of propylene carbonate with the aldehyde for the active site; thus, reducing the concentration of catalytically active species in solution. Therefore, the major species responsible for the catalysis is the isothiocyanate anion. The isothiocyanate counterion is believed to activate the TMSCN by formation of a hypervalent silicon species. This explains the decrease in the overall enantioselectivity. However, the aldehyde must be weakly coordinated to the vanadium during the transition state when the cyanohydrin is formed, otherwise only racemic cyanohydrin would be obtained. To confirm this assumption, it was decided to carry out a standard addition of TMSCN to benzaldehyde catalysed by VO(salen)$EtOSO_3$ in propylene carbonate. Since the affinity of the

$[VO(salen)]^+$ unit for the propylene carbonate and aldehyde is the same as in the case of VO(salen)NCS, it is then the nature of the counterion X that accounts for the timethylsilyl cyanide activation. Therefore, isothiocyanate anion, being a better Lewis base, should easily activate the TMSCN, whereas ethylsulfonate anion, which has never been proven to activate the TMSCN, is expected to give a very low degree of reactivity or none at all, and that was found to be the case. After 24 hours of reaction only 6% of benzaldehyde was transformed to cyanohydrin trimethylsilyl ether. Notably, when the same reaction was carried out in dichloromethane, 24 hours sufficed to achieve complete reaction.

4.8 Conclusions

VO(salen)NCS was shown to be catalytically active in propylene carbonate. This solvent is a better alternative to the usually used dichloromethane, as it has more environmentally friendly credentials. Despite the lower catalytic activity and enantioselectivity compared to those obtained in dichloromethane, these could be improved by optimizing the conditions with longer reaction times and lower temperatures, whilst maintaining the amount of catalyst used at 0.1 mol%.

Kinetic studies showed that the catalysis in propylene carbonate was entirely performed by a monometallic species, and this explains the decrease in reaction rate, which is 10-fold lower in propylene carbonate than in dichloromethane. This was confirmed by a variable temperature experiment, in which the activation parameters indicate a higher energy and more disordered transition state in propylene carbonate.

NMR studies showed that the propylene carbonate can also coordinate to the vanadium ion, thus resulting in an inhibition process.

The low reaction constant obtained in the Hammett plot study, which gave a value of 0.4 in propylene carbonate compared to 1.6 in dichloromethane, indicates that the aldehyde is not as strongly bound to the metallic centre. This also explains why we observed an overall lower enantioselectivity. Therefore, as the aldehyde is further from the chiral centre during the transition state, the asymmetric induction is reduced. Moreover, the counterion, isothiocyanate, having been shown to be a good Lewis base, can, in turn, activate the TMSCN and perform the racemic addition of cyanide to aldehydes.

5 General conclusions

The counterion has a significant influence on the catalysis, not only in the rate determining step but also in the activation of the cyanide. It has been demonstrated that during asymmetric cyanohydrin synthesis catalysed by oxovanadium(V)(salen) complexes, these are reduced to oxovanadium(IV)(salen) whilst cyanide is oxidised to cyanogen via a non-radical mechanism. Therefore, the presence of oxygen is essential to reoxidise V(IV) to V(V) and thus maintain the balance between V(V) and V(IV) species. The activation of cyanide is only achieved by the most basic counterions, followed by the formation of VO(salen)CN, a precursor of VO(salen). A Hammett plot analysis has shown that thiocyanate is a better Lewis base than the ethylsufonate. However, this was not the major Lewis base catalytic contribution. It has been suggested that a bigger contribution is given by the oxo group, this supporting the formation of bimetallic $O=V^{IV}–O=V^{V}$ species.

In accordance with previous knowledge on the catalytic cycle, the bimetallic species VO(salen)–VO(salen)X has been shown to be a superior catalyst than monometallic VO(salen)X, due to the contribution of both Lewis acid and Lewis base catalytic sites. The relative importance on the Lewis acid and Lewis base catalysis of these complexes were compared to bimetallic $[Ti(salen)]_2O_2$ and $[Al(salen)]_2O/Ph_3PO$ catalytic systems. In the case of the titanium complex, the asymmetric addition of TMSCN to aldehydes is entirely Lewis acid catalysed, while for the aluminium complex, which binds to the aldehyde very weakly, it is the Lewis basic triphenylphosphine oxide which is predominantly responsible for the catalysis. This system has also been shown to accept ketones as substrates providing moderate catalytic activities and enantioselectivities, whereas VO(salen)X has not been able to catalyse the addition of TMSCN to ketones even when used in combination with a Lewis base (Ph_3PO). This was shown to compete with the counterion and carbonyl compound for the sixth coordination site around the vanadium ion.

Propylene carbonate has been used as an alternative solvent to dichloromethane, leading to slower reactions and lower enantioselectivities, however, these could be improved by extending the reaction times and lowering the temperature. Kinetic studies have revealed that in propylene carbonate, the reaction was entirely catalysed by monometallic species, which explains the decrease in reaction rate, but not the decrease in enantioselectivity. NMR spectroscopy experiments suggested that propylene

carbonate might coordinate to the vanadium ion, resulting in a less accessible Lewis acidic site. This would position the aldehyde further from the chiral salen ligand during the transition state, and hence the transfer of chirality from the ligand would be less effective. In addition, the low reaction constant of 0.4 determined by a Hammett analysis suggests that the thiocyanate anion is at the same time activating the TMSCN catalysing the formation of racemic cyanohydrin trimethylsilyl ether. This explains the loss in enantioselectivity.

6 Future work

Following the investigations of the Lewis acid and Lewis base effect on asymmetric cyanohydrin synthesis, it would be of interest to do a secondary kinetic isotope effect study (KIE = k_H/k_D). Thus, by isotopically labelling the aldehyde with a deuterium to affect the C=O bond's zero-point vibration, this might result in a slight change in the reaction rate. This experiment would help in the understanding of the structure of the transition state; since the carbon directly bound to the hydrogen/deuterium undergoes a change in hybridisation from sp^2 to sp^3. Therefore, if the cyanide is closer to the reaction centre (aldehyde, sp^2) in the transition state, k_H/k_D would exhibit a value around 0.7, indicating a possible Lewis acid activation; whereas if the k_H/k_D value is 0, might indicate that the cyanide and not the aldehyde is being activated, thus being not as close to the reaction centre in the transition state.

In order to further understand the coordination of the aldehyde to the metal(salen) complexes, it might be revealing to isotopically label the oxygen of the aldehyde. Unlike ^{16}O, with nuclear spin I = 0, its isotope ^{17}O, with nuclear spin I = 5/2, can be observed by NMR and EPR, thus, these techniques could be used as a tool to provide more evidence on the coordination strength and hence on the Lewis acidity of the metal complexes.

Further study on the inhibitory effect of propylene carbonate as solvent during the cyanohydrin formation catalysed by oxovanadium(salen) complexes should be considered. Thus, a study on the solvent effect could be done by correlating the rate of reaction versus the Lewis basicity of solvents other than propylene carbonate, which also bear a carbonyl group such as N, N-dimethylformamide, ethyl acetate, acetone and even other cyclic and acyclic carbonates.

No reactions other than cyanohydrin synthesis and Strecker reactions have been studied in our group using oxovanadium(salen) complexes. Additional work should be addressed to the utilization of these complexes in other chiral product forming reactions involving the activation of an aldehyde.

7 Experimental Section

7.1 Chemicals and Instrumentation

Dichloromethane, tetrahydrofuran and propylene carbonate, used as solvents, were all freshly distilled under anhydrous and inert conditions prior to use.[135] For the work-up and further purification procedures, commercial grade solvents were used. Chromatographic purification employed silica gel 60 (0.040-0.063 mm) on its own or with 2.5% of triethylamine (v/v) for those products prone to decompose under acidic conditions. All the aldehydes were freshly distilled on a Büchi B-580 Kügelrohr apparatus immediately prior to use. Trimethylsilyl cyanide, which needed more care due to its toxicity, was distilled in batches using a normal distillation apparatus under nitrogen and extremely dry conditions. Other commercially available chemicals (purchased from Alfa Aesar, Aldrich, Fluka, Riedel-de Haën) were used as received.

^{1}H, ^{13}C and ^{19}F-NMR spectra were recorded on either a Bruker Avance 300 or a JEOL 400 spectrometer. ^{51}V-NMR spectra were run on a JEOL 500 spectrometer at 50 ºC. d-Chloroform was used as solvent unless specified otherwise. TMS was used as internal standard for ^{1}H and ^{13}C-NMR spectra, while ^{19}F and ^{51}V-NMR spectra were referenced to $CFCl_3$ and $VOCl_3$ respectively. Chemical shifts are expressed in parts per million (ppm) and multiplicities are described as singlet (s), doublet (d), triplet (t), quartet (q), multiplet (m), broad (br) or a combination of these.

High and low resolution mass spectrometry was conducted in a Waters LCT Premier MS apparatus using positive ion mode. A methanolic solution of the compound to be analysed was injected directly via syringe pump.

Infrared spectra were recorded on a Perkin Elmer FT-IR spectrometer using an ATR attachment. The sample was confined in a small conical cavity and pressed tightly to the lens. Peak intensities are described as broad (br), strong (s), medium (m) and weak (w).

Optical rotations were measured on a Polaar 2001 Optical Activity polarimeter. The sample concentration is reported as c (g/100mL). The solutions were prepared in a volumetric flask, and measured in a one decimetre long cuvette. Melting points were obtained using a Stuart melting point SMP3 system.

Absorbance measurements for kinetic experiments were recorded on a Biochrom Libra S12 UV-vis spectrophotometer, using 10 mm quartz cuvettes. Aliquots of the reaction were collected using a SGE Analytical Science microsyringe.

X-band EPR measurements were conducted by Victor Chechik and Marco Conte on a JEOL JES-RE1X ESR spectrometer at the University of York. The spectra simulation software used was EPR-WinSim.

The GC-MS analysis for detection of the TEMPO-CN adduct was carried out using a WATERS GCT Premier Agilent 7890A GC instrument coupled to a Restek Corp Stabilwax 30 m x 0.25 mm ID, 0.25 μm film column. The initial temperature of 50 °C was held for 5 minutes, then a ramp of 32 °C/min was applied to 220 °C. A different GC-MS instrument was used for the detection of TMS-X and $(CN)_2$ species which features are the following: A VARIAN CP-3800 gas chromatograph equipped with a SUPELCO 28055-U 30 m × 0.32 mm ID, 0.25 μm film column and coupled to a VARIAN Saturn 2200 GC/MS detector. An initial temperature of 50°C was used with a ramp of 8 °C min^{-1} to 150 °C.

Enantiomeric analysis of cyanohydrin acetates was performed using a VARIAN CP-3800 chiral gas chromatograph with a TCD detector using a Supelco Gamma DEX 120 fused silica capillary column (30 m × 0.25 mm) with hydrogen as a carrier gas. A Varian ProStar HPLC apparatus using a ChiralPak® AS column was used to determine the enantiomeric excess of methyl mandelate.

7.2 Statistical treatment of the kinetic experiments

Kinetics were all analysed by linear least squares regression. Thus, when the relationship between one independent variable *x* and a variable *y* dependent on *x* are represented in a scatter plot, these can be fitted to a straight line, fulfilling the following equation:

$$y = \beta_o + \beta_1 x + \varepsilon$$

where,

- *y* is the dependent variable
- *x* is the independent variable
- β_o is used to estimate the intercept on the Y axis
- β_1 is used to indicate the slope of the regression line
- ε is a random, independent error term or residual (the difference between the observed *y* value and that predicted by the model)

If we assume that the error terms are Normally distributed, the equation reduces to:

$$y = \beta_o + \beta_1 x$$

When the scattered plot of *y* vs. *x* looks approximately linear, the least squares method is used to achieve the best fit to a straight line. This method minimises the sum of squared vertical differences between the observed *y* values and the line.

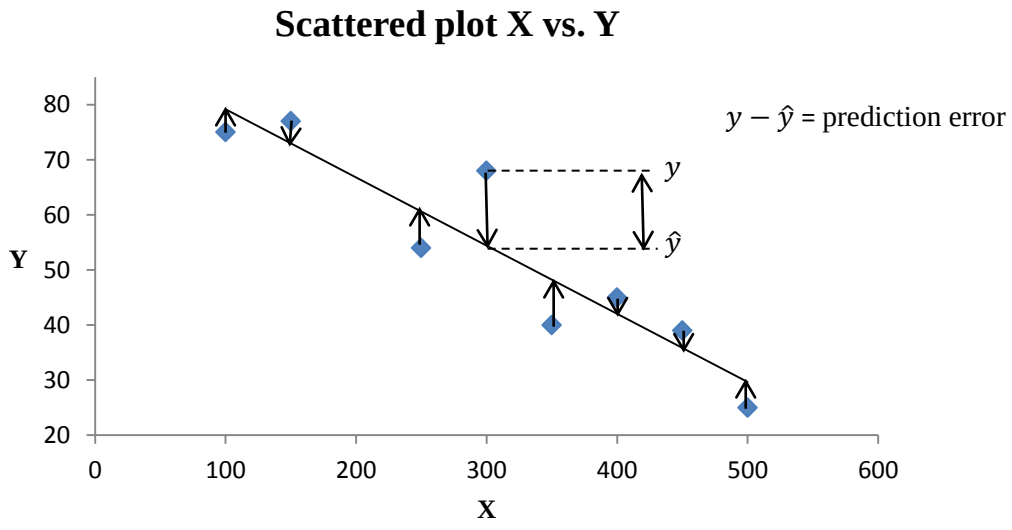

Thus, the regression equation is presented accompanied by a correlation coefficient R^2. This provides a quantitative measure of the linear relationship between *x* and *y*, and is calculated as:

$$R^2 = \frac{\sum(x_i - \overline{x})(y_i - \overline{y})}{\sqrt{\sum(x_i - \overline{x})^2 \sum(y_i - \overline{y})^2}}$$

R^2 takes values between 1 and 0. A value of $R^2 = 1$ indicates a perfect correlation, whereas a value of $R^2 = 0$ indicates no correlation.

7.3 Preparation of chiral metal(salen) complexes

7.3.1 Resolution of 1,2-diaminocyclohexane (108) [136]

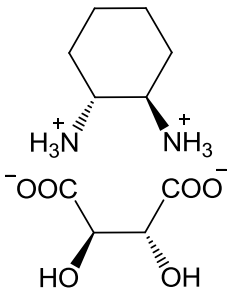

To a solution of L-(+)-tartaric acid (290 g, 1.94 mol) in distilled water (1 L), a mixture of *cis*- and racemic *trans*-1,2-diaminocyclohexane (420 g, 3.66 mol) was added *via* a dropping funnel. The reaction temperature reached 65 ºC. The resulting solution was allowed to cool to room temperature and subsequently cooled in an ice bath for one hour. The formation of a white precipitate was observed. This was filtered by suction and collected. A substantially larger crop was obtained by adding glacial acetic acid (200 mL) to the mother liquor at a rate such that the reaction temperature did not exceed 90 ºC. Another white precipitate formed immediately, which was filtered and combined with the previously collected solid. The combined solids were washed with ice cold water, ice cold methanol and dried by suction to leave the crude product as a white powder. This was recrystallised by dissolving it in the minimum volume of hot water (~1:18 w/v), and then cooled to 0 ºC (ice bath) overnight. The white precipitate was collected by suction filtration and air-dried, to leave the desired product (*R*,*R*)-cyclohexanediamine L-tartrate salt as white crystals. Yield 107.5 g, 21%; $[\alpha]^{19}_{D}$ +9.2 (c 3.9, H_2O) [lit.[136] $[\alpha]^{20}_{D}$ +12.5 (c 4.0, H_2O)].

7.3.2 Preparation of (*R*,*R*)-Salen Ligand (18e) [136]

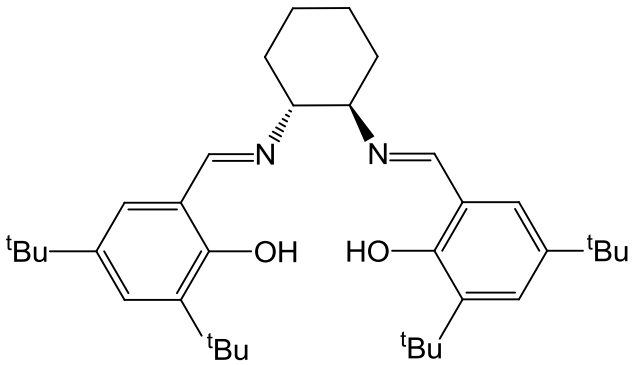

2,4-Di-*tert*-butylphenol (5.00 g, 24.2 mmol), $MgCl_2$ (4.60 g, 48.5 mmol) and paraformaldehyde (1.60 g, 53.3 mmol) were dissolved in THF (50 mL). NEt_3 (6.50 mL, 48.5 mmol) was then added dropwise to the mixture which was then allowed to reflux for 2 hours. The solution turned bright yellow. The 3,5-di-*tert*-butyl-2-hydroxybenzaldehyde produced *in situ* was used directly in the next step of the synthesis without further treatment. Therefore, (*R*,*R*)-cyclohexanediamine L-tartrate salt (3.77 g, 12.1 mmol) and K_2CO_3 were dissolved in a mixture of EtOH/H_2O (1:1) (40 mL) with heating to facilitate their complete dissolution. This solution was added *via* a dropping funnel to the previously prepared ethereal solution of 2-hydroxy-3,5-di-*tert*-butylbenzaldehyde. The resulting bright-yellow suspension was stirred under reflux for 4 hours. The reaction mixture was cooled to room temperature, the remaining $MgCl_2$ was removed by filtration and the solvent was partially removed *under vacuum*. Water was then added to the concentrated mixture and the product was extracted with dichloromethane (3 × 100 mL). The organic layer was then washed with water (3 × 100 mL) and brine (2 × 50 mL), dried over $MgSO_4$ and the solvent evaporated. After recrystallisation from acetone (1:20 w/v), 6.82 g (51% yield) of ligand **18e** could be isolated as yellow needles, $[\alpha]_D^{20}$ -306 (c 1, $CHCl_3$) [lit.[136] $[\alpha]_D^{20}$ -315 (c 1, $CHCl_3$)]; $\boldsymbol{\delta_H}$ (300 MHz, $CDCl_3$) 1.25 (18H, s, C(C*H*$_3$)$_3$), 1.43 (18H, s, C(C*H*$_3$)$_3$), 1.4-2.0 (8H, m, C*H*$_2$C*H*$_2$CHN), 3.3-3.4 (2H, m, CH$_2$CH$_2$C*H*N), 7.00 (2H, d, *J* =2.4 Hz, Ar*H*), 7.32 (2H, d, *J* =2.4 Hz, Ar*H*), 8.32 (2H, s, C*H*=N).

7.3.3 Preparation of (*R*,*R*)-Ti(salen)Cl_2 (19) [38]

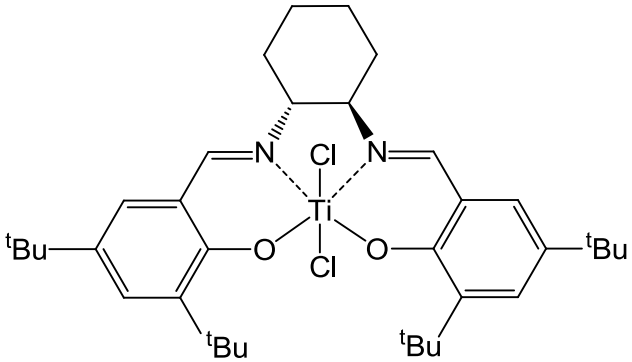

A 0.02 M solution of titanium(IV) chloride (4.03 mmol) in dichloromethane was added dropwise to a solution of salen ligand (2.00 g, 3.66 mmol) in dichloromethane (20 mL). The reaction mixture immediately became red-brown and a solid suspension was observed. The reaction mixture was stirred for 2.5 hours at room temperature, then

the solvent was evaporated and the residue was washed with diethyl ether (2 × 30 mL). The resulting brick red solid was suspended in other 30 mL of diethyl ether. This was left to precipitate and the supernatant was separated. The same operation was repeated with 1:1 hexane/diethyl ether (30 mL). The residue was dried *in vacuo*, to produce complex **19** (2.37 g, 98%) as a red-brown powder. $[\alpha]_D^{23}$ +670 (c 0.01, $CHCl_3$) [lit.[37b] $[\alpha]_D^{22}$ +736 (c 0.0125, $CHCl_3$)]; $\boldsymbol{\delta_H}$ (300 MHz, $CDCl_3$) 1.35 (18H, $C(CH_3)_3$), 1.54 (18H, $C(CH_3)_3$), 1.4-1.7 (4H, m, CH_2CH_2CHN), 2.0-2.2 (2H, m, CH_2CH_2CHN), 2.5-2.7 (2H, m, CH_2CH_2CHN), 4.0-4.1 (2H, m, CH_2CH_2CHN), 7.35 (2H, d, *J* =2.4 Hz, Ar*H*), 7.61 (2H, d, *J* =2.4, Ar*H*), 8.32 (2H, s, C*H*=N).

7.3.4 Preparation of (*R*,*R*)-[Ti(salen)O]$_2$ (20) [38]

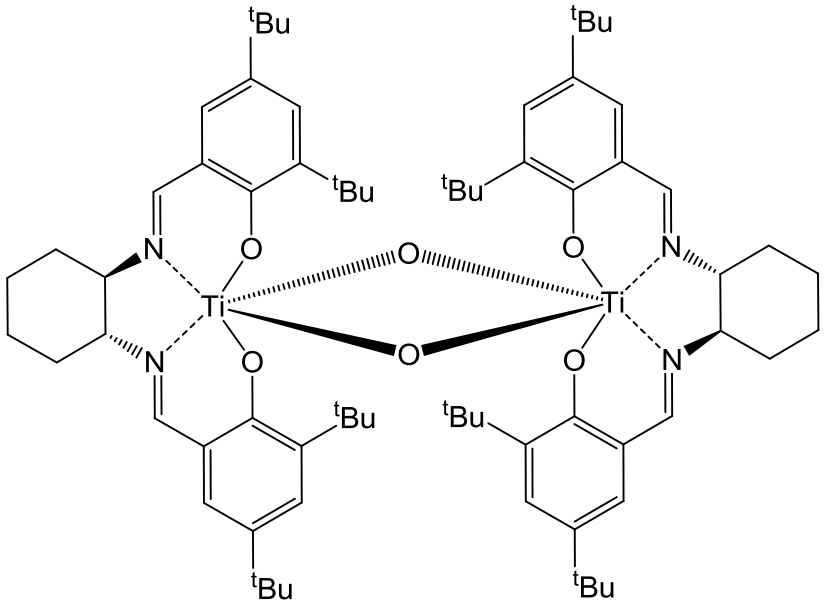

(*R*,*R*)-Ti(salen)Cl_2 (2.37 g, 3.57 mmol) was dissolved in dichloromethane (150 mL) and a pH7 phosphate buffer (200 mL) [3.5 g of $Na_2HPO_4 \cdot 7H_2O$ and 1.2 g of $NaH_2PO_4 \cdot 2H_2O$ in 200 mL of water] was added. The mixture was stirred vigorously at room temperature for 1.5 hours until the solution turned orange. The aqueous layer was removed and a new buffer solution (200 mL) was then added. The reaction mixture was stirred for another hour until the solution turned yellow. The aqueous layer was replaced again with another fresh buffer solution (100 mL), and left to stir for another 30 minutes. The organic layer was then separated, washed with distilled H_2O (200 mL) and dried over anhydrous Na_2SO_4. The solvent was removed *in vacuo* giving complex **20**

(2.15 g, 50%) as bright-yellow crystals. $[\alpha]^{20}_D$ -320 (c 0.01, $CHCl_3$) [lit.[93a] $[\alpha]^{22}_D$ -267 (c 0.01, $CHCl_3$)]; δ_H (300 MHz, $CDCl_3$) 1.04 (18H, s, C(CH_3)$_3$), 1.22 (18H, s, C(CH_3)$_3$), 1.31 (18H, s, C(CH_3)$_3$), 1.40 (18H, s, C(CH_3)$_3$), 1.7-2.6 (16H, m, CH_2CH_2CHN), 4.0-4.1 (4H, m, CH_2CH_2CHN), 6.95 (2H, s, Ar*H*), 7.05 (2H, s, Ar*H*), 7.23 (4H, s, Ar*H*), 7.42 (2H, s, Ar*H*), 7.75 (2H, s, C*H*=N), 8.15 (2H, s, C*H*=N).

7.3.5 Preparation of (*R*,*R*)-VO(salen)EtOSO$_3$ (23a) [93a]

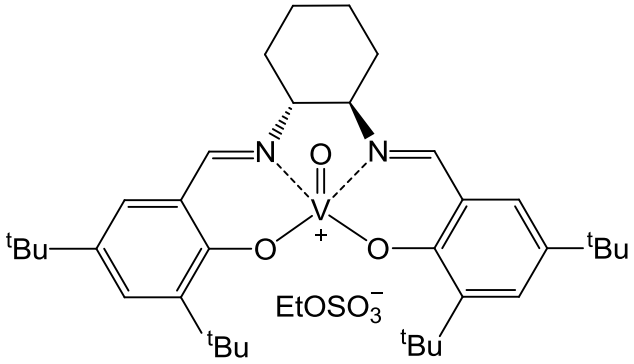

In a 250 mL two-necked round-bottomed flask, vanadyl sulphate hydrate (0.66 g, 4.02 mmol) was dissolved in hot ethanol (65 mL) producing a transparent blue solution. To this, a solution of (*R*,*R*)-salen ligand **18e** (2.0 g, 3.66 mmol) in tetrahydrofuran (40 mL) was added. The system was equipped with a Pasteur pipette, submerged into the stirring solution, fixed in place with a Suba Seal, connected to an air tap and a condenser was connected to the other inlet. The reaction mixture was refluxed for 4 hours, with air flushing to keep the solution oxygenated. Then, the dark green solution was allowed to cool to room temperature and the solvent was evaporated to leave a dark material. This was taken up in dichloromethane and passed through a flash column, eluting with dichloromethane and then with a 9:1 mixture of ethyl acetate / methanol. Unreacted salen ligand was removed first as a yellow band within the dichloromethane fraction. Further elution with dichloromethane allowed vanadium(IV)salen complex **22** (light green band) to be isolated from the vanadium(V)salen complex which was finally eluted with the ethyl acetate / methanol mixture as a dark green band. The solvent was removed *in vacuo* to give complex **23a** (1.50 g, 56%) as a dark green powder. $[\alpha]_D^{20}$ -1140 (c 0.01, $CHCl_3$), [lit.[93a] $[\alpha]_D^{25}$ -914 (c 0.01, $CHCl_3$)]; δ_H (300 MHz, $CDCl_3$) 0.89 (3H, t, *J* =6.9 Hz, $CH_3CH_2OSO_3$), 1.38 (9H, s, C(CH_3)$_3$), 1.40 (9H, s, C(CH_3)$_3$), 1.55 (18H, s, C(CH_3)$_3$), 1.6-2.9 (8H, m, CH_2CH_2CHN), 3.49 (2H, q, *J* = 6.9 Hz,

$CH_3CH_2OSO_3$), 3.6-3.8 (1H, m, CH_2CH_2CHN), 4.2-4.3 (1H, m, CH_2CH_2CHN), 7.53 (1H, s, Ar*H*), 7.59 (1H, s, Ar*H*), 7.73 (1H, s, Ar*H*), 7.78 (1H, s, Ar*H*), 8.57 (1H, s, C*H*=N), 8.79 (1H, s, C*H*=N).

7.3.6 Preparation of (*R*,*R*)-VO(salen)Cl (23f) [44a]

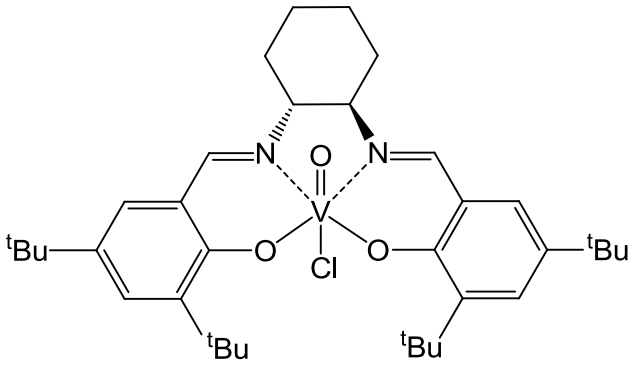

Vanadium(V) oxychloride (0.09 mL, 0.96 mmol) was added to a solution of (*R*,*R*)-salen ligand **18e** (0.34 g, 0.63 mmol) in tetrahydrofuran (20 mL). The reaction mixture immediately turned dark-green. The solution was stirred at room temperature for 30 minutes. The solvent was evaporated and the residue was purified by column chromatography eluting first with a 3:1 ethyl acetate / hexane mixture, removing the unreacted salen ligand, then with a 2:2:1 ethyl acetate/hexane/methanol mixture. The solvent of the latter combined fractions was evaporated, and the residue dried *in vacuo* to give compound **23f** (0.24 g, 60%) as dark-green crystals. $[\alpha]_D^{20}$ -1356 (c 0.01, $CHCl_3$), [lit.[44b] $[\alpha]_D^{20}$ -1340 (c 0.01, $CHCl_3$)]; $\boldsymbol{\delta_H}$ (300 MHz, $CDCl_3$) 1.35 (9H, s, $C(CH_3)_3$), 1.37 (9H, s, $C(CH_3)_3$), 1.53 (9H, s, $C(CH_3)_3$), 1.55 (9H, s, $C(CH_3)_3$), 1.5-2.8 (8H, m, CH_2CH_2CHN), 3.7-3.8 (1H, m, CH_2CH_2CHN), 4.3-4.4 (1H, m, CH_2CH_2CHN), 7.45 (1H, s, Ar*H*), 7.54 (1H, s, Ar*H*), 7.70 (1H, s, Ar*H*), 7.74 (1H, s, Ar*H*), 8.48 (1H, s, C*H*=N), 8.67 (1H, s, C*H*=N).

7.3.7 Preparation of (*R*,*R*)-VO(salen)NCS (23h) [44b]

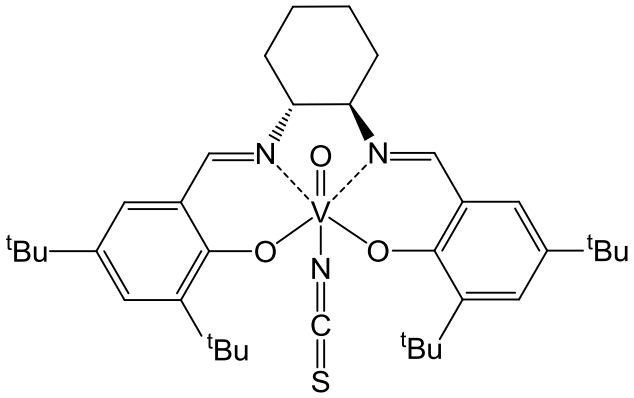

(*R*,*R*)-VO(salen)$EtOSO_3$ **23a** (1.50 g, 2.03 mmol) was dissolved in ethanol (90 mL) and potassium thiocyanate (1.90 g, 19.5 mmol) was added, resulting in an immediate change in colour to dark-green. The reaction mixture was stirred vigorously for 2.5 hours at room temperature. Removal of the solvent left a green residue, which was partly dissolved in dichloromethane and filtered through cotton wool to remove any inorganic salts. The solvent was removed *in vacuo* to give a dark green solid which was passed through a very short flash column eluting with dichloromethane followed by ethyl acetate / methanol (9:1). The first fraction gave complex **23h** (1.19 g, 88%) as a dark green powder after solvent evaporation, and the unreacted VO(salen)$EtOSO_3$ was recovered within the methanolic fraction. $[\alpha]_D^{20}$ -1340 (c 0.005, $CHCl_3$), [lit.[44b] $[\alpha]_D^{23}$ -1600 (c 0.005, $CHCl_3$)]; $\boldsymbol{\delta_H}$ (300 MHz, $CDCl_3$) 1.25 (9H, s, C(C*H*$_3$)$_3$), 1.40 (9H, s, C(C*H*$_3$)$_3$), 1.42 (9H, s, C(C*H*$_3$)$_3$), 1.54 (9H, s, C(C*H*$_3$)$_3$), 1.6-2.9 (8H, m, C*H*$_2$C*H*$_2$CHN), 3.3-3.8 (2H, m, CH_2CH_2C*H*N), 7.47 (1H, s, Ar*H*), 7.57 (1H, s, Ar*H*), 7.72 (1H, s, Ar*H*), 7.77 (1H, s, Ar*H*), 8.48 (1H, s, C*H*=N), 8.71 (1H, s, C*H*=N).

7.3.8 Preparation of (*R*,*R*)-VO(salen) (22) [93a]

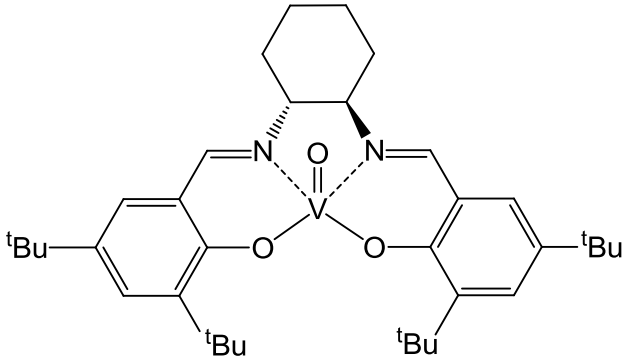

This product was isolated from the chromatographic purification of **23a** as the second product to be eluted after the unreacted salen ligand. $[\alpha]_D^{20}$ -705 (c 0.01, $CHCl_3$) [lit.[93a] $[\alpha]_D^{25}$ -442 (c 0.01, $CHCl_3$)].

7.3.9 Preparation of (*R*,*R*)-[Al(salen)]$_2$O (69) [137]

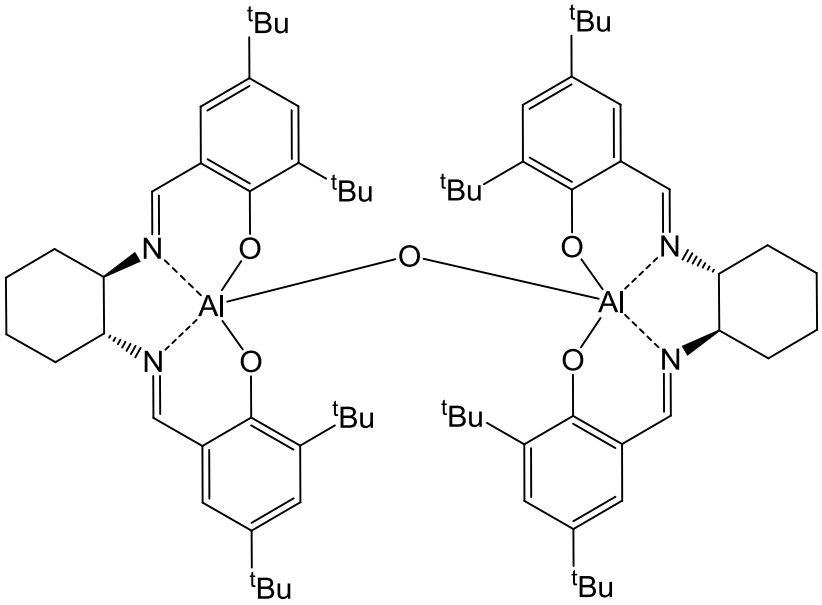

A solution of (*R*,*R*)-salen ligand **18e** (1.5 g, 2.75 mmol) in toluene (40 mL) was gently brought to reflux under nitrogen, at which point a solution of $Al(OEt)_3$ (0.89 g, 5.5 mmol) in toluene (40 mL) was added via a dropping funnel. The reaction mixture was stirred under reflux for 3–5 h before being allowed to cool to room temperature and

the solvent was evaporated. The residue was dissolved in dichloromethane (200 mL) and the remaining aluminium salts were removed by filtration using a funnel fitted with a cotton plug. The solution was washed with water (2 × 100 mL) and brine (2 × 100 mL) and the organic layer was dried over Na_2SO_4. The solvent was evaporated *in vacuo* to give a pale yellow solid, which was recrystallised from diethyl ether to give complex **69** (yield 0.95g, 63%). $[\alpha]_D^{20}$ -653 (c 0.1, toluene) [lit.[137] +715 (c 1.0, toluene, for (*S*,*S*) enantiomer)]; δ_H (300 MHz, $CDCl_3$) 1.29 (36H, s, C(C*H*$_3$)$_3$), 1.50 (36H, s, C(C*H*$_3$)$_3$), 1.8-2.7 (16H, m, C*H*$_2$C*H*$_2$CHN), 3.0-3.2 (2H, br m, CH$_2$CH$_2$C*H*N), 3.7-3.9 (2H, br m, CH$_2$CH$_2$C*H*N), 7.07 (4H, d, *J* 2.3 Hz, Ar*H*), 7.52 (4H, d, *J* 2.3 Hz, Ar*H*), 8.15 (2H, s, C*H*=N), 8.35 (2H, s, C*H*=N).

7.4 Experimental for Chapter 2

7.4.1 General procedure for the study of the redox process using electron paramagnetic resonance

In a sample vial, VO(salen)X (X = $EtOSO_3$, Cl or NCS) (2×10^{-3} mmol) was dissolved in freshly distilled dichloromethane (175 µL). The solution was transferred into a glass pipette and this was sealed. This solution was used to record the background spectrum at t = 0 (see *Appendix 1, 1.1*). In order to monitor the formation of V(IV) species during the cyanosilylation reaction, benzaldehyde (10 µL, 0.10 mmol) and TMSCN (20 µL, 0.16 mmol) were sequentially added to the solution and EPR spectra were recorded every 3.5 minutes for 0.5-1 hour (see *Appendix 1, 1.2*). When vanadium(IV) species formation by direct reaction of vanadium(V)salen complexes with cyanide was to be measured, TMSCN (20 µL, 0.16 mmol) or potassium cyanide (2 mg, 0.3 mmol) dissolved in *tert*-butanol (30 µL, 0.03 mmol) was directly added to a solution of VO(salen)X (X = $EtOSO_3$, Cl or NCS) (2×10^{-3} mmol) in dichloromethane. Thereafter, a sequence of EPR spectra was recorded at intervals of 3.5 minutes (see *Appendix 1, 1.4* and *1.5*).

In order to calculate the percentage of V(V) species converted, the intensity of the signal was compared to a sample of VO(salen) (2×10^{-3} mmol) in dichloromethane (175 µL). This was also used to centre the eight-peak signal at the middle of the spectrum.

7.4.2 Attempt to detect cyanide radicals using spin trapping chemistry

Equal volumes of a 0.1 M solution (175 µL) of spin trap (DMPO, PBN or MNP) in toluene and a 0.01 M solution (175 µL) of vanadium(V)salen complex VO(salen)X (X= $EtOSO_3$, Cl or NCS) in dichloromethane were mixed in a glass pipette. The mixture was degassed by gently bubbling N_2 through it for one minute. To promote cyanide radical formation, TMSCN (20 µL, 0.16 mmol) was then added to the solution and EPR measurements were recorded at an interval of 3.5 minutes for 10-30 min depending on the lifetime of the generated spin adduct. PBN-CN with hyperfine constants of a_N = 15.02 and a_H = 1.87 Gauss and DMPO-CN with hyperfine constants of a_N = 14.15 and a_H = 16.24 Gauss were clearly observed.

Two control experiments were carried out by adding TMSCN or vanadium(V)salen complex to a spin trap solution of DMPO (0.1 M in toluene), the

latter resulting in the detection of the oxidized form of DMPO (DMPOx) (see *Appendix 1, 1.7*).

As the hyperfine constants of DMPO-CN did not match to the ones reported in the database,[138] the authentic DMPO-CN spin adduct was prepared by irradiating with a UV light (100 W Hg/Xe lamp, for 2 minutes at a λ = 254 nm), a degassed mixture of TMSCN (20 µL, 0.16 mmol) in dichloromethane (200 µL) and a 0.1 M solution of DMPO in toluene (200 µL). The expected DMPO-CN was generated with identical a_N and a_H hyperfine constants to the ones observed for the DMPO-CN spin adduct formed in the presence of VO(salen)X species.

7.4.3 Attempted detection of cyanide radicals using TEMPO as radical scavenger.

A stock solution of 2,2',6,6'-tetramethylpiperidine N-oxide (TEMPO) (0.02 M, $2x10^{-3}$ mmol) in toluene was prepared. 100 µL of this solution were added to 100 µL dichloromethane solutions of: (**A**) TMSCN (1.6 M, 0.16 mmol), (**B**) VO(salen)NCS (0.02 M, 2×10^{-3} mmol), and (**C**) VO(salen) (0.02 M, 2×10^{-3} mmol). The resulting solutions **A**, **B** and **C** were degassed by gently bubbling N_2 through them prior to being analysed by EPR. Then, to solution **B**, TMSCN (20 µL, 0.16 mmol) was added. The course of the reaction was monitored by EPR signal intensity decay as well as by line broadening. A sample of the crude solution was further analysed by GC-MS, but none of the peaks in the chromatogram could be assigned to TEMPO-CN (m/z 182) or any derivatives such as $(TEMPO)_2CN$ or $TEMPO(CN)_2$ (see *Appendix 1, 1.8*).

7.4.4 Attempted styrene polymerization

In a 5 mL sample vial, VO(salen)NCS **23h** (15 mg, 2×10^{-2} mmol) was dissolved in freshly distilled styrene (500 µL). The solution was transferred into a glass pipette and TMSCN (20 µL, 0.16 mmol) was added. The tube was sealed in the presence of air and EPR measurements were recorded after 40 minutes, 2.5 and 18 hours. These spectra were compared to a control solution of VO(salen) complex **22** (13.5 mg, 2×10^{-2} mmol) in styrene (500 µL). The colour changed immediately after the TMSCN addition, however, after 18 hours, no apparent changes in the EPR signal could be observed. A sample from the reaction solution was analysed by ^{1}H NMR and LC-MS, which showed no evidence of polymerization.

A control experiment was conducted by dissolving TMSCN (20 µL, 0.16 mmol) in styrene (500 µL) and the mixture was UV irradiated (λ = 254nm) over a period of 18

hours. An increase in viscosity was observed, and a small sample was analysed by ^{1}H NMR spectrometry. The appearance of broad bands in the aliphatic and aromatic regions confirmed the presence of polystyrene. δ_H (300 MHz, $CDCl_3$) 1.6-1.3 (2H, br, CH_2), 2.0-1.7 (2H, br, CH_2), 6.6-6.3 (2H, br, Ar*H*) and 7.2-6.8 (3H, br, Ar*H*).

7.4.5 Attempted cyanide radical addition to electron rich alkenes.

A solution of VO(salen)NCS **23g** (6 mg, 9×10^{-3} mmol) and (*Z*)-1-(1-adamantyloxy)-2-bromoethene **92** (50 mg, 0.18 mmol) in dichloromethane (1.5 mL) was cooled to 0 °C in an ice/water bath. Then, TMSCN (30 mL, 0.24 mmol) was added via a syringe. The resulting mixture was stirred for 24 hours, while being monitored by TLC. As the reaction seemed not to be taking place, the ice/water bath was removed and the reaction mixture was warmed to room temperature and left to react for a further 24 hours. The reaction was then quenched by passing the solution through a silica plug. The solvent was evaporated and the crude material was analysed by ^{1}H-NMR spectroscopy which showed the presence of a mixture of unreacted starting materials and 1-adamantanol.

Preparation of 1-adamantyloxy-1-ethoxy-2-bromoethane **94** [103]

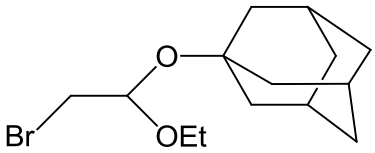

To a solution of ethyl vinyl ether (0.66 mL, 6.9 mmol) in chloroform (4 mL) at −78 °C under inert conditions, bromine (0.32 mL, 6.9 mmol) was added via a dropping funnel until a slight orange colour persisted, (this indicates when all the vinyl ether has reacted). 1-Adamantanol (1.05 g, 6.9 mmol) and triethylamine (1.05 mL, 7.5 mmol) were then dissolved in chloroform (13 mL) and added dropwise over 1 hour with vigorous stirring. The reaction mixture was then warmed to 0 °C and stirred for a further 2 hours. The cooling bath was removed and the solution was poured into H_2O (10 mL). The organic layer was separated and the aqueous layer extracted with fresh chloroform (2 x 5 mL). The combined organic extracts were then washed with a 0.5 N HCl solution (10 mL), a saturated solution of $NaHCO_3$ (10 mL), dried over $MgSO_4$ and concentrated *in vacuo*. The residue was purified by silica gel chromatography, eluting with a chloroform/hexane (1:1) mixture, to give compound **94** as a colourless oil (1.63 g, 78% yield), δ_H (300 MHz, $CDCl_3$) 1.24 (3H, t, *J* 8.5 Hz, CH_3), 1.63 (6H, m, CH_2-

Ad), 1.81 (6H, m, CH_2-Ad), 2.16 (3H, m, C*H*-Ad), 3.75-3.50 (4H, m, CH_2) and 4.96 (1H, t, *J* 6.5 Hz, C*H*).

Preparation of (Z)-1-(1-adamantyloxy)-2-bromoethene **91** [103]

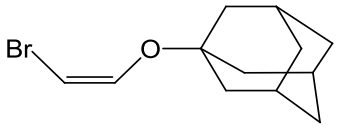

A solution of 1-adamantyloxy-1-ethoxy-2-bromoethane **94** (1.63 g, 5.4 mmol) in dichloromethane (8 mL) was added via a dropping funnel to a suspension of phosphorus pentachloride (1.35 g, 6.5 mmol) in dichloromethane (8 mL), vigorously stirred under nitrogen at 0 ºC (in an ice bath) for 30 minutes. The reaction mixture was stirred for a further 1.5 hours or until all the reagent was consumed. Keeping the temperature at 0 ºC, an excess of triethylamine (4.5 mL, 32.4 mmol) was then added dropwise. Then, the ice bath was removed and the reaction mixture was refluxed for 2.5 hours. The reaction mixture was cooled to room temperature, and then poured into an ice/water mixture (20 mL). The organic layer was separated and the aqueous layer was extracted with fresh dichloromethane (2 × 5 mL). The organic fractions were combined and washed with a 0.5 N HCl solution (10 mL), a saturated solution of $NaHCO_3$ (10 mL) and dried over $MgSO_4$. The solvent was removed *in vacuo* and the crude material was purified by chromatography using silica gel - triethylamine 2.5% (v/v) eluting with hexane. Solvent evaporation gave compound **91** as a white solid (1.23 g, 89% yield). Mp. 54-55 ºC [lit[103] 52-53 ºC], $\boldsymbol{\delta_H}$ (300 MHz, $CDCl_3$) 1.65 (6H, m, CH_2-Ad), 1.86 (6H, m, CH_2-Ad), 2.20 (3H, m, C*H*-Ad), 5.11 (1H, d, *J* 4.2 Hz, C*H*) and 6.91 (1H, d, *J* 4.2 Hz, C*H*).

7.4.6 Attempt to detect cyanogen by FT-IR

A solution of VO(salen)X complex (X= $EtOSO_3$, Cl or NCS) in dichloromethane was charged into a NaCl cell (two NaCl plates joined by a rubber gasket and tightened together by two screwed metallic hinges). The IR spectrum was recorded in the region from 1800-2400 cm^{-1}, wherein VO(salen)NCS with a signal at 2064 cm^{-1} due to the –N=C=S asymmetric stretching, was the only complex that displayed an IR signal. Then, a slight excess of TMSCN was added and a new IR spectrum was recorded. $(CN)_2$ stretching bands were not detected in any of the experiments. Interestingly

though, the –NCS band at 2064 cm^{-1} vanished and HCN and TMSCN (2190 and 2090 cm^{-1} respectively) were the only two bands observed in this region.

7.4.7 General procedure for the detection of cyanogen by GC MS

In a sample vial for chromatographic applications, VO(salen)NCS complex **23h** (1.32 mg, 2×10^{-3} mmol) was dissolved in dichloromethane (500 µL) and TMSCN (20 µL, 1.6 mmol) was added. The mixture was vigorously stirred for one hour at room temperature. This reaction mixture was directly injected by an automated system to the GC-MS apparatus. A peak at 13.54 min in the chromatogram had a molecular weight of 52 and was assigned to $(CN)_2$. A control experiment in the absence of complex VO(salen)NCS did not show the $(CN)_2$ peak. In order to rule out the formation of $(CN)_2$ in the GC-MS injection chamber, N_2 gas was bubbled through a reaction solution which contained VO(salen)NCS complex (1.32 mg, 2×10^{-3} mmol) and TMSCN (20 µL, 1.6 mmol) dissolved in dichloromethane (500 µL). The tip of the cannula where the carrier gas came out was submerged into a cold dichloromethane trap where the $(CN)_2$ was collected. This solution was then injected into the GC-MS, the chromatogram of which still clearly showed the $(CN)_2$ peak.

7.4.8 Generation of cyanogen from $CuSO_4$ and KCN in water [95]

For further evidence that the GC-MS was detecting $(CN)_2$, it was prepared by the following reaction:

$$2\ CuSO_{4\,(aq)} + 4\ KCN_{\,(aq)} \rightarrow 2\ CuCN_{\,(s)} + K_2SO_4 + (CN)_2$$

To a solution of $CuSO_4x5H_2O$ (400 mg, 1.64 mmol) in water (1 mL) at 60 ºC, an aqueous solution (10 mL) of KCN (425 mg, 6.54 mmol) was added via a dropping funnel. Formation of a turquoise precipitate as well as cyanogen bubbling out of the solution was observed. N_2 gas was flushed through the mixture and cyanogen was collected in a cold finger with dichloromethane. This solution was directly used for GC-MS analysis. The peak at 13.54 minutes in the chromatogram could be assigned as cyanogen (m/z 52).

7.4.9 General procedure for the generation and identification of TMS-NCS

A 1 mL sample vial for chromatographic applications was charged with VO(salen)NCS **23h** (6.7 mg, 0.01 mmol) dissolved in dichloromethane (500 µL) and a magnetic stirring bar. Then, TMSCN (12.5 µL, 0.1 mmol) was added and the system was appropriately sealed. The mixture was stirred at room temperature for 30 minutes then an aliquot was injected into the GC-MS apparatus by an automated system. Trimethylsilyl isothiocyanate (m/z 131, M^+) was identified, along with other species as a peak in the chromatogram with a retention time of 4.3 minutes (see *Appendix 1, 1.9*)

7.5 Experimental for Chapter 3

7.5.1 General procedure for the kinetic study of the anion effect in the addition of Bu_4N-NCS to cyanohydrin synthesis catalysed by VO(salen)NCS

VO(salen)NCS **23h** (1.32 mg, 0.2 mol%) and tetrabutylammonium thiocyanate (0.1-2 mol%) were dissolved in dichloromethane (1.75 mL). This solution was cooled to 0 °C, at which temperature the kinetics study was conducted. A 5 μL sample was taken and dissolved into dichloromethane (3.5 mL). This sample was used as the blank for the UV-vis analysis. Benzaldehyde (0.1 mL, 0.98 mmol) was then added and another 5 μL aliquot was taken and diluted into dichloromethane (3.5 mL); this, displaying the strongest absorbance at a wavelength λ 246 nm, corresponds to the t = 0 sample. Finally, TMSCN (0.15 mL, 1.14 mmol) was added at the same time as a timer was started. The reaction mixture was gently stirred and at appropriate time intervals, 5 μL aliquots were taken and quenched into dichloromethane (3.5 mL). The resulting solutions were all analysed by UV-vis spectroscopy and the absorbance was then transformed to concentrations, and these were plotted vs. time.

7.5.2 General procedure for measuring the kinetics of the addition of trimethylsilyl cyanide to aldehydes

These reactions need extremely anhydrous conditions. All the glassware must be flame-dried prior to use and disposable plastic syringes and needles were used for the addition of solutions or reagents to the reaction mixture. All material exposed to TMSCN was washed with bleach and rinsed with water.

Using (R,R)-VO(salen)X complexes as catalyst (X = $EtOSO_3$, NCS).

A solution of VO(salen)X complex (1.96 μmol, 0.2 mol%) in freshly distilled dichloromethane (1.75 mL) was prepared in a sample vial and charged, *via* syringe, to a 10 mL round-bottomed flask fitted with a magnetic stirring bar and appropriately sealed. The solution was brought to 0 ºC in an ice/water bath. An aliquot (0.5 μL) was taken and diluted into dichloromethane (3.5 mL). This was used as the reference sample for UV-vis analysis and was subtracted from the following measurements. Then, freshly distilled aldehyde (0.985 mmol, 1eq) was added to the solution and another aliquot (0.5 μL) was taken and diluted into dichloromethane (3.5 mL). The absorbance at the λ_{max}

was recorded and was used as the t = 0 value. Finally, TMSCN (1.182 mmol, 1.2 eq) was added at the same time that a stopwatch was started. Aliquots (0.5 µL) were taken and quenched into dichloromethane (3.5 mL) at appropriate time intervals over a period of 1 to 2 hours for the complex with X = NCS, depending on the nature of the aldehyde substituent, always reaching conversions up to 80%. In the case of the complex with X = $EtOSO_3$, the kinetics had to be monitored over longer periods of time (generally 8 hours or longer). Within this time, 80% conversion was achieved for the electron-deficient aldehydes; whereas for the more electron-rich aldehydes only a 30% conversion could be monitored. The solution was then passed through a silica plug eluting with dichloromethane and the solvent was evaporated. Conversions could be directly determined by ^{1}H-NMR by integration of the peaks corresponding to C*H*(CN) and ArC*H*O of the cyanohydrin and the unreacted aldehyde respectively. Then, the O-TMS derivative was transformed to the acetate to allow the enantiomeric excess to be determined (see *Section 7*).

*Using (R,R)-[Ti(salen)O]$_2$ complex **20** as catalyst.*

A solution of catalyst **20** (0.98 µmol, 0.1 mol%) in dry dichloromethane (1.75 mL) was charged into a 10 mL round-bottomed flask fitted with a magnetic stirring bar and appropriately sealed. The solution was brought to 0 ºC using a water/ice bath. An aliquot (0.5 µL) was taken and diluted into dichloromethane (3.5 mL), and this solution was used as the reference sample for UV-vis analysis. Then, freshly distilled aldehyde (0.985 mmol, 1eq) was added to the solution and another aliquot (0.5µL) was taken and diluted into dichloromethane (3.5 mL). The absorbance was measured at the λ_{max} of each aldehyde to give a t = 0 value. Finally, TMSCN (1.182 mmol, 1.2eq) was added and a stopwatch was started. Aliquots (0.5 µL) of the reaction were taken and quenched into dichloromethane (3.5 mL) at appropriate time intervals over a period of 1 minute to 1 hour depending on the nature of the aldehyde substituents, during which time all the aldehyde was converted to product. The solution was then passed through a silica plug eluting with dichloromethane and the solvent was evaporated. The residue was directly used to determine the conversion and enantiomeric excess as described in *Section 7*.

7.5.3 General procedure for the preparation of racemic cyanohydrins

An aldehyde (0.985 mmol, 1 eq) was added to a solution of Bu_4NSCN (15 mg, 0.05 mmol) in dry dichloromethane (1.75 mL). To this solution, TMSCN (1.182 mmol, 1.2 eq) was added and the reaction mixture was stirred for 2 hours at room temperature.

The solution was then passed through a short silica plug eluting with dichloromethane and the solvent was evaporated giving the cyanohydrin trimethylsilyl ether. The conversion was determined by ^{1}H NMR spectroscopy.

7.5.4 General procedure for trimethylsilyl cyanide addition to ketones

A solution of triphenylphosphine oxide (12 mg, 0.04 mmol) and $[Al(salen)]_2O$ (10 mg, 8.4 μmol) in dichloromethane (1.0 mL) was added to a 10 mL round-bottomed flask. The temperature was adjusted to 20°C in a water bath and ketone (0.42 mmol) was then added. TMSCN (66 mg, 0.67 mmol) was added and the resulting solution stirred for 48 hours. After this time, the reaction mixture was passed through a short silica plug eluting with dichloromethane, and concentrated *in vacuo*. The conversion was determined by ^{1}H NMR spectroscopy from the protected product ($C(CH_3)CN$) and the unreacted ketone ($C(CH_3)O$). To determine the enantiomeric excesses, a chiral shift reagent was used from the unprotected cyanohydrin (see *section 7.2*).

7.6 Experimental for Chapter 4

7.6.1 General procedure for the catalytic asymmetric addition of trimethylsilyl cyanide to aldehydes in different solvents.

An aldehyde (0.98 mmol) was added to a solution of catalyst ([Ti(salen)O]$_2$ or VO(salen)NCS (0.98 µmol, 0.1mol%)) in dichloromethane or propylene carbonate (1.75 mL). The temperature was then adjusted by an ice/water bath for reactions at 0 ºC or cryostat in an ethanol bath to achieve temperatures lower than 0 ºC. At the appropriate temperature, TMSCN (0.15 mL, 1.12 mmol) was added and the reaction mixture was left to react for the specified time (from 2-24 hours). The catalyst was then removed through a silica plug eluting with the same solvent used during the reaction (dichloromethane or propylene carbonate). When the solvent was dichloromethane, it was removed under reduced pressure and the conversion was determined by ^{1}H NMR by comparing the integrals of the unreacted aldehyde with the protected cyanohydrin. The remaining cyanohydrin trimethylsilyl ether solution was transformed to the acetate derivative in order to determine the enantiomeric excess (see *section 7*).

7.6.2 Synthesis of (*S*)-mandelic acid [139]

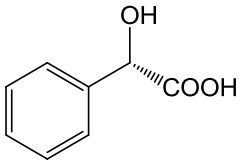

To the reaction obtained during the addition of TMSCN to benzaldehyde using propylene carbonate as the solvent, a 12 N aqueous solution of HCl (10 mL) was added. The mixture was stirred vigorously under reflux for 6 hours. The mixture was brought to basic pH with a 1 M aqueous solution of NaOH, and this was washed with diethyl ether (3 × 10mL) (to remove the diol from the propylene carbonate decomposition). The aqueous layer was then brought back to acidic pH with a 12 N solution of HCl and extracted with diethyl ether (3 × 10mL). The ethereal fractions were combined and dried over anhydrous sodium sulphate and evaporated to afford a pale yellow solid which was recrystallized at 4 °C in an ether/hexane mixture giving 91 mg of mandelic acid as white crystals with a yield of 60%. $\boldsymbol{\delta_H}$ (300 MHz, $CDCl_3$) 5.26 (1H, s, C*H*COOH), 7.3-7.4 (3H, m, Ar*H*), 7.4-7.5 (2H, m, Ar*H*).

7.6.3 Synthesis of (*S*)-methyl mandelate [140]

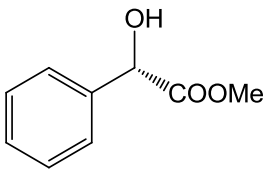

Mandelic acid (80 mg, 0.53mmol) was first suspended in toluene (20 mL), followed by addition of methanol (2 mL) to form a homogeneous solution. Then, a drop of concentrated H_2SO_4 was added. The mixture was heated to reflux and left to react for 4 hours. When the solution had cooled, the solvent was removed and the residue was dissolved in ether (15 mL) and washed with water (2 × 10mL) and saturated $NaHCO_3$. The ethereal layer was dried over anhydrous sodium sulphate and concentrated, affording the desired product as a pale yellow solid (28 mg, 50% yield). The enantiomeric excess was determined by chiral HPLC using 80% hexane and 20% isopropanol at a flow rate of 1mL/min in a ChiralPak® AS column. t_R = 6.72 (major), 9.59 (minor) minutes. 81%*ee*, $\boldsymbol{\delta_H}$ (300 MHz, $CDCl_3$) 3.77 (3H, s, OC*H*$_3$), 5.20 (1H, s, C*H*COOMe), 7.3-7.5 (5H, m, Ar*H*).

7.6.4 General procedure to study the kinetics of the addition of trimethylsilyl cyanide to aldehydes in propylene carbonate

A solution of VO(salen)NCS **23h** (0.2-0.8 mol%) in freshly distilled propylene carbonate (1.75mL) was charged, via a syringe, into a flamed-dried round-bottomed flask fitted with a stirrer bar and appropriately sealed. The temperature was adjusted in an ice/water bath for reactions at 0 °C, or in an ethanol bath using a cryostat for reactions at temperatures below 0 °C. Reaction temperatures above 0 °C were kept within a ±0.5 °C range, by adding small amounts of crushed ice to a water bath. A 0.5 µL sample was extracted and diluted into 3.5 mL of dichloromethane. This solution was used as the reference for UV analysis at the wavelength where the aldehyde absorbs at its maximum (λ_{max} = 230-310 nm). Freshly distilled aldehyde (0.96 mmol) was then added and another 0.5 µL aliquot was collected and diluted into 3.5 mL of dichloromethane. The value at the λ_{max} was recorded as t =0. Finally, TMSCN (0.15 mL, 1.12 mmol) was added at the same time as a stopwatch was started. Aliquots of the reaction were taken and diluted at appropriate time intervals for 2 hours. The reaction mixture was passed through a silica plug eluting with dichloromethane, solvent was removed under reduced pressure and the cyanohydrin trimethylsilyl ether recovered was

converted to the acetate as described in *section 7* and the enantiomeric excesses were determined.

8 Enantiomeric analysis

8.1 Chiral Gas Chromatography[110]

The cyanohydrin trimethylsilyl ether obtained by the addition of TMSCN to aldehydes or ketones, was dissolved in acetonitrile (2 mL). Acetic anhydride (1.5 mL, 1.58 mmol, 1.6 eq) and $Sc(OTf)_3$ (5 mg, 0.01 mmol) were then added, and the mixture was stirred for 30 minutes at room temperature. The resulting solution was passed through a short silica plug eluting with acetonitrile (2-4 mL) and directly injected into the gas chromatograph to determine the enantiomeric excess of the product according to the appropriated method:

Method 1 initial temperature 95 °C, hold for 2 minutes then ramp rate of 3 °C/minute to 180 °C, then hold for another 5 minutes. Flow rate: 2 mL/ min.

Method 2 initial temperature 95 °C, hold for 2 minutes then ramp rate of 5 °C/minute to 180 °C, then hold for another 5 minutes. Flow rate: 1 mL/min.

Method 3 initial temperature 95 °C, hold for 2 minutes then ramp rate of 2 °C/minute to 180 °C, then hold for another 5 minutes. Flow rate: 2 mL/ min.

Method 4 initial temperature 95 °C, hold for 5 minutes then ramp rate of 0.5 °C/minute to 180 °C, then hold for another 5 minutes. Flow rate: 2 mL/ min.

Method 5 initial temperature 100 °C, hold for 5 minutes then ramp rate of 1 °C/minute to 180 °C, then hold for another 5 minutes. Flow rate: 2 mL/ min.

8.2 Chiral Resolution using a Chiral Shift Reagent

For those acetates that could not be resolved by chiral gas chromatography, a chiral shift reagent was used instead, and their enantiomeric excesses were determined by ^{1}H NMR spectroscopy from the unprotected cyanohydrins, which were prepared as described below:

To a solution of cyanohydrin acetate (0.985 mmol, 1 eq) in ethanol (3 mL), *p*-toluenesulphonic acid monohydrate (187 mg, 0.985 mmol, 1eq) was added, and the mixture was stirred at room temperature for 2 days. The solvent was evaporated and the

product was purified by column chromatography eluting first with a 1:15 mixture of ethyl acetate/hexane then increasing the polarity to a 1:6 mixture of ethyl acetate/hexane.[112]

In an NMR tube, mandelic acid (2.74 mg, 18 μmol) and $CDCl_3$ (0.6 mL) were mixed, and DMAP (1.73 mg, 18 μmol) was then added. Mandelic acid is poorly soluble in $CDCl_3$, but it readily goes into solution upon addition of DMAP. Finally, chiral cyanohydrin (18μmol) was added and the ^1H NMR spectrum was recorded.[111]

9 Characterization data

9.1 Aldehydes

9.1.1 Phenyl-2-trimethylsilyloxy-acetonitrile.[44b, 66]

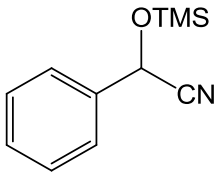

The product was obtained as an oil. **δ_H** (300 MHz, $CDCl_3$) 0.24 (9H, s, Si(C*H*$_3$)$_3$), 5.50 (1H, s, C*H*CN), 7.3-7.5 (5H, m, Ar*H*); **δ_C** (75 MHz, $CDCl_3$) -0.3, 63.6, 119.2, 126.3, 128.9, 129.3, 136.2; ee determined by chiral GC analysis of the corresponding acetate using *Method 1*. R_t(*R*) 19.3 min., R_t(*S*) 19.6 min.

9.1.2 2-(3,5-Difluorophenyl)-2-trimethylsilyloxy-acetonitrile.

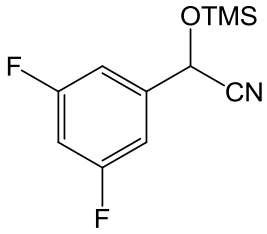

The product was obtained as an oil. $[\alpha]^{20}_D$ = -18.4 (c = 1.0 in $CHCl_3$); **δ_H** (400 MHz, $CDCl_3$) 0.27 (9H, s, Si(C*H*$_3$)$_3$), 5.47 (1H, s, C*H*CN), 6.84 (1H, tt, *J* (H,F)=8.8, *J* (H,H) 2.4 Hz, Ar*H*), 6.9–7.1 ppm (2H, m, Ar*H*); **δ_C** (100 MHz, $CDCl_3$) -0.4, 62.4, 104.8 (t, J (C,F) 25.1 Hz), 109.3 (d, J (C,F) 26.9 Hz), 118.2, 140.0 (t, J (C,F) 9.1 Hz), 163.2 ppm (dd, J(CF) 249.4, J (C,F) 12.4 Hz); **δ_F** (376 MHz, $CDCl_3$) 107.6 ppm (t, J(FH) = 7.5 Hz); IR (neat): υ = 3096, 2962, 2903, 2243, 1626, 1602 cm^{-1}; MS (ESI): m/z (%): 259 (25) $[M+H_2O]^+$, 185 (100); HRMS (ESI): calculated for $C_{11}H_{13}NOF_2Si$ $[M]^+$: 241.0735; found: 241.0731; ee determined by chiral GC analysis of the corresponding acetate by using *Method 2*: R_t(R) 14.8 min, R_t(S) 15.1 min.

9.1.3 2-(3,4-Dichlorophenyl)-2-trimethylsilyloxy-acetonitrile.

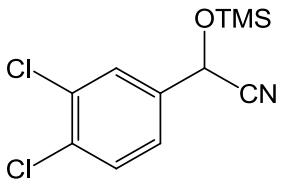

The product was obtained as an oil. $[\alpha]^{20}_{D}$ = -15.9 (c = 1.0 in $CHCl_3$); **δ_H** (400 MHz, $CDCl_3$) 0.26 (9H, s, Si(C*H*$_3$)$_3$), 5.44 (1H, s, C*H*CN), 7.31 (1H, dd, *J* 8.4, 2.0 Hz, Ar*H*), 7.50 (1H, d, *J* 8.4 Hz, Ar*H*), 7.57 ppm (1H, d, *J* 2.0 Hz, Ar*H*); **δ_C** (100 MHz, $CDCl_3$) -0.3, 62.4, 118.4, 125.4, 128.3, 131.0, 133.3, 133.7, 136.3 ppm; IR (neat): υ = 3094, 3025, 2961, 2901, 2242, 1595, 1568 cm^{-1}; MS (ESI): m/z (%): 296 (100) $[M+Na]^+$; HRMS (ESI): calculated for $C_{11}H_{13}NOCl_2SiNa$ $[M+Na]^+$: 296.0041; found: 296.0026; ee determined by ^{1}H NMR spectroscopy of the unprotected cyanohydrin in the presence of (R)-mandelic acid and DMAP: δ_H (400 MHz, $CDCl_3$) ((R)-C*H*CN) = 5.30 ppm, ((S)-C*H*CN) = 5.22 ppm.

2-Hydroxy-2-(3,4-dichlorophenyl)acetonitrile

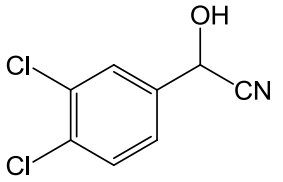

The product was obtained as a white solid (118mg) with a yield of 84%, **δ_H** (300 MHz, $CDCl_3$) 2.88 (1H, br, O*H*), 5.55 (1H, s, C*H*CN), 7.39 (1H, d, *J* 8.3 Hz, Ar*H*), 7.54 (1H, d, *J* 8.3 Hz, Ar*H*), 7.66 (1H, s, Ar*H*).

9.1.4 2-(4-Trifluoromethylphenyl)-2-trimethylsilyloxy-acetonitrile.[66]

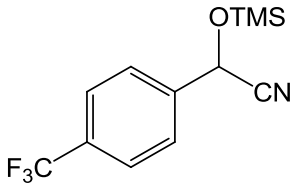

The product was obtained as an oil. δ_H (300 MHz, $CDCl_3$) 0.27 (9H, s, Si(CH_3)$_3$), 5.55 (1H, s, C*H*CN), 7.61 (2H, d, *J* 8.2 Hz, Ar*H*), 7.70 (2H, d, *J* 8.2 Hz, Ar*H*); δ_C (75 MHz, $CDCl_3$) -0.3, 62.9, 118.5, 122.3, 126.0 (q, *J* 4.0 Hz), 126.6, 131.5 (q, *J* 33 Hz), 140.0; δ_F (376 MHz, $CDCl_3$) 62.7; ee determined by chiral GC analysis of the corresponding acetate using *Method 2*. R_t(*R*) 16.3 min., R_t(*S*) 16.6 min.

9.1.5 2-(3-Chlorophenyl)-2-trimethylsilyloxy-acetonitrile.[44b]

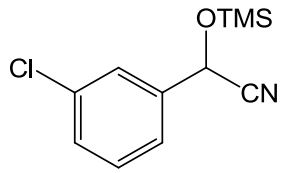

The product was obtained as an oil. δ_H (300 MHz, $CDCl_3$) 0.26 (9H, s, Si(CH_3)$_3$), 5.55 (1H, s, C*H*CN), 7.3-7.4 (2H, m, Ar*H*), 7.4-7.5 (2H, m, Ar*H*); δ_C (75 MHz, $CDCl_3$) -0.3, 62.9, 118.6, 124.3, 126.4, 129.5, 130.2, 134.9, 138.1; ee determined by chiral GC analysis of the corresponding acetate using *Method 4*. R_t(*R*) 76.7 min., R_t(*S*) 78.4 min.

9.1.6 2-(3-Fluorophenyl)-2-trimethylsilyloxy-acetonitrile.[141]

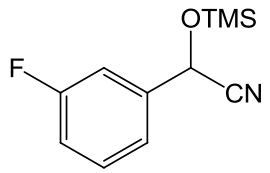

The product was obtained as an oil. δ_H (300 MHz, $CDCl_3$) 0.25 (9H, s, Si(CH_3)$_3$), 5.49 (1H, s, C*H*CN), 7.07 (1H, *apparent* tdd, *J* 6.3, 2.1, 0.6 Hz, Ar*H*), 7.19 (1H, *apparent* dt, *J* (H-F) 7.2, *J* (H-H) 1.8 Hz, Ar*H*), 7.2-7.3 (1H, m, Ar*H*), 7.38 (1H, td, *J* (H-F) 6.0, *J* (H-H) 4.2 Hz, *ArH*); δ_C (75 MHz, $CDCl_3$) -0.3, 62.9, 113.5 (d, *J* 23 Hz), 116.4 (d, *J* 21 Hz), 118.8, 121.9 (d, *J* 3.0 Hz), 130.7 (d, *J* 8.0 Hz), 138.7 (d, *J* 7.0 Hz) 163.0 (d, *J* 246

Hz); δ_F (376 MHz, $CDCl_3$) 111.3; ee determined by chiral GC analysis of the corresponding acetate using *Method 3*. R_t(*R*) 22.7 min., R_t(*S*) 23.3 min.

9.1.7 2-(4-Chlorophenyl)-2-trimethylsilyloxy-acetonitrile.[44b]

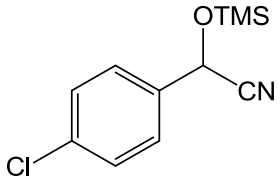

The product was obtained as an oil. δ_H (300 MHz, $CDCl_3$) 0.24 (9H, s, Si(C*H*$_3$)$_3$), 5.46 (1H, s, C*H*CN), 7.3-7.5 (4H, m, Ar*H*); δ_C (75 MHz, $CDCl_3$) -0.2, 63.0, 118.8, 127.7, 129.2, 134.8, 135.3; ee determined by chiral GC analysis of the corresponding acetate using *Method 3*. R_t(*R*) 34.0 min., R_t(*S*) 34.6 min.

9.1.8 2-(4-Bromophenyl)-2-trimethylsilyloxy-acetonitrile.[141]

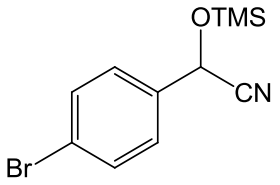

The product was obtained as an oil. δ_H (300 MHz, $CDCl_3$) 0.24 (9H, s, Si(C*H*$_3$)$_3$), 5.45 (1H, s, C*H*CN), 7.35 (2H, d, *J* 8.3 Hz, Ar*H*), 7.55 (2H, d, *J* 8.3 Hz, Ar*H*); δ_C (75 MHz, $CDCl_3$) -0.3, 63.0, 118.7, 123.5, 127.9, 132.1, 135.3; ee determined by chiral GC analysis of the corresponding acetate using *Method 3*. R_t(*R*) 39.4 min., R_t(*S*) 39.9 min.

9.1.9 2-(4-Fluorophenyl)-2-trimethylsilyloxy-acetonitrile.[44b]

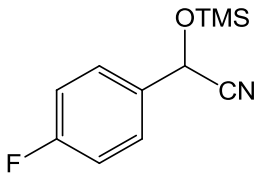

The product was obtained as an oil. δ_H (300 MHz, $CDCl_3$) -0.24 (9H, s, Si(CH_3)$_3$), 5.47 (1H, s, C*H*CN), 7.09 (2H, t, *J* 6.3 Hz, Ar*H*), 7.42 (2H, dd, *J* 6.3, 3.9 Hz, Ar*H*); δ_C (75 MHz, $CDCl_3$) -0.3, 62.9, 116.1 (d, *J* 22 Hz), 119.1, 128.4 (d, *J* 9.0 Hz), 132.3 (d, *J* 3.0 Hz,), 163.2 (d, *J* 247 Hz); δ_F (376 MHz, $CDCl_3$) 111.8; ee determined by chiral GC analysis of the corresponding acetate using *Method 2*. R_t(*R*) 16.9 min., R_t(*S*) 17.2 min.

9.1.10 2-(2-Methylphenyl)-2-trimethylsilyloxy-acetonitrile.[66]

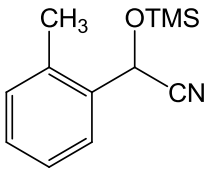

The product was obtained as an oil. δ_H (300 MHz, $CDCl_3$) 0.23 (9H, s, Si(CH_3)$_3$), 2.45 (3H, s, CH_3), 5.58 (1H, s, C*H*CN), 7.15-7.4 (4H, m, Ar*H*); δ_C (100 MHz, $CDCl_3$) -0.2, 18.7, 62-0, 118.8, 126.5, 127.1, 129.4, 131.1, 134.1, 135.7; ee determined by chiral GC analysis of the corresponding acetate using *Method 3*. R_t(*R*) 27.2 min., R_t(*S*) 27.4 min.

9.1.11 2-(3-Methylphenyl)-2-trimethylsilyloxy-acetonitrile.[44b, 66]

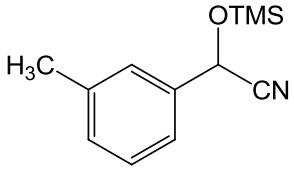

The product was obtained as an oil. δ_H (300 MHz, $CDCl_3$) 0.23 (9H, s, Si(CH_3)$_3$), 2.39 (3H, s, CH_3), 5.45 (1H, s, C*H*CN), 7.1-7.2 (1H, m, Ar*H*), 7.2-7.3 (3H, m, Ar*H*); δ_C (75 MHz, $CDCl_3$) -0.3, 21.4, 63.7, 119.3, 123.5, 127.0, 128.8, 130.1, 136.1, 138.8; ee determined by chiral GC analysis of the corresponding acetate using *Method 4*. R_t(*R*) 60.7 min., R_t(*S*) 62.2 min.

9.1.12 2-(4-Methylphenyl)-2-trimethylsilyloxy-acetonitrile.[44b, 66]

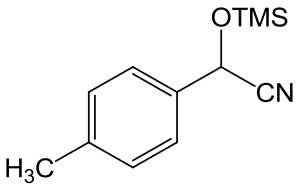

The product was obtained as an oil. δ_H (300 MHz, $CDCl_3$) 0.22 (9H, s, Si(CH_3)$_3$), 2.37 (3H, s, C*H*$_3$), 5.45 (1H, s, C*H*CN), 7.22 (2H, d, *J* 7.9 Hz, Ar*H*), 7.35 (2H, d, *J* 7.9 Hz, Ar*H*); δ_C (75 MHz, $CDCl_3$) -0.3, 21.2, 63.5, 119.3, 126.4, 129.6, 133.4, 139.3; ee determined by chiral GC analysis of the corresponding acetate using *Method 3*. R_t(*R*) 29.0 min., R_t(*S*) 29.5 min.

9.1.13 2-(3,4-Dimethylphenyl)-2-trimethylsilyloxy-acetonitrile.

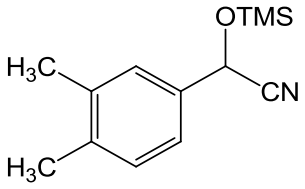

The product was obtained as a white solid. m.p. 31–32 °C; $[\alpha]^{20}_D$ = -24.1 (c = 1.0 in $CHCl_3$); δ_H (400 MHz, $CDCl_3$) 0.21 (9H, s, Si(CH_3)$_3$), 2.26 (3H, s, C*H*$_3$), 2.28 (3H, s, CH_3), 5.41 (1H, s, C*H*CN), 7.1–7.3 ppm (3H, m, Ar*H*); δ_C (100 MHz, $CDCl_3$) -0.2, 19.6, 19.8, 63.6, 119.4, 123.9, 127.6, 130.1, 133.7, 137.4, 138.0 ppm; IR (ATR): υ =

3017, 2960, 2924, 2239 cm^{-1}; MS (ESI): m/z (%): 251 (100) $[M+H_2O]^+$, 207 (95) $[M-CN]^+$, 185 (40); HRMS (ESI): calculated for $C_{13}H_{19}NOSi$ $[M+H]^+$: 234.1314; found: 234.1305; ee determined by ^1H NMR spectroscopy of the unprotected cyanohydrin in the presence of (R)-mandelic acid and DMAP: δ_H (400 MHz, $CDCl_3$) ((R)-C*H*CN) = 5.36 ppm, ((S)-C*H*CN) = 5.31 ppm.

2-Hydroxy-2-(3,4-dimethylphenyl)acetonitrile

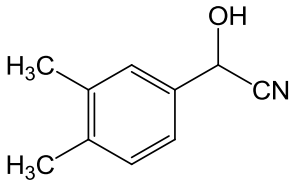

The product was obtained as a colourless oil (101mg) with a yield of 72%, δ_H (300 MHz, $CDCl_3$) 2.29 (3H, s, C*H*$_3$), 2.31 (3H, s, C*H*$_3$), 2.55 (1H, br, O*H*), 7.2-7.3 (3H, m, Ar*H*).

9.1.14 2-(4-Thiomethylphenyl)-2-trimethylsilyloxy-acetonitrile.[142]

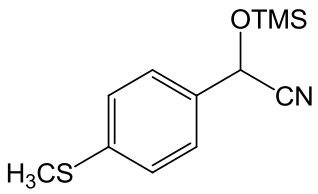

The product was obtained as an oil. δ_H (300 MHz, $CDCl_3$) 0.23 (9H, s, Si(C*H*$_3$)$_3$), 2.50 (3H, s, C*H*$_3$), 5.45 (1H, s, C*H*CN), 7.27 (2H, d, *J* 7.6 Hz, Ar*H*), 7.38 (2H, d, *J* 7.7 Hz, Ar*H*); δ_C (75 MHz, $CDCl_3$) -0.3, 15.4, 63.3, 119.1, 126.4, 126.8, 127.1, 139.3; ee determined by chiral GC analysis of the corresponding acetate using *Method 4*. R_t(*R*) 136.4 min., R_t(*S*) 138.4 min.

9.1.15 2-(4-Methoxyphenyl)-2-trimethylsilyloxy-acetonitrile.[44b, 66]

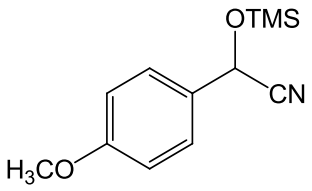

The product was obtained as an oil. δ_H (300 MHz, $CDCl_3$) 0.21 (9H, s, Si(CH_3)$_3$), 3.83 (3H, s, OCH_3), 5.44 (1H, s, C*H*CN), 6.93 (2H, d, *J* 8.5 Hz, Ar*H*), 7.39 (2H, d, *J* 8.5 Hz, Ar*H*); δ_C (75 MHz, $CDCl_3$) -0.2, 55.3, 63.3, 114.2, 119.3, 127.9, 128.4, 160.3. The optical rotation was used to determine the enantiomeric excesses: [lit.[113] for (*R*)-enantiomer: $[\alpha]^{20}_D$ = +22 (c = 1, $CHCl_3$)].

9.1.16 2-(4-*Tert*-butoxyphenyl)-2-trimethylsilyloxy-acetonitrile.

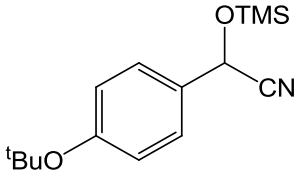

The product was obtained as an oil. $[\alpha]^{20}_D$ = -17.4 (c = 1.0 in $CHCl_3$); δ_H (400 MHz, $CDCl_3$) 0.22 (9H, s, Si(CH_3)$_3$), 1.36 (9H, s, OC(CH_3)$_3$), 5.46 (1H, s, C*H*CN), 7.02 (2H, d, *J* 8.4 Hz, Ar*H*), 7.36 ppm (2H, d, *J* 8.4 Hz, Ar*H*); δ_C (100 MHz, $CDCl_3$) -0.2, 28.8, 63.4, 79.0, 119.3, 124.2, 127.2, 130.9, 156.4 ppm; IR (neat): υ = 3063, 3036, 2978, 2904, 2240, 1608, 1508 cm^{-1}; MS (ESI): m/z (%): 278 (50) $[M+H]^+$, 276 (70), 242 (100); HRMS (ESI): calculated for $C_{15}H_{23}NO_2SiNa$ $[M+Na]^+$: 300.1396; found: 300.1371; ee determined by chiral GC analysis of the corresponding acetate by using *Method 5*: R_t=72.9 min (R), R_t= 73.7 min (S).

9.1.17 2-Trimethylsilyloxy-decanenitrile.[143]

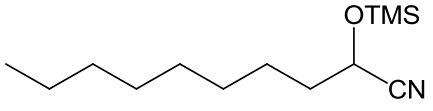

The product was obtained as an oil. δ_H (300 MHz, $CDCl_3$) 0.23 (9H, s, Si(CH_3)$_3$), 0.90 (3H, t, *J* 7.0 Hz, CH_3), 1.22-1.40 (10H, m, CH_2), 1.40-1.52 (2H, m, CH_2), 1.80 (2H, *apparent* q, *J* 8.2 Hz, CH_2), 4.40 (1H, t, *J* 6.6 Hz, C*H*CN); δ_C (100 MHz, $CDCl_3$) -0.4, 14.1, 22.6, 24.6, 28.9, 29.1, 29.3, 31.8, 36.2, 61.5, 120.1; ee determined by chiral GC analysis of the corresponding acetate using *Method 5*. R_t(*R*) 15.4 min., R_t(*S*) 15.6 min.

9.1.18 2-Trimethylsilyloxy-3,3-dimethyl-butanonitrile.[143]

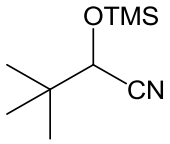

The product was obtained as an oil. δ_H (300 MHz, $CDCl_3$) 0.20 (9H, s, Si(CH_3)$_3$), 1.00 (9H, s, C(CH_3)$_3$), 3.98 (1H, C*H*CN); δ_C (100 MHz, $CDCl_3$) -0.5, 24.9, 35.8, 70.8, 119.3; ee determined by chiral GC analysis of the corresponding acetate using *Method 5*. R_t(*R*) 4.5 min., R_t(*S*) 4,7 min.

9.1.19 2-Cyclohexyl-2-trimethylsilyloxy-acetonitrile.[143]

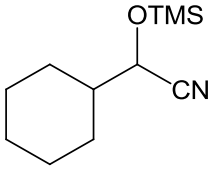

The product was obtained as an oil. δ_H (300 MHz, $CDCl_3$) 0.22 (9H, s, Si(CH_3)$_3$), 0.98-1.36 (5H, m, CH_2, C*H*CHCN), 1.75 (2H, m, CH_2), 1.75-1.83 (4H, m, CH_2), 4.16 (1H, d, *J* 6.4 Hz, C*H*CN); δ_C (100 MHz, $CDCl_3$) -0.5, 25.5, 26.0, 27.9, 28.2, 42.9, 66.5, 119.5 (this proton and carbon NMR corresponds to the chiral compound, that is the reason of observing an extra peak in the ^{13}C-NMR); ee determined by chiral GC analysis of the corresponding acetate using *Method 5*. R_t(*R*) 13.3 min., R_t(*S*) 13.5 min.

9.2 Ketones

9.2.1 2-Phenyl-2-trimethylsilyloxy-propionitrile.[39, 40b]

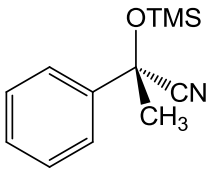

The product was obtained as an oil. **δ_H** (300 MHz, $CDCl_3$) 0.18 (9H, s, Si(C*H*$_3$)$_3$), 1.86 (3H, s, C*H*$_3$), 7.3-7.6 (5H, m, Ar*H*); **δ_C** (75 MHz, $CDCl_3$) 1.04, 33.55, 71.59, 121.62, 124.59, 128.28, 128.54, 141.96; ee was determined by ^{1}H NMR spectroscopy of the unprotected cyanohydrin in the presence of (*R*)-mandelic acid and DMAP. δ_H (300 MHz, $CDCl_3$) (*(R)*-CH_3CCN) 1.85 ppm, (*(S)*-CH_3CCN) 1.83 ppm.

9.2.2 2-(4-Chlorophenyl)-2-trimethylsilyloxy-propionitrile.[144]

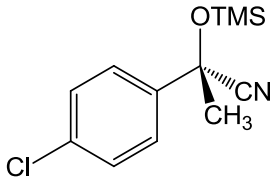

The product was obtained as an oil. **δ_H** (300 MHz, $CDCl_3$) 0.19 (9H, s, Si(C*H*$_3$)$_3$), 1.83 (3H, s, C*H*$_3$), 7.37 (2H, d, *J* 8.5 Hz, Ar*H*), 7.48 (2H, d, *J* 8.5 Hz, Ar*H*); **δ_C** (75 MHz, $CDCl_3$) 1.04, 33.51, 71.04, 121.22, 126.05, 128.81, 134.57, 140.67; ee was determined by ^{1}H NMR spectroscopy of the unprotected cyanohydrin in the presence of (*R*)-mandelic acid and DMAP. δ_H (300 MHz, $CDCl_3$) (*(R)*-CH_3CCN) 1.82 ppm, (*(S)*-CH_3CCN) 1.80 ppm.

9.2.3 2-(3-Chlorophenyl)-2-trimethylsilyloxy-propionitrile.[81b]

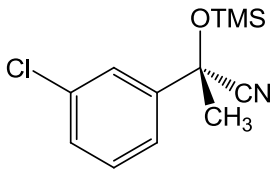

The product was obtained as an oil. **δ_H** (300 MHz, $CDCl_3$) 0.21 (9H, s, Si(CH_3)$_3$), 1.84 (3H, s, CH_3), 7.3-7.4 (2H, m, Ar*H*), 7.4-7.5 (1H, m, Ar*H*), 7.5-7.6 (1H, m, Ar*H*); **δ_C** (75 MHz, $CDCl_3$) 1.1, 33.5, 71.0, 121.1, 122.8, 124.9, 128.8, 130.0, 134.7, 144.1; ee was determined by ^{1}H NMR spectroscopy of the unprotected cyanohydrin in the presence of (*R*)-mandelic acid and DMAP. δ_H (300 MHz, $CDCl_3$) (*(R)*-CH_3CCN) 1.83 ppm, (*(S)*-CH_3CCN) 1.80 ppm.

9.2.4 2-(4-Bromophenyl)-2-trimethylsilyloxy-propionitrile.[80]

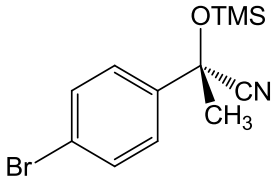

The product was obtained as an oil. **δ_H** (300 MHz, $CDCl_3$) 0.19 (9H, s, Si(CH_3)$_3$), 1.83 (3H, s, CH_3), 7.42 (2H, d, *J* 8.7 Hz, Ar*H*), 7.53 (2H, d, *J* 8.7 Hz, Ar*H*); **δ_C** (75 MHz, $CDCl_3$) 1.0, 33.5, 71.1, 121.2, 122.7, 126.4, 131.8, 141.2; ee was determined by ^{1}H NMR spectroscopy of the unprotected cyanohydrin in the presence of (*R*)-mandelic acid and DMAP. **δ_H** (300 MHz, $CDCl_3$) (*(R)*-CH_3CCN) 1.75 ppm, (*(S)*-CH_3CCN) 1.72 ppm.

9.2.5 2-(4-Fluorophenyl)-2-trimethylsilanoxy-propionitrile.[81b]

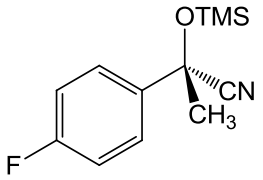

The product was obtained as an oil. **δ_H** (300 MHz, $CDCl_3$) 0.18 (9H, s, Si(CH_3)$_3$), 1.84 (3H, s, CH_3), 7.0-7.1 (2H, t, *J* (H-F) 8.8 Hz, Ar*H*), 7.5-7.6 (2H, dd, *J* (H-F) 8.8 and *J* (H-H) 5.2 Hz, Ar*H*); **δ_C** (75 MHz, $CDCl_3$) 1.0, 33.6, 71.0, 115.5 (d, *J* 21.8 Hz), 121.4, 126.67 (d, *J* 8.4 Hz,), 137.9 (d, *J* 3.2 Hz), 162.7 (d, *J* 247.8 Hz); **δ_F** (376 MHz, $CDCl_3$) -113.2; ee was determined by ^{1}H NMR spectroscopy of the unprotected cyanohydrin in the presence of (*R*)-mandelic acid and DMAP. δ_H (300 MHz, $CDCl_3$) (*(R)*-CH_3CCN) 1.82 ppm, (*(S)*-CH_3CCN) 1.79 ppm.

9.2.6 2-(4-Methylphenyl)-2-trimethylsilyloxy-propionitrile.[39, 40b]

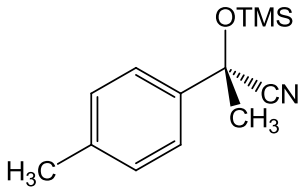

The product was obtained as an oil. **δ_H** (300 MHz, $CDCl_3$) 0.16 (9H, s, Si(CH_3)$_3$), 1.84 (3H, s, C(CH_3)CN), 2.37 (3H, s, CH_3), 7.20 (2H, d, *J* 8.1 Hz, Ar*H*), 7.42 (2H, d, *J* 8.1 Hz, Ar*H*); **δ_C** (75 MHz, $CDCl_3$) 1.1, 21.1, 33.5, 71.5, 121.7, 124.6, 129.2, 138.5, 143.8; ee was determined by ^{1}H NMR spectroscopy of the unprotected cyanohydrin in the presence of (*R*)-mandelic acid and DMAP. **δ_H** (300 MHz, $CDCl_3$) (*(R)*-CH_3CCN) 1.84 ppm, (*(S)*-CH_3CCN) 1.82 ppm.

9.2.7 2-(4-Methoxyphenyl)-2-trimethylsilyloxy-propionitrile.[39, 40b]

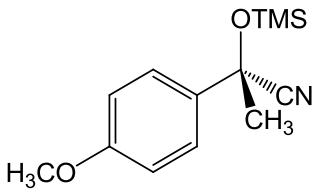

The product was obtained as an oil. **δ_H** (300 MHz, $CDCl_3$) 0.15 (9H, s, Si(CH_3)$_3$), 1.84 (3H, s, CH_3), 3.82 (3H, s, OCH_3), 6.90 (2H, d, *J* 8.8 Hz, Ar*H*), 7.46 (2H, d, *J* 8.8 Hz, Ar*H*); **δ_C** (75 MHz, $CDCl_3$) 1.1, 33.4, 55.3, 71.2, 113.8, 121.8, 126.0, 134.0, 159.7; ee was determined by ^{1}H NMR spectroscopy of the unprotected cyanohydrin in the presence of (*R*)-mandelic acid and DMAP. **δ_H** (300 MHz, $CDCl_3$) (*(R)*-CH_3CCN) 1.79 ppm, (*(S)*-CH_3CCN) 1.78 ppm.

9.2.8 2-Methyl-2-trimethylsilyloxy-pentanonitrile.[145]

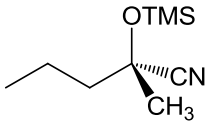

The product was obtained as an oil. **δ_H** (300 MHz, $CDCl_3$) 0.23 (9H, s, Si(CH_3)$_3$), 0.96 (3H, t, *J* 7.0 Hz, CH_3), 1.56 (3H, s, C(CH_3)CN), 1.3-1.6 (2H, m, CH_2), 1.6-1.8 (2H, m, CH_2); **δ_C** (75 MHz, $CDCl_3$) 1.3, 13.8, 17.6, 28.9, 45.5, 69.6, 122.2; ee was determined by ^{1}H NMR spectroscopy of the unprotected cyanohydrin in the presence of (*R*)-mandelic acid and DMAP. **δ_H** (300 MHz, $CDCl_3$) (*(R)*-CH_3CCN) 1.55 ppm, (*(S)*-CH_3CCN) 1.54 ppm.

10 References

[1] Pasteur, *Ann. Chim. Phys*. **1848**, *24*, 442.

[2] a) D. Enders, *Chem. Tech.* **1981**, 504; b) D. Enders, *Chemica Scripta*. **1985**, *25*, 139.

[3] C. P. Decicco, P. Grover, *Synlett* **1997**, 529-530.

[4] A. Gaucher, J. Ollivier, J. Salaun, *Synlett* **1991**, 151-153.

[5] M. A. Schwindt, D. T. Belmont, M. Carlson, L. C. Franklin, V. S. Hendrickson, G. L. Karrick, R. W. Poe, D. M. Sobieray, J. Van De Vusse, *J. Org. Chem.* **1996**, *61*, 9564-9568.

[6] M. F. Parisi, G. Gattuso, A. Notti, F. M. Raymo, R. H. Abeles, *J. Org. Chem.* **1995**, *60*, 5174-5179.

[7] a) Y. Lu, C. Miet, N. Kunesch, J. E. Poisson, *Tetrahedron: Asymmetry* **1993**, *4*, 893-902; b) R. F. C. Brown, A. C. Donohue, W. R. Jackson, T. D. McCarthy, *Tetrahedron* **1994**, *50*, 13739-13752; c) I. Tellitu, D. Badía, E. Domíguez, F. J. García, *Tetrahedron: Asymmery* **1994**, *5*, 1567-1578; d) F. Effenberger, J. Eichhorn, *Tetrahedron: Asymmetry* **1997**, *8*, 469-476.

[8] F. Effenberger, U. Stelzer, *Angew. Chem. Int. Ed.* **1991**, *30*, 873-874.

[9] F. Winkler, *Liebigs Ann. Chem.* **1832**, *4*, 242.

[10] F. Wöhler, *Liebigs J. Ann. Chim.* **1837**, *22*, 1.

[11] L. Rosenthaler, *Biochem. Z.* **1908**, *14*, 238-253.

[12] A. Lapworth, *J. Am. Chem. Soc.* **1903**, 995-1005.

[13] A. I. Mori, Y.; Kinoshita, K.; Inoue, S. , *Chem. Lett.* **1989**, 2119-2122.

[14] M. T. Reetz, F. Kunisch, P. Heitmann, *Tetrahedron Lett.* **1986**, *27*, 4721-4724.

[15] K. Y. Narasaka, T. Minamikawa, *Chem. Lett.* **1987**, 2073.

[16] S. K. Sung, M. K. Ju, G. Rajagopal, *Bull. Korean Chem. Soc.* **2006**, *27*, 1638-1640.

[17] M. Hayashi, T. Matsuda, N. Oguni, *J. Chem. Soc., Chem. Commun.* **1990**, 1364-1365.

[18] M. Wada, T. Takahashi, T. Domae, T. Fukuma, N. Miyoshi, K. Smith, *Tetrahedron: Asymmetry* **1997**, *8*, 3939-3946.

[19] D. Callant, D. Stanssens, J. G. de Vries, *Tetrahedron: Asymmetry* **1993**, *4*, 185-188.

[20] M. C. K. Choi, S. S. Chan, K. Matsumoto, *Tetrahedron Lett.* **1997**, *38*, 6669-6672.

[21] A. Mori, H. Nitta, M. Kudo, S. Inoue, *Tetrahedron Lett.* **1991**, *32*, 4333-4336.

[22] H. Ohno, H. Nitta, K. Tanaka, A. Mori, S. Inoue, *J. Org. Chem.* **1992**, *57*, 6778-6783.

[23] a) M. Hayashi, Y. Miyamoto, T. Inoue, N. Oguni, *J. Chem. Soc., Chem. Commun.* **1991**, 1752-1753; b) M. Hayashi, T. Inoue, Y. Miyamoto, N. Oguni, *Tetrahedron* **1994**, *50*, 4385-4398.

[24] M. Hayashi, Y. Miyamoto, T. Inoue, N. Oguni, *J. Org. Chem.* **1993**, *58*, 1515-1522.

[25] a) Y. Jiang, X. Zhou, W. Hu, Z. Li, A. Mi, *Tetrahedron: Asymmetry* **1995**, *6*, 2915-2916; b) Y. Jiang, X. Zhou, W. Hu, L. Wu, A. Mi, *Tetrahedron: Asymmetry* **1995**, *6*, 405-408.

[26] L. Z. Flores-Lopéz, M. Parra-Hake, R. Somanathan, P. J. Walsh, *Organometallics* **2000**, *19*, 2153-2160.

[27] A. Gama, L. Z. Flores-López, G. Aguirre, M. Parra-Hake, R. Somanathan, P. J. Walsh, *Tetrahedron: Asymmetry* **2002**, *13*, 149-154.

[28] R. M. Moreno, M. Rosol, A. Moyano, *Tetrahedron: Asymmetry* **2006**, *17*, 1089-1103.

[29] J.-S. You, H.-M. Gau, M. C. K. Choi, *Chem. Commun.* **2000**, 1963-1964.

[30] K. Yoshinaga, T. Nagata, *Adv. Synth. Cat.* **2009**, *351*, 1495-1498.

[31] a) T. Katsuki, *Coord. Chem. Rev.* **1995**, *140*, 189-214; b) W. Zhang, E. N. Jacobsen, *J. Org. Chem.* **1991**, *56*, 2296-2298.

[32] a) T. Fukuda, T. Katsuki, *Tetrahedron* **1997**, *53*, 7201-7208; b) T. Niimi, T. Uchida, R. Irie, T. Katsuki, *Tetrahedron Lett.* **2000**, *41*, 3647-3651; c) T. Uchida, R. Irie, T. Katsuki, *Synlett* **1999**, 1793-1795.

[33] B. Saito, T. Katsuki, *Tetrahedron Lett.* **2001**, *42*, 3873-3876.

[34] a) Y. Yamashita, T. Katsuki, *Synlett* **1995**, 829-830; b) Y. Huang, T. Iwama, V. H. Rawal, *J. Am. Chem. Soc.* **2000**, *122*, 7843-7844.

[35] Y. Jiang, L. Gong, X. Feng, W. Hu, W. Pan, Z. Li, A. Mi, *Tetrahedron* **1997**, *53*, 14327-14338.

[36] a) Y. Belokon, N. Ikonnikov, M. Moscalenko, M. North, S. Orlova, V. Tararov, L. Yashkina, *Tetrahedron: Asymmetry* **1996**, *7*, 851-855; b) Y. Belokon, M. Flego, N. Ikonnikov, M. Moscalenko, M. North, C. Orizu, V. Tararov, M. Tasinazzo, *J. Chem. Soc., Perkin Trans. 1* **1997**, 1293-1296.

[37] a) M. North, C. Orizu, V. I. Tararov, N. S. Ikonnikov, Y. N. Belokon, D. E. Hibbs, M. B. Hursthouse, K. M. Abdul Malik, *Chem. Commun.* **1998**, 387-388; b) Y. N. Belokon, S. Caveda-Cepas, B. Green, N. S. Ikonnikov, V. N. Krustalev, V. S. Larichev, M. A. Moscalenko, M. North, C. Orizu, V. I. Tararov, M. Tasinazzo, G. I. Timofeeva, L. V. Yashkina, *J. Am. Chem. Soc.* **1999**, *121*, 3968-3973.

[38] Y. N. Belokon, B. Green, N. S. Ikonnikov, V. S. Larichev, B. V. Lokshin, M. A. Moscalenko, M. North, C. Orizu, A. S. Peregudov, G. I. Timofeeva, *Eur. J. Org. Chem.* **2000**, 2655-2661.

[39] Y. N. Belokon, B. Green, N. S. Ikonnikov, M. North, V. I. Tararov, *Tetrahedron Lett.* **1999**, *40*, 8147-8150.

[40] a) Y. N. Belokon, A. V. Gutnov, M. A. Moskalenko, L. V. Yashkina, D. E. Lesovoy, N. S. Ikonnikov, V. S. Larichev, A. N. Michael North, *Chem. Commun.* **2002**, 244-245; b) Y. N. Belokon, B. Green, N. S. Ikonnikov, M. North, T. Parsons, V. I. Tararov, *Tetrahedron* **2001**, *57*, 771-779; c) Y. N. Belokon, A. J. Blacker, L. A. Clutterbuck, M. North, *Org. Lett.* **2003**, *5*, 4505-4507; d) Y. N. Belokon, E. Ishibashi, H. Nomura, M. North, *Chem. Commun.* **2006**, 1775-1777.

[41] S. Liang, X. R. Bu, *J. Org. Chem.* **2002**, *67*, 2702-2704.

[42] Y. N. Belokon, J. Hunt, M. North, *Synlett* **2008**, 2150-2154.

[43] Y. N. Belokon, M. North, T. Parsons, *Org. Lett.* **2000**, *2*, 1617-1619.

[44] a) Y. N. Belokon, V. I. Maleev, M. North, D. L. Usanov, *Chem. Commun.* **2006**, 4614-4616; b) Y. N. Belokon, W. Clegg, R. W. Harrington, V. I. Maleev, M. North, M. O. Pujol, D. L. Usanov, C. Young, *Chem. Eur. J.* **2009**, *15*, 2148-2165.

[45] a) Y. N. Belokon, M. North, V. I. Maleev, N. V. Voskoboev, M. A. Moskalenko, A. S. Peregudov, A. V. Dmitriev, N. S. Ikonnikov, H. B. Kagan, *Angew. Chem. Int. Ed.* **2004**, *43*, 4085-4089; b) Y. N. Belokon, W. Clegg, R. W. Harrington, C. Young, M. North, *Tetrahedron* **2007**, *63*, 5287-5299; c) Y. N. Belokon, W. Clegg, R. W. Harrington, M. North, C. Young, *Inorg. Chem.* **2008**, *47*, 3801-3814.

[46] Z. Zhang, Z. Wang, R. Zhang, K. Ding, *Angew. Chem. Int. Ed.* **2010**, *49*, 6746-6750.

[47] a) S. S. Kim, S. H. Lee, *Synth. Commun.* **2005**, *35*, 751-759; b) F. X. Chen, H. Zhou, X. Liu, B. Qin, X. Feng, G. Zhang, Y. Jiang, *Chem. Eur. J.* **2004**, *10*,

4790-4797; c) S. S. Kim, D. H. Song, *Eur. J. Org. Chem.* **2005**, *2005*, 1777-1780.

[48] M. T. K. Reetz, F.; Heitmann, P. , *Tetrahedron Lett.* **1986**, *27*, 4721.

[49] M. Mori, H. Imma, T. Nakai, *Tetrahedron Lett.* **1997**, *38*, 6229-6232.

[50] C. Qian, C. Zhu, T. Huang, *J. Chem. Soc., Perkin Trans. 1* **1998**, 2131-2132.

[51] Z.-B. Li, A. R. Rajaram, N. Decharin, Y.-C. Qin, L. Pu, *Tetrahedron Lett.* **2005**, *46*, 2223-2226.

[52] a) Y. N. Belokon, D. Chusov, D. A. Borkin, L. V. Yashkina, A. V. Dmitriev, D. Katayev, M. North, *Tetrahedron: Asymmetry* **2006**, *17*, 2328-2333; b) Y. Belokon, D. Chusov, T. Skrupskaya, D. Bor'kin, L. Yashkina, K. Lyssenko, M. Il'in, T. Strelkova, G. Timofeeva, A. Peregudov, M. North, *Russ. Chem. Bull.* **2008**, *57*, 1981-1988.

[53] X.-G. Zhou, J.-S. Huang, P.-H. Ko, K.-K. Cheung, C.-M. Che, *J. Chem. Soc., Dalton Trans.* **1999**, 3303-3309.

[54] a) Y. Hamashima, D. Sawada, M. Kanai, M. Shibasaki, *J. Am. Chem. Soc.* **1999**, *121*, 2641-2642; b) Y. Hamashima, D. Sawada, H. Nogami, M. Kanai, M. Shibasaki, *Tetrahedron* **2001**, *57*, 805-814; c) J. Casas, C. Nájera, J. M. Sansano, J. M. Saá, *Org. Lett.* **2002**, *4*, 2589-2592; d) J. Casas, C. Nájera, J. M. Sansano, J. M. Saá, *Tetrahedron* **2004**, *60*, 10487-10496; e) Y.-C. Qin, L. Liu, L. Pu, *Org. Lett.* **2005**, *7*, 2381-2383; f) F. Yang, S. Wei, C.-A. Chen, P. Xi, L. Yang, J. Lan, H.-M. Gau, J. You, *Chem. Eur. J.* **2008**, *14*, 2223-2231.

[55] C.-D. Hwang, D.-R. Hwang, B.-J. Uang, *J. Org. Chem.* **1998**, *63*, 6762-6763.

[56] C.-W. Chang, C. TzuYang, C.-D. Hwang, B.-J. Uang, *Chem. Commun.* **2002**, 54-55.

[57] O. Belda, S. Duquesne, A. Fischer, C. Moberg, *J. Organomet. Chem.* **2004**, *689*, 3750-3755.

[58] Y. Liu, X. Liu, J. Xin, X. Feng, *Synlett* **2006**, 1085-1089.

[59] H. Deng, M. P. Isler, M. L. Snapper, A. H. Hoveyda, *Angewandte Chemie - International Edition* **2002**, *41*, 1009-1012.

[60] J.-M. Brunel, O. Legrand, G. Buono, *Tetrahedron: Asymmetry* **1999**, *10*, 1979-1984.

[61] Z. Yang, Z. Zhou, K. He, L. Wang, G. Zhao, Q. Zhou, C. Tang, *Tetrahedron: Asymmetry* **2003**, *14*, 3937-3941.

[62] K. He, Z. Zhou, L. Wang, K. Li, G. Zhao, Q. Zhou, C. Tang, *Tetrahedron* **2004**, *60*, 10505-10513.

[63] a) K. Sato, M. Kira, H. Sakurai, *Tetrahedron Lett.* **1989**, *30*, 4375-4378; b) B. Liu, X. Feng, F. Chen, G. Zhang, X. Cui, Y. Jiang, *Synlett* **2001**, 1551-1554; c) H. Zhou, F. X. Chen, B. Qin, X. Feng, G. Zhang, *Synlett* **2004**, 1077-1079.

[64] a) Y. Shen, X. Feng, Y. Li, G. Zhang, Y. Jiang, *Tetrahedron* **2003**, *59*, 5667-5675; b) Y. Shen, X. Feng, Y. Li, G. Zhang, Y. Jiang, *Eur. J. Org. Chem.* **2004**, *2004*, 129-137.

[65] a) S. S. Kim, D. W. Kim, G. Rajagopal, *Synthesis* **2004**, 213-216; b) S. S. Kim, G. Rajagopal, D. W. Kim, D. H. Song, *Synth. Commun.* **2004**, *34*, 2973-2980; c) Y. Li, B. He, X. Feng, G. Zhang, *Synlett* **2004**, 1598-1600.

[66] Y. Wen, X. Huang, J. Huang, Y. Xiong, B. Qin, X. Feng, *Synlett* **2005**, *2005*, 2445-2448.

[67] B. Zeng, X. Zhou, X. Liu, X. Feng, *Tetrahedron* **2007**, *63*, 5129-5136.

[68] a) C. Puigjaner, A. Vidal-Ferran, A. Moyano, M. A. Pericàs, A. Riera, *J. Org. Chem.* **1999**, *64*, 7902-7911; b) M. Pastó, A. Riera, Miquel A. Pericàs, *Eur. J. Org. Chem.* **2002**, *2002*, 2337-2341; c) S. l. Ferrer, M. Pastó, B. Rodríguez, A. Riera, M. A. Pericàs, *Tetrahedron: Asymmetry* **2003**, *14*, 1747-1752; d) M. A. Pericàs, C. Puigjaner, A. Riera, A. Vidal-Ferran, M. Gómez, F. Jiménez, G. Muller, M. Rocamora, *Chem. Eur. J.* **2002**, *8*, 4164-4178.

[69] B. Rodríguez, M. Pastó, C. Jimeno, M. A. Pericàs, *Tetrahedron: Asymmetry* **2006**, *17*, 151-160.

[70] Y.-Q. Wen, W.-M. Ren, X.-B. Lu, *Org. Biomol. Chem.* **2011**, *9*, 6323-6330.

[71] M. North, P. Villuendas, C. Williamson, *Tetrahedron* **2010**, *66*, 1915-1924.

[72] Y. Xiong, X. Huang, S. Gou, J. Huang, Y. Wen, X. Feng, *Adv. Synth. Cat.* **2006**, *348*, 538-544.

[73] M. Yoshioka, T. Kawakita, M. Ohno, *Tetrahedron Lett.* **1989**, *30*, 1657-1660.

[74] B. M. Trost, S. Martínez-Sánchez, *Synlett* **2005**, 627-630.

[75] Y. B. Kim, M. K. Kim, S. H. Kang, Y. H. Kim, *Synlett* **2005**, 1995-1998.

[76] M. Kanai, Y. Hamashima, M. Shibasaki, *Tetrahedron Lett.* **2000**, *41*, 2405-2409.

[77] a) Y. Hamashima, M. Kanai, M. Shibasaki, *J. Am. Chem. Soc.* **2000**, *122*, 7412-7413; b) Y. Hamashima, M. Kanai, M. Shibasaki, *Tetrahedron Lett.* **2001**, *42*, 691-694; c) S. Masumoto, K. Yabu, M. Kanai, M. Shibasaki, *Tetrahedron Lett.* **2002**, *43*, 2919-2922.

[78] E. J. Corey, W. Zhe, *Tetrahedron Lett.* **1993**, *34*, 4001-4004.

[79] D. H. Ryu, E. J. Corey, *J. Am. Chem. Soc.* **2004**, *126*, 8106-8107.

[80] D. H. Ryu, E. J. Corey, *J. Am. Chem. Soc.* **2005**, *127*, 5384-5387.

[81] a) F. Chen, X. Feng, B. Qin, G. Zhang, Y. Jiang, *Org. Lett.* **2003**, *5*, 949-952; b) F.-X. Chen, B. Qin, X. Feng, G. Zhang, Y. Jiang, *Tetrahedron* **2004**, *60*, 10449-10460.

[82] a) B. He, F.-X. Chen, Y. Li, X. Feng, G. Zhang, *Tetrahedron Lett.* **2004**, *45*, 5465-5467; b) B. He, F.-X. Chen, Y. Li, X. Feng, G. Zhang, *Eur. J. Org. Chem.* **2004**, *2004*, 4657-4666.

[83] a) S. S. Kim, J. M. Kwak, *Tetrahedron* **2006**, *62*, 49-53; b) S. S. Kim, S. H. Lee, J. M. Kwak, *Tetrahedron: Asymmetry* **2006**, *17*, 1165-1169.

[84] a) J. Meléndez, M. North, R. Pasquale, *Eur. J. Inorg. Chem.* **2007**, 3323-3326; b) M. North, R. Pasquale, *Angew. Chem. Int. Ed.* **2009**, *48*, 2946-2948; c) W. Clegg, R. W. Harrington, M. North, R. Pasquale, *Chem. Eur. J.* **2010**, *16*, 6828-6843.

[85] M. North, C. Williamson, *Tetrahedron Lett.* **2009**, *50*, 3249-3252.

[86] C. Lv, Q. Cheng, D. Xu, S. Wang, C. Xia, W. Sun, *Eur. J. Org. Chem.* **2011**, *2011*, 3407-3411.

[87] Q. Li, X. Liu, J. Wang, K. Shen, X. Feng, *Tetrahedron Lett.* **2006**, *47*, 4011-4014.

[88] K. Shen, X. Liu, Q. Li, X. Feng, *Tetrahedron* **2008**, *64*, 147-153.

[89] S. S. Kim, J. M. Kwak, G. Rajagopal, *Bull. Korean Chem. Soc.* **2006**, *27*, 1638-1640.

[90] a) J. A. Bonadies, W. M. Butler, V. L. Pecoraro, C. J. Carrano, *Inorg. Chem.* **1987**, *26*, 1218-1222; b) J. R. Zamian, E. R. Dockal, G. Castellano, G. Oliva, *Polyhedron* **1995**, *14*, 2411-2418; c) H. Schmidt, M. Bashirpoor, D. Rehder, *J. Chem. Soc., Dalton Trans.* **1996**, 3865-3870.

[91] K. Nakajima, M. Kojima, S. Azuma, R. Kasahara, M. Tsuchimoto, Y. Kubozono, H. Maeda, S. Kashino, S. Ohba, Y. Yoshikawa, J. Fujita, *Bull. Chem. Soc. Jpn.* **1996**, *69*, 3207-3216.

[92] a) K. Oyaizu, K. Yamamoto, K. Yoneda, E. Tsuchida, *Inorg. Chem.* **1996**, *35*, 6634-6635; b) N. F. Choudhary, N. G. Connelly, P. B. Hitchcock, G. Jeffery Leigh, *J. Chem. Soc., Dalton Trans.* **1999**, 4437-4446.

[93] a) Y. N. Belokon, P. Carta, A. V. Gutnov, V. Maleev, M. A. Moskalenko, L. V. Yashkina, N. S. Ikonnikov, N. V. Voskoboev, V. N. Khrustalev, M. North, *Helv. Chim. Acta* **2002**, *85*, 3301-3312; b) W. Huang, Y. Song, J. Wang, G. Cao, Z. Zheng, *Tetrahedron* **2004**, *60*, 10469-10477.

[94] R. J. Blanch, A. McCluskey, *Chem. Phys. Lett.* **1995**, *241*, 116-120.

[95] T. K. Brotherton, J. W. Lynn, *Chem. Rev.* **1959**, *59*, 841-883.

[96] U. Thewalt, W. Nuding, *J. Organomet. Chem.* **1996**, *512*, 127-130.

[97] a) D. Li, S. Parkin, G. Wang, G. T. Yee, S. M. Holmes, *Inorg. Chem.* **2006**, *45*, 2773-2775; b) I. S. Lee, J. R. Long, *Dalton Transactions* **2004**, 3434-3436; c) S. Gambarotta, C. Floriani, A. Chiesi-Villa, C. Guastini, *Inorg. Chem.* **1984**, *23*, 1739-1747.

[98] a) W.-L. Man, H.-K. Kwong, W. W. Y. Lam, J. Xiang, T.-W. Wong, W.-H. Lam, W.-T. Wong, S.-M. Peng, T.-C. Lau, *Inorg. Chem.* **2008**, *47*, 5936-5944; b) N. Matsumoto, Y. Sunatsuki, H. Miyasaka, Y. Hashimoto, D. Luneau, J.-P. Tuchagues, *Angew. Chem. Int. Ed.* **1999**, *38*, 171-173; c) D. Zhang, H. Wang, Y. Chen, L. Zhang, L. Tian, Z.-H. Ni, J. Jiang, *Dalton Transactions* **2009**, 9418-9425; d) P. Albores, J. Seeman, E. Rentschler, *Dalton Transactions* **2009**, 7660-7668.

[99] C. Chatgilialoglu, B. C. Gilbert, B. Gill, M. D. Sexton, *J. Chem. Soc., Perkin Trans. 2* **1980**, 1141-1150.

[100] A. R. Forrester, V. Purushotham, *J. Chem. Soc., Faraday Trans. 1* **1987**, *83*, 211-217.

[101] L. Eberson, O. Persson, *Acta Chem. Scand.* **1998**, *52*, 608-621.

[102] a) S.-H. Qin, K.-Y. Qiu, *Polym. Bull. (Berlin)* **2000**, *44*, 123-128; b) J.-Y. Huang, Y.-S. Zou, *Gaodeng Xuexiao Huaxue Xuebao* **2008**, *29*, 1689-1693.

[103] M. A. Pericàs, F. Serratosa, E. Valentà-, *Tetrahedron* **1987**, *43*, 2311-2316.

[104] M. Tsuchimoto, G. Hoshina, N. Yoshioka, H. Inoue, K. Nakajima, M. Kamishima, M. Kojima, S. Ohba, *Journal of Solid State Chemistry* **2000**, *153*, 9-15.

[105] a) D. H. Paull, C. J. Abraham, M. T. Scerba, E. Alden-Danforth, T. Lectka, *Acc. Chem. Res.* **2008**, *41*, 655-663; b) S. Matsunaga, M. Shibasaki, *Bull. Chem. Soc. Jpn.* **2008**, *81*, 60-75; c) M. Shibasaki, M. Kanai, S. Matsunaca, N. Kumagai, *Acc. Chem. Res.* **2009**, *42*, 1117-1127; d) J. Gawronski, N. Wascinska, J. Gajewy, *Chem. Rev.* **2008**, *108*, 5227-5252; e) C. Schneider, *Angew. Chem. Int. Ed.* **2009**, *48*, 2082-2084; f) C. Nájera, J. M. Sansano, J. M. Saá, *Eur. J. Org. Chem.* **2009**, 2385-2400.

[106] E. J. Corey, Z. Wang, *Tetrahedron Lett.* **1993**, *34*, 4001-4004.

[107] S. S. Kim, J. M. Kwak, S. C. George, *Appl. Organomet. Chem.* **2007**, *21*, 809-813.

[108] H. Minamikawa, S. Hayakawa, T. Yamada, N. Iwasawa, K. Narasaka, *Bull. Chem. Soc. Jpn.* **1988**, *61*, 4379-4383.

[109] L. P. Hammett, *Chem. Rev.* **1935**, *17*, 125-136.

[110] S. Norsikian, I. Holmes, F. Lagasse, H. B. Kagan, *Tetrahedron Lett.* **2002**, *43*, 5715-5717.

[111] L. S. Moon, R. S. Jolly, Y. Kasetti, P. V. Bharatam, *Chem. Commun.* **2009**, 1067-1069.

[112] T. Sakai, K. Wang, T. Ema, *Tetrahedron* **2008**, *64*, 2178-2183.

[113] J. Brussee, E. C. Roos, A. Van Der Gen, *Tetrahedron Lett.* **1988**, *29*, 4485-4488.

[114] a) D. A. Evans, L. K. Truesdale, *Tetrahedron Lett.* **1973**, *14*, 4929-4932; b) J. K. Whitesell, R. Apodaca, *Tetrahedron Lett.* **1996**, *37*, 2525-2528; c) P. G. Cozzi, C. Floriani, *J. Chem. Soc., Perkin Trans. 1* **1995**, 2557-2563; d) R. J. Capon, D. Vuong, M. McNally, T. Peterle, N. Trotter, E. Lacey, J. H. Gill, *Org. Biomol. Chem.* **2005**, *3*, 118-122.

[115] a) M. G. Dekamin, S. Sagheb-Asl, M. Reza Naimi-Jamal, *Tetrahedron Lett.* **2009**, *50*, 4063-4066; b) S. E. Denmark, W.-j. Chung, *J. Org. Chem.* **2006**, *71*, 4002-4005; c) I. Amurrio, R. Córdoba, A. G. Csákÿ, J. Plumet, *Tetrahedron* **2004**, *60*, 10521-10524.

[116] M. North, M. Omedes-Pujol, C. Williamson, *Chem. Eur. J.* **2010**, *16*, 11367-11375.

[117] a) Y. N. Belokon, P. Carta, M. North, *Tetrahedron Lett.* **2005**, *46*, 4483-4486; b) Y. N. Belokon, A. J. Blacker, P. Carta, L. A. Clutterbuck, M. North, *Tetrahedron* **2004**, *60*, 10433-10447.

[118] a) Y. N. Belokon, W. Clegg, R. W. Harrington, E. Ishibashi, H. Nomura, M. North, *Tetrahedron* **2007**, *63*, 9724-9740; b) E. Wingstrand, S. Lundgren, M. Penhoat, C. Moberg, *Pure Appl. Chem.* **2006**, *78*, 409-414; c) S. Lundgren, E. Wingstrand, M. Penhoat, C. Moberg, *J. Am. Chem. Soc.* **2005**, *127*, 11592-11593.

[119] M. Tilliet, S. Lundgren, C. Moberg, V. Levacher, *Adv. Synth. Catal.* **2007**, *349*, 2079-2084.

[120] N. U. H. Khan, S. Agrawal, R. I. Kureshy, S. H. R. Abdi, K. Jeya Prathap, R. V. Jasra, *Eur. J. Org. Chem.* **2008**, 4511-4515.

[121] C. Baleizão, B. Gigante, H. Garcia, A. Corma, *Green Chem.* **2002**, *4*, 272-274.

[122] Y. Qu, L. Jing, Z. Wu, D. Wu, X. Zhou, *Tetrahedron: Asymmetry* **2010**, *21*, 187-190.

[123] a) A. M. Delaite, Fr. . **2007**, p. 5pp; b) A. Ansmann, B. Boutty, M. Dierker, Cognis IP Management GmbH, Germany . **2008**, p. 14 pp.

[124] K. Xu, *Chem. Rev.* **2004**, *104*, 4303-4418.

[125] B. Schäffner, F. Schäffner, S. P. Verevkin, A. Börner, *Chem. Rev.* **2010**, *110*, 4554-4581.

[126] M. T. Reetz, G. Lohmer, *Chem. Commun.* **1996**, 1921-1922.

[127] B. Schäffner, J. Holz, S. P. Verevkin, A. Börner, *Tetrahedron Lett.* **2008**, *49*, 768-771.

[128] B. Schäffner, J. Holz, S. P. Verevkin, A. Börner, *ChemSusChem* **2008**, *1*, 249-253.

[129] N. Mase, Y. Nakai, N. Ohara, H. Yoda, K. Takabe, F. Tanaka, C. F. Barbas Iii, *J. Am. Chem. Soc.* **2006**, *128*, 734-735.

[130] M. North, F. Pizzato, P. Villuendas, *ChemSusChem* **2009**, *2*, 862-865.

[131] M. Morcillo, M. North, P. Villuendas, *Synthesis* **2011,** 1918-1925.

[132] a) J. H. Clements, *Ind. Eng. Chem. Res.* **2003**, *42*, 663-674; b) M. Yoshida, M. Ihara, *Chem. Eur. J.* **2004**, *10*, 2886-2893; c) J. Sun, S. I. Fujita, M. Arai, *J. Organomet. Chem.* **2005**, *690*, 3490-3497; d) R. Zevenhoven, S. Eloneva, S. Teir, *Catal. Today* **2006**, *115*, 73-79; e) M. North, R. Pasquale, C. Young, *Green Chem.* **2010**, *12*, 1514-1539.

[133] a) A. H. Tullo, P. L. Short, *Chem. Eng. News* **2006**, *84*, 22-23; b) Q. Chen, E. J. Beckman, *Green Chem.* **2007**, *9*, 802-808; c) Q. Chen, E. J. Beckman, *Green Chem.* **2008**, *10*, 934-938.

[134] a) J. M. Brunel, I. P. Holmes, *Angew. Chem. Int. Ed.* **2004**, *43*, 2752-2778; b) A. J. Blacker, M. North, Y. N. Belokon, *Chimica Oggi* **2004**, *22*, S30-S32; c) J. Blacker, M. North, *Chemistry and Industry (London)* **2005**, 22-25.

[135] W. L. F. Armarego, C. L. L. Chai, Knovel (Firm), *Purification of laboratory chemicals*, 5th ed., Butterworth-Heinemann, Amsterdam ; Boston, **2003**.

[136] J. F. Larrow, E. N. Jacobsen, Y. Gao, Y. Hong, X. Nie, C. M. Zepp, *J. Org. Chem.* **1994**, *59*, 1939-1942.

[137] a) M. S. Taylor, E. N. Jacobsen, *J. Am. Chem. Soc.* **2003**, *125*, 11204-11205; b) G. M. Sammis, H. Danjo, E. N. Jacobsen, *J. Am. Chem. Soc.* **2004**, *126*, 9928-9929.

[138] http://tools.niehs.nih.gov/stdb/index.cfm

[139] K. Tanaka, A. Mori, S. Inoue, *J. Org. Chem.* **1990**, *55*, 181-185.

[140] P. V. R. Acharyulu, P. K. Dubey, P. V. V. P. Reddy, T. Suresh, *Synth. Commun.* **2009**, *39*, 3217-3231.

[141] M. Hatano, T. Ikeno, T. Miyamoto, K. Ishihara, *J. Am. Chem. Soc.* **2005**, *127*, 10776-10777.

[142] K. Mai, G. Patil, *Tetrahedron Lett.* **1984**, *25*, 4583-4586.

[143] Y. N. Belokon, J. Hunt, M. North, *Tetrahedron: Asymmetry* **2008**, *19*, 2804-2815.

[144] K. Yabu, S. Masumoto, S. Yamasaki, Y. Hamashima, M. Kanai, W. Du, D. P. Curran, M. Shibasaki, *J. Am. Chem. Soc.* **2001**, *123*, 9908-9909.

[145] F.-X. Chen, H. Zhou, X. Liu, B. Qin, X. Feng, G. Zhang, Y. Jiang, *Chem Eur. J.* **2004**, *10*, 4790-4797.

Appendix 1

1.1- *Solutions of Oxovanadium(salen) complexes in dichloromethane.*

The spectrum of VO(salen) on the top, shows the characteristic eight line signal of paramagnetic vanadium(IV) with nuclear spin I=7/2. In descending order, next come the spectra of VO(salen)NCS, VO(salen)Cl and VO(salen)$EtOSO_3$ complexes. These complexes, bearing a vanadium(V) nuclei with all paired electrons, should be invisible to electron paramagnetic resonance. However, all contained VO(salen) impurity, 4.8, 2.0 and 4.2% respectively.

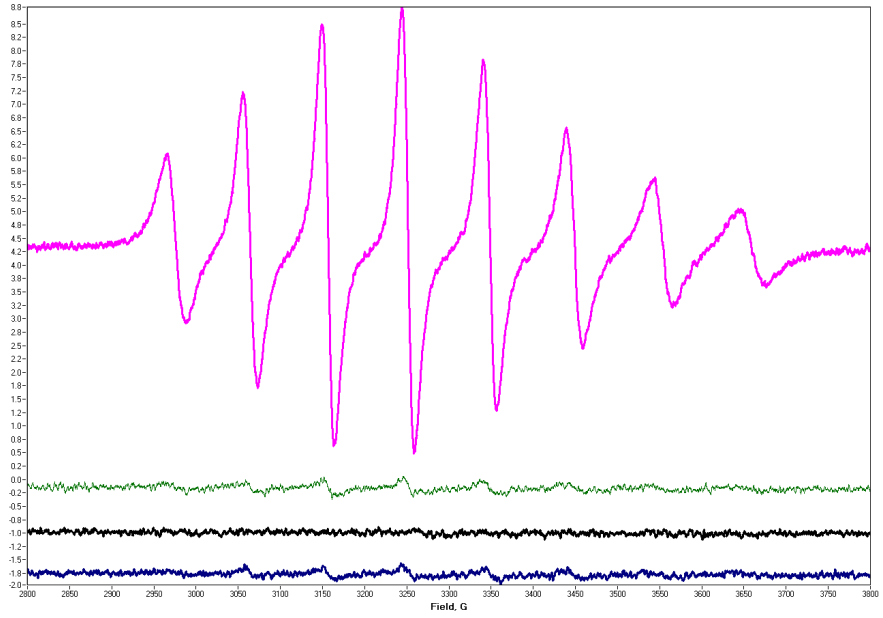

1.2- *Trimethylsilyl cyanide addition to solutions of benzaldehyde and vanadium complex.*

Here are presented the spectra evolution versus time (from bottom to top) of the addition of TMSCN to a solution of benzaldehyde and vanadium complex. Each spectrum was recorded 3.5 minutes after the TMSCN addition (time that the EPR spectrometer takes to record a spectrum).

VO(salen)$EtOSO_3$ – 12 % of vanadium(V) was reduced to vanadium(IV):

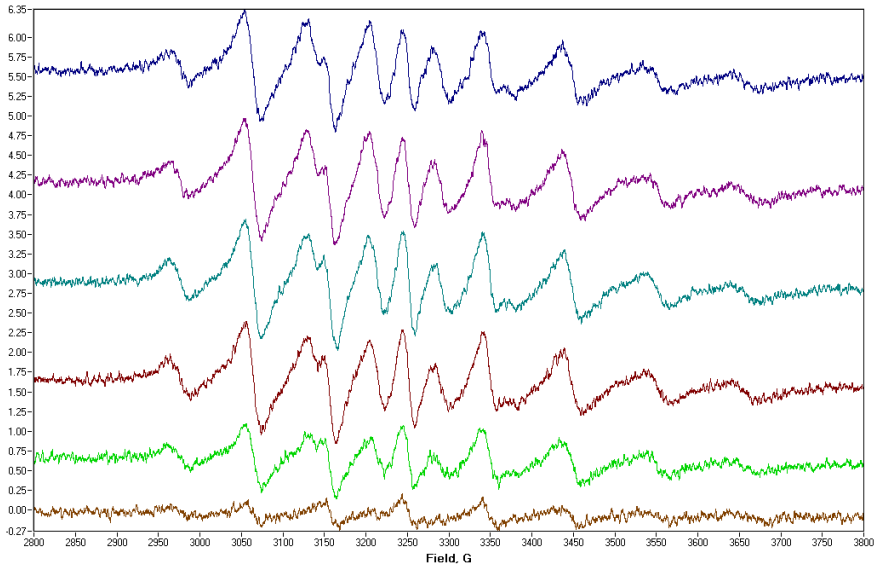

VO(salen)Cl – 10 % of vanadium(V) was reduced to vanadium(IV):

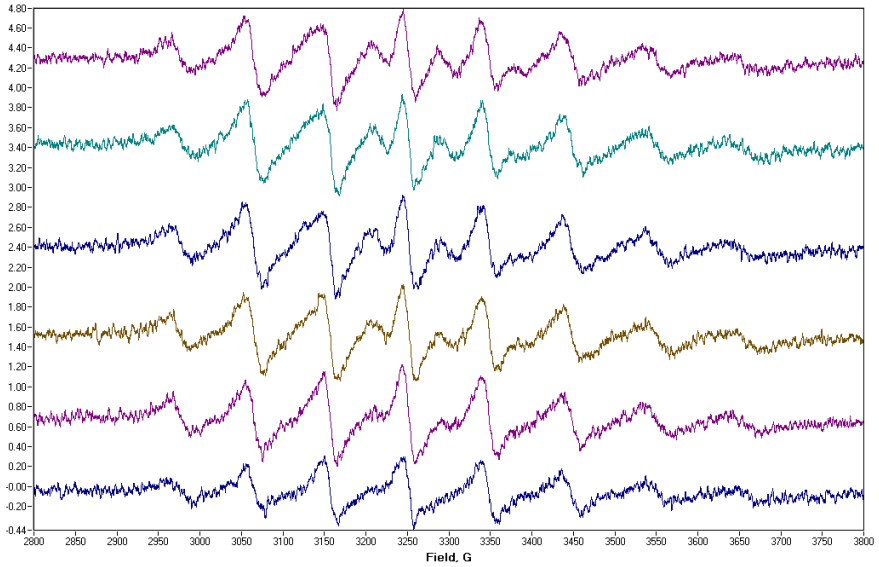

VO(salen)NCS – 40 % of vanadium(V) was reduced to vanadium(IV):

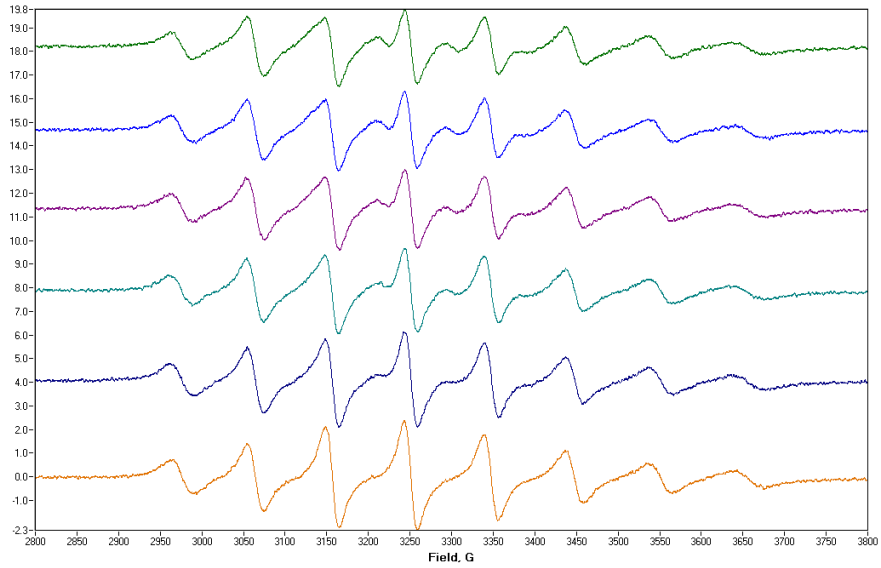

1.3- *Testing benzaldehyde as the reducing agent.*

The aldehyde was thought to be the reducing agent. Therefore, a control experiment was conducted in which EPR spectra of a solution of vanadium(V) complex in dichloromethane were recorded before and after the addition of benzaldehyde (bottom and top respectively).

VO(salen)EtOSO$_3$

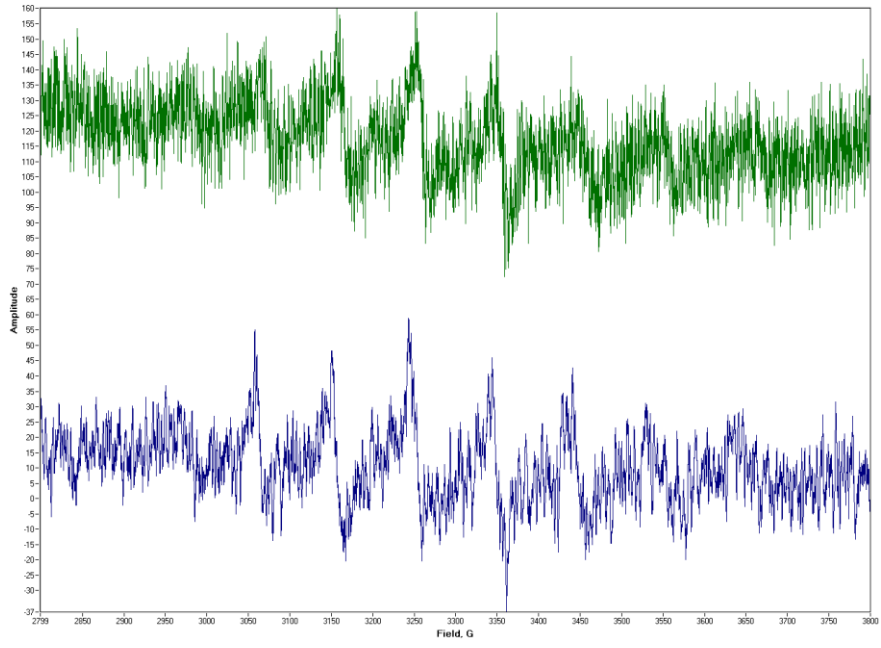

VO(salen)Cl

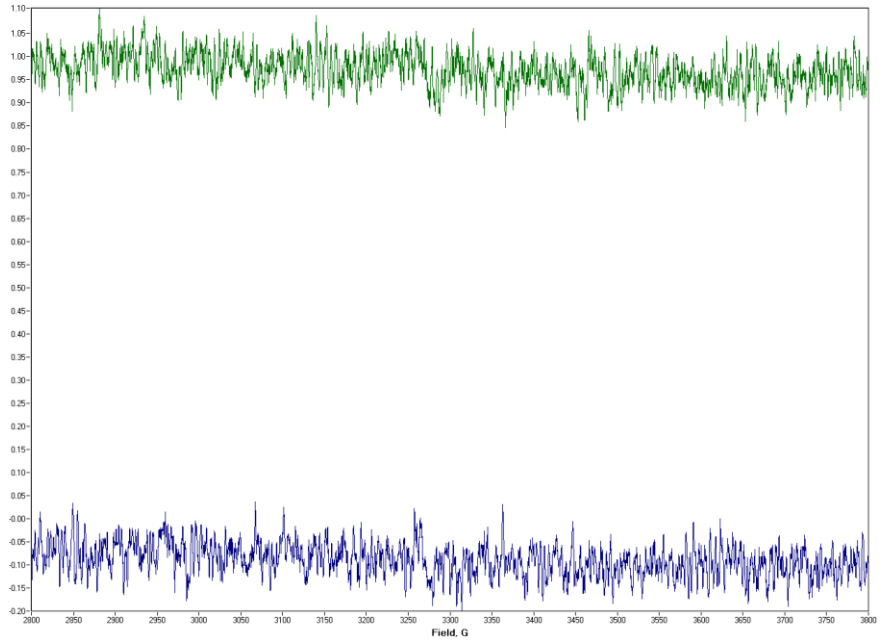

VO(salen)NCS

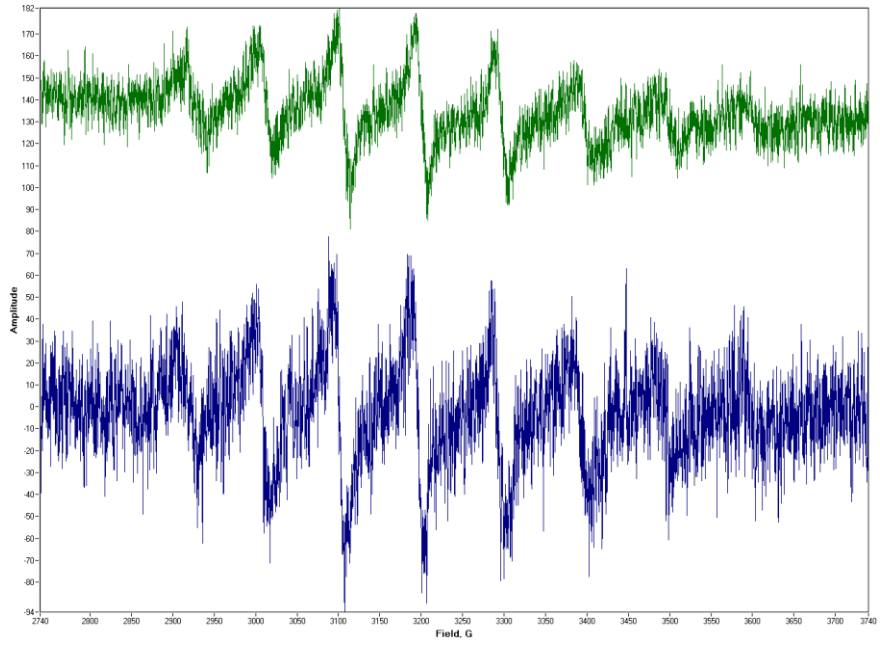

1.4- *Testing trimethylsilyl cyanide as the reducing agent.*

Below are reported the spectra evolution versus time (from bottom to top) of the addition of TMSCN to a solution of vanadium complex in dichloromethane. Each spectrum is recorded every 3.5 minutes, starting from minute 3.5 (time that the EPR spectrometer takes to record a spectrum).

VO(salen)EtOSO$_3$ – after 30 minutes, 5% of vanadium V(V) was reduced to V(IV):

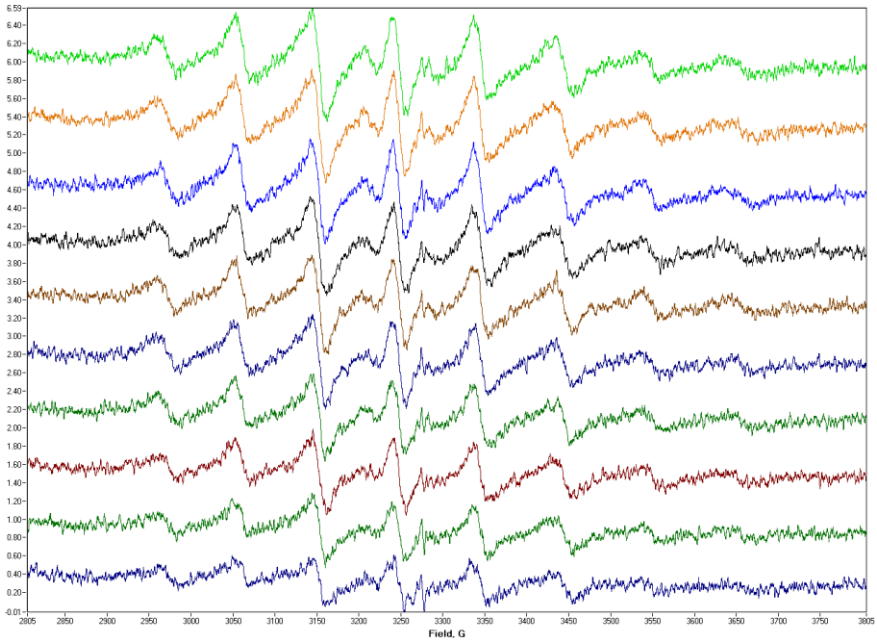

VO(salen)Cl – after 60 minutes, 20% of vanadium V(V) was reduced to V(IV):

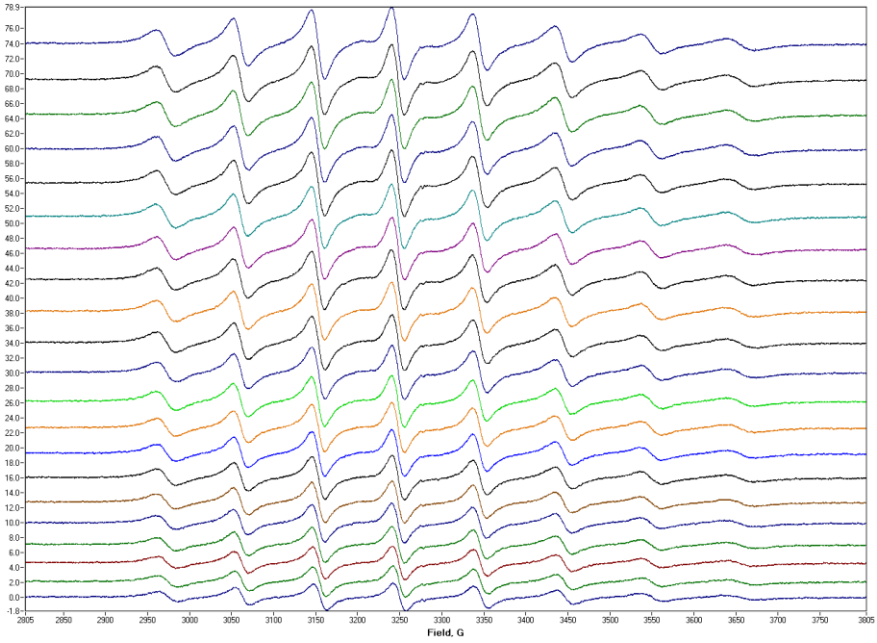

VO(salen)NCS – after 60 minutes, 40% of vanadium V(V) was reduced to V(IV):

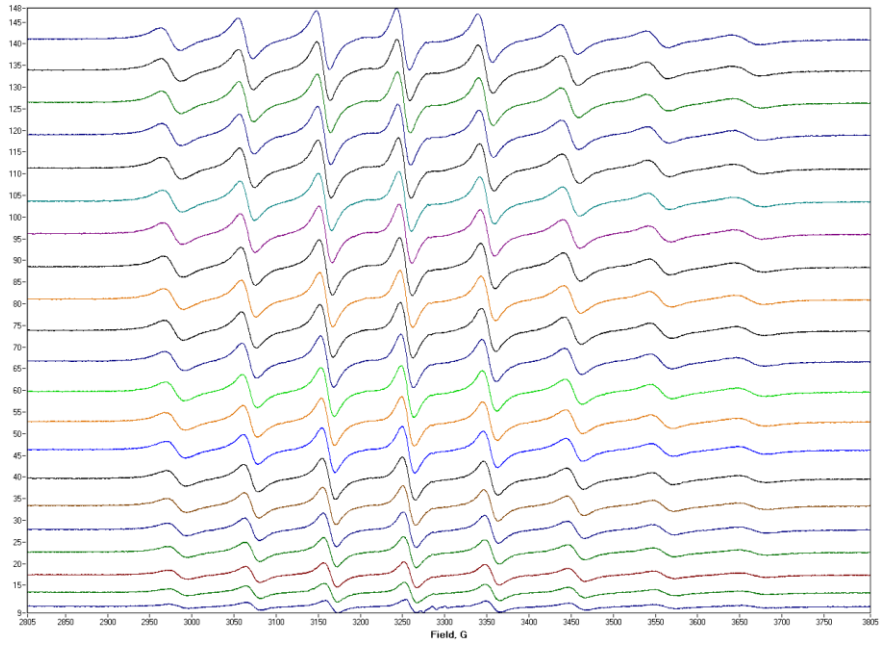

1.5- *Potassium cyanide addition to a solution of VO(salen)NCS.*

Below are shown the spectra of a solution of VO(salen) complex (blue line) and a mixture of KCN/^{t}BuOH(1:1) and VO(salen)NCS in dichloromethane (green line). 16 % of V(IV) was detected in the VO(salen)NCS spectrum after 3.5 minutes of reaction.

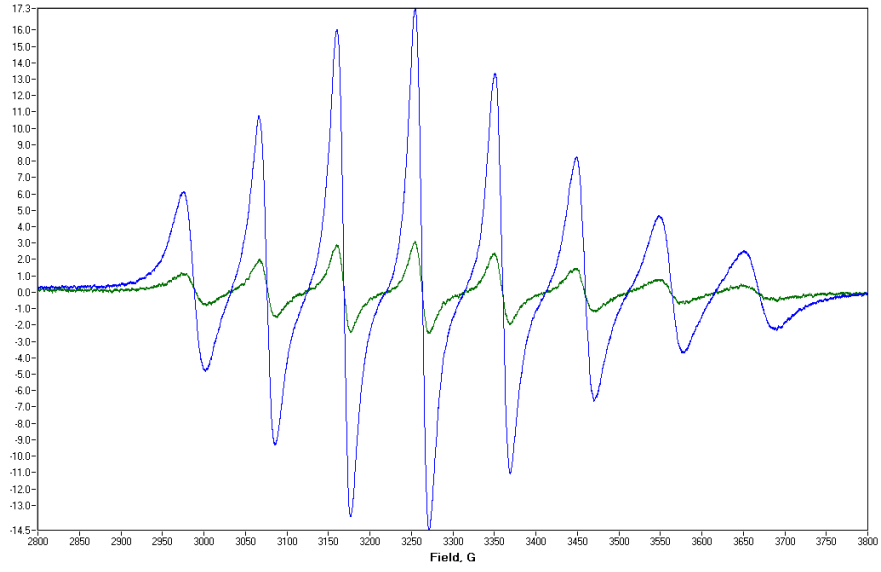

1.6- *Cyanogen detection by GCMS.*

Chromatographic evidence for cyanogen detection (13.54 minutes): (A) $(CN)_2$ formed by mixing $CuSO_4$ and KCN in water; (B) $(CN)_2$ formed in the reaction of VO(salen)NCS and TMSCN by direct injection; and (C) $(CN)_2$ formed in the reaction of VO(salen)NCS and TMSCN and carried by N_2 gas into a cold trap. The peak at 17.41

minutes is a spike due to the DCM solvent which occurs as a large peak at 20 minutes. The peaks at 28 minutes and beyond are trimethylsilyl derivatives.

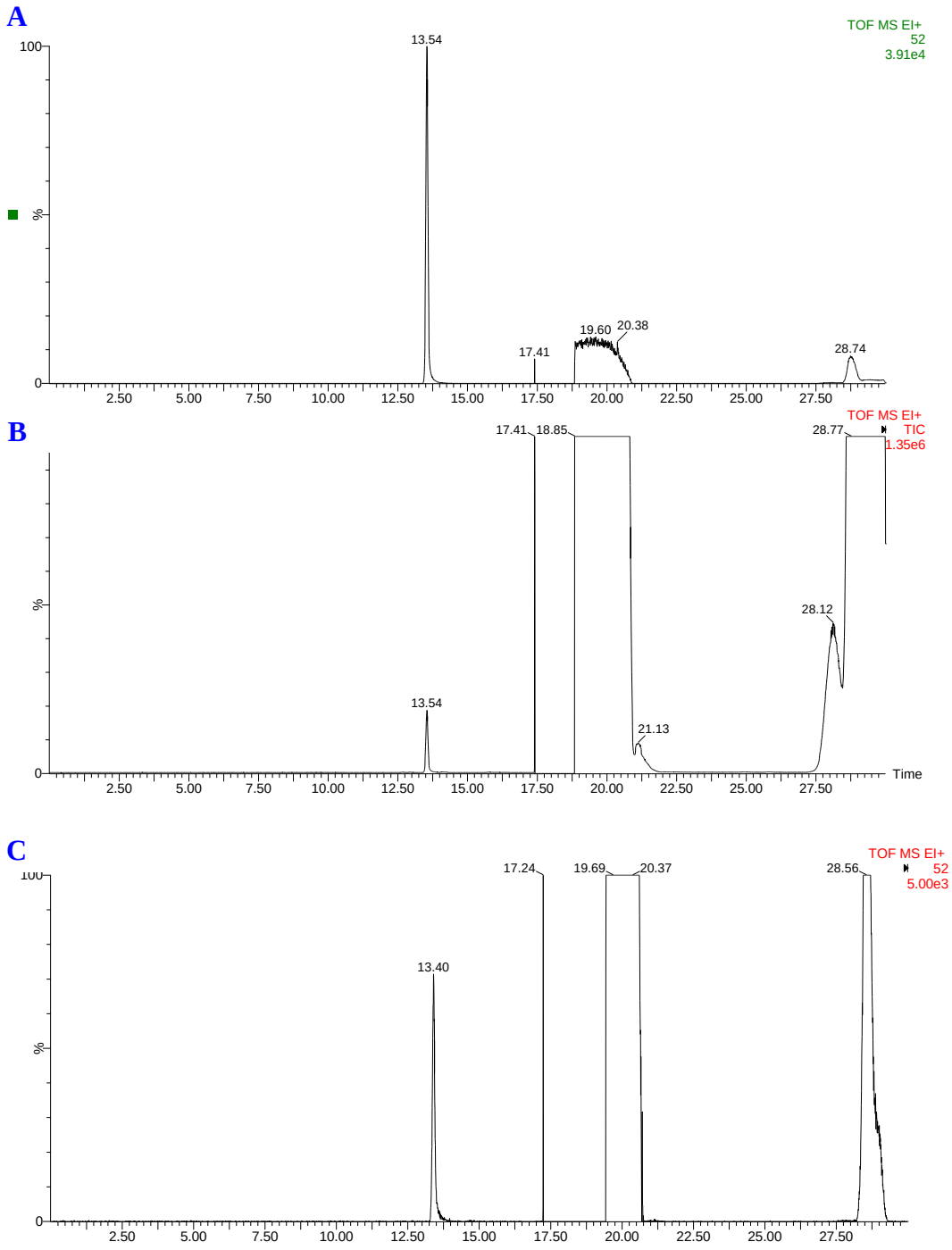

Mass spectrum of $(CN)_2$ peak at 13.54 minutes from $CuSO_4$/KCN reaction:

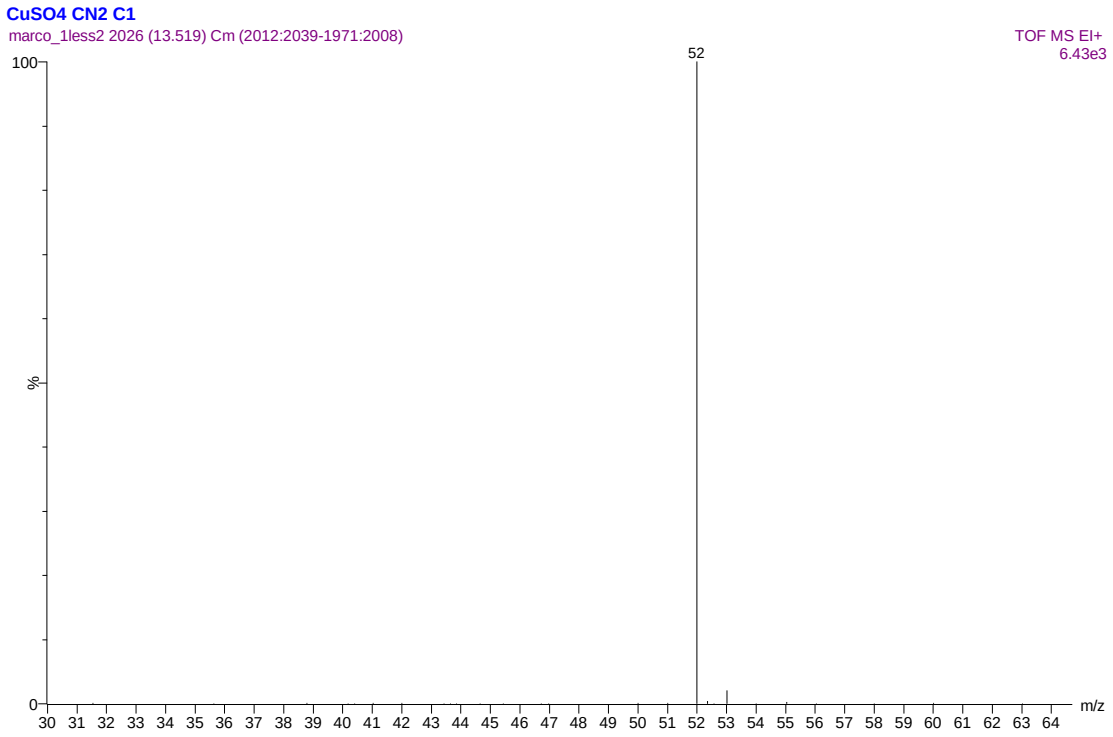

1.7- *Spin trapping experiments.*

The following charts show the spin adduct spectra of (a) PBN-CN and (b) DMPO-CN obtained by mixing a vanadium(V)(salen) complex and TMSCN in the presence of the corresponding spin trap. (c) Corresponds to the oxidized form of DMPO (DMPOx) which was detected when a vanadium(V)(salen) complex was mixed with the spin trap in absence of TMSCN.

VO(salen)EtOSO$_3$ – the signal intensity was increasing vs. time. Slow radical formation.

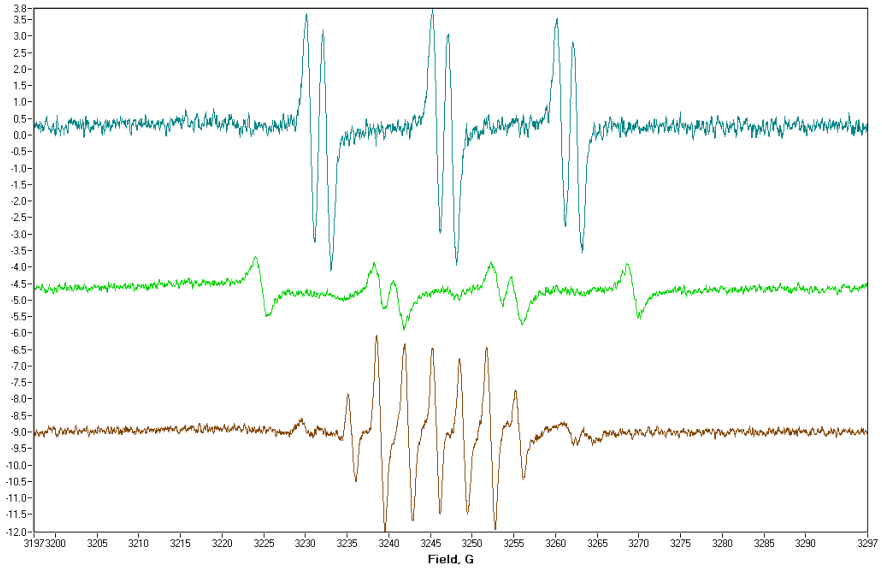

(a)

(b)

(c)

VO(salen)Cl – The signal intensity was decreasing vs. time. Fast radical generation.

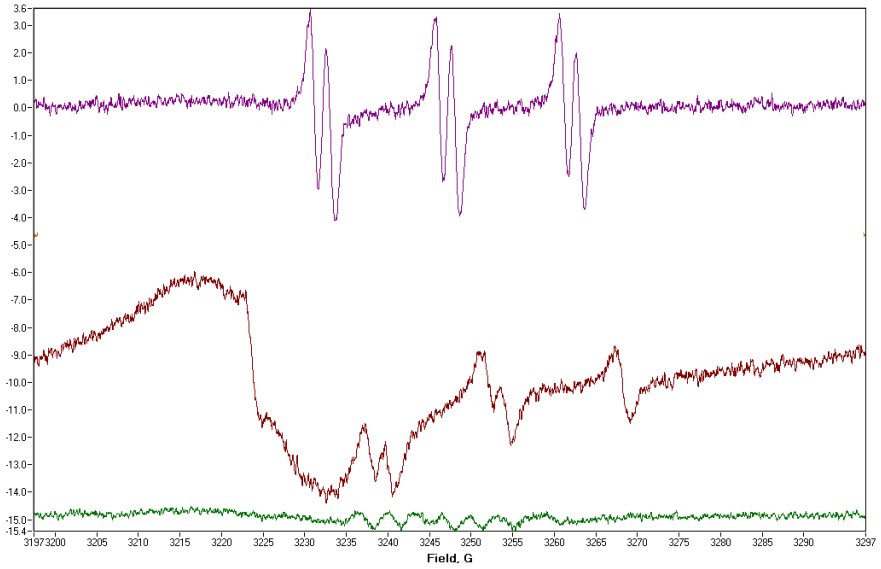

VO(salen)NCS – The signal intensity was initially very weak and disappeared after the third measurement (after 10 minutes) The spin adduct lifetime was very short.

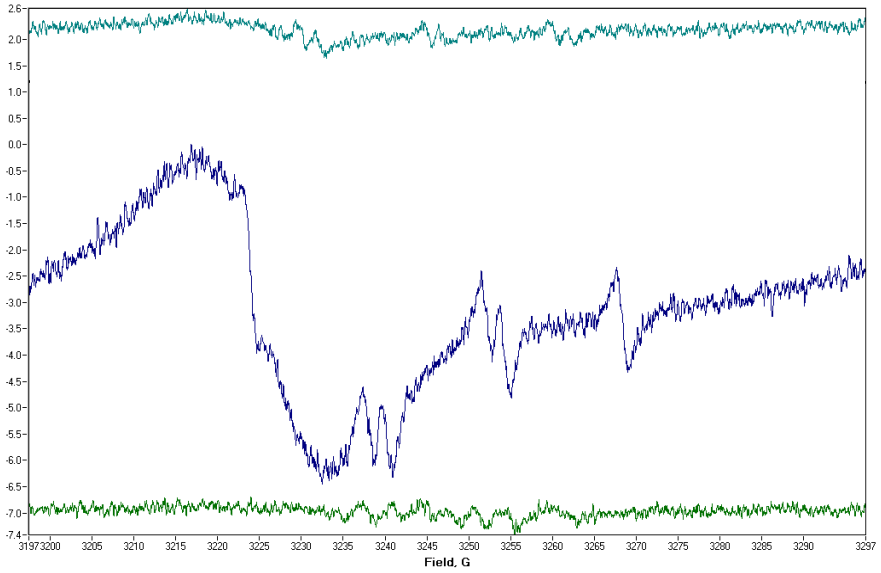

1.8- *TEMPO experiments.*

The spectra below show the TEMPO EPR signal intensity decay when TEMPO was added to a mixture of VO(salen)NCS and TMSCN.

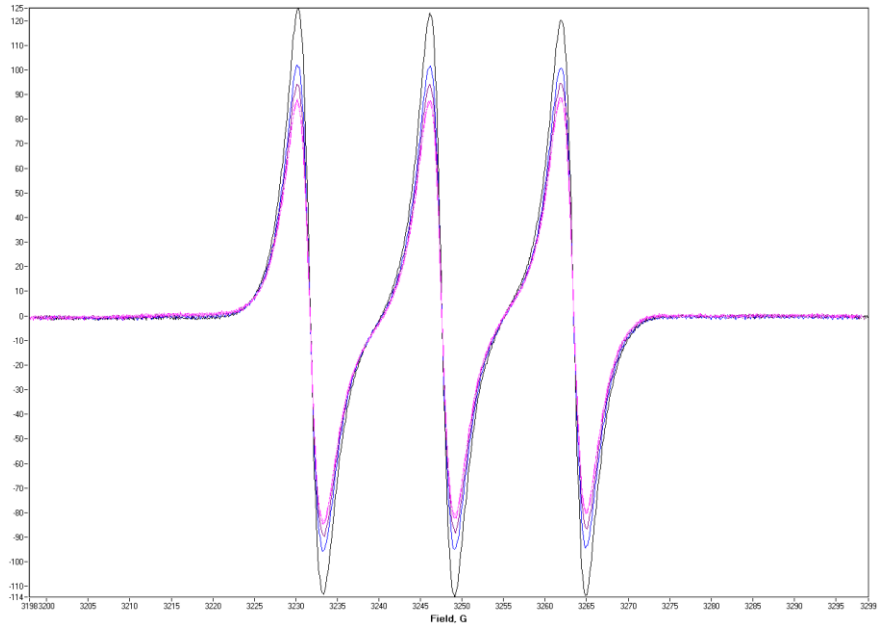

The plot below shows the electron impact GCMS chromatogram of a mixture of TEMPO, TMSCN and VO(salen)NCS in dichloromethane, in which none of the peaks could be assigned to TEMPO-CN adduct (m/z) 182. According to the MS, the peaks at 2.2, 3.54, 6.69, and 9.70 minutes could be associated to a trimethylsilyl derivative, $(CH_3)_3$-Si-NCS, unreacted TEMPO, and TEMPO derivative with molecular weight larger than TEMPO-CN (m/z 239 and 254) respectively.

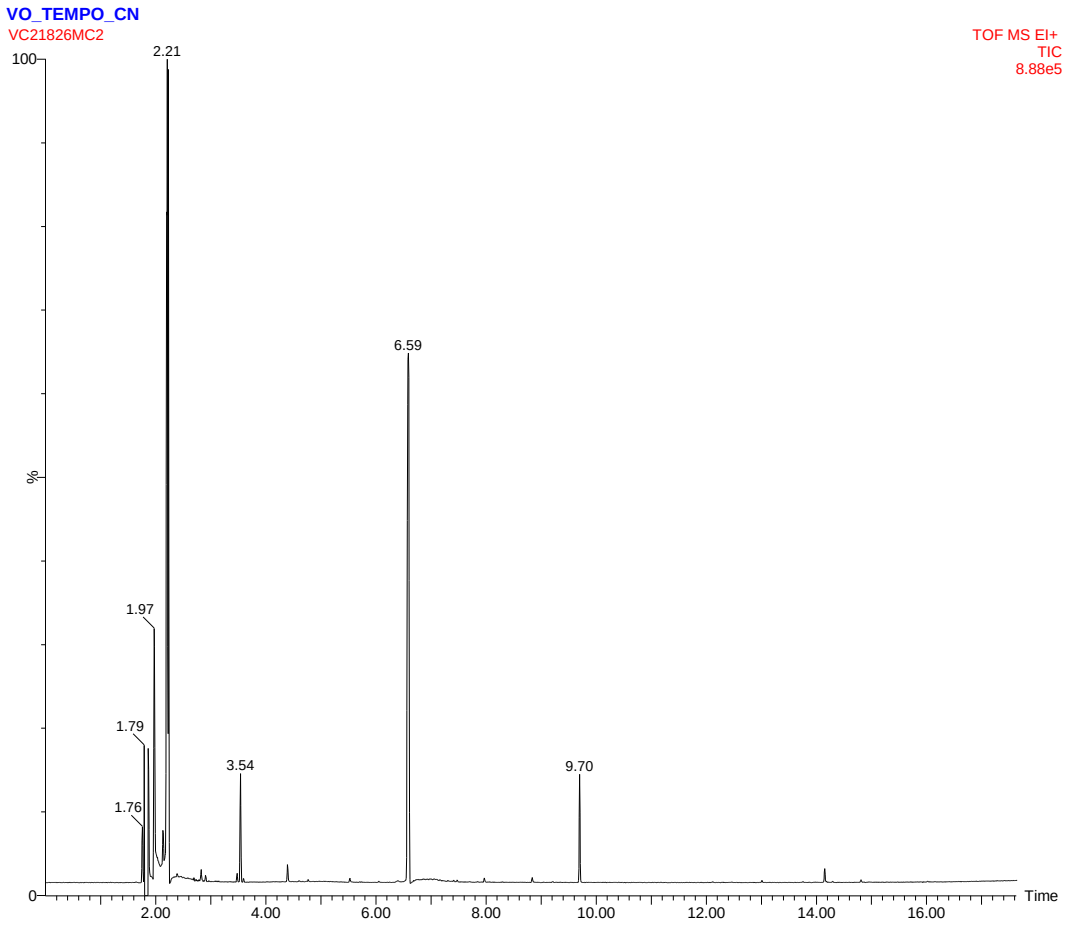

1.9- *Detection of trimethylsilyl derivatives from the reaction between VO(salen)X and trimethylsilyl cyanide.*

Chromatogram of TMS-SCN from the reaction between VO(salen)NCS and TMSCN. The detector was switched off for the first 3.5 minutes to avoid seeing the solvent signal.

TMS-SCN detection:

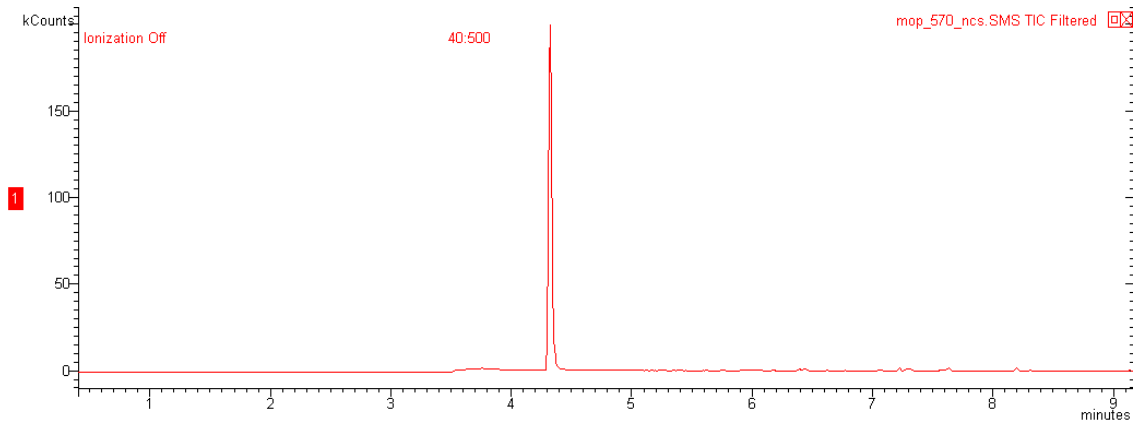

Mass spectrum of the TMS-SCN, peak at 4.33 minutes during the reaction between VO(salen)NCS and TMSCN (m/z 131).

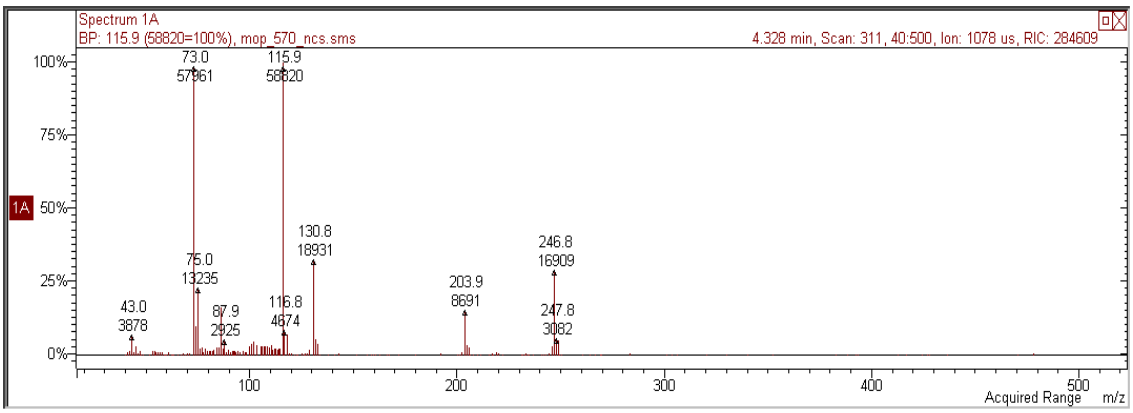

APPENDIX 2

2.1. Counterion effect using tetrabutylammonium thiocyanate.

The kinetics are presented according to the amount of tetrabutylammonium thiocyanate in mol %, while the concentration of VO(salen)NCS **23h** is kept constant at 0.2 mol%.

Bu$_4$N-SCN (0 mol%)

R^2 = 0.9918

Order 2

k = 0.0035 M s^{-1}

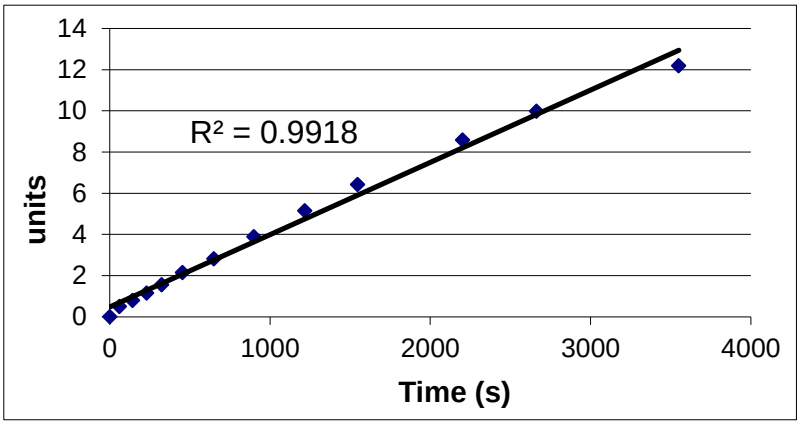

Bu$_4$N-SCN (0.1 mol%)

R^2 = 0.9994

Order 2

k = 0.0078 M s^{-1}

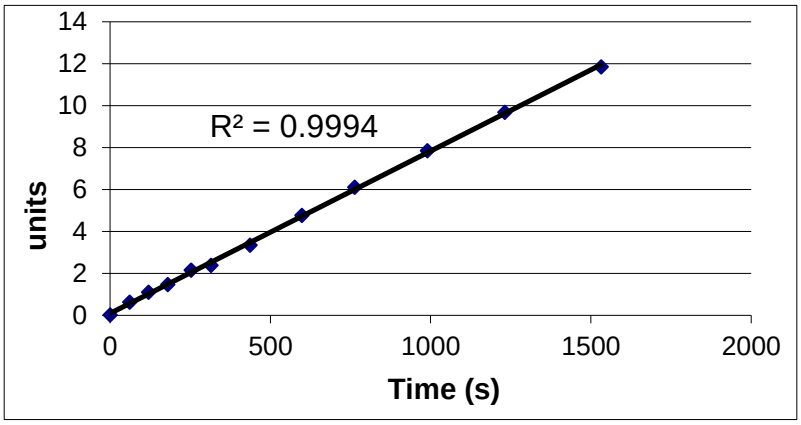

Bu$_4$N-SCN (0.2 mol%)

R^2 = 0.9890

Order 2

k = 0.0095 M s^{-1}

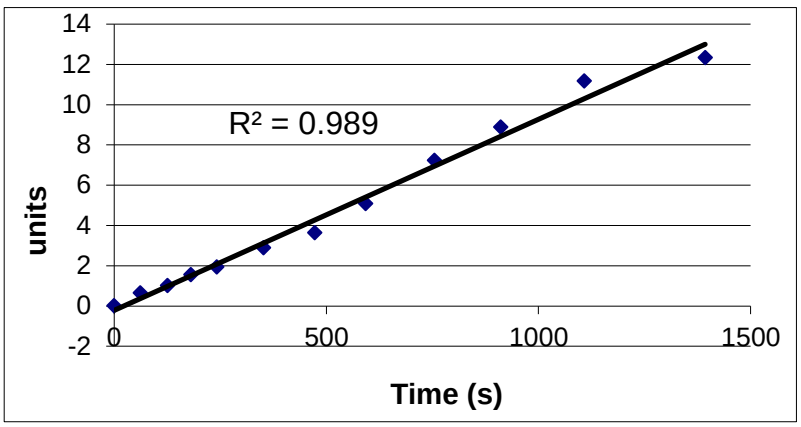

Bu$_4$N-SCN (0.5 mol%)

R^2 = 0.9948

Order 2

k = 0.0093 M s^{-1}

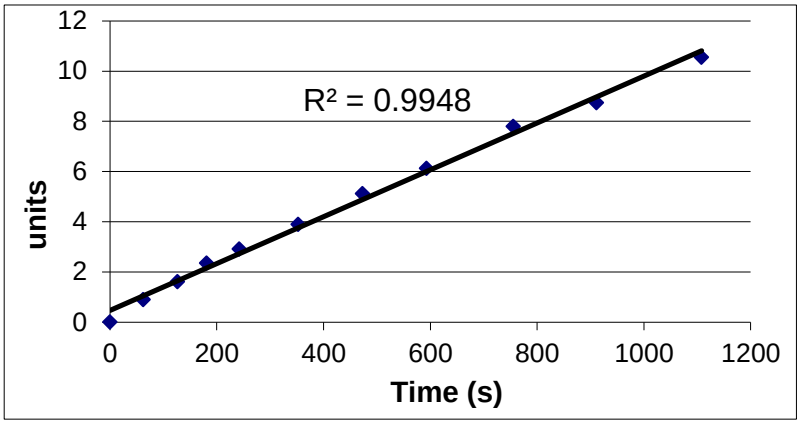

Bu$_4$N-SCN (1.0 mol%)

R^2 = 0.9974

Order 2

k = 0.0089 M s^{-1}

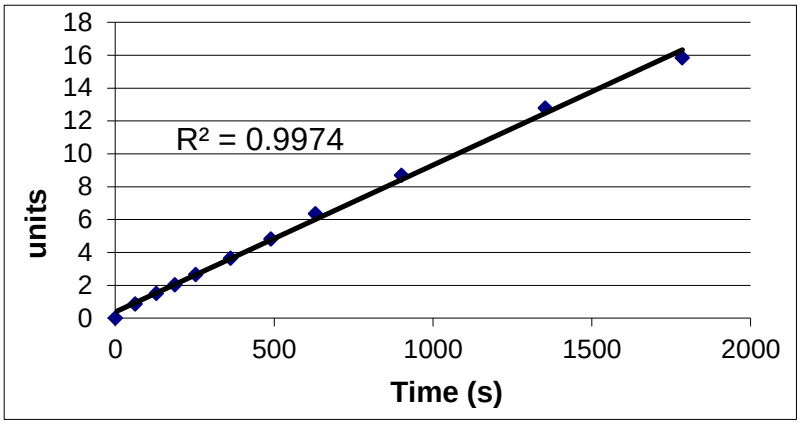

Bu$_4$N-SCN (2.0 mol%)

R^2 = 0.9627

Order 2

k = 0.0080 M s^{-1}

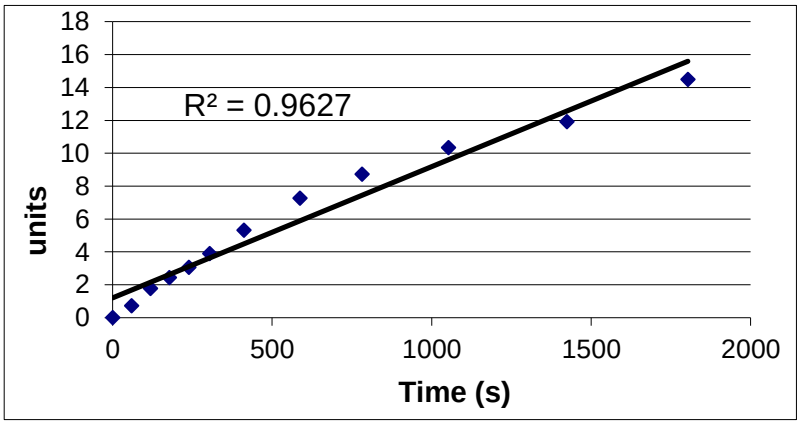

2.2. Kinetic experiments at different catalyst concentrations using tert-butylamonium isothiocyanate

All the kinetic experiments are conducted at 0°C using from $5x10^{-3}$ to $2x10^{-2}$ M of **Bu_4-SCN** catalyst in dichloromethane, at a substrate concentration of 0.49 and 0.56 M of benzaldehyde and TMSCN respectively.

Bu_4N-SCN ($5x10^{-3}$M)

$R^2 = 0.9991$

Order 2

$k = 0.0020$ M s^{-1}

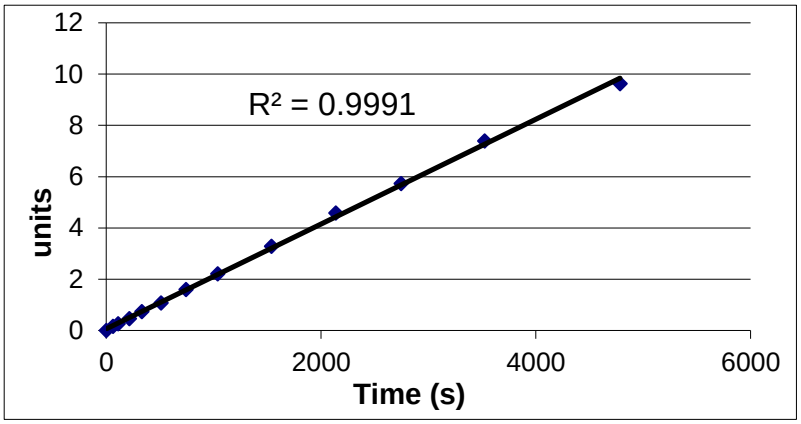

Bu_4N-SCN ($1x10^{-2}$M)

$R^2 = 0.9979$

Order 2

$k = 0.0039$ M s^{-1}

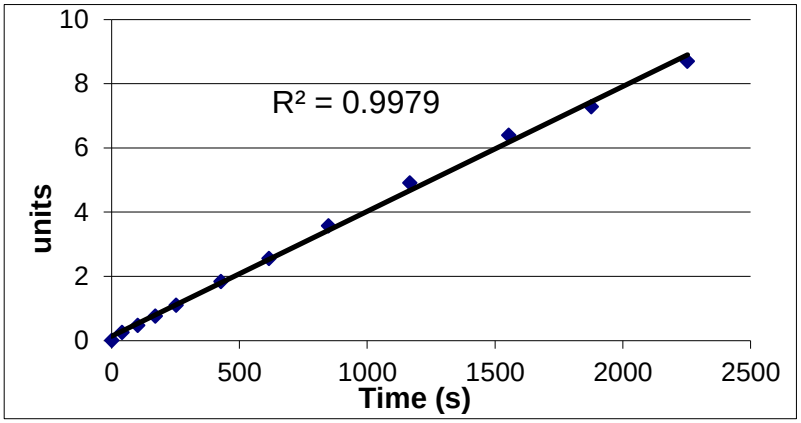

Bu_4N-SCN ($2x10^{-2}$M)

$R^2 = 0.9724$

Order 2

$k = 0.0076$ M s^{-1}

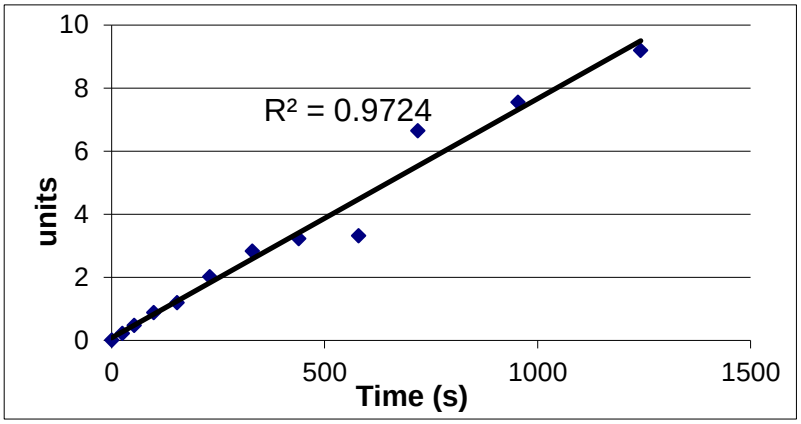

2.3. Kinetics for the Hammett plot

The kinetics are presented according to the catalyst and the aldehyde

1 **- [Ti(salen)O]$_2$**

PhCHO

R^2 = 0.9834

Order 1

k = 0.0075 s^{-1}

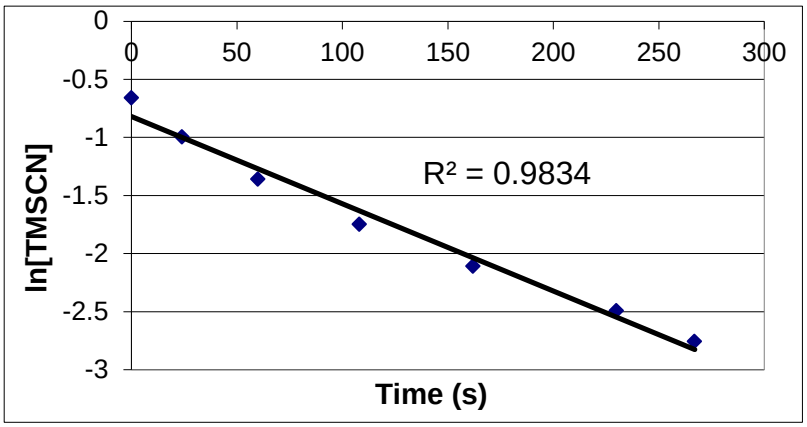

2 **- [Ti(salen)O]$_2$**

PhCHO

R^2 = 0.9897

Order 1

k = 0.0066 s^{-1}

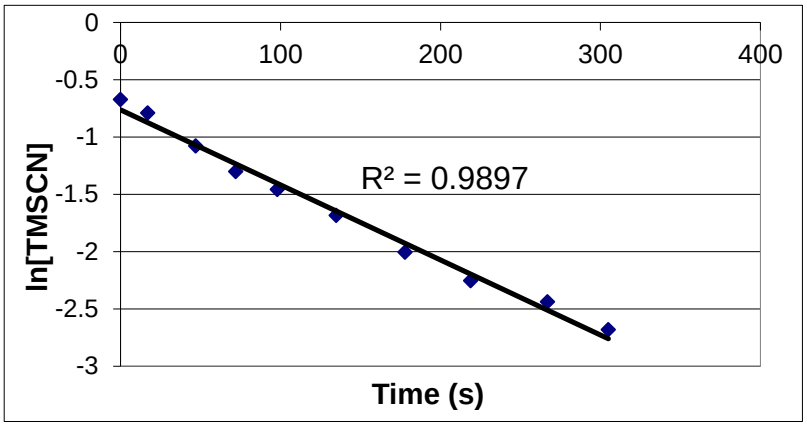

1 **- [Ti(salen)O]$_2$**

m-ClC$_6$H$_4$CHO

R^2 = 0.9789

Order 1

k = 0.0422 s^{-1}

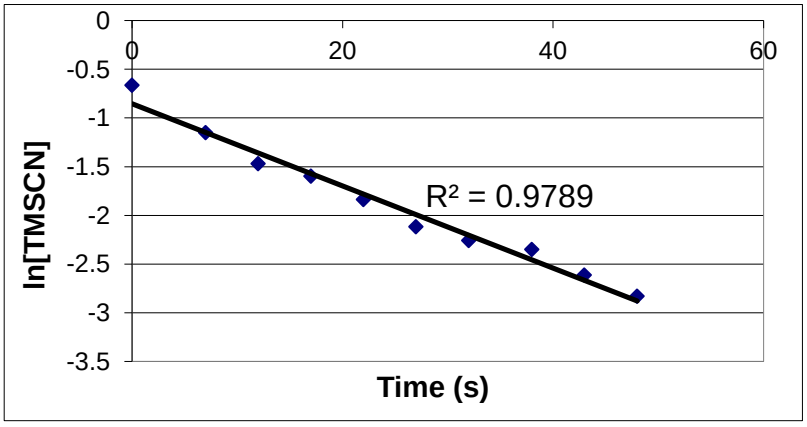

***2* - [Ti(salen)O]$_2$**

m-ClC$_6$H$_4$CHO

R^2 = 0.9627

Order 1

k = 0.0432 s^{-1}

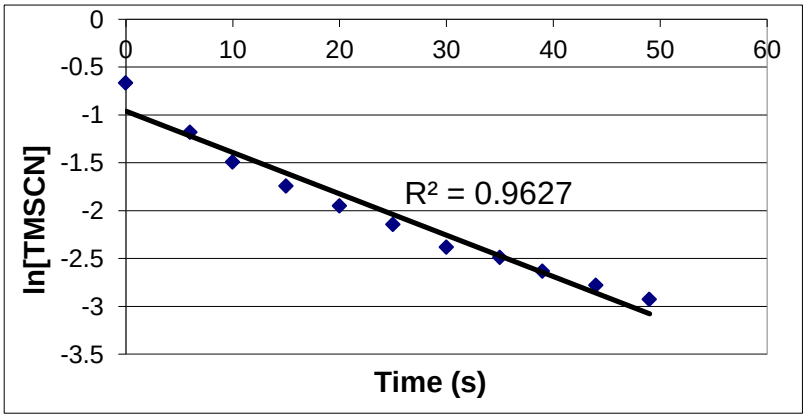

***1* - [Ti(salen)O]$_2$**

m-FC$_6$H$_4$CHO

R^2 = 0.9610

Order 1

k = 0.0371 s^{-1}

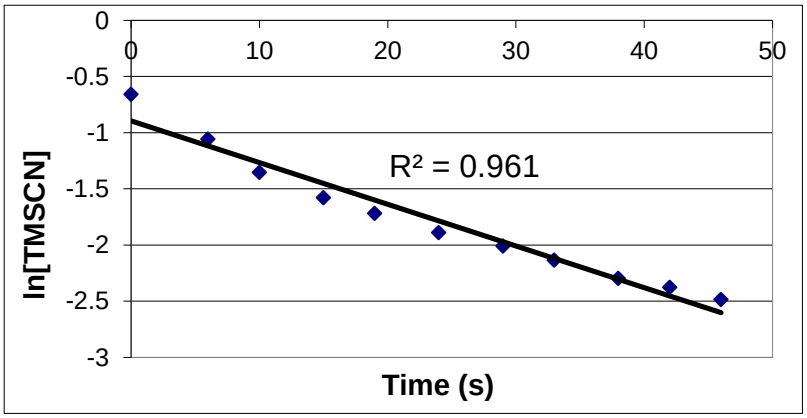

***2* - [Ti(salen)O]$_2$**

m-FC$_6$H$_4$CHO

R^2 = 0.9737

Order 1

k = 0.0375 s^{-1}

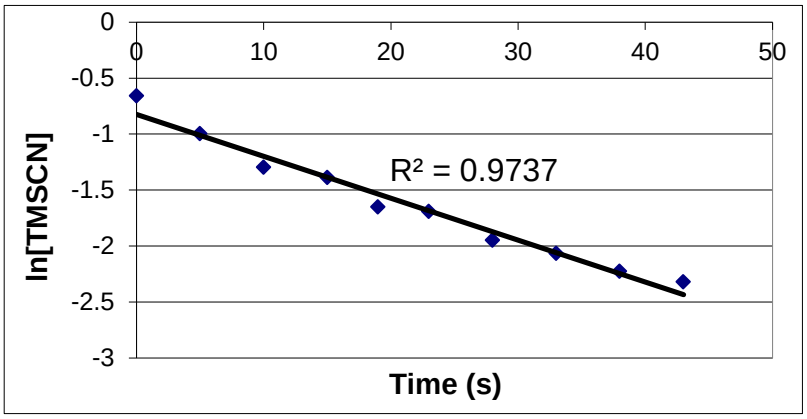

***1* - [Ti(salen)O]$_2$**

p-ClC$_6$H$_4$CHO

R^2 = 0.9559

Order 1

k = 0.0311 s^{-1}

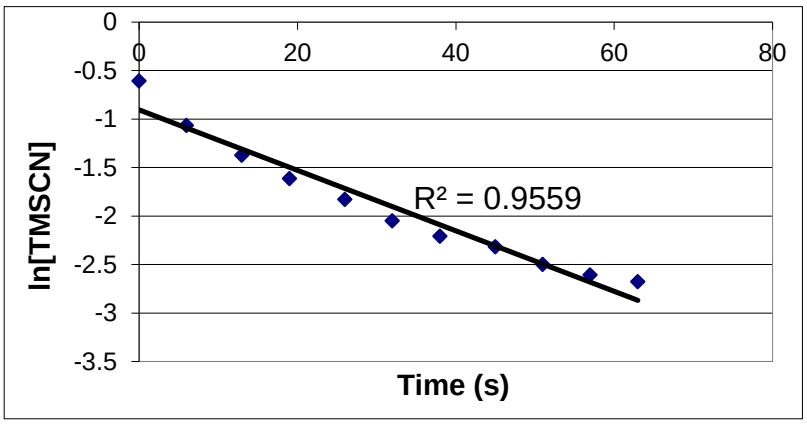

***2* - [Ti(salen)O]$_2$**

p-ClC$_6$H$_4$CHO

R^2 = 0.9604

Order 1

k = 0.0319 s^{-1}

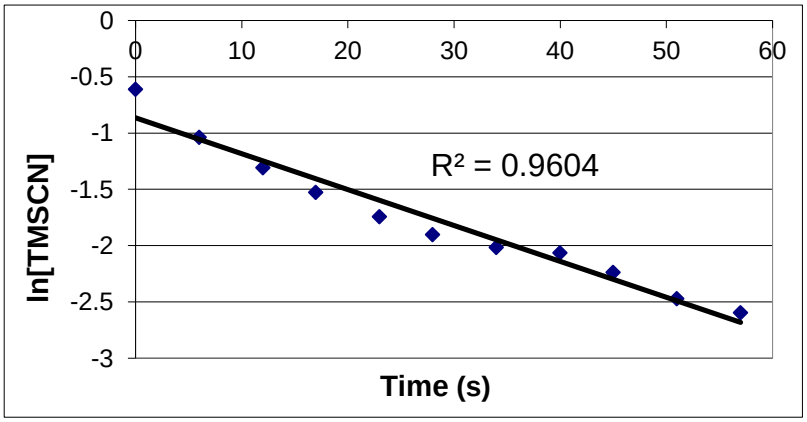

***1* - [Ti(salen)O]$_2$**

p-FC$_6$H$_4$CHO

R^2 = 0.9554

Order 1

k = 0.0086 s^{-1}

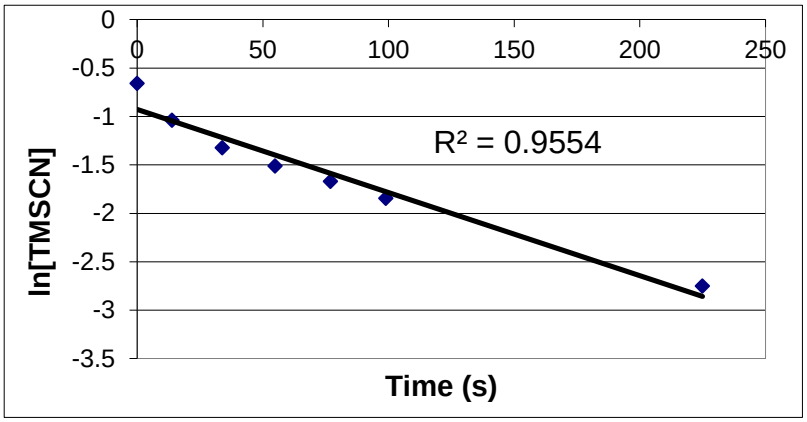

***2* - [Ti(salen)O]$_2$**

p-FC$_6$H$_4$CHO

R^2 = 0.9748

Order 1

k = 0.0101 s^{-1}

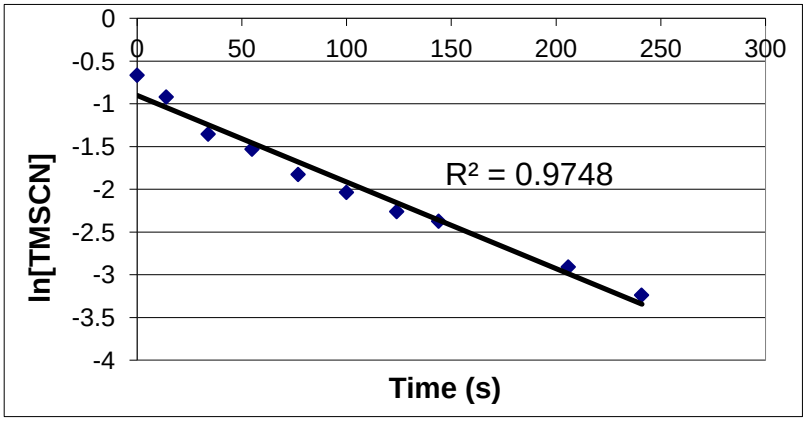

***1* - [Ti(salen)O]$_2$**

p-CH$_3$C$_6$H$_4$CHO

R^2 = 0.9891

Order 1

k = 0.0025 s^{-1}

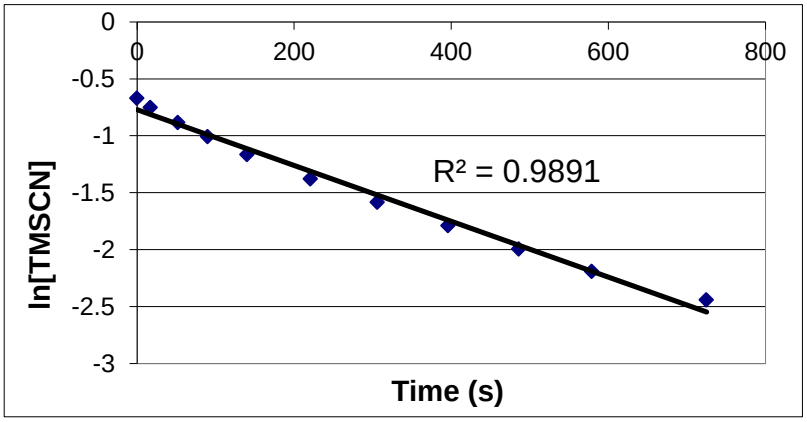

***2* - [Ti(salen)O]$_2$**

p-$CH_3C_6H_4CHO$

R^2 = 0.9900

Order 1

k = 0.0020 s^{-1}

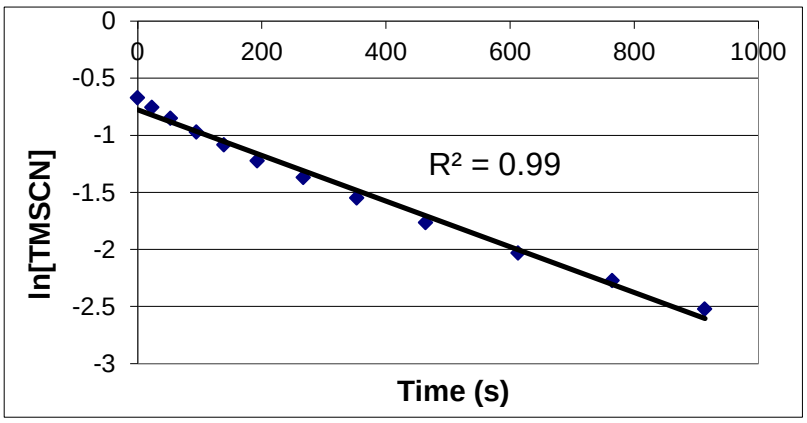

***1* - [Ti(salen)O]$_2$**

m-$CH_3C_6H_4CHO$

R^2 = 0.9976

Order 1

k = 0.0072 s^{-1}

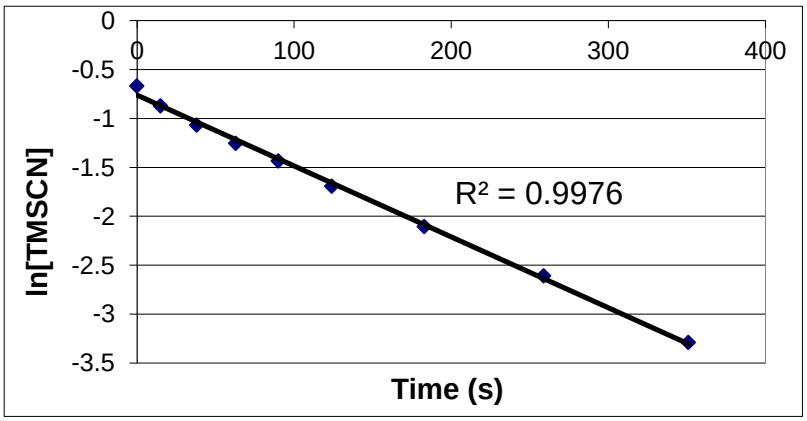

***2* - [Ti(salen)O]$_2$**

m-$CH_3C_6H_4CHO$

R^2 = 0.9858

Order 1

k = 0.0062 s^{-1}

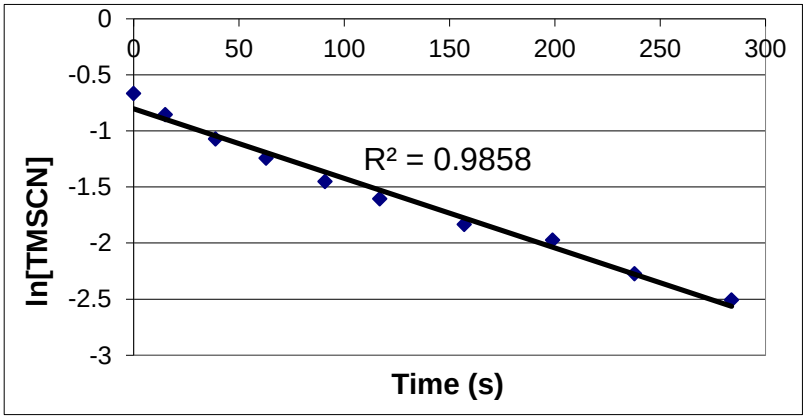

***1* - [Ti(salen)O]$_2$**

3,4-$CH_3C_6H_3CHO$

R^2 = 0.9864

Order 1

k = 0.0033 s^{-1}

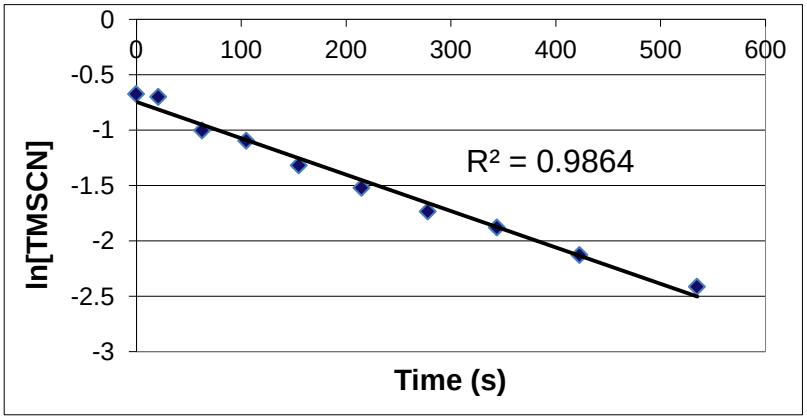

***2* - [Ti(salen)O]$_2$**

3,4-$CH_3C_6H_3CHO$

R^2 = 0.9871

Order 1

k = 0.0033 s^{-1}

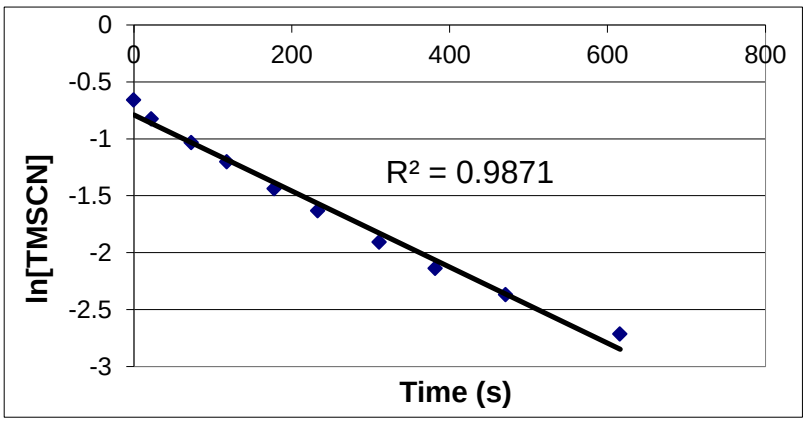

***1* - [Ti(salen)O]$_2$**

p-$CH_3OC_6H_4CHO$

R^2 = 0.9790

Order 1

k = 0.0012 s^{-1}

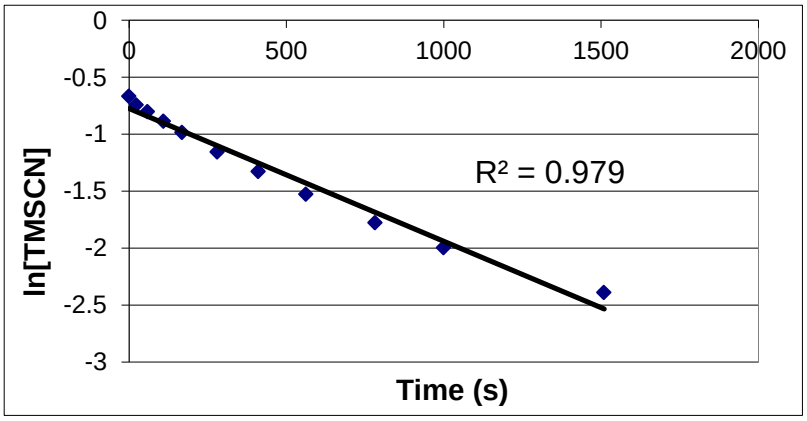

***2* - [Ti(salen)O]$_2$**

p-$CH_3OC_6H_4CHO$

R^2 = 0.9771

Order 1

k = 0.0011 s^{-1}

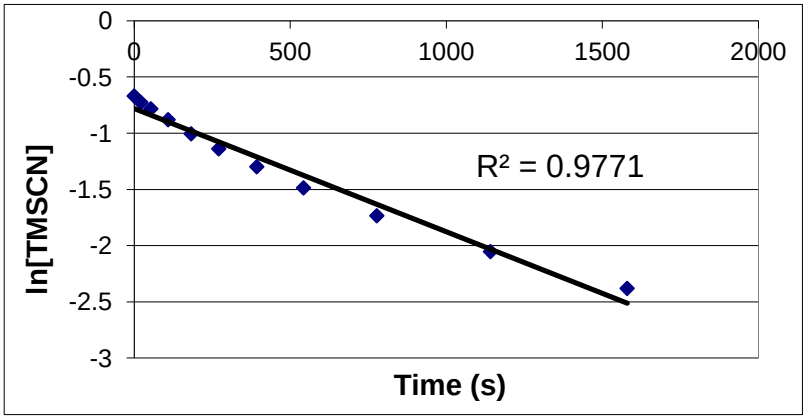

***1* - [Ti(salen)O]$_2$**

p-$CH_3SC_6H_4CHO$

R^2 = 0.9782

Order 1

k = 0.0040 s^{-1}

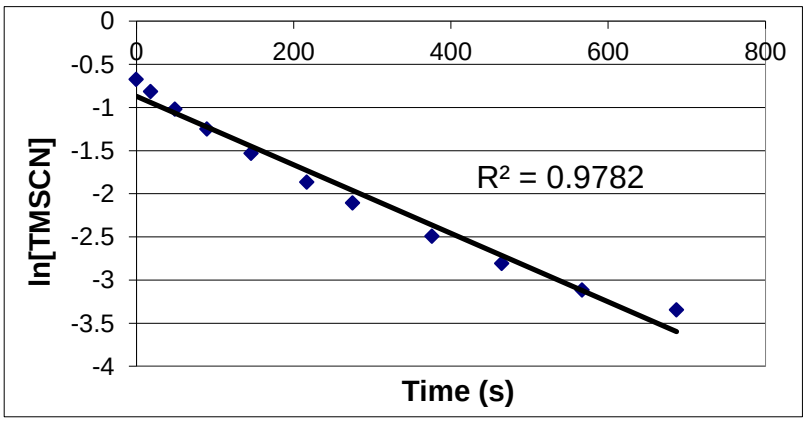

***2* - [Ti(salen)O]$_2$**

p-$CH_3SC_6H_4CHO$

R^2 = 0.9820

Order 1

k = 0.0047 s^{-1}

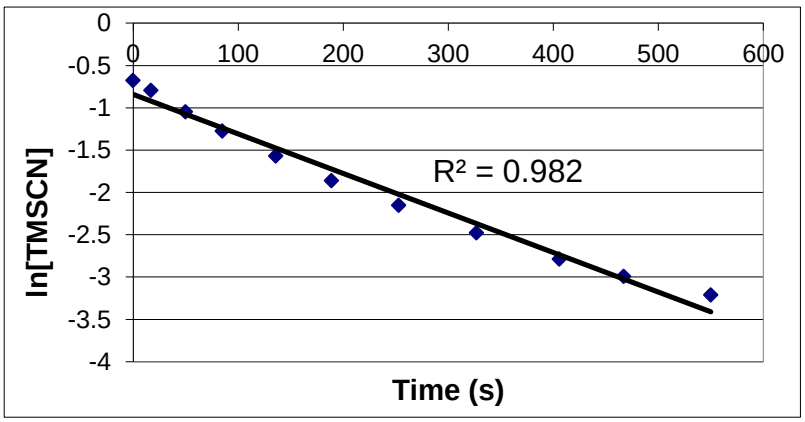

***1* – VO(salen)NCS**

PhCHO

R^2 = 0.9961

Order 2

k = 0.0041 $M^{-1}.s^{-1}$

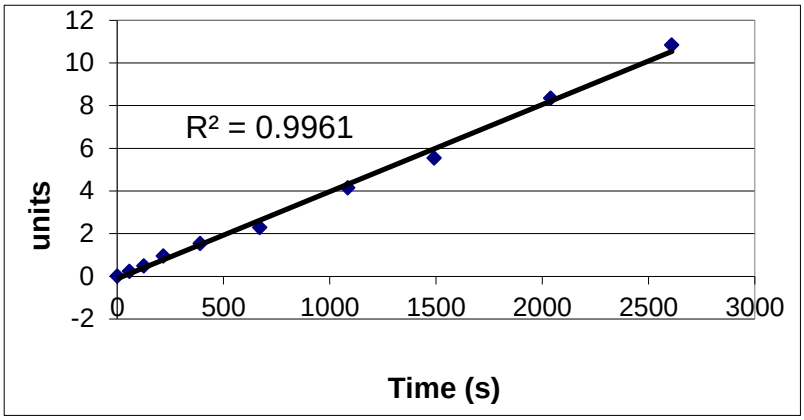

***2* – VO(salen)NCS**

PhCHO

R^2 = 0.9964

Order 2

k = 0.0034 $M^{-1}.s^{-1}$

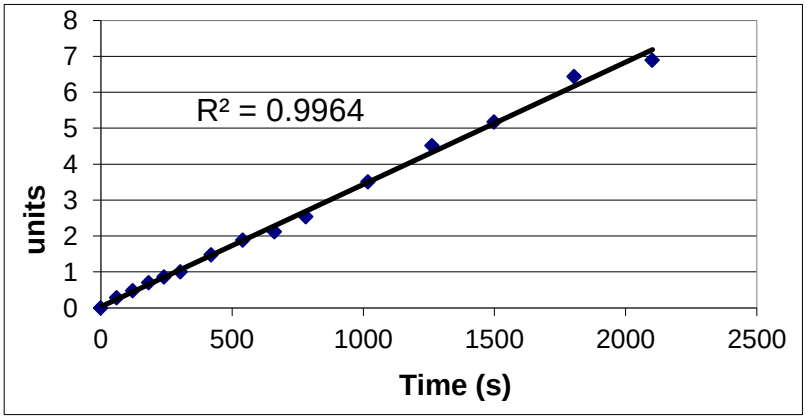

***1* – VO(salen)NCS**

3,5-FC_6H_3CHO

R^2 = 0.9929

Order 2

k = 0.0318 $M^{-1}.s^{-1}$

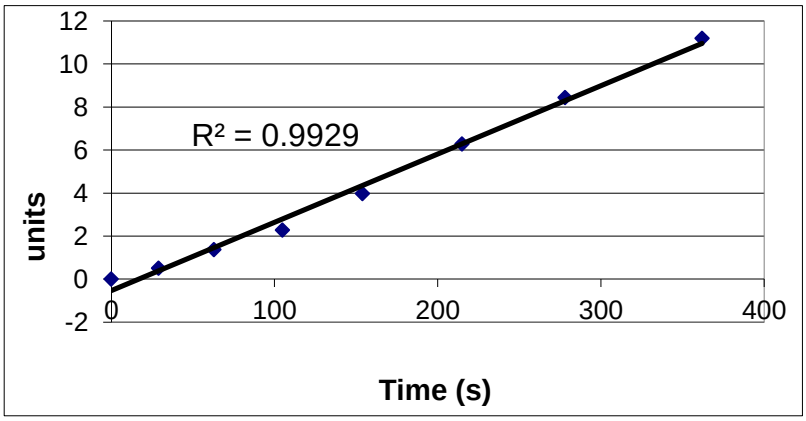

***2* – VO(salen)NCS**

3,5-FC_6H_3CHO

R^2 = 0.9933

Order 2

k = 0.0338 $M^{-1}.s^{-1}$

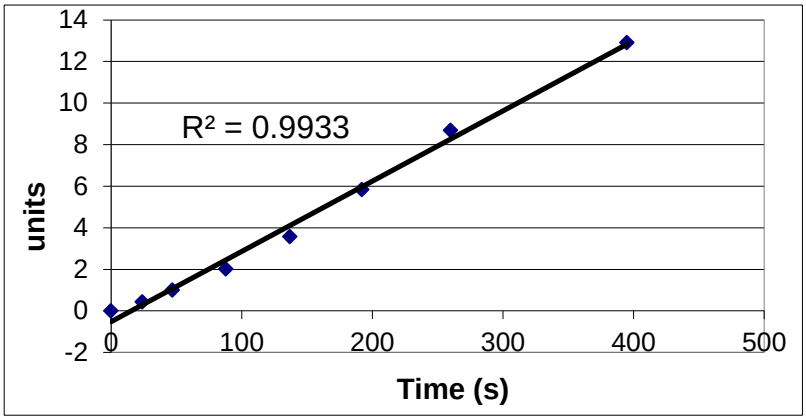

***1* – VO(salen)NCS**

3,4-ClC_6H_3CHO

R^2 = 0.9933

Order 2

k = 0.0091 $M^{-1}.s^{-1}$

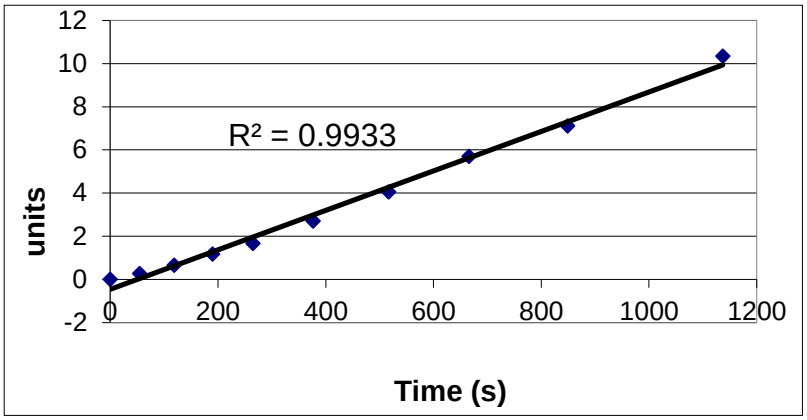

***2* – VO(salen)NCS**

3,4-ClC_6H_3CHO

R^2 = 0.9902

Order 2

k = 0.0113 $M^{-1}.s^{-1}$

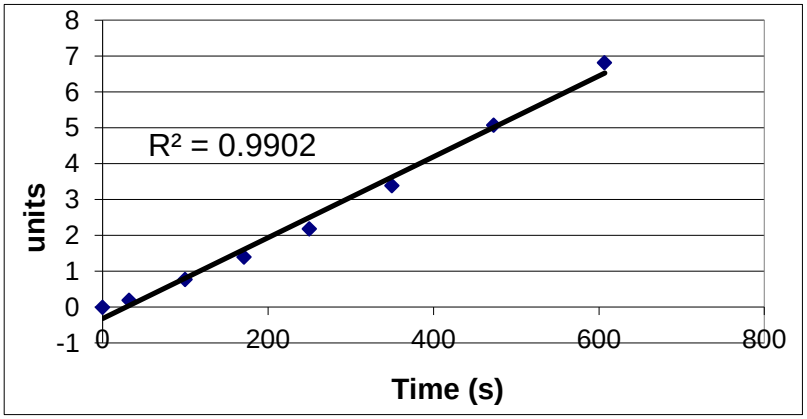

***1* – VO(salen)NCS**

4-$CF_3C_6H_4CHO$

R^2 = 0.9919

Order 2

k = 0.0105 $M^{-1}.s^{-1}$

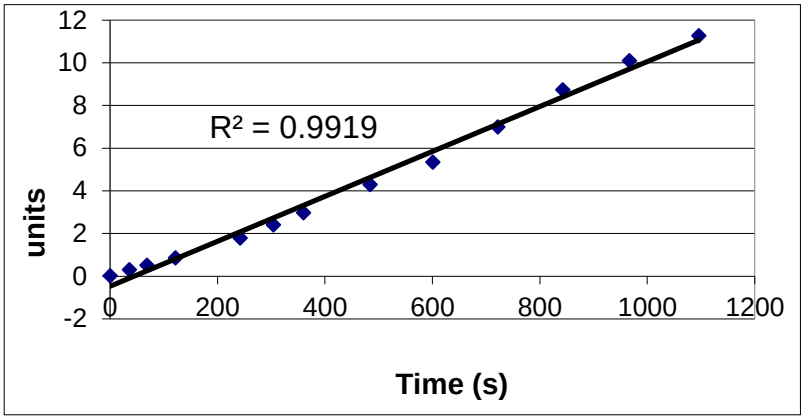

***2* – VO(salen)NCS**

4-$CF_3C_6H_4CHO$

R^2 = 0.9870

Order 2

k = 0.0095 $M^{-1}.s^{-1}$

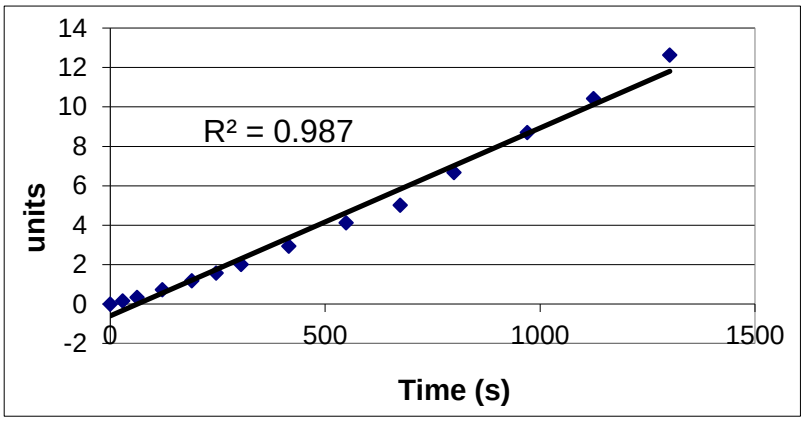

***1* – VO(salen)NCS**

3-ClC_6H_4CHO

R^2 = 0.9918

Order 2

k = 0.0083 $M^{-1}.s^{-1}$

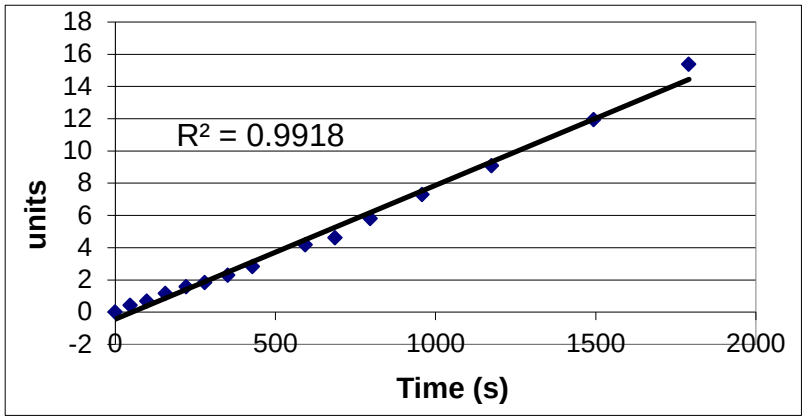

***2* – VO(salen)NCS**

3-ClC_6H_4CHO

R^2 = 0.9979

Order 2

k = 0.0081 $M^{-1}.s^{-1}$

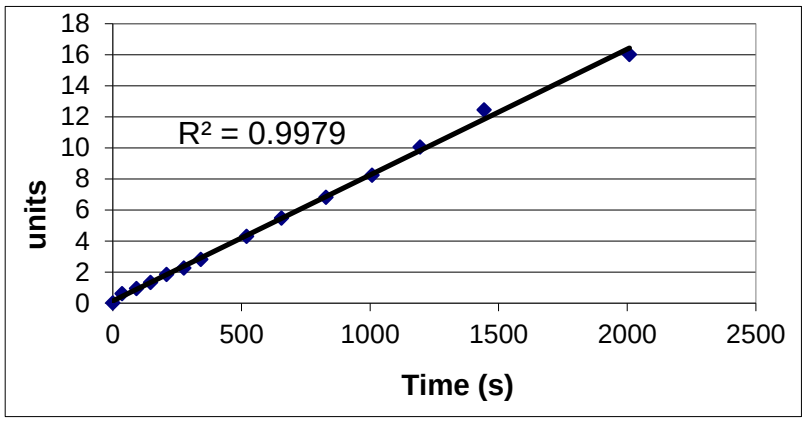

***1* – VO(salen)NCS**

3-FC_6H_4CHO

R^2 = 0.9909

Order 2

k = 0.0108 $M^{-1}.s^{-1}$

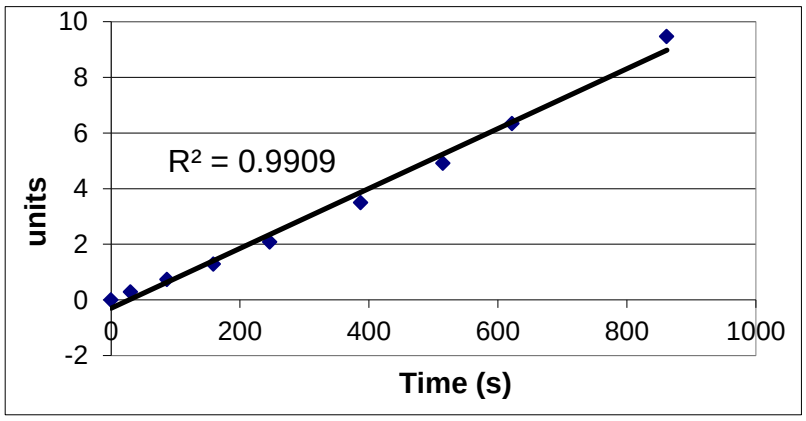

***2* – VO(salen)NCS**

3-FC_6H_4CHO

$R^2 = 0.9737$

Order 2

$k = 0.0111\ M^{-1}.s^{-1}$

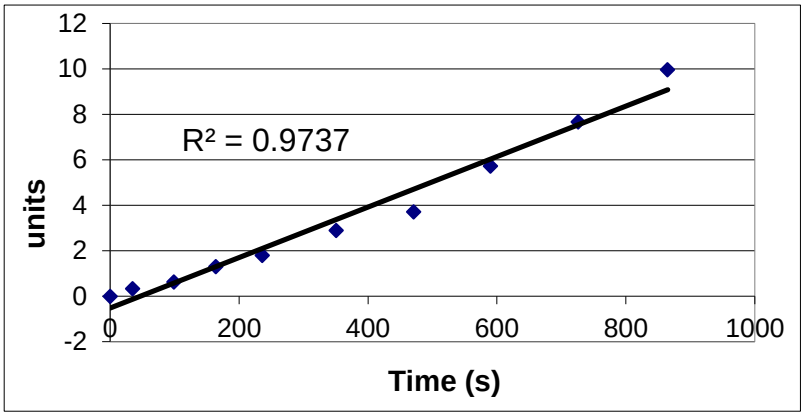

***1* – VO(salen)NCS**

4-ClC_6H_4CHO

$R^2 = 0.9891$

Order 2

$k = 0.0067\ M^{-1}.s^{-1}$

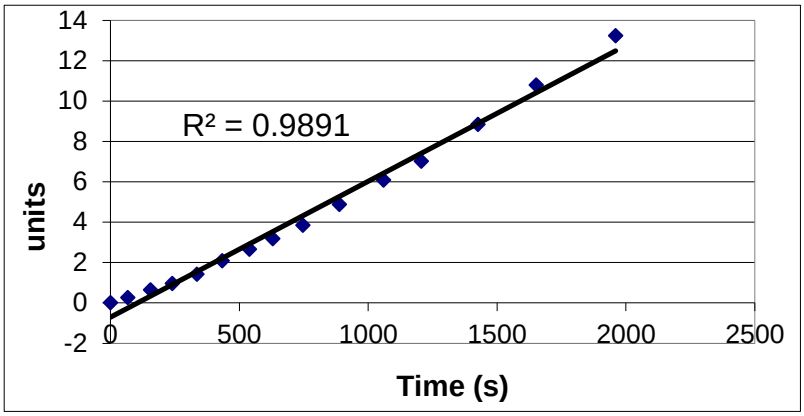

***2* – VO(salen)NCS**

4-ClC_6H_4CHO

$R^2 = 0.9773$

Order 2

$k = 0.0062\ M^{-1}.s^{-1}$

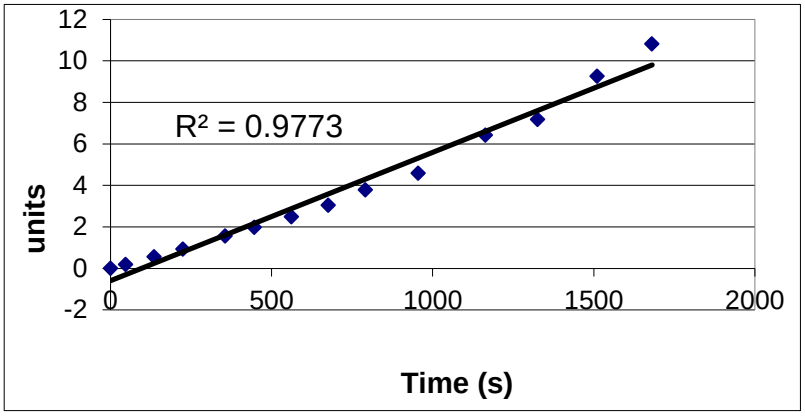

***1* – VO(salen)NCS**

4-BrC_6H_4CHO

$R^2 = 0.9922$

Order 2

$k = 0.0071\ M^{-1}.s^{-1}$

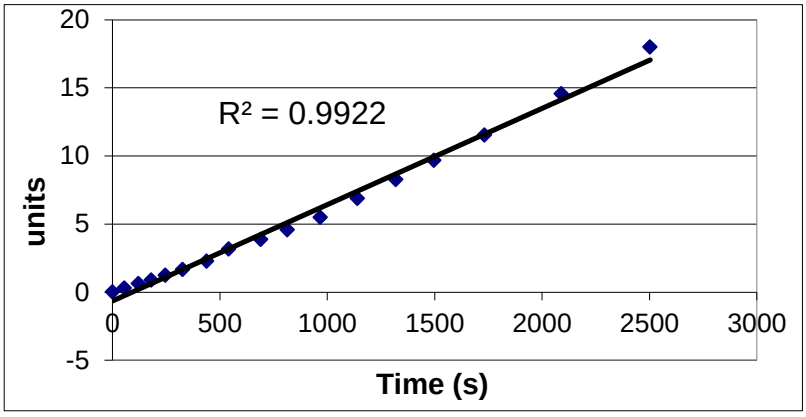

***2* – VO(salen)NCS**

4-BrC$_6$H$_4$CHO

R^2 = 0.9918

Order 2

k = 0.0070 $M^{-1}.s^{-1}$

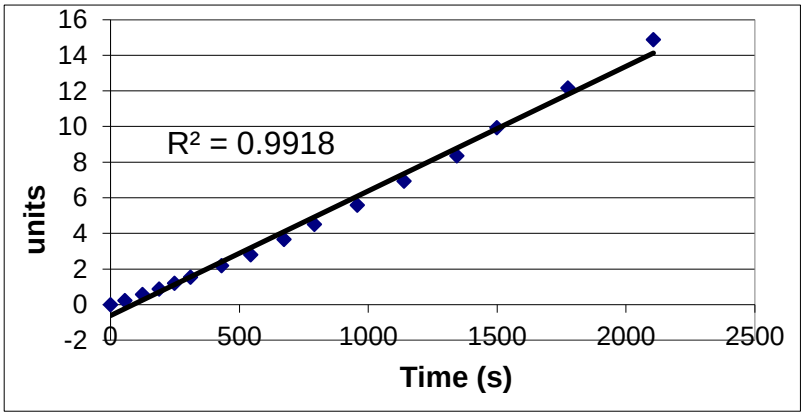

***1* – VO(salen)NCS**

4-FC$_6$H$_4$CHO

R^2 = 0.9864

Order 2

k = 0.0048 $M^{-1}.s^{-1}$

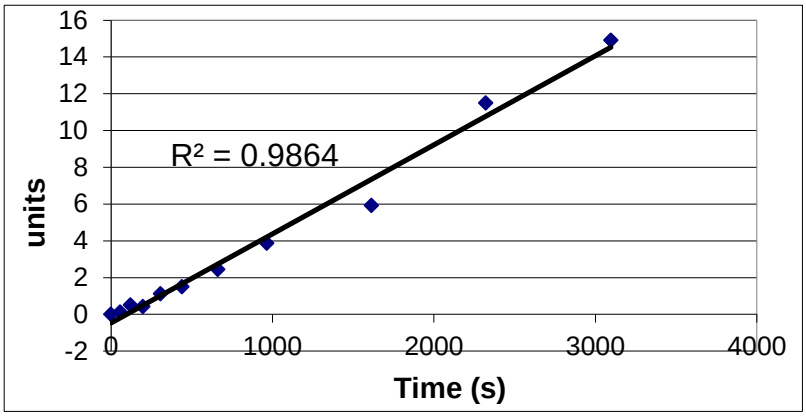

***2* – VO(salen)NCS**

4-FC$_6$H$_4$CHO

R^2 = 0.9917

Order 2

k = 0.0048 $M^{-1}.s^{-1}$

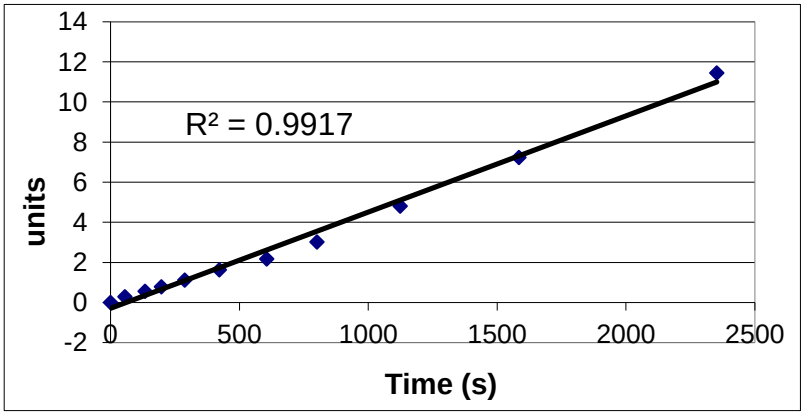

***1* – VO(salen)NCS**

3-CH$_3$C$_6$H$_4$CHO

R^2 = 0.9969

Order 2

k = 0.0035 $M^{-1}.s^{-1}$

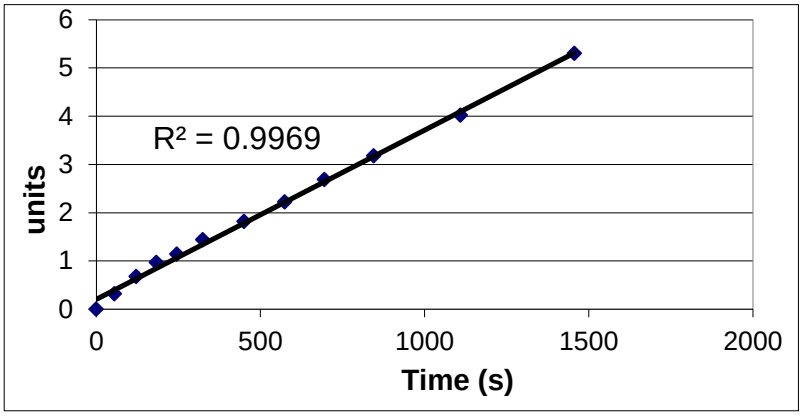

***2* – VO(salen)NCS**

3-$CH_3C_6H_4CHO$

$R^2 = 0.9817$

Order 2

$k = 0.0037\ M^{-1}.s^{-1}$

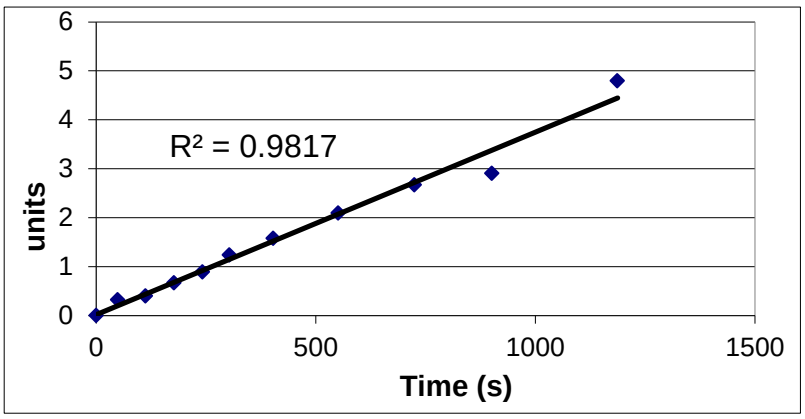

***1* – VO(salen)NCS**

4-$CH_3C_6H_4CHO$

$R^2 = 0.9937$

Order 2

$k = 0.0021\ M^{-1}.s^{-1}$

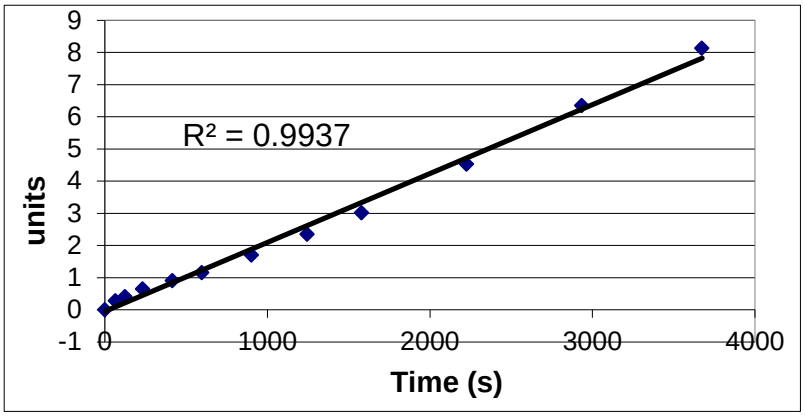

***2* – VO(salen)NCS**

4-$CH_3C_6H_4CHO$

$R^2 = 0.9936$

Order 2

$k = 0.0018\ M^{-1}.s^{-1}$

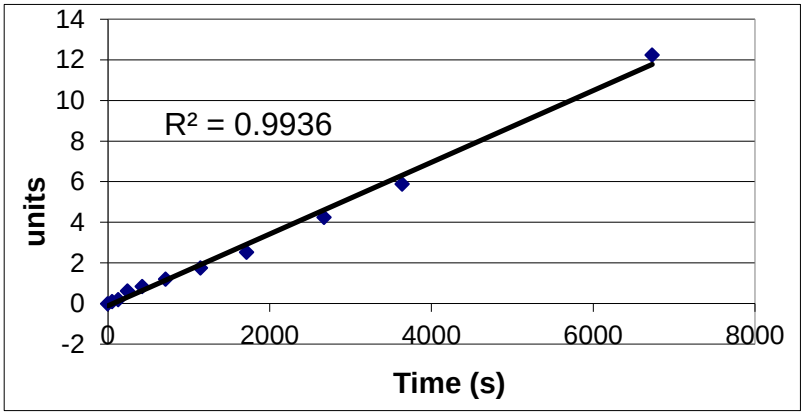

***1* – VO(salen)NCS**

3,4-$CH_3C_6H_3CHO$

$R^2 = 0.9922$

Order 2

$k = 0.0012\ M^{-1}.s^{-1}$

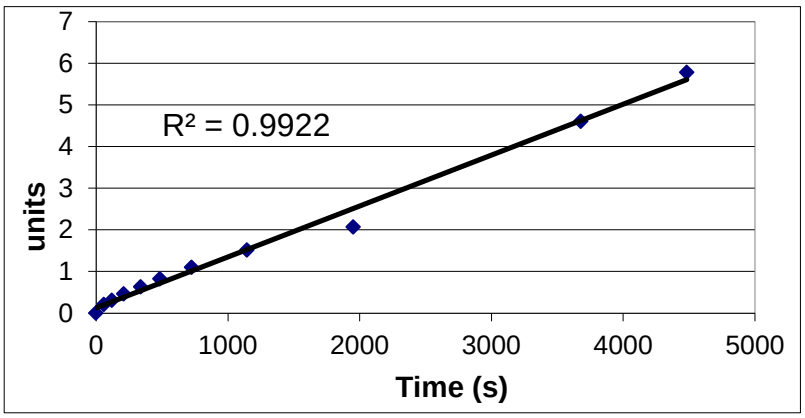

***2* – VO(salen)NCS**

3,4-$CH_3C_6H_3CHO$

R^2 = 0.9755

Order 2

k = 0.0013 $M^{-1}.s^{-1}$

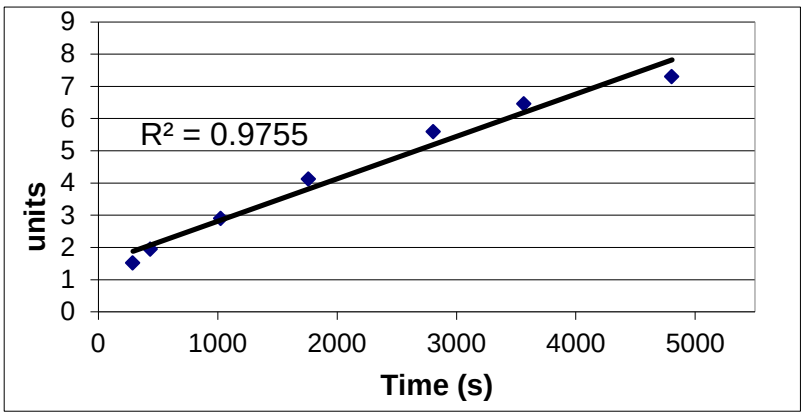

***1* – VO(salen)NCS**

p-$CH_3OC_6H_4CHO$

R^2 = 0.9972

Order 2

k = 0.0003 $M^{-1}.s^{-1}$

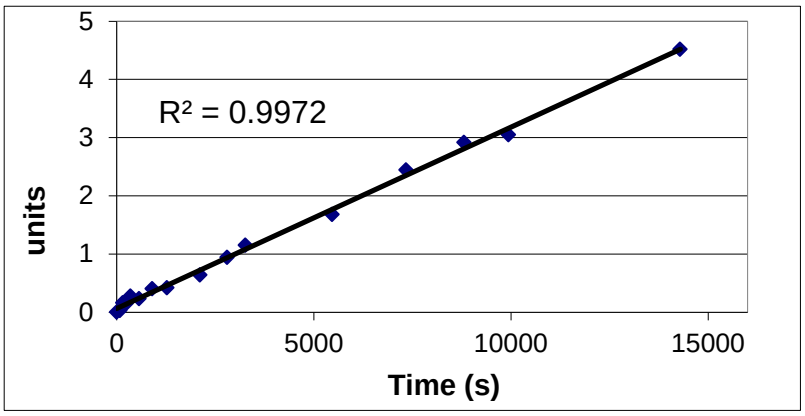

***2* – VO(salen)NCS**

p-$CH_3OC_6H_4CHO$

R^2 = 0.9967

Order 2

k = 0.0003 $M^{-1}.s^{-1}$

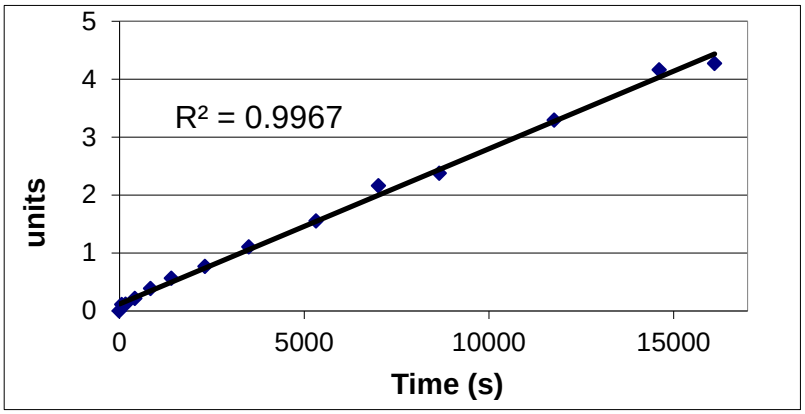

***1* – VO(salen)NCS**

p-$^tBuOC_6H_4CHO$

R^2 = 0.9893

Order 2

k = 0.0012 $M^{-1}.s^{-1}$

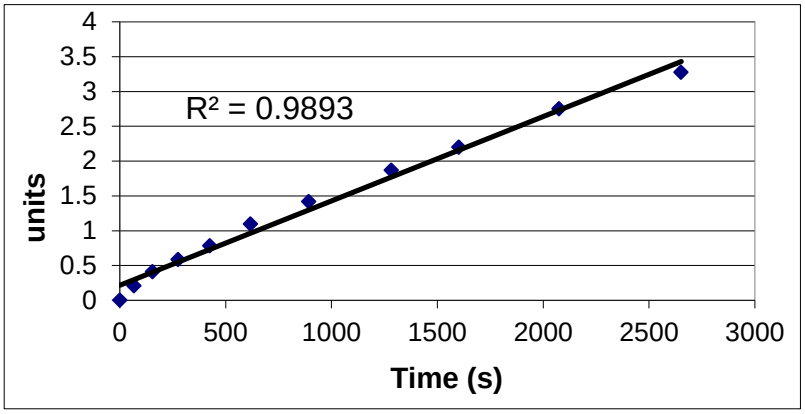

***2* – VO(salen)NCS**

p-^{t}BuOC$_6$H$_4$CHO

R^2 = 0.9988

Order 2

k = 0.0013 $M^{-1}.s^{-1}$

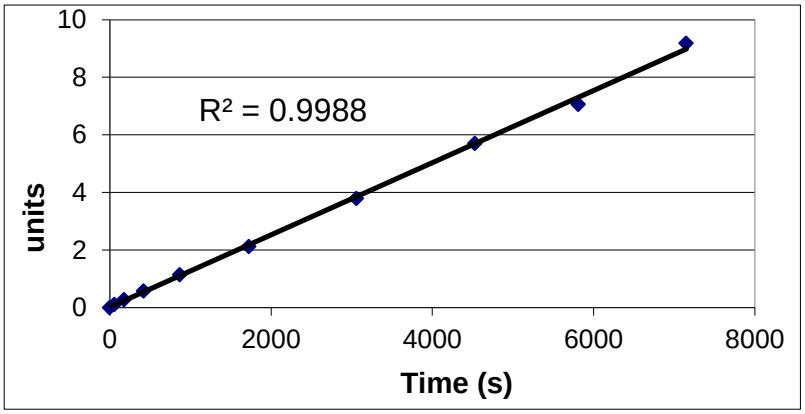

***1* – VO(salen)NCS**

p-CH$_3$SC$_6$H$_4$CHO

R^2 = 0.9978

Order 2

k = 0.0023 $M^{-1}.s^{-1}$

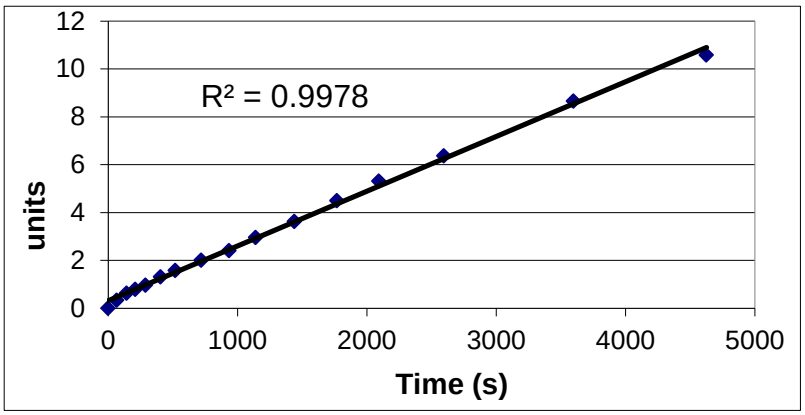

***2* – VO(salen)NCS**

p-CH$_3$SC$_6$H$_4$CHO

R^2 = 0.9972

Order 2

k = 0.0032 $M^{-1}.s^{-1}$

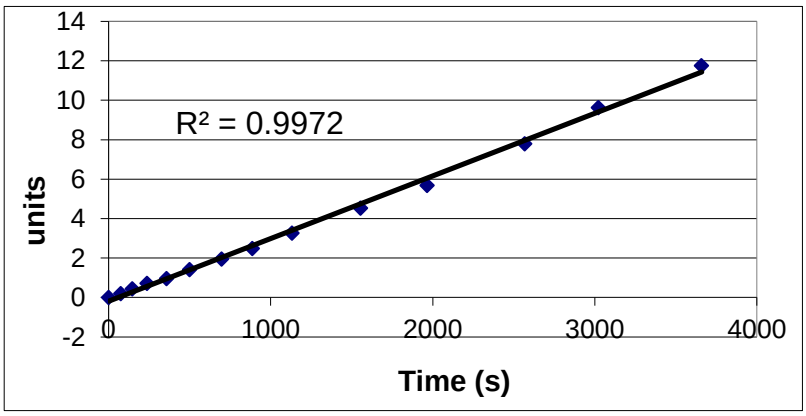

***1* – VO(salen)EtOSO$_3$**

PhCHO

R^2 = 0.9948

Order 2

k ($x10^{-4}$)= 0.70 $M^{-1}.s^{-1}$

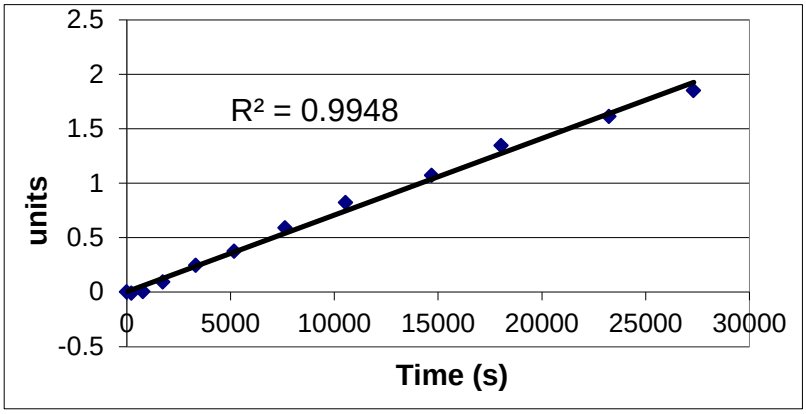

***2* – VO(salen)EtOSO$_3$**

PhCHO

R^2 = 0.9883

Order 2

k (x10^{-4})= 0.61 $M^{-1}.s^{-1}$

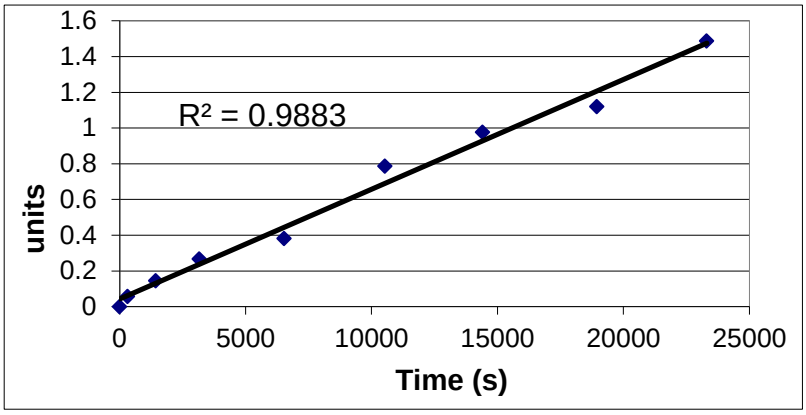

***1* – VO(salen)EtOSO$_3$**

3,5-FC_6H_3CHO

R^2 = 0.9993

Order 2

k (x10^{-4})= 5.73 $M^{-1}.s^{-1}$

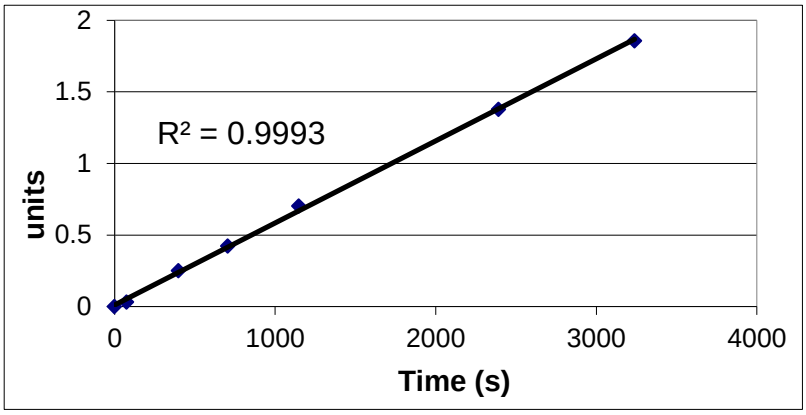

***2* – VO(salen)EtOSO$_3$**

3,5-FC_6H_3CHO

R^2 = 0.9971

Order 2

k (x10^{-4})= 5.00 $M^{-1}.s^{-1}$

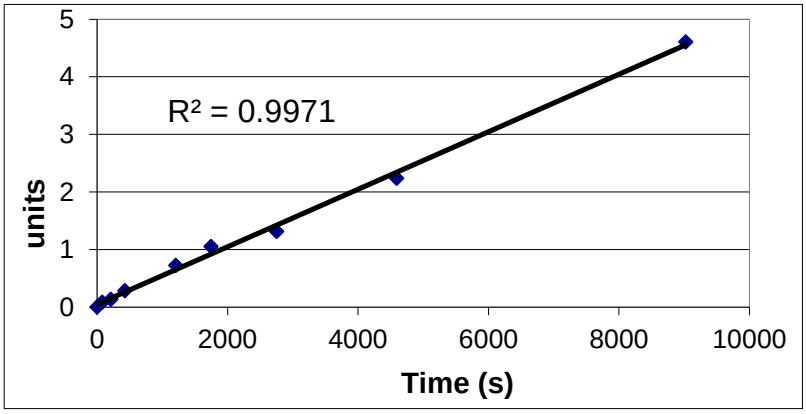

***1* – VO(salen)EtOSO$_3$**

3,4-ClC_6H_3CHO

R^2 = 0.9996

Order 2

k (x10^{-3})= 1.506 $M^{-1}.s^{-1}$

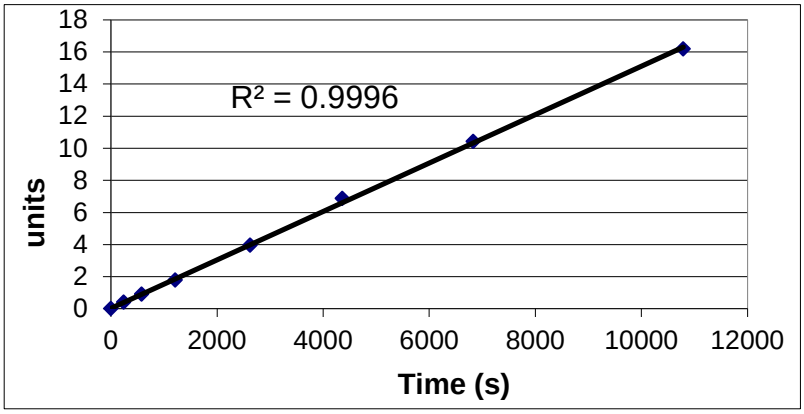

***2* – VO(salen)EtOSO$_3$**

3,4-ClC$_6$H$_3$CHO

R^2 = 0.9979

Order 2

k (x10^{-3})= 1.425 M^{-1}.s^{-1}

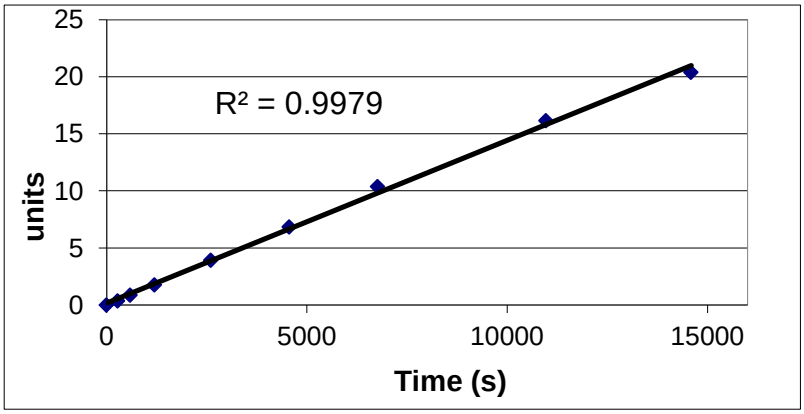

***1* – VO(salen)EtOSO$_3$**

4-CF$_3$C$_6$H$_4$CHO

R^2 = 0.9971

Order 2

k (x10^{-4})= 2.42 M^{-1}.s^{-1}

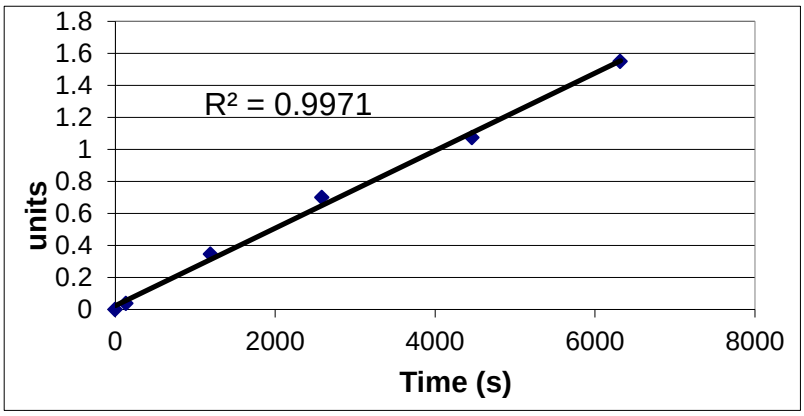

***2* – VO(salen)EtOSO$_3$**

4-CF$_3$C$_6$H$_4$CHO

R^2 = 0.9795

Order 2

k (x10^{-4})= 2.86 M^{-1}.s^{-1}

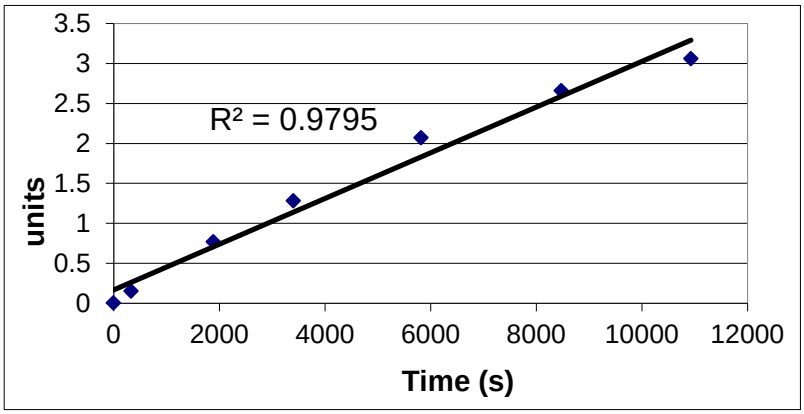

***1* – VO(salen)EtOSO$_3$**

3-ClC$_6$H$_4$CHO

R^2 = 0.9982

Order 2

k (x10^{-4})= 2.95 M^{-1}.s^{-1}

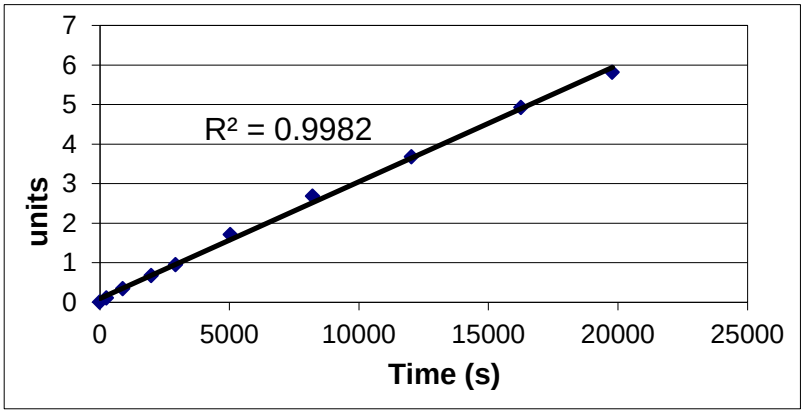

***2* – VO(salen)EtOSO$_3$**

3-ClC$_6$H$_4$CHO

R^2 = 0.9983

Order 2

k (x10^{-4})= 3.55 M^{-1}.s^{-1}

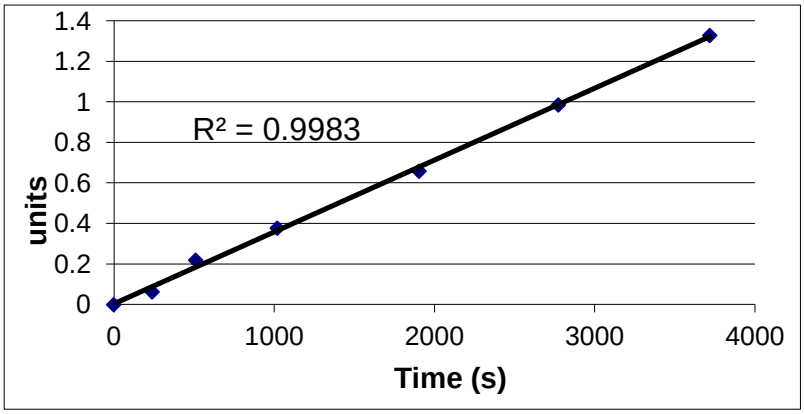

***1* – VO(salen)EtOSO$_3$**

3-FC$_6$H$_4$CHO

R^2 = 0.9993

Order 2

k (x10^{-4})= 2.76 M^{-1}.s^{-1}

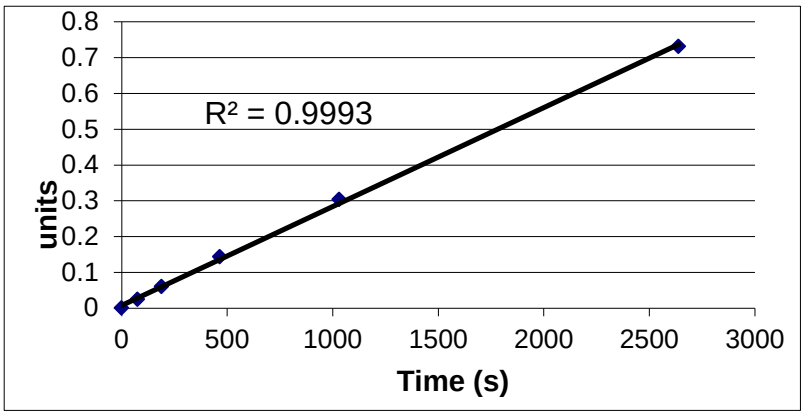

***2* – VO(salen)EtOSO$_3$**

3-FC$_6$H$_4$CHO

R^2 = 0.9960

Order 2

k (x10^{-4})= 2.50 M^{-1}.s^{-1}

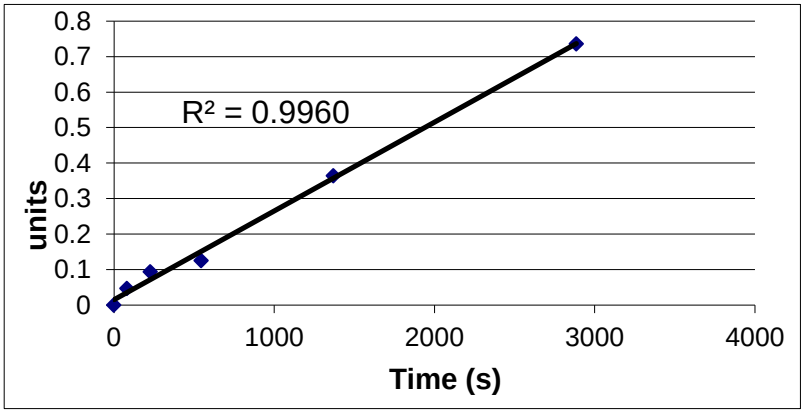

***1* – VO(salen)EtOSO$_3$**

4-ClC$_6$H$_4$CHO

R^2 = 0.9946

Order 2

k (x10^{-4})= 1.29 M^{-1}.s^{-1}

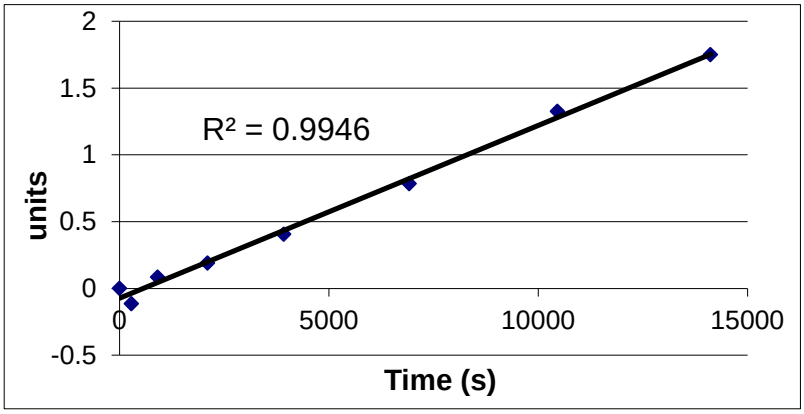

2 **– VO(salen)EtOSO$_3$**

4-ClC$_6$H$_4$CHO

R^2 = 0.9978

Order 2

k (x10^{-4})= 1.52 M^{-1}.s^{-1}

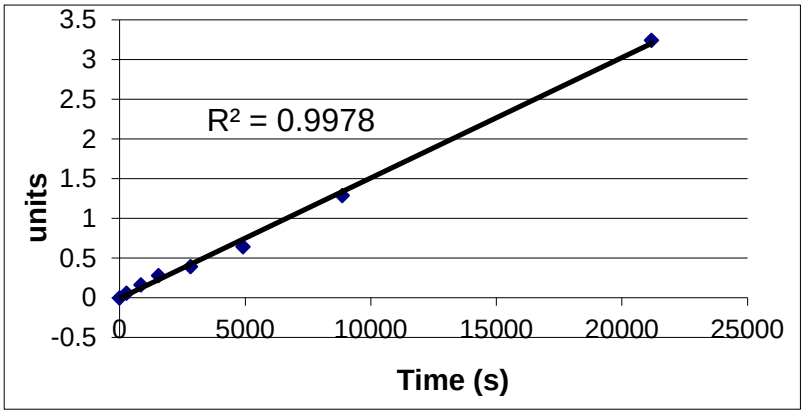

1 **– VO(salen)EtOSO$_3$**

4-BrC$_6$H$_4$CHO

R^2 = 0.9958

Order 2

k (x10^{-4})= 1.22 M^{-1}.s^{-1}

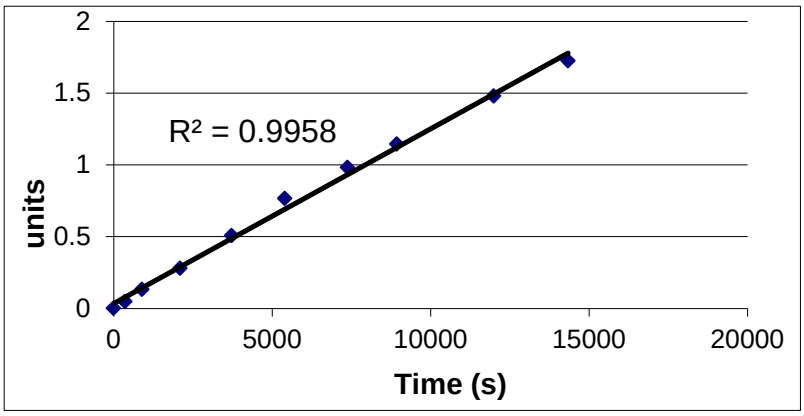

2 **– VO(salen)EtOSO$_3$**

4-BrC$_6$H$_4$CHO

R^2 = 0.9364

Order 2

k (x10^{-4})= 1.14 M^{-1}.s^{-1}

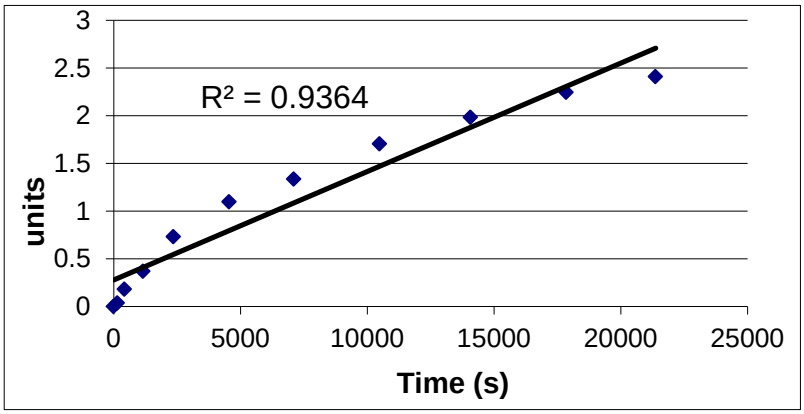

1 **– VO(salen)EtOSO$_3$**

4-FC$_6$H$_4$CHO

R^2 = 0.9977

Order 2

k (x10^{-4})= 0.88 M^{-1}.s^{-1}

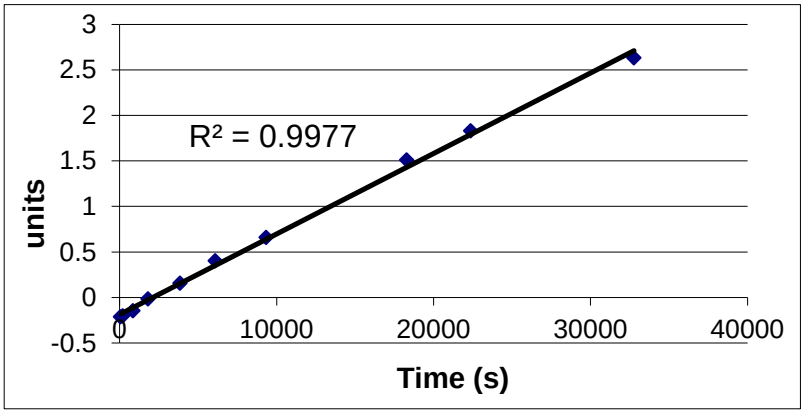

2 **– VO(salen)EtOSO$_3$**

4-FC$_6$H$_4$CHO

R^2 = 0.9266

Order 2

k (x10^{-4})= 0.82 M^{-1}.s^{-1}

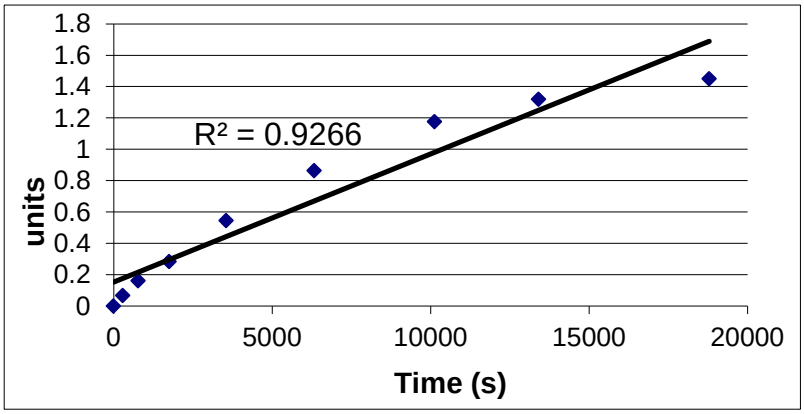

1 **– VO(salen)EtOSO$_3$**

3-CH$_3$C$_6$H$_4$CHO

R^2 = 0.9562

Order 2

k (x10^{-4})= 0.33 M^{-1}.s^{-1}

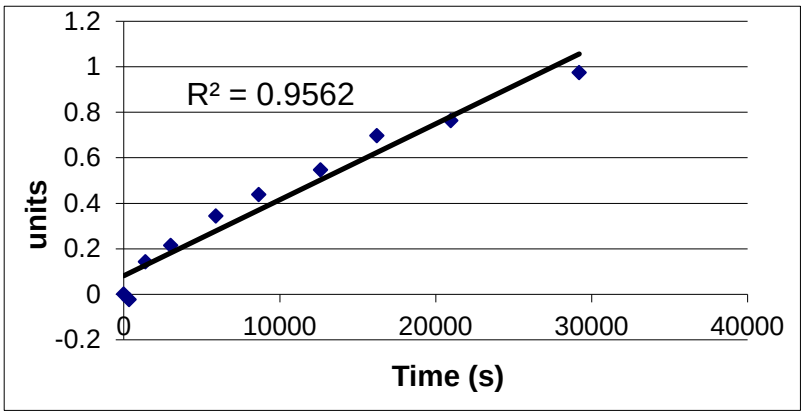

2 **– VO(salen)EtOSO$_3$**

3-CH$_3$C$_6$H$_4$CHO

R^2 = 0.9985

Order 2

k (x10^{-4})= 0.31 M^{-1}.s^{-1}

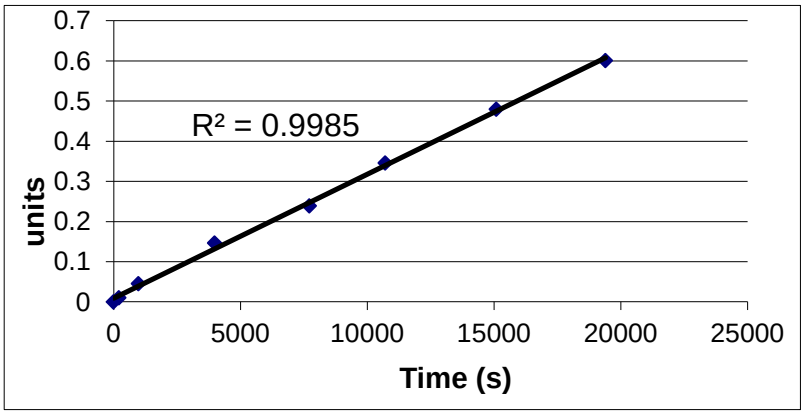

1 **– VO(salen)EtOSO$_3$**

4-CH$_3$C$_6$H$_4$CHO

R^2 = 0.9863

Order 2

k (x10^{-4})= 0.23 M^{-1}.s^{-1}

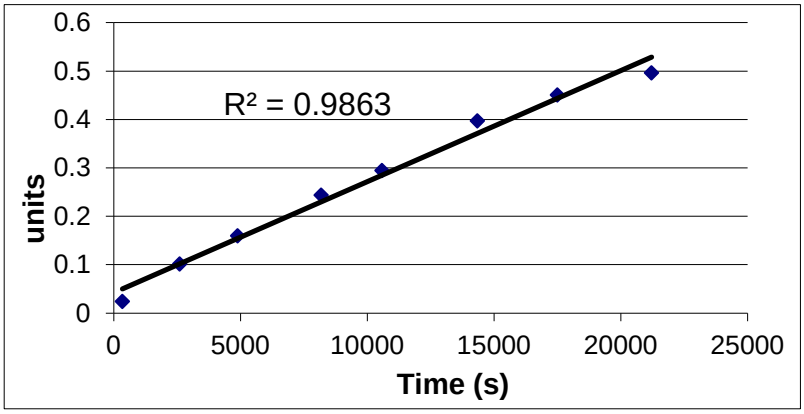

2 **– VO(salen)EtOSO$_3$**

4-CH$_3$C$_6$H$_4$CHO

R^2 = 0.9840

Order 2

k (x10^{-4})= 0.21 M^{-1}.s^{-1}

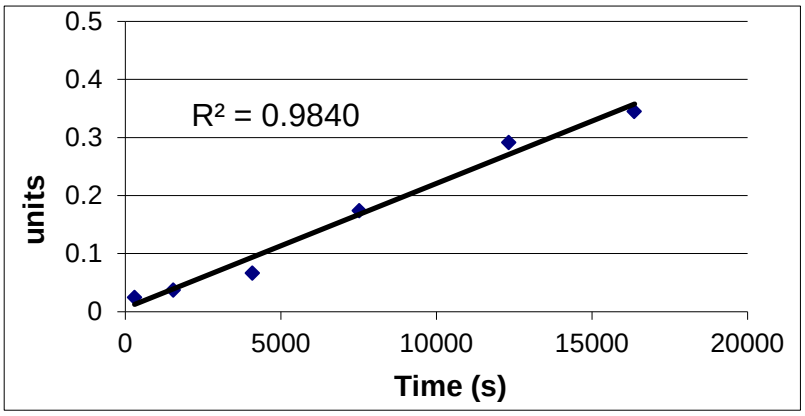

1 **– VO(salen)EtOSO$_3$**

3,4-CH$_3$C$_6$H$_3$CHO

R^2 = 0.9714

Order 2

k (x10^{-4})= 0.16 M^{-1}.s^{-1}

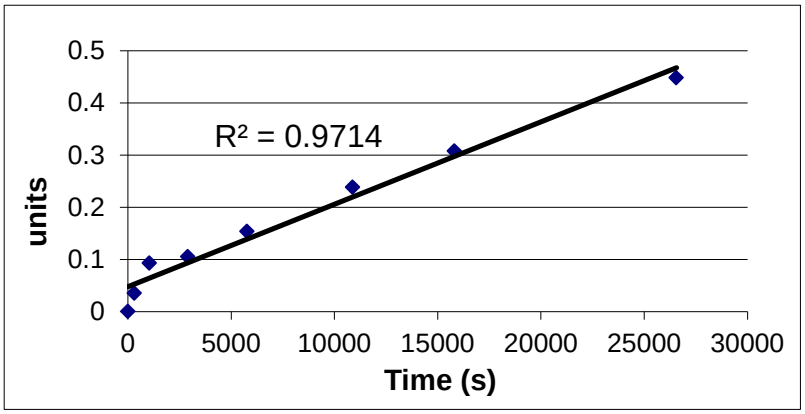

2 **– VO(salen)EtOSO$_3$**

3,4-CH$_3$C$_6$H$_3$CHO

R^2 = 0.9933

Order 2

k (x10^{-4})= 0.17 M^{-1}.s^{-1}

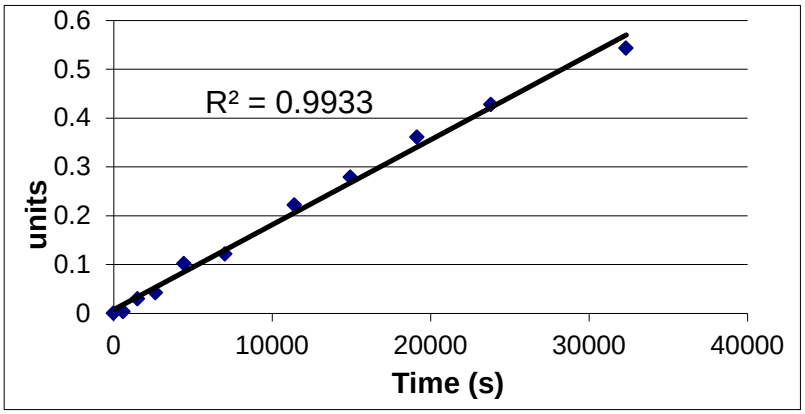

1 **– VO(salen)EtOSO$_3$**

4-^{t}BuOC$_6$H$_4$CHO

R^2 = 0.9852

Order 2

k (x10^{-4})= 0.24 M^{-1}.s^{-1}

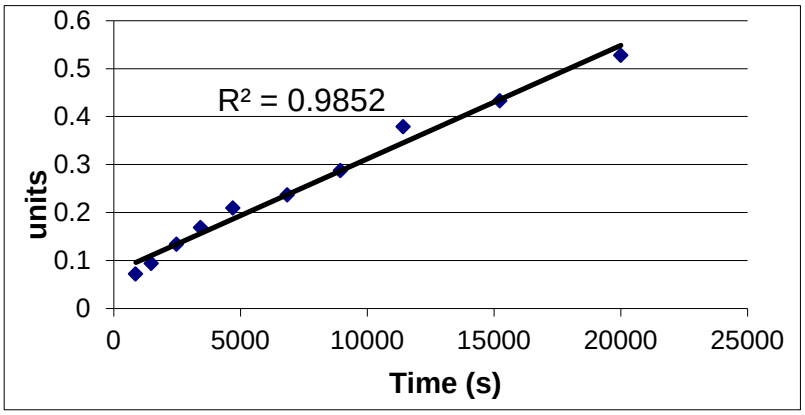

2 **– VO(salen)EtOSO$_3$**

4-^{t}BuOC$_6$H$_4$CHO

R^2 = 0.9971

Order 2

k (x10^{-4})= 0.12 $M^{-1}.s^{-1}$

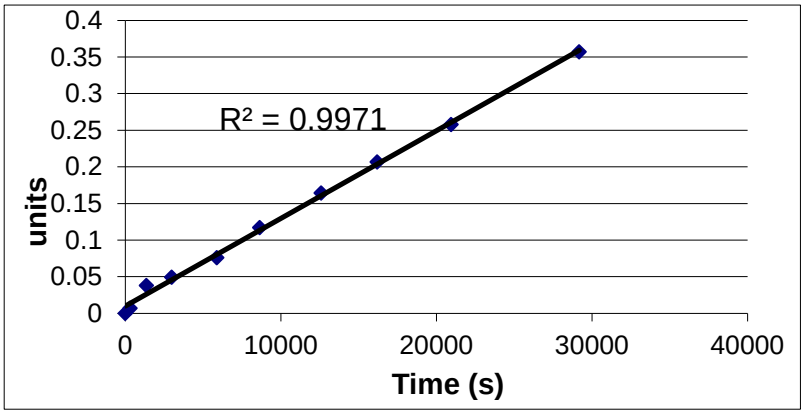

APPENDIX 3

3.1. Kinetic experiments at different catalyst concentrations using PC as solvent

All the kinetic experiments are conducted at 0°C using from 0.2 to 0.8 mol% of VO(salen)NCS catalyst in propylene carbonate, at a substrate concentration of 0.49 and 0.56 M of benzaldehyde and TMSCN.

1- VO(salen)NCS

1.13 mM, (0.2 mol%)

R^2 = 0.9941

Order 2

k = $5.72 \times 10^{-4} M.s^{-1}$

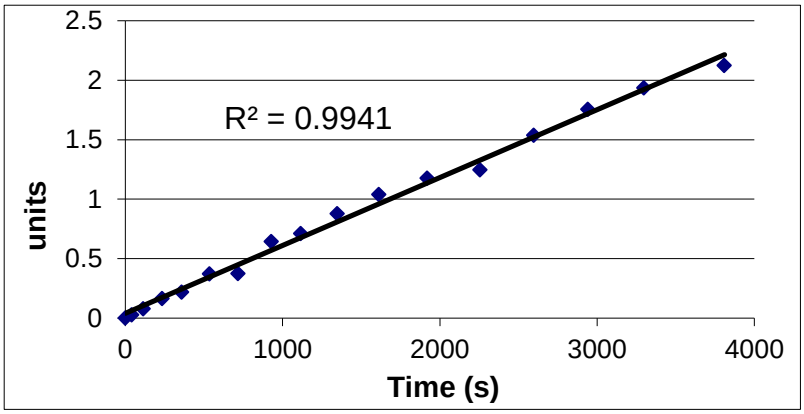

2- VO(salen)NCS

1.13 mM, (0.2 mol%)

R^2 = 0.9994

Order 2

k = $9.90 \times 10^{-4} M.s^{-1}$

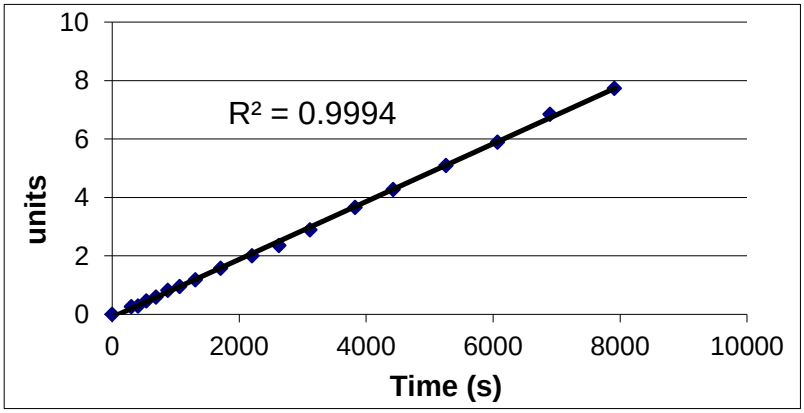

3- VO(salen)NCS

1.13 mM, (0.2 mol%)

R^2 = 0.9942

Order 2

k = $9.02 \times 10^{-4} M.s^{-1}$

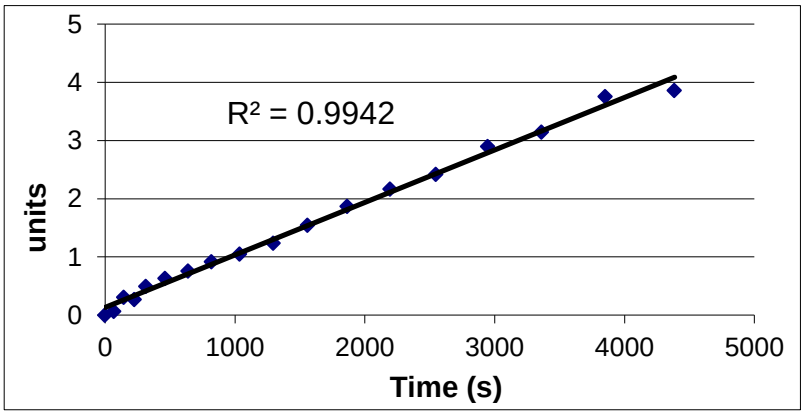

1- VO(salen)NCS

1.69 mM, (0.3 mol%)

R^2 = 0.9936

Order 2

k = $8.68x10^{-4}M.s^{-1}$

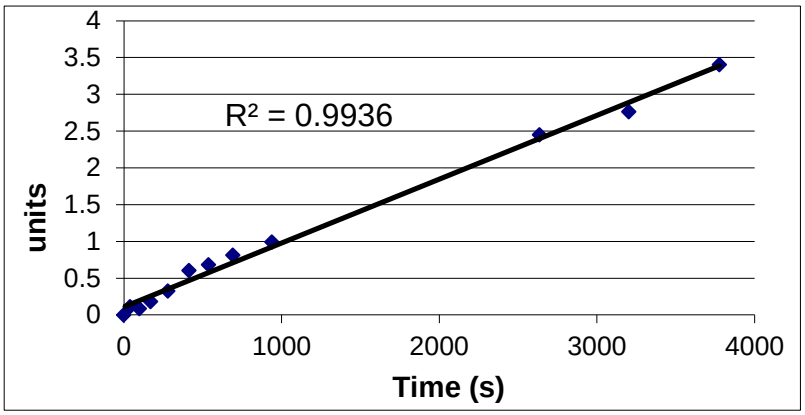

2- VO(salen)NCS

1.69 mM, (0.3 mol%)

R^2 = 0.9965

Order 2

k = $1.16x10^{-3}M.s^{-1}$

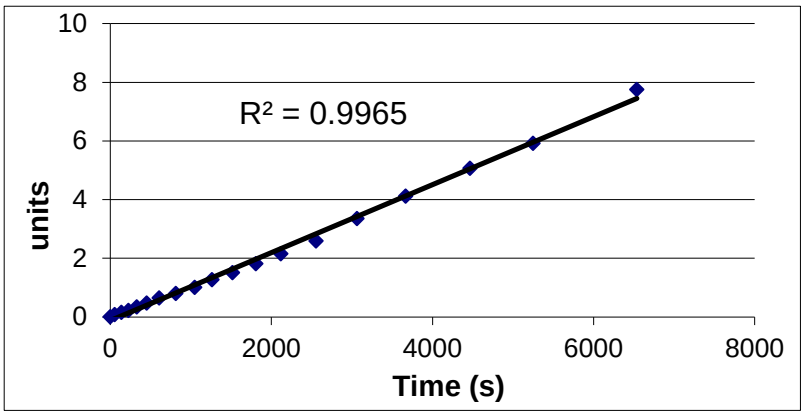

3- VO(salen)NCS

1.69 mM, (0.3 mol%)

R^2 = 0.9993

Order 2

k = $1.27x10^{-3}M.s^{-1}$

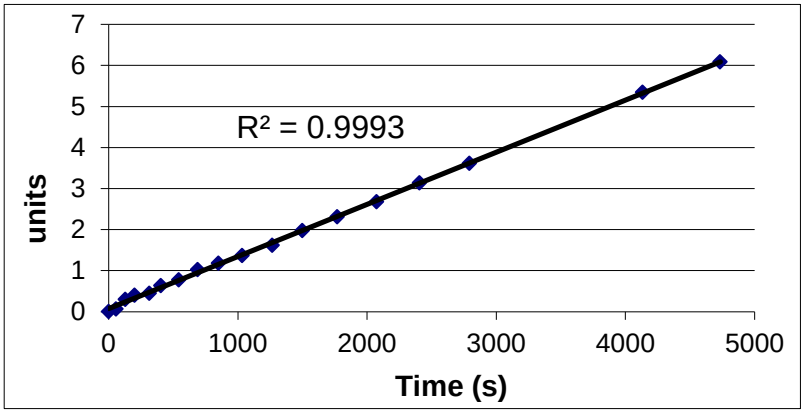

1- VO(salen)NCS

2.25 mM, (0.4 mol%)

R^2 = 0.9730

Order 2

k = $1.00x10^{-3}M.s^{-1}$

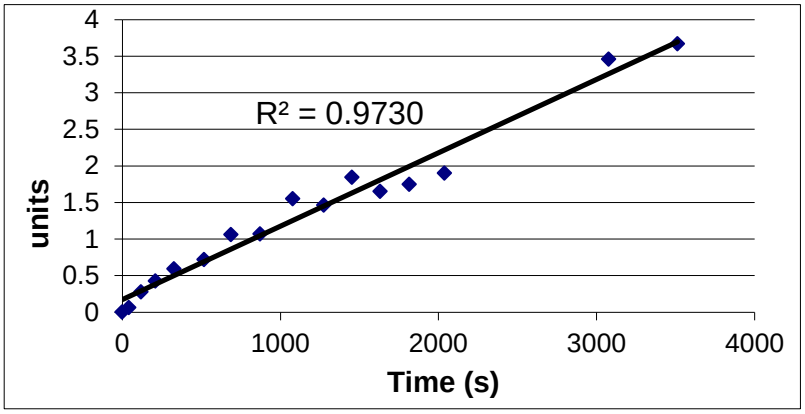

2- VO(salen)NCS

2.25 mM, (0.4 mol%)

R^2 = 0.9946

Order 2

k = $1.70x10^{-3}M.s^{-1}$

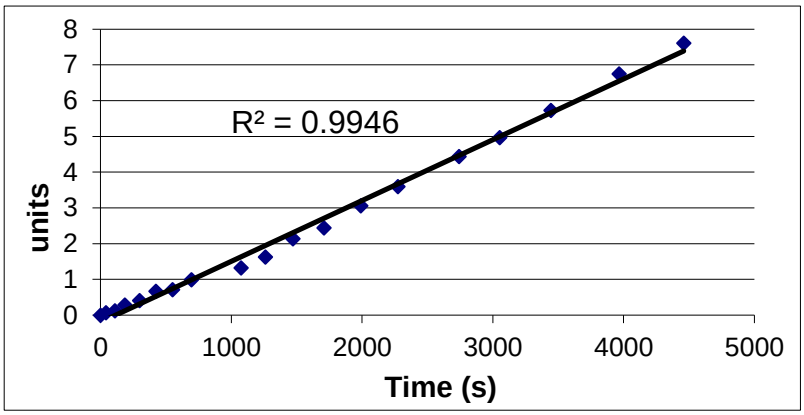

3- VO(salen)NCS

2.25 mM, (0.4 mol%)

R^2 = 0.9995

Order 2

k = $1.55x10^{-3}M.s^{-1}$

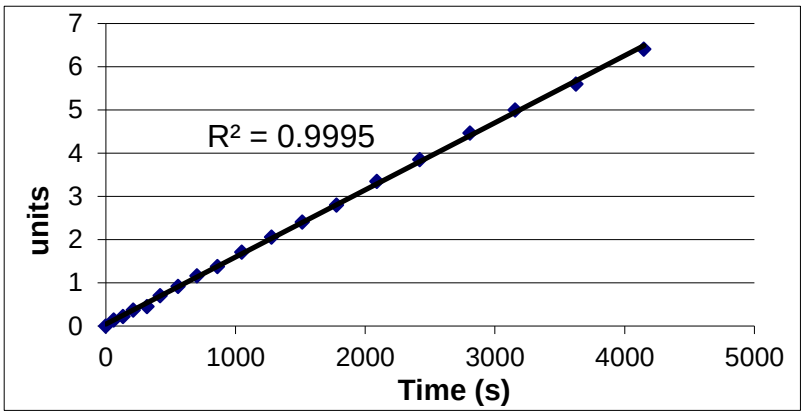

1- VO(salen)NCS

3.38 mM, (0.6 mol%)

R^2 = 0.9932

Order 2

k = $2.22x10^{-3}M.s^{-1}$

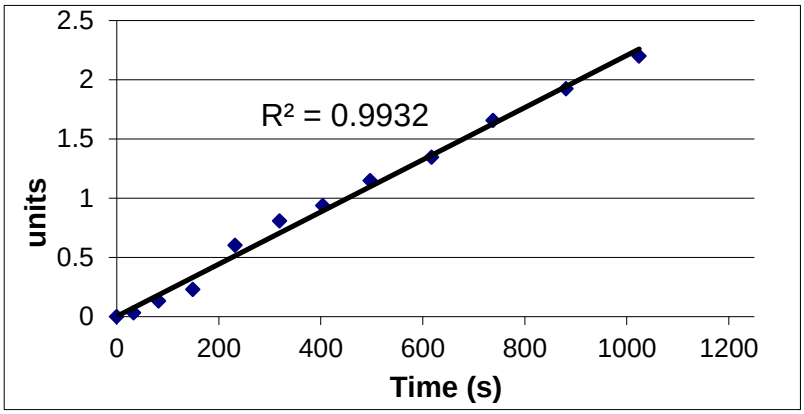

2- VO(salen)NCS

3.38 mM, (0.6 mol%)

R^2 = 0.9931

Order 2

k = $2.05x10^{-3}M.s^{-1}$

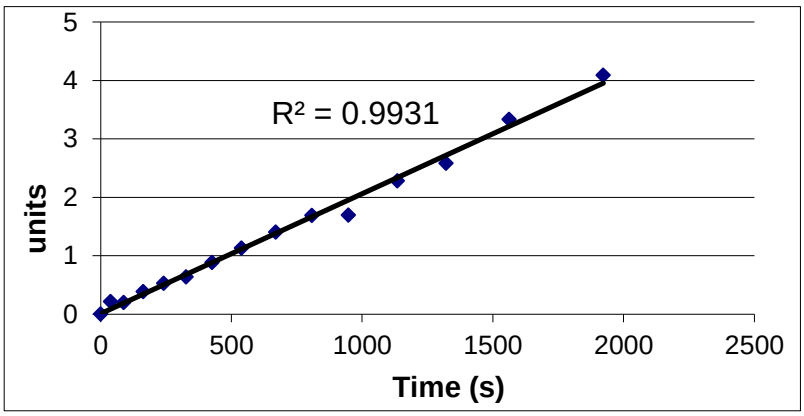

3- VO(salen)NCS

3.38 mM, (0.6 mol%)

$R^2 = 0.9973$

Order 2

$k = 2.29x10^{-3}M.s^{-1}$

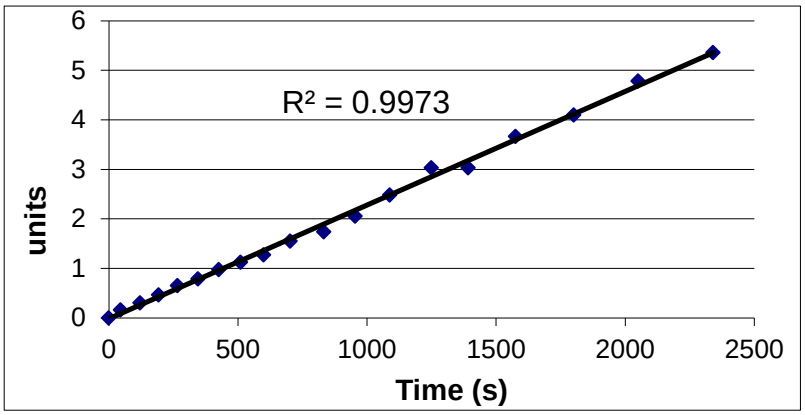

1- VO(salen)NCS

4.50 mM, (0.8 mol%)

$R^2 = 0.9937$

Order 2

$k = 2.96x10^{-3}M.s^{-1}$

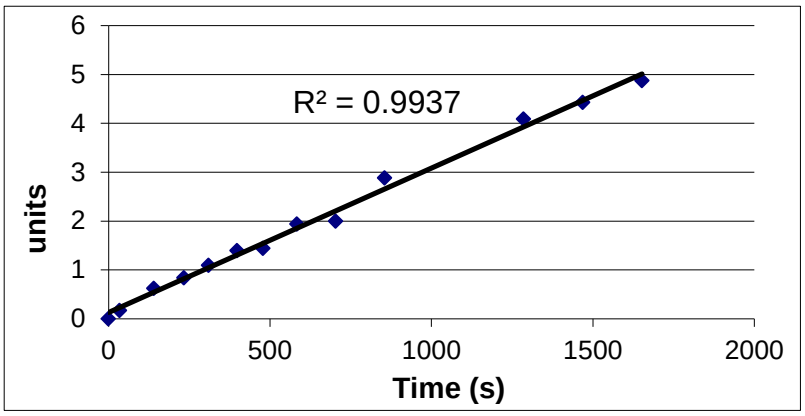

2- VO(salen)NCS

4.50 mM, (0.8 mol%)

$R^2 = 0.9976$

Order 2

$k = 3.70x10^{-3}M.s^{-1}$

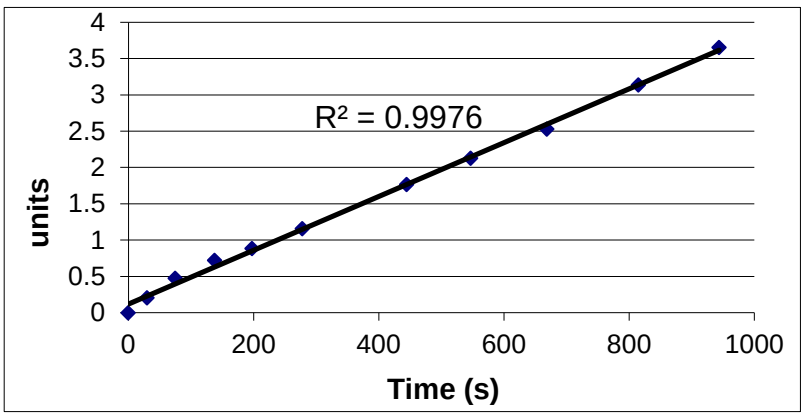

3- VO(salen)NCS

4.50 mM, (0.8 mol%)

$R^2 = 0.9985$

Order 2

$k = 2.96x10^{-3}M.s^{-1}$

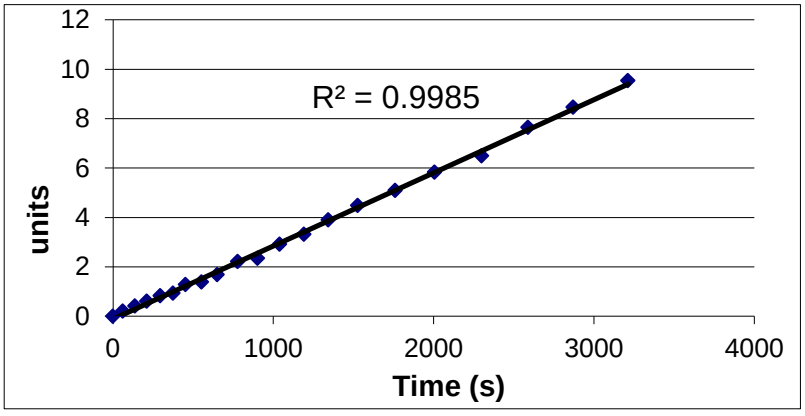

3.2.Variable temperature kinetic experiments in propylene carbonate

All the kinetic experiments are conducted at different temperatures from 20 to -20°C using 0.2 mol% of VO(salen)NCS catalyst in propylene carbonate, at a substrate concentration of 0.49 and 0.56 M of benzaldehyde and TMSCN.

1- VO(salen)NCS

T = 253 K

R^2 = 0.9955

Order 2

k = $0.58x10^{-4}M.s^{-1}$

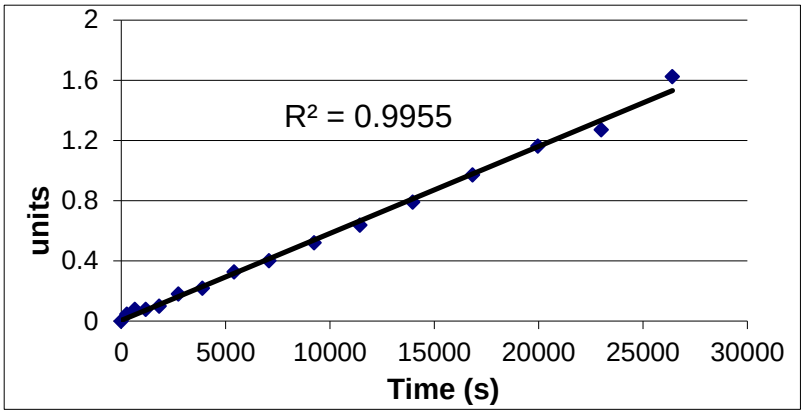

2- VO(salen)NCS

T = 253 K

R^2 = 0.9768

Order 2

k = $1.07x10^{-4}M.s^{-1}$

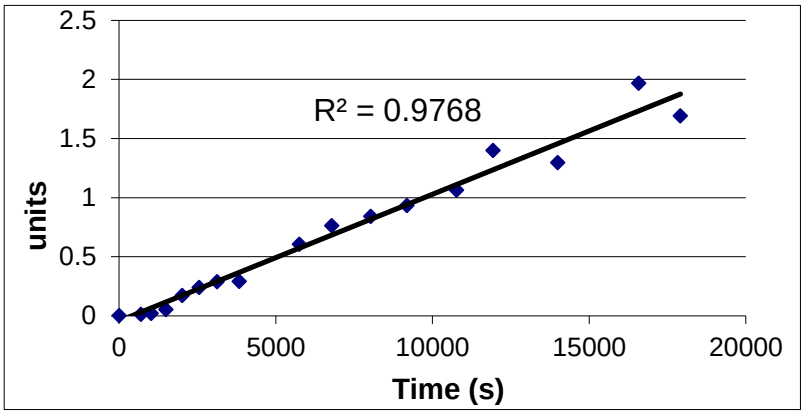

1- VO(salen)NCS

T = 263 K

R^2 = 0.9987

Order 2

k = $2.03x10^{-4}M.s^{-1}$

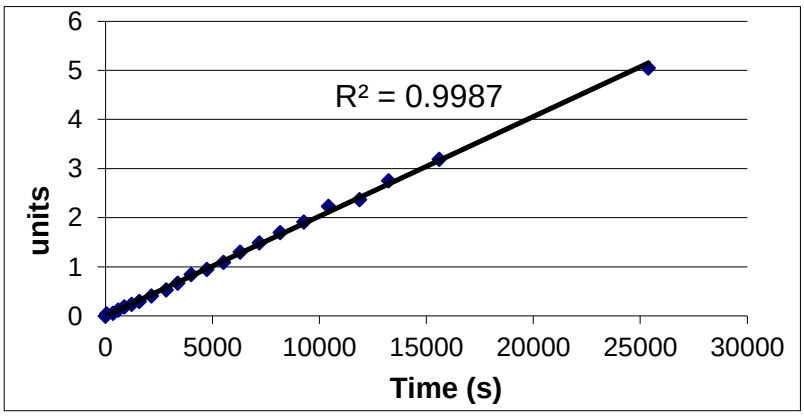

2- VO(salen)NCS

T = 263 K

R^2 = 0.9986

Order 2

k = 2.85x10^{-4}M.s^{-1}

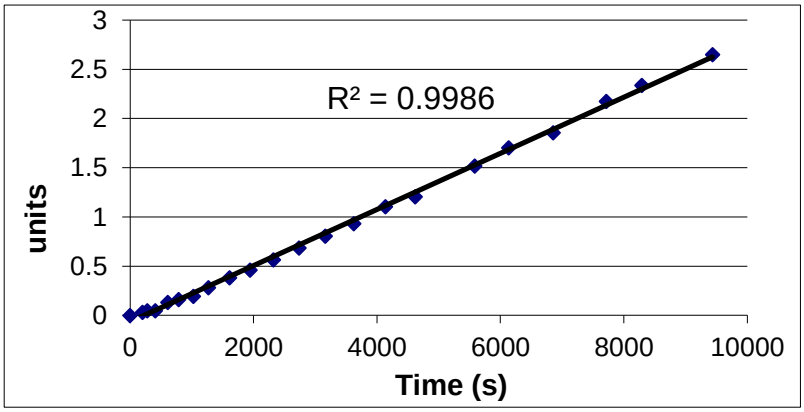

1- VO(salen)NCS

T = 273 K

R^2 = 0.9967

Order 2

k = 4.72x10^{-4}M.s^{-1}

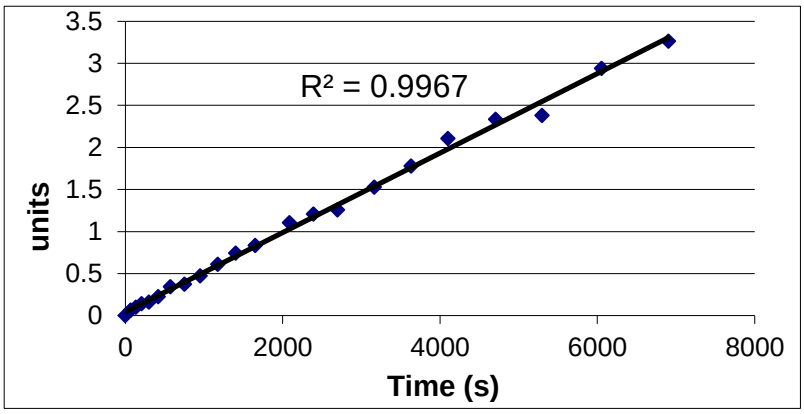

2- VO(salen)NCS

T = 273 K

R^2 = 0.9941

Order 2

k = 5.72x10^{-4}M.s^{-1}

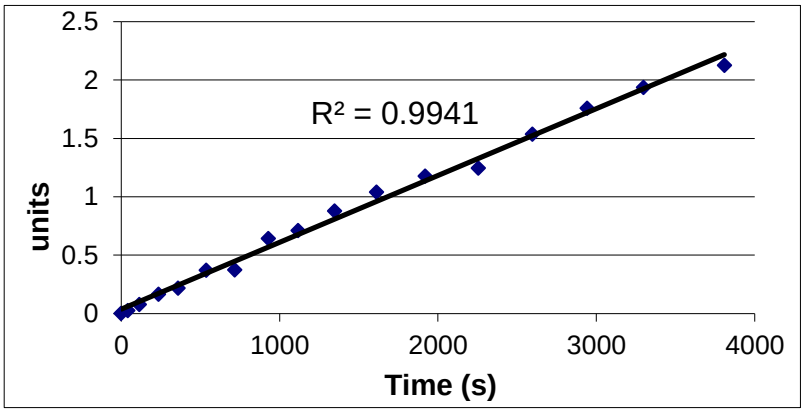

1- VO(salen)NCS

T = 283 K

R^2 = 0.9981

Order 2

k = 1.73x10^{-3}M.s^{-1}

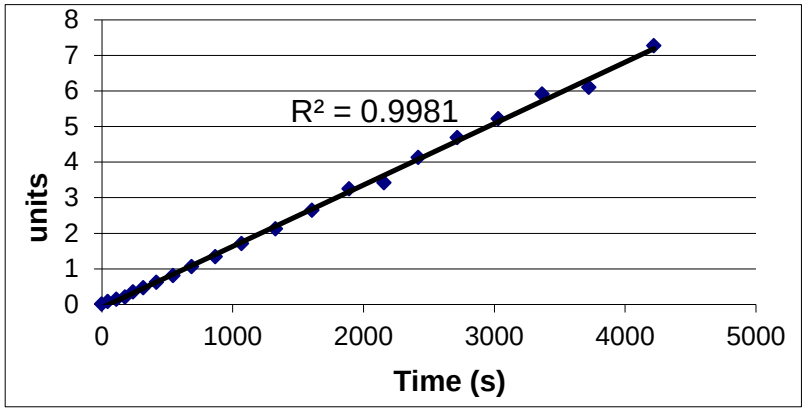

2- VO(salen)NCS

T = 283 K

R^2 = 0.9947

Order 2

k = 1.50x10^{-3}M.s^{-1}

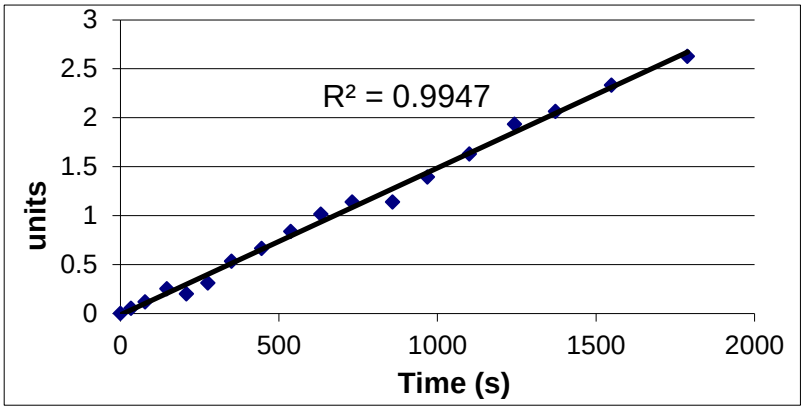

1- VO(salen)NCS

T = 293 K

R^2 = 0.9961

Order 2

k = 3.25x10^{-3}M.s^{-1}

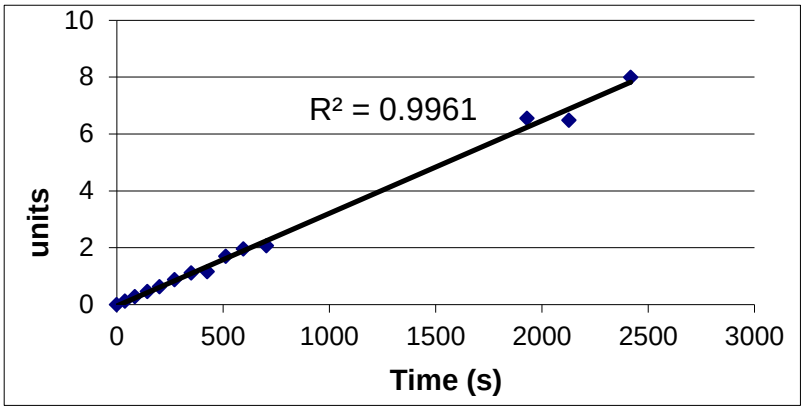

2- VO(salen)NCS

T = 293 K

R^2 = 0.9926

Order 2

k = 2.55x10^{-3}M.s^{-1}

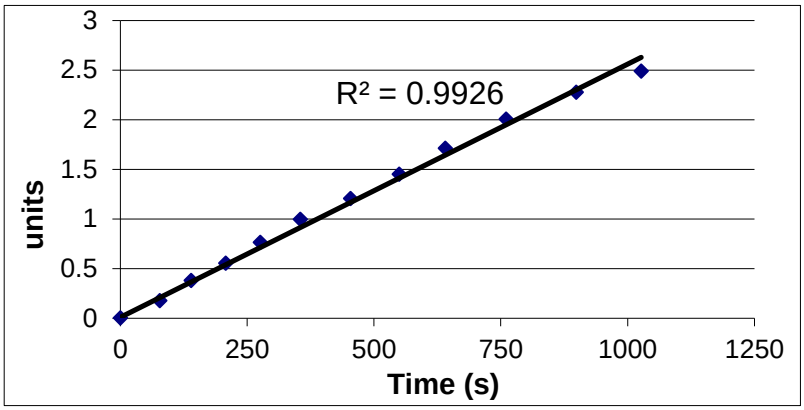

3.3. Kinetics for the Hammett plot in propylene carbonate

The kinetics experiments are conducted in propylene carbonate at 0 ºC using 0.2 mol% of catalyst loading. The second order correlations are presented according to the aldehyde employed. The aldehyde and TMSCN concentrations are 0.49 and 0.56 M respectively.

1 – VO(salen)NCS

PhCHO

$R^2 = 0.9977$

Order 2

$k = 0.90 \times 10^{-3}$ M.s^{-1}

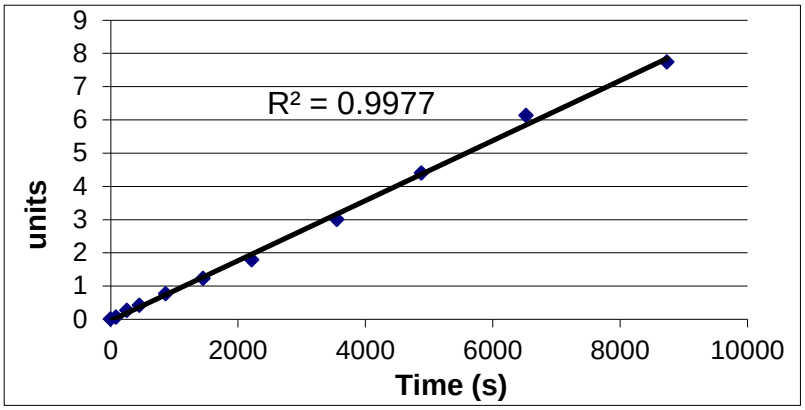

2 – VO(salen)NCS

PhCHO

$R^2 = 0.9942$

Order 2

$k = 0.90 \times 10^{-3}$ M.s^{-1}

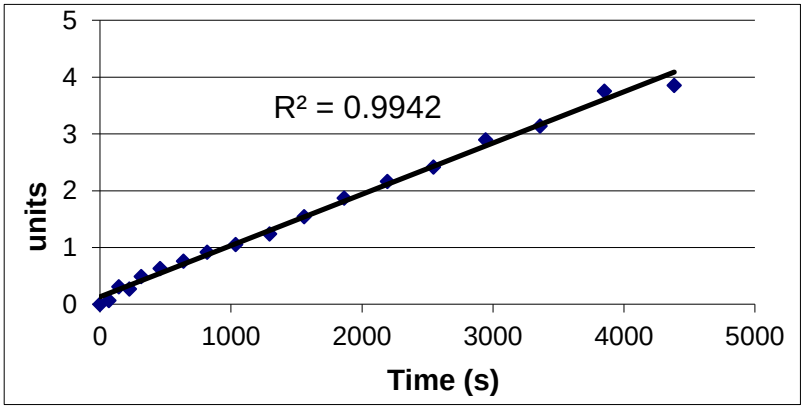

1 – VO(salen)NCS

3,5-$F_2C_6H_3CHO$

$R^2 = 0.9884$

Order 2

$k = 0.84 \times 10^{-3}$ M.s^{-1}

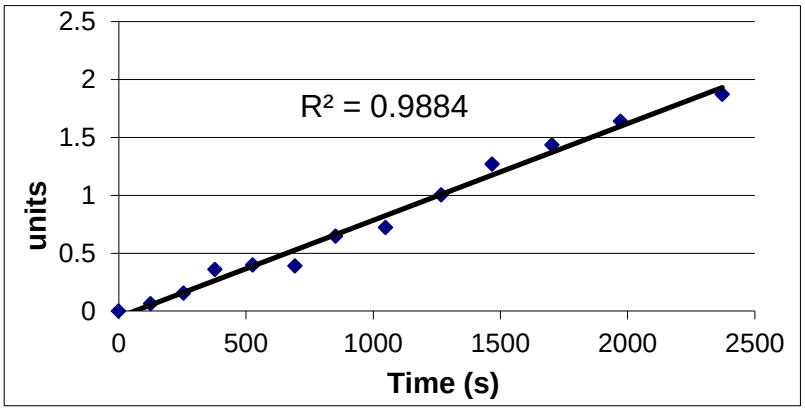

2 – VO(salen)NCS

3,5-$F_2C_6H_3CHO$

R^2 = 0.9900

Order 2

k = 1.10x10^{-3} M.s^{-1}

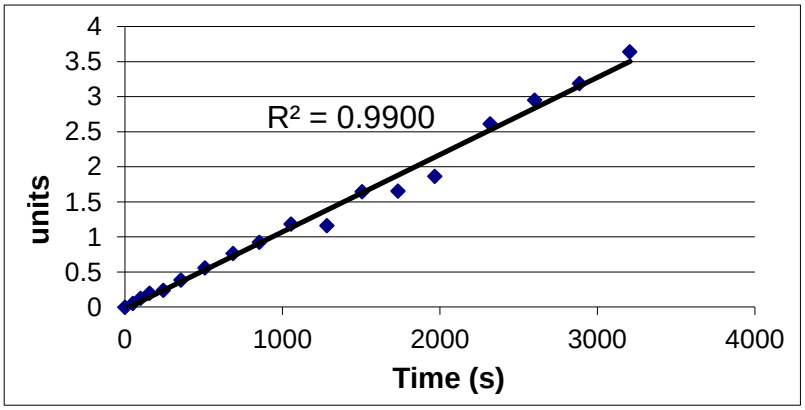

1 – VO(salen)NCS

3,4-$Cl_2C_6H_3CHO$

R^2 = 0.9984

Order 2

k = 1.17x10^{-3} M.s^{-1}

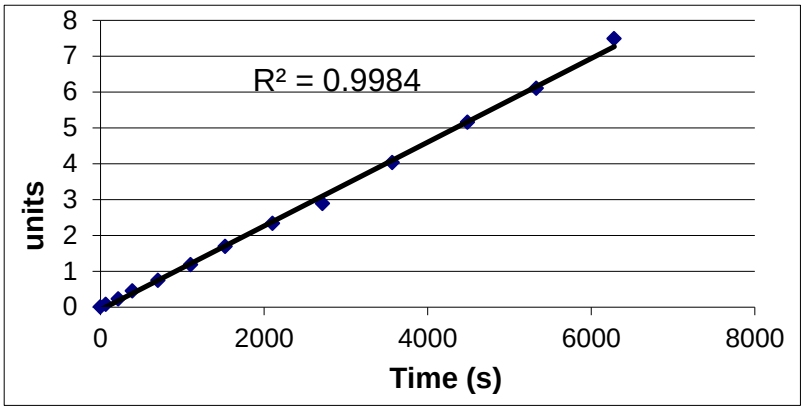

2 – VO(salen)NCS

3,4-$Cl_2C_6H_3CHO$

R^2 = 0.9992

Order 2

k = 1.24x10^{-3} M.s^{-1}

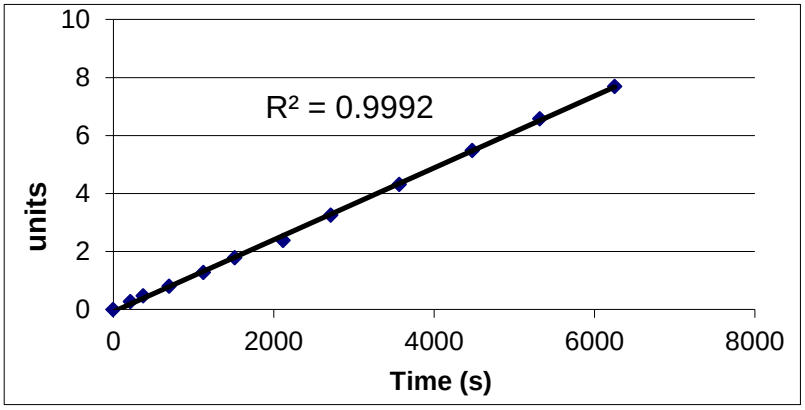

1– VO(salen)NCS

4-$CF_3C_6H_4CHO$

R^2 = 0.9982

Order 2

k = 1.53x10^{-3} M.s^{-1}

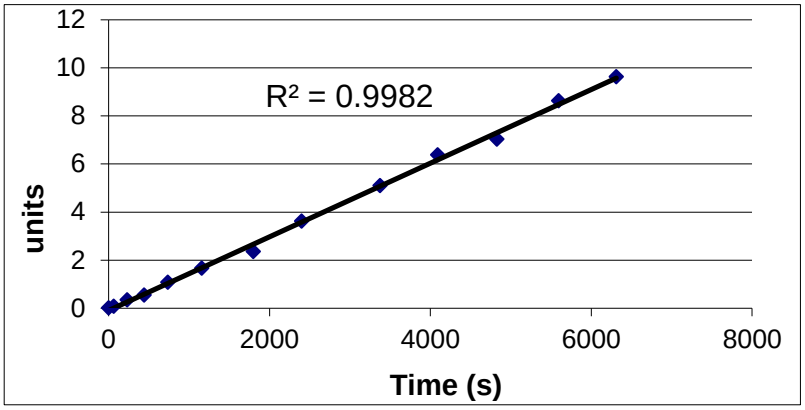

2– VO(salen)NCS

4-$CF_3C_6H_4CHO$

R^2 = 0.9964

Order 2

k = 1.73x10^{-3} M.s^{-1}

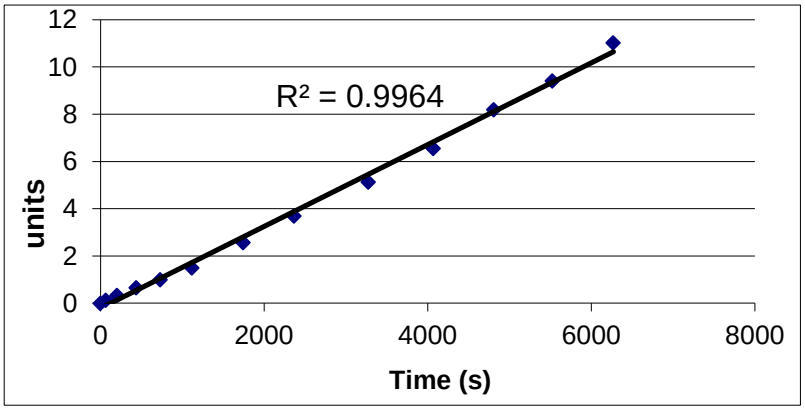

1– VO(salen)NCS

3-ClC_6H_4CHO

R^2 = 0.9948

Order 2

k = 0.78x10^{-3} M.s^{-1}

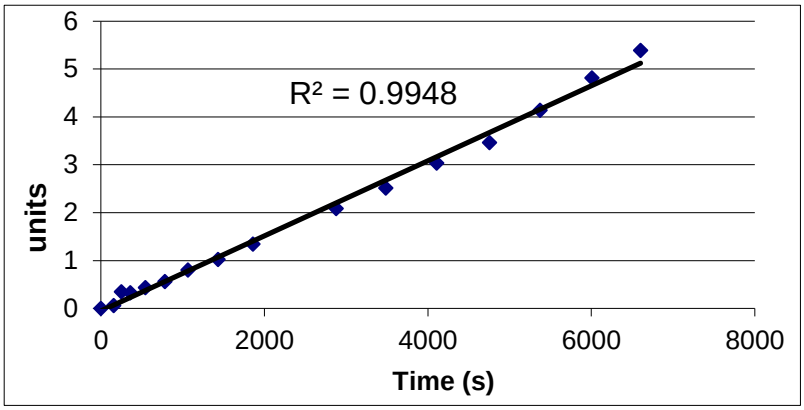

2– VO(salen)NCS

3-ClC_6H_4CHO

R^2 = 0.9962

Order 2

k = 0.90x10^{-3} M.s^{-1}

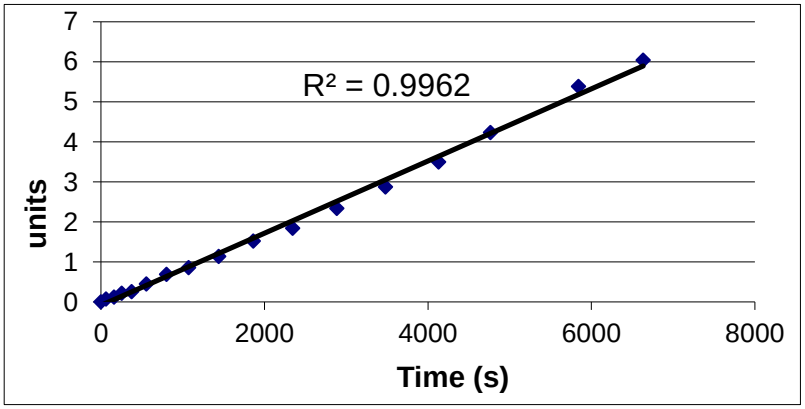

1– VO(salen)NCS

3-FC_6H_4CHO

R^2 = 0.9989

Order 2

k = 1.04x10^{-3} M.s^{-1}

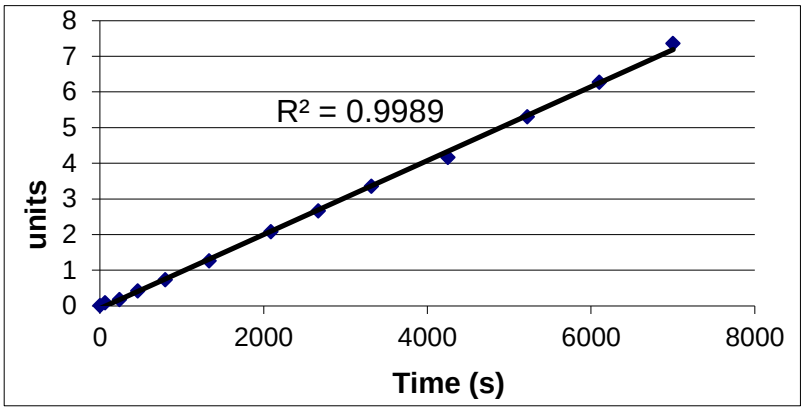

2– VO(salen)NCS

3-FC_6H_4CHO

R^2 = 0.9993

Order 2

k = 1.00x10^{-3} M.s^{-1}

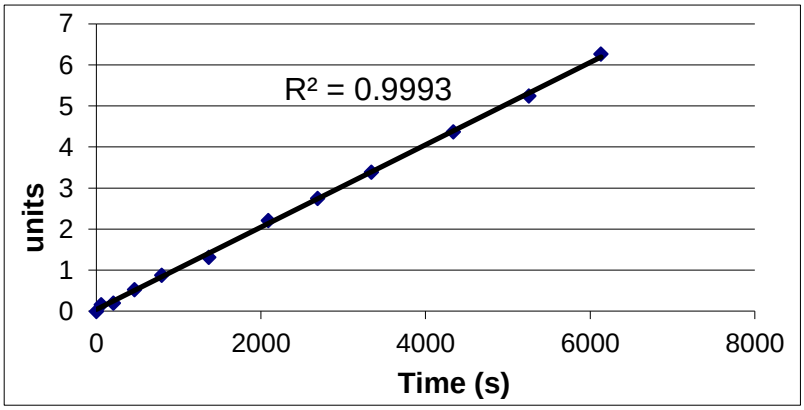

1– VO(salen)NCS

4-ClC_6H_4CHO

R^2 = 0.9988

Order 2

k = 0.93x10^{-3} M.s^{-1}

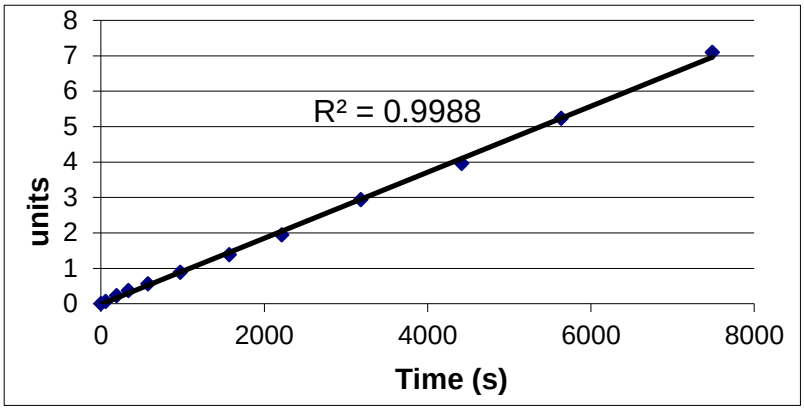

2– VO(salen)NCS

4-ClC_6H_4CHO

R^2 = 0.9978

Order 2

k = 0.99x10^{-3} M.s^{-1}

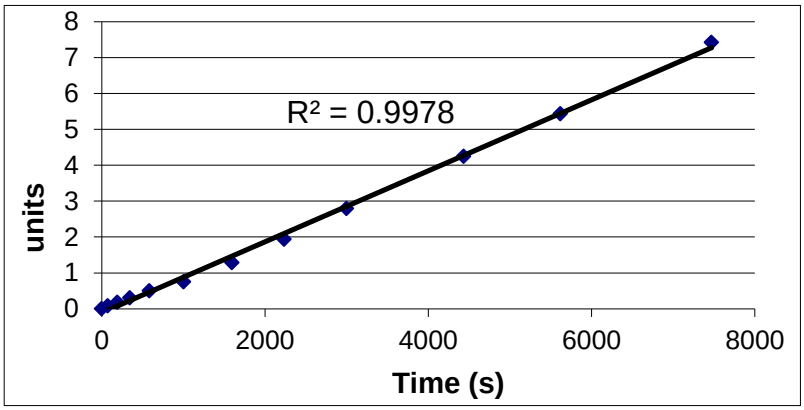

1– VO(salen)NCS

4-BrC_6H_4CHO

R^2 = 0.9987

Order 2

k = 0.89x10^{-3} M.s^{-1}

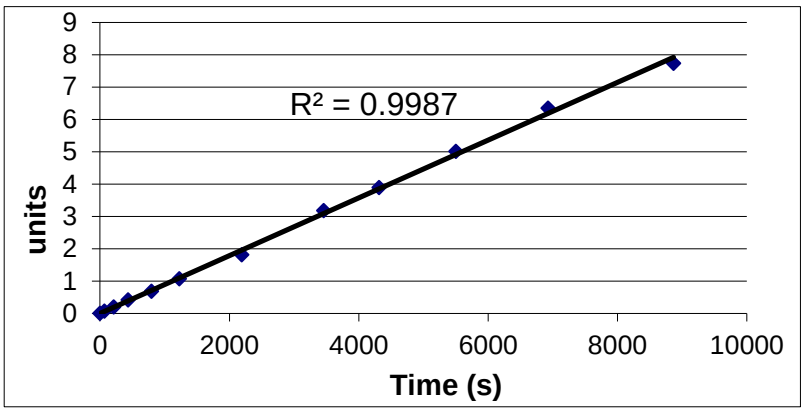

2– VO(salen)NCS

4-BrC$_6$H$_4$CHO

R^2 = 0.9981

Order 2

k = 0.76x10^{-3} M.s^{-1}

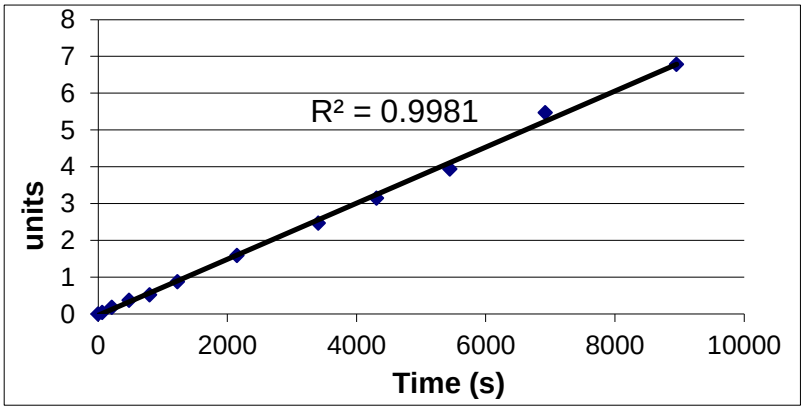

1– VO(salen)NCS

4-FC$_6$H$_4$CHO

R^2 = 0.9907

Order 2

k = 0.56x10^{-3} M.s^{-1}

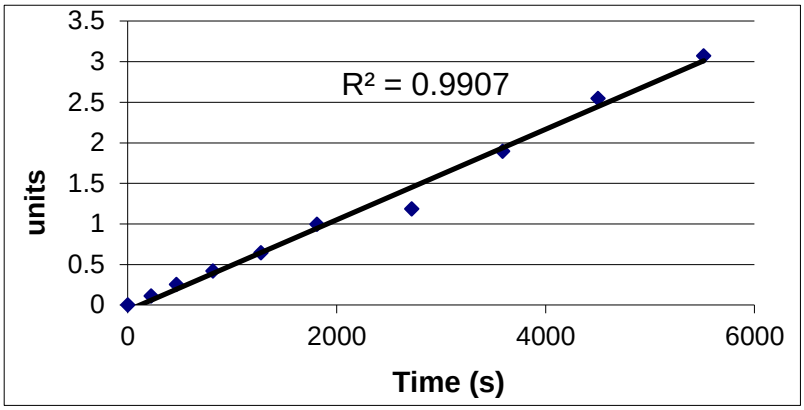

2– VO(salen)NCS

4-FC$_6$H$_4$CHO

R^2 = 0.9937

Order 2

k = 0.48x10^{-3} M.s^{-1}

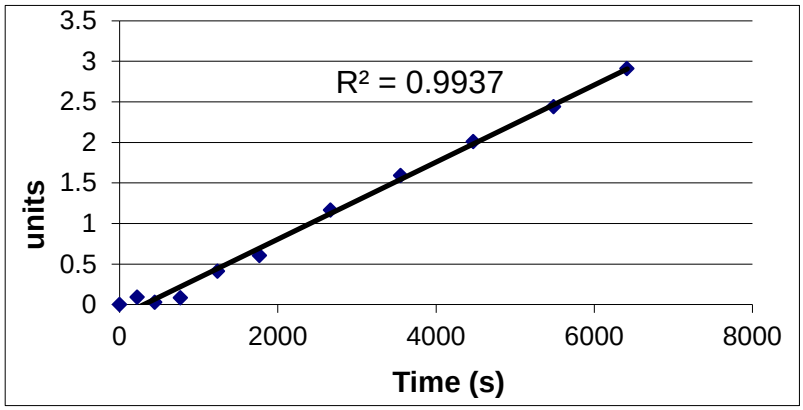

1– VO(salen)NCS

4-CH$_3$SC$_6$H$_4$CHO

R^2 = 0.9795

Order 2

k = 0.26x10^{-3} M.s^{-1}

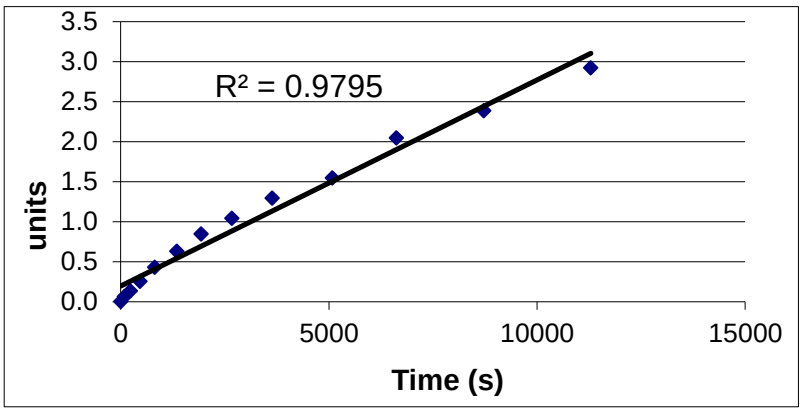

2– VO(salen)NCS

4-$CH_3SC_6H_4CHO$

R^2 = 0.9667

Order 2

k = 0.25x10^{-3} M.s^{-1}

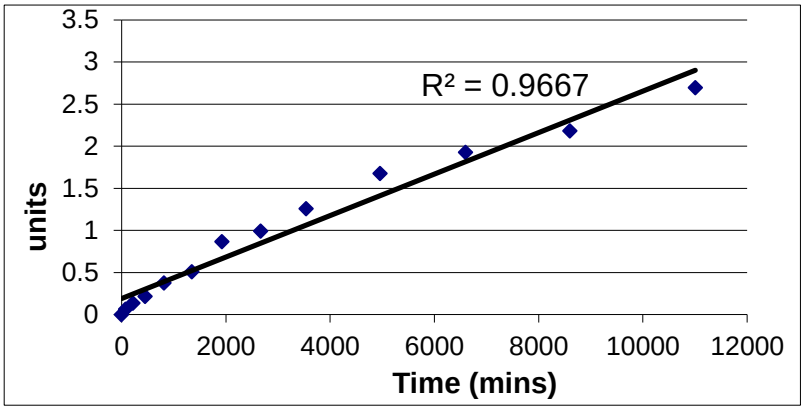

1– VO(salen)NCS

3-$CH_3C_6H_4CHO$

R^2 = 0.9920

Order 2

k = 0.68x10^{-3} M.s^{-1}

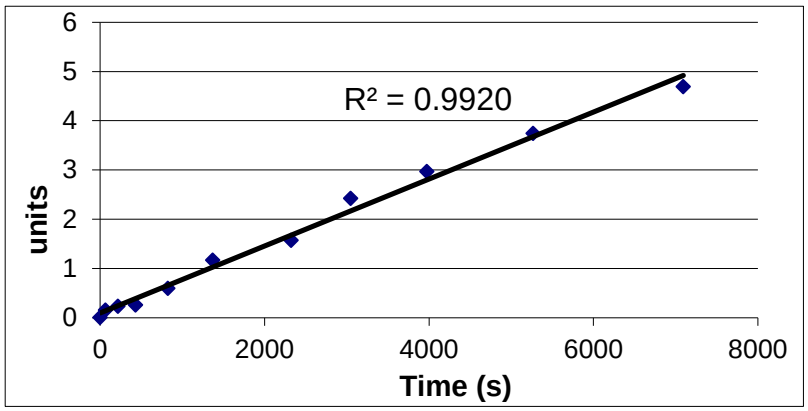

2– VO(salen)NCS

3-$CH_3C_6H_4CHO$

R^2 = 0.9967

Order 2

k = 0.74x10^{-3} M.s^{-1}

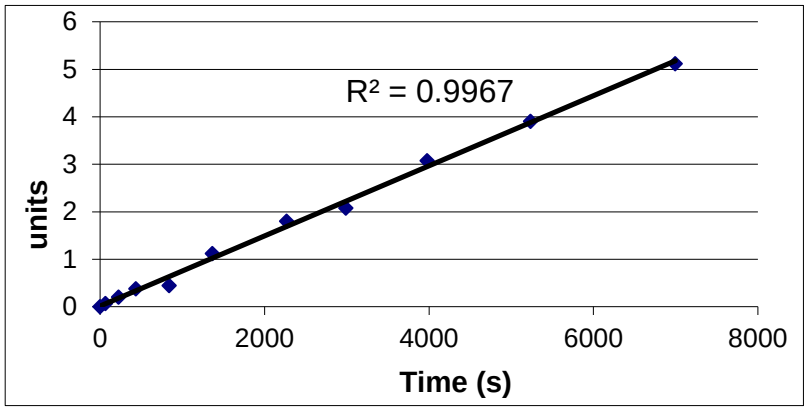

1– VO(salen)NCS

4-$CH_3C_6H_4CHO$

R^2 = 0.9986

Order 2

k = 0.58x10^{-3} M.s^{-1}

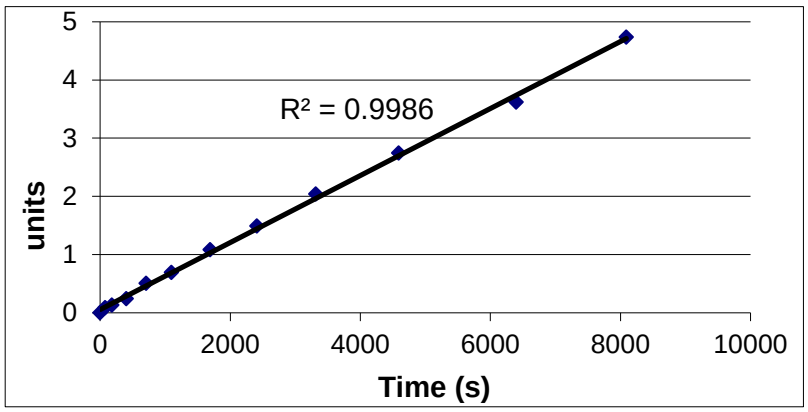

2– VO(salen)NCS

4-$CH_3C_6H_4CHO$

$R^2 = 0.9918$

Order 2

$k = 0.58x10^{-3}$ $M.s^{-1}$

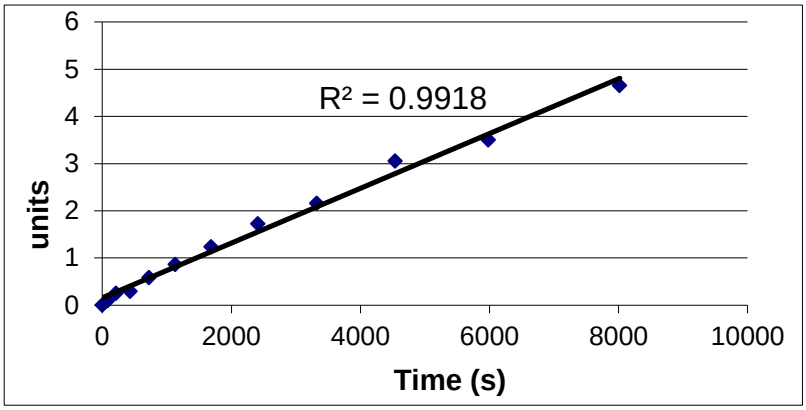

1– VO(salen)NCS

3,4-$(CH_3)_2C_6H_3CHO$

$R^2 = 0.9982$

Order 2

$k = 0.55x10^{-3}$ $M.s^{-1}$

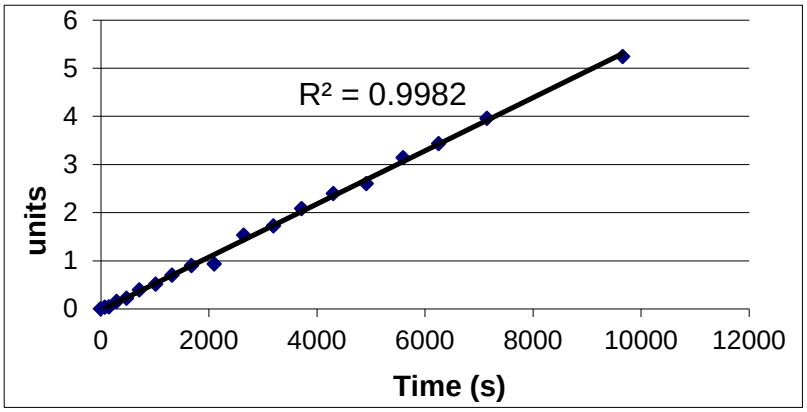

2– VO(salen)NCS

3,4-$(CH_3)_2C_6H_3CHO$

$R^2 = 0.9962$

Order 2

$k = 0.48x10^{-3}$ $M.s^{-1}$